5TH INTERNATIONAL CONFERENCE

ON

SIMULATION AND MODELLING

IN THE

FOOD AND BIO-INDUSTRY

2008

FOODSIM'2008

EDITED BY

Enda Cummins

and

Daniel Thiel

JUNE 26-28, 2008

DUBLIN, IRELAND

A Publication of EUROSIS-ETI

Printed in Ghent, Belgium

5th International Conference on
Simulation and Modelling
In the
Food and Bio-Industry

DUBLIN, IRELAND

JUNE 26-28, 2008

Organised by

ETI
The European Technology Institute

UCD
University College Dublin

Sponsored by

SFI
Science Foundation Ireland

EUROSIS
The European Simulation Society

NIZO FOOD Research

Ghent University

ENITIAA

Hosted by

UCD

And

The Montrose Hotel

Dublin, Ireland

EXECUTIVE EDITOR

PHILIPPE GERIL
(BELGIUM)

EDITORS

General Conference Chair

Enda Cummins

University College Dublin, Dublin, Ireland

General Program Chair

Daniel Thiel, ENITIAA, Nantes, France

International Programme Committee

Simulation in Food Engineering and Processing
Cedric Brandam, ENSIACET - Laboratoire de Génie Chimique, Toulouse, France
Peter de Jong, NIZO food research, Ede, The Netherlands
Jean-Yves Monteau, ENITIAA, Nantes cedex 3, France
Maarten Schutyser, NIZO food research B.V, Ede, The Netherlands
Jan L. Top, Agrotechnology and Food Innovations B.V., Wageningen, The Netherlands
Olivier Vitrac, INRA-UMR FARE, Reims Cedex 2, France .

Simulation in Food Sciences and Biotechnology
Francis Butler, UCD, Dublin, Ireland
Enda Cummins, UCD, Dublin, Ireland
Imogen Foubert, Ghent University, Ghent, Belgium .
Martin Mitzscherling, Universität Hohenheim, Stuttgart, Germany

Simulation in Food Economics
Vincent Hovelaque, UMR INRA-Agrocampus SENAH, Rennes, France
Daniel Thiel, ENITIAA, Nantes, France

Methods and Tools Applied to Food and Bio-Industries
Kristel Bernaerts, Katholieke Universiteit Leuven, Leuven, Belgium
Paolo Masi, University of Naples Federico II, Portici (NA), Italy
Pierre-Sylvain Mirade, INRA-Theix, St.Genes Champanelle, France
Annalisa Romano, University of Naples Federico II, Portici (NA), Italy
Leon Rothkrantz, Delft University of Technology, Delft, The Netherlands

Energy efficiency improvement
Lionel Boillereaux, ENITIAA, Nantes, France

Sustainable Food Production
Karin Östergren, SIK, Sweden
Ulf Sonesson, SIK, Sweden
Björn Johansson, Chalmers University of Technology, Sweden

FOODSIM 2008

All articles published in these Proceedings have been peer reviewed

EUROSIS-ETI Publications are ISI-Thomson and INSPEC referenced

For permission to publish a complete paper write EUROSIS, c/o Philippe Geril, ETI Executive Director, Greenbridge NV, Wetenschapspark 1, Plassendale 1, B-8400 Ostend Belgium

EUROSIS is a Division of ETI Bvba, The European Technology Institute, Torhoutsesteenweg 162, Box 4, B-8400 Ostend, Belgium

Printed in Belgium by Reproduct NV, Ghent, Belgium
Cover Design by Grafisch Bedrijf Lammaing, Ostend, Belgium

EUROSIS-ETI Publication

ISBN: 978-90-77381-41-0
EAN : 978-90-77381-41-0

Preface

It is with great pleasure we welcome you to Dublin for the 5th International Conference on Simulation and Modelling in the Food and Bio industries (FOODSIM'08). The FOODSIM conference, conceived in 2000 by a team of five Professors from ENITIAA (Daniel Thiel, Jean-Yves Monteau, Lionel Boilleraux, Dominique Della Valle and Michel Havet) in cooperation with the European Simulation Office, has gone from strength to strength, bringing together model developers, food experts and industrial users of model simulation tools.

Mathematical and computing techniques play an important role in simulation, optimisation and management of food and bio-processing techniques. The effectiveness and reliability of modelling procedures has become a valuable alternative for, and support to, the traditional experimental approach. In that respect, mathematical simulation is of paramount importance in describing phenomena, solving problems, testing new ideas for a better representation of reality.

FOODSIM'08 aims to present a broad overview of the state-of-the art in using computer models in the development and operation of food and bio-processes. This event provides a great opportunity for scientists from all over the world to share their thoughts, findings and progress in this field and facilitates cooperation and interaction between international experts in food and biological sciences, engineering, computer science, and mathematics.

We would like to thank all the authors for sharing their research and the reviewers for their diligent work in assessing papers. We would also like to thank the various organisations for assistance and sponsorship of this year's event (UCD, SFI, ENITIAA, ETI, EUROSIS, Ghent University, NIZO Food Research).

Finally we wish you all a pleasant and enjoyable time in Dublin at FOODSIM'08.

Dr. Enda Cummins, University College Dublin, Belfield, Dublin, Ireland

and

Prof. Daniel Thiel, ENITIAA, Nantes, France

CONTENTS

CONTENTS

CONTENTS

CONTENTS

SCIENTIFIC PROGRAMME

KEYNOTE SPEECHES

Modelling and simulation of dynamical systems with a dynamical structure

Jean-Louis Giavitto
IBISC FRE 3190 CNRS – Université d'Evry, Genopole,
523 place des Terrasses de l'Agora, 91000 Evry, France
giavitto@ibisc.univ-evry.fr
http://mgs.ibisc.univ-evry.fr

The dynamical system approach characterizes a system by its state and models its evolution by a transition function (or a relation). This approach is widely used in system's simulation and there exists several formalisms used to describe a dynamical system: ordinary differential equations, partial differential equations, iterated equations (finite set of coupled difference equations), cellular automata, etc., following the discrete or continuous nature of the time, the space and the value used in the modelling.

However, some dynamical systems exhibit a dynamical structure, that is, the structure of the state cannot be fixed *a priori* and changes in the course of the time *and/or* the evolution function is also susceptible to evolve, cf. [Gia03]. We call such systems *dynamical systems with a dynamical structure* or $(DS)^2$ in short. Examples of such systems include the modeling of elastic and soft bodies, dynamical networks (like the Internet, mobile network, etc.) and numerous biological systems, especially in morphogenesis [GGMP02].

$(DS)^2$ cause specific and hard problems for their simulation. For example the transition function cannot be defined globally and once and for all: the dynamics of the whole system must be specified as several *local* competing transformations occurring in an organized set of simpler entities (the elements of the system). Locality means that the system can be decomposed into parts, either statically or dynamically [GMCS05], these parts being small with respect to the whole, and such that computation proceeds by evolution of these parts.

In this presentation, we introduce the notion of $(DS)^2$ and one approach for their simulation based on the specification of local evolution rules specifying the system's element interactions. This framework, based on elementary notions borrowed from algebraic topology [GS08], encompasses previous well known formalisms like Lindenmayer systems (used in the modelling of plant growth) or cellular automata. The rule application strategy can be used to achieve synchronous, asynchronous or stochastic evolutions.

The corresponding tool, instantiated in a domain specific programming language[1] (DSL) called **MGS**, has been successfully used in various applications. We will present here two examples: the simulation of the growth of the meristem of *Arabidopsis* at a cellular level [dRBCL+06] and an example of synthetic multicellular bacteria designed for the iGEM competition in synthetic biology [IGE07].

References

[dRBCL+06] Pierre Barbier de Reuille, Isabelle Bohn-Courseau, Karin Ljung, Halima Morin, Nicola Carraro, Christophe Godin, and Jan Traas. Computer simulations reveal

[1] see the project web page at http://mgs.ibisc.univ-evry.fr

properties of the cell-cell signaling network at the shoot apex in Arabidopsis. *PNAS*, 103(5):1627–1632, 2006.

[GGMP02] Jean-Louis Giavitto, Christophe Godin, Olivier Michel, and Przemyslaw Prusinkiewicz. *Modelling and Simulation of biological processes in the context of genomics*, chapter "Computational Models for Integrative and Developmental Biology". Hermes, July 2002. Also republished as an high-level course in the proceedings of the Dieppe spring school on "Modelling and simulation of biological processes in the context of genomics", 12-17 may 2003, Dieppes, France.

[Gia03] Jean-Louis Giavitto. Topological collections, transformations and their application to the modeling and the simulation of dynamical systems. In *Rewriting Technics and Applications (RTA'03)*, volume LNCS 2706 of *LNCS*, pages 208 – 233, Valencia, June 2003. Springer.

[GMCS05] J.-L. Giavitto, O. Michel, J. Cohen, and A. Spicher. Computation in space and space in computation. In *Unconventional Programming Paradigms (UPP'04)*, volume 3566 of *LNCS*, pages 137–152, Le Mont Saint-Michel, September 2005. Springer.

[GS08] Jean-Louis Giavitto and Antoine Spicher. Topological rewriting and the geometrization of programming. *Physica D*, 2008. (accepted for publication).

[IGE07] IGEM. Modeling a synthetic multicellular bacterium. Modeling page of the Paris team wiki at iGEM'07, 2007. `http://parts.mit.edu/igem07/index.php/Paris/Modeling`.

Predictive Microbiology Tools for Evaluating the Compliance of RTE Foods with the New European Union Safety Criteria for *Listeria monocytogenes*

Kostas Koutsoumanis

Laboratory of Food Microbiology and Hygiene, Department of Food Science and Technology, Faculty of Agriculture, Aristotle University of Thessaloniki, Thessaloniki, 54124, Phone +30 2310 991647. Fax: +30 2310 991647. E-mail: kkoutsou@agro.auth.gr.

Abstract

This study presents predictive microbiology tools for evaluating the compliance of RTE foods with the new safety criteria for *L. monocytogenes.* A probabilistic modeling approach is described that combines: a) growth/no growth boundary models, b) kinetic growth models, c) data on product characteristics (pH, a_w, shelf-life) and d) storage temperature data recorded from 50 retail stores in Greece. The probabilistic analysis of the above components using Monte Carlo simulation, which takes into account the variability of factors affecting microbial growth, can lead to a realistic estimation of *L. monocytogenes* levels in the products throughout the food-supply chain. The developed approach was also used for evaluating the probability of food spoilage. The quantitative output generated can be further used by food managers as a decision-making tool regarding the design or modification of a product's formulation or its "use-by-date" in order to ensure compliance with the new safety criteria and quality of the products.

INTRODUCTION

According to the new EU Regulation (EC 2073/2005), food safety criteria are those that "define the acceptability of a product or a batch of foodstuff applicable to products placed on the market". Of particular interest in the food safety criteria-compared to the previously existing legislation- are the legislative amendments regarding *L. monocytogenes* in RTE foods. RTE foods other than those intended for infants or special medical purposes are sub-divided into those that are able to support the growth of *L. monocytogenes* and into those that are not. Products "with pH $\leq$ 4.4 or a_w $\leq$ 0.92, products with pH $\leq$ 5.0 and a_w $\leq$ 0.94 and products with a shelf-life of less than five days" are automatically considered to belong to the category of RTE foods that are unable to support the growth of *L. monocytogenes*. The Regulation also states that "other categories of products can also belong this category, subject to scientific justification". Last, the food safety criteria for *L. monocytogenes* are adjusted according to their temporal stage in the food-chain. Thus, for RTE foods that are able to support the growth of *L. monocytogenes*, the new Regulation demands the absence of the pathogen (in 25 g) "before the food has left the immediate control of the food business operator, who has produced it", but allows for up to 100 CFU/g for "products placed on the market during their shelf-life". The 100 CFU/g limit also applies throughout the shelf-life of marketed RTE foods unable of supporting *L. monocytogenes* growth.

At a first glance, the new safety criteria for *L. monocytogenes* might appear more lenient towards food manufacturers; however, this is not necessarily the case. Rather, the new Regulation can be viewed as more pragmatic, albeit not comprehensive (see Discussion), and certainly generates novel responsibilities for food manufacturers. For RTE foods that are able to support the growth of *L. monocytogenes*, Regulation 2073 specifies that the "100 CFU/g" criterion "applies if the manufacturer is able to demonstrate, to the satisfaction of the competent authority, that the product will not exceed the limit of 100 CFU/g throughout the shelf-life" and the "absence in 25 g" criterion applies only when the manufacturer is "not able to demonstrate, to the satisfaction of the competent authority, that the product will not exceed the limit of 100 CFU/ml throughout the shelf-life". It is therefore the responsibility of the manufacturer to engage into research and generate product-specific data in order to

provide scientific proof to meet the above requirements.

The purpose of this work was to illustrate the usefulness of predictive modeling as a tool for assessing the compliance of RTE foods with the new safety criteria for *L. monocytogenes*. For this purpose we used a stochastic modeling approach based on published data on the prevalence of the pathogen in RTE deli meats together with data on product characteristics from 160 deli meat samples (such as pH and water activity that affect the behavior of food-borne pathogens in foods) and data on the temperature distribution of refrigerators in retail stores in Greece (Koutsoumanis and Angelidis, 2007). This approach was also used for the evaluation of deli meat spoilage.

MATERIALS AND METHODS

For all RTE meat samples shelf-life was calculated as the difference between the expiration and production dates specified on the label. However, the shelf-life of some products could not be calculated as no production information was recorded on the label. The temperature in 50 display cabinet refrigerators for deli meat products was monitored in six super markets located at five cities in Greece. Temperature data were then fitted to various distributions using the @Risk Software (version 4.5, Palisade Corporation, Newfield, NY USA).

The ability of the tested RTE meat products to support the growth of *L. monocytogenes* was evaluated using the growth/no growth interface model published by Koutsoumanis and Sofos (10). The measured pH and a_w values for each product as well as the temperature distribution of retail refrigerators were introduced into the model and the distribution of the probability of growth of the pathogen was estimated based on a Monte Carlo Simulation technique (30.000 iterations) using the @Risk Software. The percentage of the packages of each product which are able or unable to support growth of the pathogen during storage in retail was calculated by treating the data on the probability of growth derived from the Monte Carlo Simulation as a Binomial random variable with parameter *Pg*:

$$\text{if Binomial}(1,Pg) = \begin{cases} 0 & \text{the package is unable to support growth} \\ 1 & \text{the package is able to support growth} \end{cases}$$

where *Pg* is the probability of growth

The concentration of *L. monocytogenes* in RTE meat products at the end of shelf-life was estimated using a combination of a growth/no growth and a kinetic model. The exponential growth rate (μ) and the lag phase was calculated from the models of Buchanan and Phillips (2).Growth of the pathogen was calculated using a modification of the three-phase linear model (3):

$$N_t = \begin{cases} N_0 & \text{for } t \le \text{lag} \\ N_0 + \alpha\mu\left(t - t_{lag}\right) & \text{for } t_{lag} < t < t_{max} \\ N_{max} & \text{for } t \ge t_{max} \end{cases} \qquad \text{eq.1}$$

where: N_t=log of the population density at time t [log(CFU/g)]; N_o=log of the initial population density [log(CFU/g)]; N_{max}=log of the maximum population density [log(CFU/g)]; t=Elapsed time (h); t_{lag}=time when the lag phase ends (h); t_{max}=time when the maximum population density is reached (h); μ=exponential growth rate [log(CFU/g)]/h and α is the output of the Binomial (1, *Pg*) distribution, where *Pg* is the probability of growth. Based on the above modification, equation 1 predicts no growth of the pathogen when the parameter α is equal to 0, whereas when α is equal to 1 growth is predicted with both μ and lag phase. The initial contamination level (N_o) of *L. monocytogenes* was assumed to follow a normal distribution Normal (-9, 3.5) log CFU/g truncated to -2.3 log CFU/g based on an average package weight of 200 g. The maximum population density (N_{max}) was assumed to be constant with a mean value of 10 log CFU/g. For products with a known shelf-life, the

distribution of the concentration of *L. monocytogenes* at the end of shelf-life was calculated based on the above modeling procedure using a Monte Carlo Simulation technique (30.000 iterations) with the @Risk Software.

The approach described above was also applied for evaluating spoilage of deli meats. In foods where spoilage is caused by microbial activity, shelf life can be defined as the time required by the specific spoilage organisms (the organism responsible for spoilage) to grow from the initial level to a spoilage level (level at which spoilage is observed) (Koutsoumanis and Nychas, 2000). In the case of vaccum packed deli meats, Lactobacillus sake was chosen as the specific spoilage organisms with a spoilage level of 10^7 cfu/g (Devlieghere et al., 2000). Spoilage of deli meat products was estimated using the extended Ratkowsky model of L. sake developed by Devlieghere et al., (1999). For the initial level of L. sake in deli meats a custom distribution was used based on data collected in our lab.

RESULTS AND DISCUSSION

The pH and a_w values of each tested product are shown in Figure 1. According to the regulation criteria, only 8.2% of these products belong to the category of not supporting *L. monocytogenes* growth. This indicates that for the majority of the RTE meat products that are available in the market the food industry should evaluate their ability to support growth of *L. monocytogenes*.

The characteristics of the tested meat products (pH and a_w) were compared with the pH and a_w limits of growth predicted by equation 1 at 4, 10 and 15°C (Fig. 1a). The results showed that 121 out of 160 products (75.6 %) are predicted to be able to support growth at 4°C. Increasing storage temperature however, leads to a shift in the growth limits. As a result, the percent of the tested meat products that are predicted to be able to support growth at 10 and 15°C increased to 85.0% and 89.4%, respectively (Fig. 1). For example, this means that, depending on their pH and a_w, some products are unable to support growth at 4°C, but are able of doing so at 10°C. However, Regulation 2073/2005 does not include a clear guideline regarding the temperature at which the industry should evaluate the ability of its products to support or not the growth of *L. monocytogenes.* The only reference on temperature in the Regulation is under the General requirements of Article 3 where it is stated that "Food business operators shall ensure that the food safety criteria applicable throughout the shelf-life of the products can be met under reasonably foreseeable conditions of distribution, storage and use". In the present study, in order to evaluate the "reasonably foreseeable conditions" of storage of RTE meat products we recorded the temperature in 50 retail refrigerators for deli meats. The results showed that temperature can vary significantly among retail refrigerators (Fig. 1b). Temperature data were fitted to various distributions and a Normal distribution with a mean value of 4.42°C and a standard deviation of 2.63°C provided the best fit based on the χ^2 test.

(a)

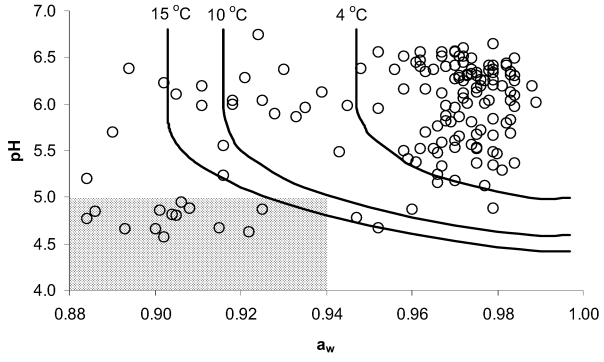

(b)

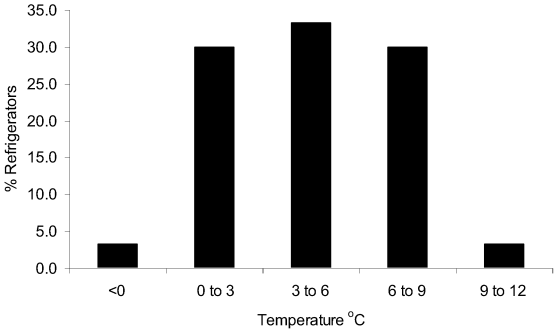

Figure 1. (a): pH and a_w values of sliced ready-to-eat meat products and growth/no growth boundaries (50% probability level) of *Listeria monocytogenes* at 4, 10 and 15°C The shaded area indicates products that are automatically considered as unable to support growth of *L. monocytogenes* according to EC Regulation 2073/2005. (b): Mean temperature in display cabinet refrigerators of the Greek retail market.

The increased variability observed in the storage temperature of RTE foods leads to the conclusion that a probabilistic approach would be more appropriate for evaluating both the ability of products to support growth of *L. monocytogenes* and the total growth of the pathogen during the products' shelf-life. Indeed, by combining figures 1a and 1b, it becomes evident that, for many RTE meat products, the ability of a product unit (retail package) to support the growth of *L. monocytogenes* as well as the total growth of the pathogen during the unit's shelf-life are strongly dependent on the temperature of the refrigerator that the package will be stored in. Thus, more realistic estimations can be obtained by taking the variability of storage temperature into account.

Using the probabilistic approach proposed in the present study both the distribution of the probability of growth of *L. monocytogenes* in a given product and the percent of the product's packages in the market that are able or unable to support growth of the pathogen can be estimated. The cumulative distributions of the probability of growth of *L. monocytogenes* in two representative products as predicted by the model are shown in Fig. 2. For bresaola (pH=6.75 and a_w=0.924) only 0.1% of the packages is predicted to support growth of the pathogen (Fig. 2a). For a pork-shoulder product (pH=5.49 and a_w=0.943) however, it is predicted that 33.3% of the packages will be able to support the growth of *L. monocytogenes* (Fig. 2b). The question arising for the latter product is whether it should be categorized in the group of RTE foods that are able of supporting the growth of *L. monocytogenes* or to the group of RTE foods that are unable of supporting the growth of the pathogen. Interestingly, as in the case of the pork shoulder example, for most of the RTE products available in the market the answer to the above question is not clear. From the 160 RTE meat products tested in the present study in only 27 (16.9%) was the percent of packages that are able to support the growth of *L. monocytogenes* equal to zero. The above results indicate the need for guidelines on categorizing the products in a more probabilistic way. Although it is not easy to include such guidelines in a regulation some recommendation on the "level of agreement" of a product to each category is required.

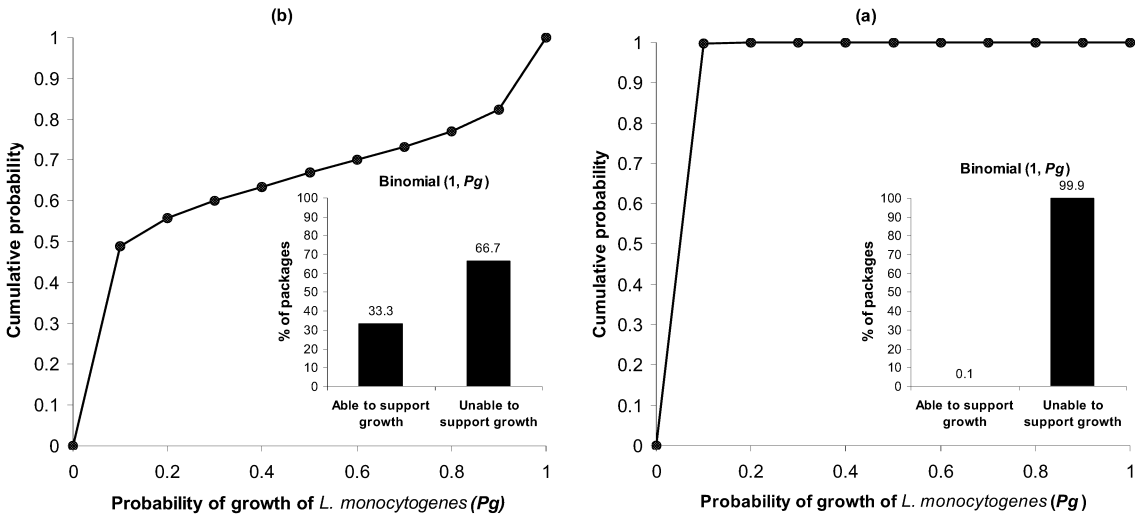

Figure 2. Cumulative distribution of the probability of growth of *Listeria monocytogenes* in (a) bresaola and (b) pork shoulder and percent of packages that is able or unable to support growth of the pathogen during storage in retail.

The distributions of the *L. monocytogenes* concentration in the packages of bresaola (shelf-life=98 days) and pork shoulder products (shelf-life=113 days) at the end of their shelf-life are shown in Fig. 3. The simulation results showed that the pathogen will exceed the criterion of 100 CFU/g in 3.3% of contaminated bresaola packages at the end of shelf-life (Fig. 3a). This means that the level of compliance of this product to the safety criterion is 96.7%. For the pork shoulder product the simulation results showed that the pathogen will exceed the criterion of 100 CFU/g in 35.3% of the packages at the end of shelf-life (Fig 3b). The estimated concentration of the pathogen at the end of the shelf-life of the latter product varies significantly from -2.3 to 10 log CFU/g. As it is shown in Fig. 4b there are two groups of packages, with low and high concentration of the pathogen, respectively. This bi-modal pattern of the distribution can be attributed to the variability of the storage temperature in retail (Fig. 2). The group of packages with *L. monocytogenes* concentration less than 2 log CFU/g (64.5% of the total packages) are those exposed at temperature conditions which do not allow growth of the pathogen and thus the *L. monocytogenes* concentration at the end of shelf life is predicted to be equal to the initial level of contamination. In about 22.4% of the packages the predicted total growth of the pathogen during the shelf life ranged from 2 to 9 log CFU/g depending on the storage temperature while in 13.1% of the packages the pathogen reached the assumed maximum population density (10 log CFU/g) at the end of shelf life. The above results indicate that depending on the storage temperature some packages will not allow growth of the pathogens, whereas in some other packages the pathogen can reach high levels, especially when the product has a long shelf life as in the case of pork shoulder (113 days).

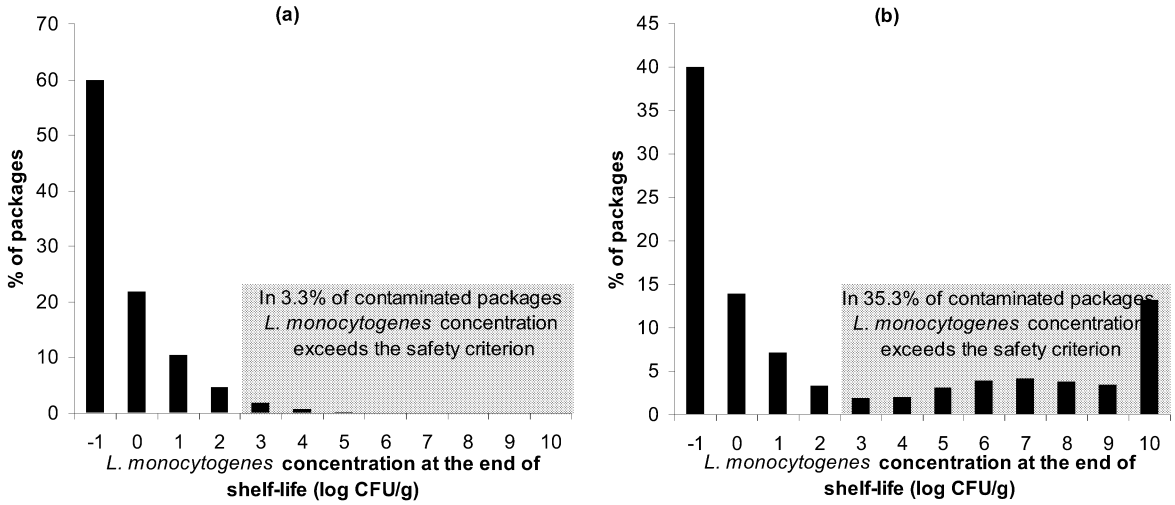

Figure 3. Distribution of the predicted *Listeria monocytogenes* concentration in contaminated (a) bresaola) and (b) pork shoulder packages at the end of shelf-life in retail.

In 66.1% of the products tested in this work the level of compliance was less than 50% (i.e. 66.1% of the products tested are expected to have more than 50% of their contaminated packages exceeding 100 CFU/g by the end of their shelf-life), while only in 25% the level of compliance was found to be higher than 90%. However, 100% compliance was not observed

for any of the tested products. Indeed, achieving absolute (100%) compliance to the safety criterion may not be practically feasible because even for contaminated products that do not support growth of *L. monocytogenes* there is a finite probability for the initial contamination to exceed 100 cells/g.

Given a desired level of compliance, the proposed approach can estimate an appropriate adjustment of the product's shelf-life or a modification in its formulation in order to achieve this compliance. For example, for the pork shoulder product discussed above, in order to increase the level of compliance from the value of 64.7% (that is predicted with its current shelf-life of 113 days) to 90 or 95%, the shelf-life would have to be decreased to 50 or 36 days, respectively (Fig. 4a). Alternatively, a 90% level of compliance could be achieved by maintaining a shelf-life of 113 days, but decreasing the a_w of the product from 0.943 to 0.930 and increasing the concentration of $NaNO_2$ from 50 to 100 ppm (Fig. 4b). This capability of the proposed approach can be also utilized by the food industry for the development of new products. The approach can provide useful information, which can serve as the basis for an appropriate product design that will assure placement of the product to the desired food category. It should be noted that it may be beneficial for the food industry to prove that a product does not support *L. monocytogenes* growth since in this case the zero tolerance limit for the time period until "the food has left the immediate control of the food business operator who has produced it" does not apply.

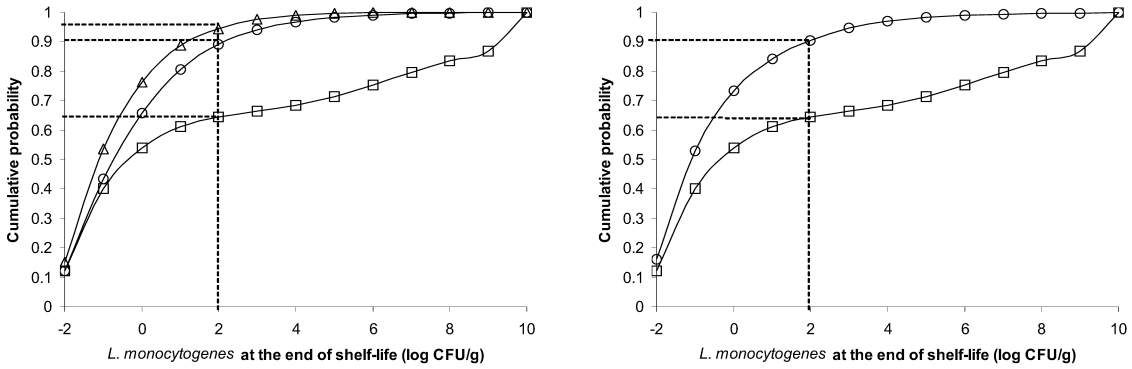

Figure 4.. Effect of shelf-life or product formulation modifications on the cumulative probability distribution of the *Listeria monocytogenes* concentration in contaminated pork shoulder packages at the end of shelf-life (a: □: Current shelf-life of 113 days, ○: Shelf-life of 50 days, △: Shelf-life of 36 days. b: □: Current formulation (pH=5.49, a_w=0.943, $NaNO_2$=50 ppm), ○: Modified formulation (pH=5.49, a_w=0.930, $NaNO_2$=100 ppm).Dotted lines indicate the level of compliance with the new safety criteria).

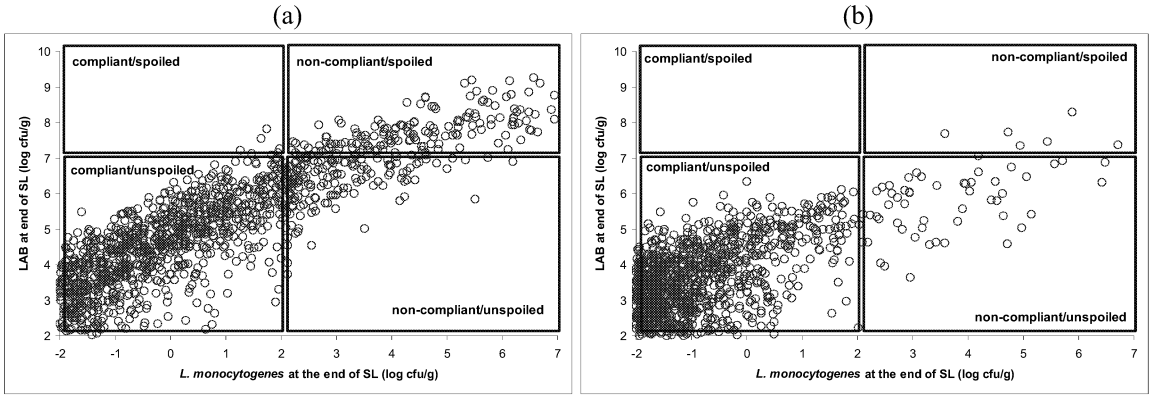

Figure 5. Effect of shelf-life modifications on the cumulative probability distribution of the Listeria monocytogenes and L. sake concentration in contaminated pork shoulder packages at the end of shelf-life (a: Current shelf-life of 113 days, b: Shelf-life of 36 days.

The proposed approach can be also applied for evaluating the probability of food spoilage. In figure 5a the distribution of the level of both *L. sake* and *L. monocytogenes* in pork shoulder at the end of shelf life (113 days) is presented. As it is mentioned above the level of compliance to the safety criteria is 64.7%. In addition this figure shows that 17.5% of the packages will be spoiled before the end of shelf life (L sake level > 10^7 cfu/g). In this case decreasing the shelf life to 36 days will increase the compliance level to 95% and at the same time eliminate the spoiled packages before the end of shelf life (Fig. 5b). Consequently, this approach can be used for optimizing both safety and quality of foods.

REFERENCES

Buchanan, R. L., and J. G. Phillips. 2000. Updated models for the effects of temperature, initial pH, NaCl and $NaNO_2$ on the aerobic and anaerobic growth of *Listeria monocytogenes.* Quant. Microbiol. 2, 103-128.

Buchanan, R. L., R. C. Whiting, and W. C. Damert. 1997. When is simple good enough: a comparison of the Gompertz, Baranyi, and three-phase linear models for fitting bacterial growth curves. Food Microbiol. 14,313-326.

Devlieghere, F., Van Belle B. and Debevere, J., 1999. Shelf life of modified atmosphere packed cooked meat products: a predictive model, International Journal of Food Microbiology 46, 57-70

Devlieghere, F., A. H. Geeraerd, K. J. Versyck, H. Bernaert, J. F. Van Impe and J. Debevere. 2000. Shelf life of modified atmosphere packed cooked meat products: addition of Na-lactate as a fourth shelf life determinative factor in a model and product validation, Int International Journal of Food Microbiology 58, 93-106

Koutsoumanis K., and J. N. Sofos. 2005. Effect of inoculum size on the combined temperature, pH and a_w limits for growth of *Listeria monocytogenes*. Int. J. Food Microbiol. 104:83-91.

Koutsoumanis, K., Angelidis, A.S. 2007 Probabilistic modeling approach for evaluating the compliance of ready-to-eat foods with new European union safety criteria for Listeria monocytogenes Applied and Environmental Microbiology 73, 4996-5004

MODELLING OF HEAT TRANSFER AND SIMULATION OF THERMAL PROCESSES

Global and local optimization of food quality in batch thermal processes

Taghi Miri
University of Birmingham, Edgbaston, Birmingham B15 2TT, UK.
E-mail: mirishst@adf.bham.ac.uk

Serafim Bakalis
University of Birmingham, Edgbaston, Birmingham B15 2TT, UK.

Berc Rustem
Imperial College of Science, Technology & Medicine 180 Queen's Gate, London SW7, UK

Angelos Tsoukalas
Imperial College of Science, Technology & Medicine 180 Queen's Gate, London SW7, UK

Efstratios Pistikopoulos
Imperial College of Science, Technology & Medicine 180 Queen's Gate, London SW7, UK

Peter Jonathan Fryer
University of Birmingham, Edgbaston, Birmingham B15 2TT, UK.

KEYWORDS
Food process optimisation, Food quality, Global optimisation, Thermal inactivation

ABSTRACT
Conventionally, food is significantly over-processed to ensure safety. Dynamic optimization can be used to compute optimal thermal operation condition to ensure maximum product quality while assuring food safety. Local optimization (LO) algorithms have been used to compute optimal profiles. However, LO is not guaranteed to find the best solution. We show that the problem can be formulated as a convex problem with a reverse convex constraint and we implement Tuy's algorithm to optimize globally. The method is deterministic and guaranteed to find the global optimum and therefore it is suitable to evaluate the effectiveness local optimization to compute global optima. We compared the results of LO and global optimization (GO) to find that GO gives significantly better results for 2 and 3 heating time periods. However, for 4 periods the local optimizer catches up. This suggests that LO is good enough for this problem if we consider strategies with more than 4 periods implementable. However for many commercial processes less than 4 heating-cooling stages are used.

INTRODUCTION

The main goal of thermal processing is inactivating pathogenic micro-organisms to make the food safe to the consumer (Bellara et al., 1999).

Thermal Processing of Foods

Thermal processing, i.e. heating, is one of the most important operations in food processing (Balsa-Canto et al., 2002). Conventionally, food is significantly over-processed to ensure safety (Fryer and Robbins, 2005). Requirements for microbial safety and food acceptability and its quality are conflicting, as a certain amount of chemical change will occur during adequate sterilization of the food. Therefore it is important to ask what is meant by quality and what is the scope for improving it (Lewis and Heppell, 2000).

However, heating needs to be done without the over-processing which results in low quality. For obvious reasons a decline in sensory quality is undesirable. If over-processing is not excessive, then sensory quality may be acceptable. Nevertheless, this will still lower the nutritional value of the food as vitamins and micro-nutrients are decomposed by heating process. In this case, the consumer will not be able to distinguish between high and low quality food. The price the consumer is prepared to pay reflects the quality of the product (real or perceived), and so maximizing quality is critical for commercial success. The manufacturers on the other hand, fear microbial safety and tend to over-process while ensuring that the consumer will not notice the loss in nutrition quality since sensory quality is maintained.

Batch thermal processing is widely used in food canning plants as continuous thermal processing is only economical for very large processes (Norback and Rattunde, 1991; Richardson, 2004) i.e. majority of canneries are small to medium size. Batch thermal processing involves following stages 1. heating stage: food temperature (already packed in the can) is raised to the set temperature; 2. holding stage: food is held at the set temperature for a set time; 3. cooling temperature: the food is cooled down to a point were reactions no longer occur.

Optimization of Food Processes

The literature in thermal processing of food is very extensive. Thermal processing of canned foods reviews can be found at Silva et al. (1993) and Durance (1997). Local optimization of thermal processing has also been studied by many authors, but global optimization method is rarely explored in this area. Reviews on optimization of thermal processing can be found in Holdsworth (1985) and Banga et al. (2003).

Food systems have a non-linear dynamic nature described by PDE's such as the equations for heat transfer. The corresponding optimization problems that need to be solved are in general not convex. Consequently, LO methods can only locate a local optimum. It is impossible to know how close the obtained local optimum is to global optimality. Hence, GO methods are needed to find the globally best solution (Banga and Seider, 1996; Esposito and Floudas, 2000). Deterministic GO methods (Horst and Tuy, 1996; Floudas, 1999) prove that a point is a global optimum or an ε-global optimum usually by searching the whole feasible region. The main challenge is to locate in an efficient manner sub regions that may include a solution and exclude partitions that are guaranteed to be suboptimal.

In this paper we adopt a deterministic GO approach and use Tuy's algorithm to solve it.

MATHEMATICAL MODELS

The objective is to find the optimal retort temperature, which maximizes the final nutrient retention. The casestudy is one particular example from Banga et al. (1991) and Garcia et al. (2006). Here, the formulation of the maximization of the final nutrient retention is considered, using both local and global optimization techniques. The constraint for the optimization is the microbiological lethality at coldest spot at a final time (safety).

The container considered is a cylinder of volume V_T with a radius R and height $2L$, filled with a conduction heated (solid) food. Because of symmetry half of the can simulated as it shown in Fig. 1. The food is pork puree and the parameters for simulation of this system are shown in Table 1.

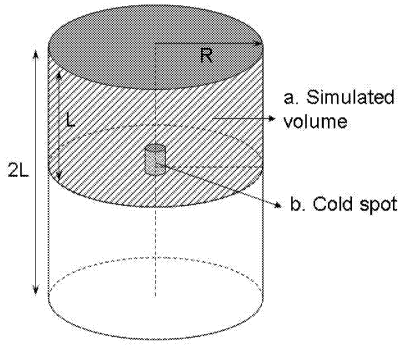

Fig. 1. Schematic diagram of simulated volumes in the can.

Heat transfer dynamics are given by conduction (Fourier) equation

$$\frac{\partial T}{\partial t}=\alpha\left[\frac{1}{r}\frac{\partial}{\partial r}\left(r\frac{\partial T}{\partial r}\right)+\frac{\partial^2 T}{\partial z^2}\right] \quad (1)$$

Where $T=T(r,z,t)$ with following boundary conditions

$$\frac{\partial T(0,z,t)}{\partial r}=0 \quad (2)$$

$$\frac{\partial T(r,0,t)}{\partial z}=0 \quad (3)$$

$$T(r,L,t)=T_{ret}(t) \quad (4)$$

$$T(R,z,t)=T_{ret}(t) \quad (5)$$

Where $T_{ret}(t)$ is the retort temperature

Initial condition is

$$T(R,z,0)=T_0 \quad (6)$$

the microbiological lethality indicator, F-value, is calculated using first-order inactivation kinetic as

$$F_0(t_g)=\int_0^{t_s} 10^{\frac{T(t)-T_{ref,F}}{Z_F}}\,dt=D_{ref,F}.\log\left(\frac{N_F(0)}{N_F(t_g)}\right) \quad (7)$$

Where Z_F is the thermal destruction rate and $N_F(0)$ and $N_F(t_g)$ are the concentration of micro-organisms alive at time 0 and time t_g respectively.

A quantitative measure of the heating effect on quality factors, C-value or cooking value, the same manner as the F-value defined as

$$C_0(t_g)=\int_0^{t_s} 10^{\frac{T(t)-T_{ref,C}}{Z_C}}\,dt=D_{ref,C}.\log\left(\frac{N_C(0)}{N_C(t_g)}\right) \quad (8)$$

As it can be seen from Eq. (8), C_0 has a reverse relation to the retention of nutrient.

Table 1. Parameters for the processing model of pork puree from Garcia et al.(2006)

Parameter	Value
Container diameter (2R)	0.088 m
Container height (2L)	0.116 m
Thermal diffusion coefficient (alpha)	$1.561\text{x}10^{-7}$ m^2s^{-1}
Initial temperature (T_0)	71 °C
Micro-organism	*Baccillus stearothermophilus*
Z_F	10 °C
$D_{ref,F}$	240 s
$T_{ref,F}$	121.11 °C
F_{SD}	1200 s
Nutrient	Thiamine
Z_C	25.56 °C
$D_{ref,C}$	10716 s
$T_{ref,C}$	121.11 °C

The system is modelled using generalised PRocess Modelling Systems (gPROMS) package. For local optimisation the build-in optimiser package was used while for global optimisation Tuy's algorithm was implemented in C++.

GLOBAL OPTIMIZATION FOR FOOD PROCESSING

We divide the time horizon into multiple intervals (periods) and control the retort temperature separately in each of this. That is, we compute piecewise linear strategies. The solution of the heat equation gives the temperature as a function of position and time. However, in most optimization problems the control is the temperature applied externally which appears into the model as a boundary condition and therefore the effect of a change in the controls is not directly visible.

F0,av, C0,av are convex functions in $\{T_1,...,T_n\}$. In addition the final temperature at any given point is an affine and therefore convex function of $T_1,...,T_n$.

The problem we wish to solve is

$$\min_{T_1,...,T_n} C_{0,av} \quad (9)$$

Subject to

$$F_{0,av}\geq 1200s$$

$$30°C\leq T_i\leq 180°C$$

The method is deterministic which means that the optimal point attained by the method is guaranteed to be the global minimum. Apart from the obvious benefit of selecting a good point, the confidence that we know the global

optimum is important for the evaluation of other faster methods, such as Garcia et al. (2006) local optimization approach.

NUMERICAL RESULTS

Figure 2 shows temperature at the centre of the can for the three external temperature profiles.

The numerical results for a heating length of 12,000 s are given in Table 2 in which F_0 is the safety indicator (and should be at least 1200 s) while C_0 is the quality degradation indicator because of heating. These results reveals that for two and three heating periods the global optimizations provides a significant improvement in the food quality (i.e. provide lower C_0 value). However, the local optimizer catches up for four periods. Since we used a deterministic global optimization algorithm, this shows that there is no room for improvement and local solution is optimal for more than four periods.

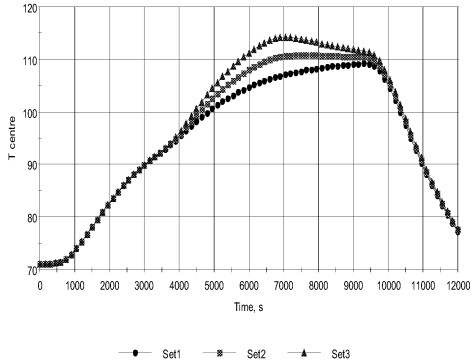

Figure 2: Temperature at the centre of the can for the three external temperature profiles: set1[100,110,110,60], set2[100,115,110,60], set3[100,120,110,60]

CONCLUSIONS

We have addressed the problem of computing globally optimal heating strategies for food sterilization process. We have showed that the food canning problem can be formulated as a convex problem with a reverse convex constrain, and can thus be solved to global optimality by Tuy's deterministic GO algorithm. Tuy's algorithm has been implemented and result compared with the gPROMS local optimization algorithm in the calculation of optimal process conditions for food sterilization. The results demonstrate that for small numbers of intervals, global optimization gives better results, and that, as would be expected, the local optimization accuracy depends on the initial guess. The importance of using global optimization is demonstrated by these results, as the majority of commercial heat-hold-cool systems use only a few temperature intervals.

ACKNOWLEDGEMENTS

We wish to acknowledge financial support from EPSRC.

Table 2: Local optimization vs. global optimization

Local Optimization

Periods	External Temperature	C0	F0
2	92.09 21.266	4746	1200
3	98.1 124.3 66.4	4086	1200
4	862 113.5 124.0 65.7	4051	1200
8	85 99 112 122 124 106 20 20	3920	1200

Global Optimization

Periods	External Temperature	C0	F0
2	121.5 50.7	4174	1200
3	102.9 123.1 59.7	4062	1200
4	85.6 113.7 123.9 66.6	4050	1200

REFERENCES

Balsa-Canto, E., Alonso, A., Banga, J., 2002. A novel, efficient and reliable method for thermal process design and optimization. Part I. Theory. Journal of Food Engineering 52 (May), 227–234.

Banga, J., Balsa-Canto, E., Moles, C., Alonso, A., 2003. Improving food processing using modern optimization methods. Trends in Food Science and Technology 14, 131–144.

Banga, J., Perez-Martin, R., Gallardo, J., Casares, J., 1991. Optimization of the thermal processing of conduction-heated canned foods: study of several objective functions. Journal of Food Engineering 14, 25–51.

Banga, J., Seider, W., 1996. Global optimization of chemical processes using stochastic algorithms. In: Floudas, C., Pardalos, P. (Eds.), State of the Art in Global Optimization. Kluwer Academic Publication, Dordrecht, pp. 563–583.

Bellara, S.R., Fryer, P.J., McFarlane, C.M., Thomas, C.R., Hocking, P.M., Mackey, B.M., 1999. Visualization and modelling of the thermal inactivation of bacteria in a model food. Applied and Environmental Microbiology 65, 3095–3099.

Durance, T., 1997. Improving canned food quality with variable retort temperature processes. Trends in Food Science and Technology 8, 113–118.

Floudas, C., 1999. Deterministic Global Optimization: Theory, Methods and Applications. Kluwer Academic Publishers. Fryer, P., Robbins, P., 2005. Heat transfer in food processing: ensuring product quality and safety. Applied Thermal Engineering 25 (Nov), 2499–2510.

Garcia, M., Balsa-Canto, E., Banga, A.A.J., 2006. Computing optimal operating policies for the food industry. Journal of Food Engineering 74, 13–23.

Holdsworth, S., 1985. Optimisation of thermal processing – a review. Journal of Food Engineering 4, 89–116.

Horst, R., Tuy, H., 1996. Global optimization. In: Deterministic Approaches. Springer.

MODELLING OF HEAT TRANSFER TO FOODS INCORPORATING UNCERTAINTY IN THE LOCATION OF EXPERIMENTAL TEMPERATURE MEASUREMENT

Kevin Cronin[1*],
[1]Dept. of Process & Chemical Engineering,
University College Cork
*Corresponding author, k.cronin@ucc.ie

Jose Caro Corrales[2]
[2]Maestria en Ciencia y Tecnología de Alimentos
and Programa Regional del Noroeste para el
Doctorado en Biotecnología, Universidad
Autónoma de Sinaloa

KEYWORDS
Cheese cooling, Measurement uncertainty

ABSTRACT

A cheese product in the shape of a rectangular slab is cooled by immersion in brine. The temperature of the cheese during cooling was measured by inserting thermocouples into the product. As the cheese is very soft and deformable, it is not possible to exactly identify the measurement location. The Uniform and Exponential probability distributions were found to best represent the variability in thermocouple location at the centre and surface respectively. Cooling of the product was modelled with the one dimensional Fourier field equation. Expressions for the mean measured temperature at the centre and surface that result from the distributed nature of thermocouple location were obtained. These expressions were used to derive equivalent locations in the cheese which should be used when comparing model and experimental temperature predictions. Experiments were conducted to quantify the variability in thermocouple location and the associated dispersion in temperature readings. It was shown that when validating model temperature versus time histories against experimental readings that this phenomenon must be taken into account.

1. INTRODUCTION

Validation of the output from analytical models of heat transfer to food products is generally accomplished by comparison with experimentally obtained heating or cooling curves in the product. To achieve this aim, precise thermocouple location is crucially important in model validation studies (Erdogdu, 2005). The issue is complicated by the fact that there may be unpredictability about the exact location of the thermocouples used to record temperature. The influence of imprecision on thermocouple location has been examined by Gordon & Thorne (1990) and Erdogdu (2005). In some foods, the location can be determined experimentally by subsequent cutting of thin slices from the product or alternatively through remote sensing such as X rays. For the particular product, that is the focus of this work, (soft cheese) these methods were not appropriate.

The impetus for this work is that a cheese product in the form of a slab with a thickness of 60 mm, width of 500 mm and length of 600 mm is produced at a temperature of 40 °C. The product is cooled down to 2 °C by forced immersion in brine; itself maintained at a constant temperature of 0 °C. The temperature of the cheese during cooling is monitored by inserting thermocouples into the cheese at its centre and under the surface. Over the cooling process the rheology of the cheese changes substantially. At its initial temperature of 40 °C, the cheese is extremely soft making accurate placement of the thermocouple tip very difficult. After the cheese has cooled and hardened, it is not possible to subsequently, unambiguously identify the tip location. Hence there is uncertainty in experimental temperature histories which must be considered when comparing them to theoretical predictions. If this issue is not considered, it maybe erroneously concluded that there are errors either in the model or the input data (product thermal properties) that it uses. Specifically where product thermal properties are estimated from the lag or intercept methods, then it is essential that any thermocouple positional error is considered.

2. THEORY

The cheese product is taken to be homogeneous in terms of its composition. The dependence of thermal properties on temperature is ignored because of the relatively small temperature change involved in this cooling operation. Shrinkage and latent heat effects are neglected so product mass and dimensions are constant with respect to time; experiments confirmed this assumption. Thus an analytical solution for temperature versus time is available. Furthermore because the plane dimensions of the product (its width and length) are many times greater than its thickness, heat transfer is regarded as essentially one dimensional. Hence the equation of conservation of energy, for one-dimensional unsteady state conduction in a plane

forms, the basis of this model. The first n terms of the analytical solution (assuming convective boundary conditions and a uniform initial temperature distribution) is given as (Incropera and DeWitt, 1990):

$$\frac{T(x,t)-T_\infty}{T_i-T_\infty}=\sum_{i=1}^{n} A_i\, e^{-\lambda_i^2 Fo}\cos\left(\lambda_i\frac{x}{L}\right) \tag{1}$$

where the constants A_i and λ_i are functions of the Biot Number only. The term, L is half product thickness (i.e. 30 mm). Using the first term expansion of equation (1) is sufficiently accurate for temperature prediction for Fourier Numbers in excess of 0.2, (Incropera and DeWitt, 1990) giving an expression for temperature

$$T(x,t)=(T_i-T_\infty)A_1\, e^{-\frac{\lambda_1^2\,\alpha\, t}{L^2}}\cos\left(\frac{\lambda_1 x}{L}\right)+T_\infty \tag{2}$$

Note the Biot Number for the particular thermal process under review here is in excess of 100 (due to the very high surface heat transfer coefficient between the cheese and brine) so that temperature within the cheese is quite insensitive to any uncertainty in the boundary condition. The temperature gradient through the cheese slab is given as (again for Fourier Numbers in excess of 0.2)

$$\frac{dT(x,t)}{dx}=(T_i-T_\infty)A_1\, e^{-\frac{\lambda_1^2\,\alpha\, t}{L^2}}-\sin\left(\frac{\lambda_1 x}{L}\right)\frac{\lambda_1}{L} \tag{3}$$

indicating that local temperature gradient close to the surface will be significantly larger than at the centre and this effect (which is always present) will be particularly important for this cooling situation due to high value for λ_1 resulting from the high Biot number.

As thermocouple location is generally unknown, its position x_T can be considered as a random variable. The origin for position is taken to be at the centre of the product. In the experiments, thermocouples were inserted into the cheese to a nominal centre position and at the surface. From analysis of experimental data, the Uniform distribution was selected as the appropriate probability density function for x_T for centre temperature while the Exponential distribution was found to best represent the variation in surface thermocouple position. Both distributions have the advantage that they are fully characterised by a single parameter. For the former, the probability density function of thermocouple location will simply be the reciprocal of its range, x_{TR} or imprecision given that the distribution commences at zero (Law & Kelton, 1991)

$$p(x_T)=\frac{1}{x_{TR}} \tag{4}$$

while the density function for measured surface temperature position will be

$$p(x_T)=\frac{1}{x_{TM}}e^{-\frac{(L-x_T)}{x_{TM}}} \tag{5}$$

where x_{TM} is the mean location of the probe. Because measured position of temperature, x_T is now distributed, corresponding measured temperature will also be distributed. The predicted mean of measured temperature can be found using:

$$\mu_T=\int f(x_T)\,p(x_T)\,dx_T \tag{6}$$

where $f(x_T)$ is the functional relationship between temperature and location and $p(x_T)$ is the probability density function of thermocouple location. The full solution contained in equation (1) can be used as the functional relationship or alternatively and more simply, the single cosine function within equation (2). For this work the integral of equation (6) will be evaluated using the simplified thermal model of equation (2) with the appropriate limits and thus the obtained mean value will also be subject to the Fourier time limit.

For centre temperature, the limits of integration in equation (6) will be 0 and x_{TR} while at the surface the corresponding limits are $L-x_{TM}$ and L. Hence mean experimental temperature at the centre will be:

$$\mu_T=(T_i-T_\infty)A_1\, e^{-\frac{\lambda_1^2\,\alpha\, t}{L^2}}\frac{\sin\left(\frac{\lambda_1 x_{TR}}{L}\right)}{\frac{\lambda_1 x_{TR}}{L}}+T_\infty \tag{7}$$

Note as the factor, x_{TR} goes to zero, (no error in thermocouple location) the expression for mean measured centre temperature converges to theoretical centre temperature. The corresponding statistic for surface temperature will be:

$$\mu_T=(T_i-T_\infty)A_1\, e^{-\frac{\lambda_1^2\,\alpha\, t}{L^2}}\frac{\left(L/\lambda_1 x_{TM}\right)^2\left(\lambda_1 x_{TM}/L\sin\lambda_1+\cos\lambda_1-e^{-\frac{L}{x_{TM}}}\right)}{1+\left(L/\lambda_1 x_{TM}\right)^2}+T_\infty\left(1-e^{-\frac{L}{x_{TM}}}\right) \tag{8}$$

Again as the factor, x_{TM} goes to zero, (no error in thermocouple location) the expression for mean measured surface temperature converges to theoretical surface temperature.

For nominal centre temperature, it can be shown that all individual recorded histories will be equal to or less than the true centre temperature. For surface temperature, they will be greater. Thus averaging individual temperature time histories will give a mean that will always be offset from the true value. In fact the expressions for mean centre and surface temperature can be manipulated to give the equivalent locations at which the average of the experimental readings will correspond to. For 'centre'

temperature the equivalent position, x_{ec} is

$$x_{ec} = \frac{\cos^{-1}\left[\dfrac{\sin\left(\dfrac{\lambda_1 x_{TR}}{L}\right)}{\dfrac{\lambda_1 x_{TR}}{L}}\right]}{\dfrac{\lambda_1}{L}} \quad (9)$$

and for 'surface' temperature the equivalent position, x_{es} is approximately given as

$$x_{es} = \frac{\cos^{-1}\left\{\dfrac{\left(\dfrac{L}{\lambda_1 x_{TM}}\right)^2\left(\dfrac{\lambda_1 x_{TM}}{L}\sin\lambda_1 + \cos\lambda_1\right)}{1+\left(\dfrac{L}{\lambda_1 x_{TM}}\right)^2}\right\}}{\dfrac{\lambda_1}{L}} \quad (10)$$

When comparing the average of the experimental temperature histories for centre and surface to the theoretical values, the analytical model should not be evaluated at locations 0 (true centre) and L (surface) respectively but rather at the equivalent locations given by the above analysis. Broadly it can be seen that the greater the local temperature spatial gradient and the larger the dispersion in thermocouple position, the more important is this phenomenon.

3. MATERIALS & METHODS

Initially a series of trials were carried out where the thermocouple was inserted into the warm cheese to assess the imprecision in location. Over thirty samples were cut from the slab and dye marker was placed at the tip of the thermocouple wire. Thirty minutes after each insertion when the cheese had cooled down, the sample was cut open and the location of the thermocouple tip identified as best as possible. This methodology enabled an indication of the distribution of location to be quantified for the centre and surface regions.

The temperature histories of 10 slabs in brine were recorded. Prior to each experiment, the slabs were forcibly, completely submerged in warm water, maintained at a temperature of 40 °C, for a period of 30 minutes to ensure an even initial temperature through them. For each experiment, two thermocouples were inserted into each slab at a position near the centre of the slab and just under the surface of the slab. As far as was practical, the two thermocouple locations were collinear on the same vertical line in the cheese slab, between the different experiments. This was to satisfy the one dimensional analysis of the heat transfer. Temperature data was logged to a computer. Temperature was recorded over the full cooling cycle but only data from the intermediate cooling period was used.

Furthermore, the Monte Carlo method was utilized to estimate the effect of uncertainty in thermocouple location when validating the experimental results and to numerically check the theoretical predictions. The Monte Carlo method can be applied to the full temperature model and thus avoids the limitations of the Fourier time limit. Hence the first four terms of equation (1) formed the deterministic sub-model of the Monte Carlo approach. Random thermocouple locations were sampled from the governing Uniform distribution using

$$x_T = u\,x_{TR} \quad (11)$$

where u is a uniformly distributed random number on the interval [0,1]. Temperature was evaluated at each sampled location with the first four terms of equation (1). These were then averaged to produce an estimate of centre temperature incorporating location uncertainty. The same procedure was followed to obtain an estimate of mean surface temperature by sampling from the governing Exponential distribution with the formula

$$x_T = \ln(1-u)x_{TM} \quad (12)$$

with again temperatures evaluated at each sampled location and then averaged. The Monte Carlo approach was used to act as a check on the validity of the assumptions used in the variability analysis.

4. RESULTS

The cheese thermal properties were measured as a density of 1060 kg/m^3, thermal conductivity of 0.35 W/mK and thermal diffusivity of 1.19 x 10^{-7} m^2/s. The measured convective heat transfer coefficient in the brine was 1300 W/m^{2}K. These properties imply that the Biot Number is 111, the λ_1 and A_1 constants in equation (2) are 1.555 and 1.2731 respectively and the Fourier time limit for the validity of equation (2) is 1512 s.

Analysis of the dispersion in centre thermocouple tip location revealed that its position could vary symmetrically by ± 3 mm on either side of the centre. Figure 1 depicts in frequency histogram form the measured data; locations were banded into 1 mm intervals and the mid-point is given on the graph. With no discernable peak, the Uniform distribution was selected to represent the dispersion. Applying symmetry about product centerline, the value for the appropriate range parameter, x_{TR} is 3 mm.

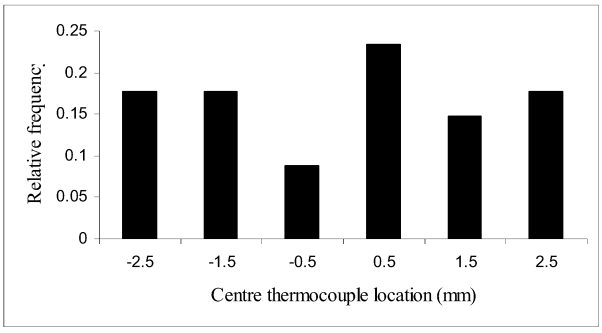

Figure 1: Distribution in Centre Thermocouple Location

A different pattern was evident for thermocouple location under the surface; the location could vary from just under the surface to just over 5 mm below the surface. However the deeper the location below the surface, the less likely was a thermocouple to be situated. Figure 2 illustrates the distribution; again 1 mm bands are used and the mid-point shown. From its general shape, an Exponential distribution was fitted to the data and the analysis gave a value for the mean location, x_{TM} of 28.15 mm (or 1.85 mm from the surface).

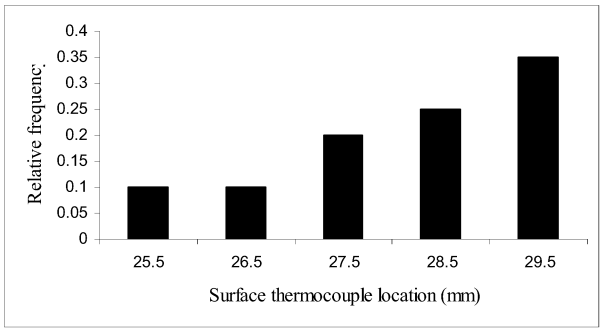

Figure 2: Distribution in Surface Thermocouple Location

Using the data from both distributions, equivalent centre temperature location x_{ec} from equation (9) is 1.73 mm from the centre and equivalent surface temperature location x_{es} is 28.2 mm from the centre or 1.8 mm under the surface (from equation 10). Note that mean temperature in either region (centre or surface) is not equal to temperature evaluated at the mean thermocouple location.

The 10 individual experimental temperature versus time histories recorded at the centre were averaged to produce a single mean experimental history. The analytical solution (equation 2) was used to calculate centre temperature at the exact centre (x = 0) and at the equivalent centre location ($x = x_{ec}$). Figure 3 displays the average of the experimentally recorded centre temperatures, the exact centre temperature, the temperature at the equivalent centre location and the Monte Carlo prediction of measured centre temperature. The curves are only given for times in excess of 1512 s to satisfy the restrictions on the use of equation (2) that was used in the derivation of equivalent position. Figure 4 gives the same temperature-time histories for surface temperature again with the same time limits.

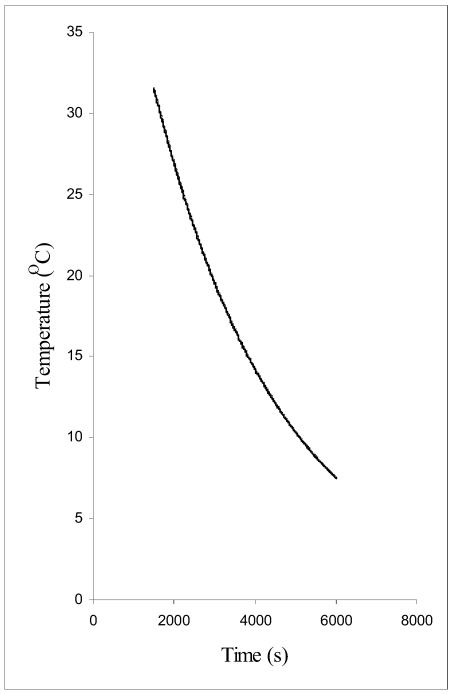

Figure 3: Centre Temperature Histories

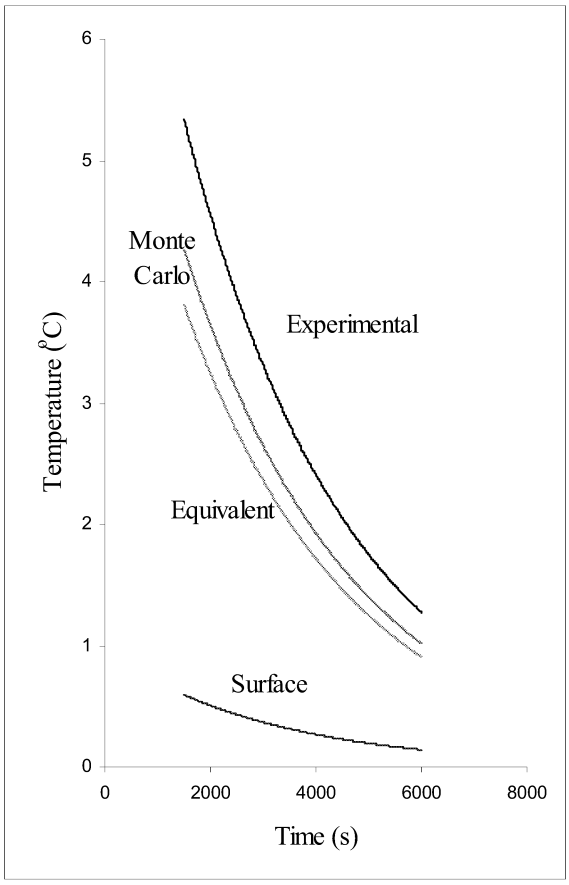

Figure 4: Surface Temperature Histories

Examining figures 3 and 4 it is clear the issue of uncertainty in thermocouple location is much more of an issue for surface temperature prediction than centre temperature. The curves are almost coincident at the centre though

considerably different at the surface. This is partly accounted for by a scale effect as temperature change with time at the surface is considerably smaller than that at the centre at times in excess of the Fourier limit. There are two more fundamental reasons that are also relevant:
1] Temperature gradients close to the surface (evaluated at the location x_{es}) is 11 times larger than temperature gradient in the centre region (evaluated at x_{ec}). Hence any uncertainty in thermocouple location has its influence magnified accordingly.
2] The level of dispersion in thermocouple location (as measured by the standard deviation) is greater for surface readings than centre readings. Standard deviation for centre location is 0.87 mm (i.e. = $x_{TR}/\sqrt{12}$) while for the surface it is 1.85 mm (= x_{TM}).

Nonetheless for both locations, the agreement between the experimental mean temperature history and the temperature history evaluated at the appropriate equivalent location is much superior than the agreement with the temperature history evaluated at the nominal position. This is markedly evident for the surface location as depicted in figure 4. Table 1 quantifies the agreement where the average temperature difference between the experimental and equivalent position histories is compared with the same statistic for the experimental and nominal histories at the centre and surface.

Table 1: Average Temperature Difference between Experimental and Equivalent and Nominal Temperature Histories

Location	Average Temperature Difference	
	Equivalent	Nominal
Centre	0.003 °C	0.07 °C
Surface	0.81 °C	2.52 °C

As is clear, the agreement between theory and experiment is much superior when the dispersion in thermocouple position is accounted for. Specifically the average difference between experimentally measured temperature readings and those evaluated at the appropriate equivalent location is much smaller than the difference found between experiment and nominal values. Any remaining differences between the equivalent and experimental curves may be due to sampling errors; equations (7) and (8) give expressions for the population mean; the larger the number of individual histories that are averaged the closer the results will be to its predictions. Also issues such as thermocouple accuracy and any other sources of error in addition to location imprecision will affect the level of agreement.

The results described here are all limited to times in excess of 1500 s. Studies with the Monte Carlo model to analyse the influence of thermocouple location effects at shorter times demonstrated that the difference between averaged experimental histories and equivalent / nominal theoretical histories are even more pronounced at early stages of cooling. Also note equation (6) can be applied to determine the equivalent location at which temperatures should be verified for, in principle, any thermocouple location distribution function (uniform, normal, exponential etc.). A useful heuristic that can be used without the need to evaluate the integral is that the equivalent location will be the nominal location offset by an amount equal to the mean of the distribution that describes the thermocouple positional imprecision. Finally the results can be manipulated to examine the probability distribution that describes the measured temperature gradient in the cheese i.e. the temperature difference measured between centre and surface locations divided by the (expected) distance between both thermocouples.

5. CONCLUSIONS

The effect of thermocouple positional inexactness should be included in comparing experimental and theoretical temperature predictions where this is an important effect. Such a phenomenon is generally significant when examining surface region temperatures with a high convective heat transfer coefficient. The analysis of this paper can be used to quantify how significant this effect can be and thus suggest whether it should be taken into account. The adoption of an equivalent position rather than the nominal position when comparing experimental and theoretical (or model) temperature histories has been shown to have advantages. The approach of this paper is equally applicable to heating processes with the same assumptions and restrictions. The underlying theory as expressed by equation (6) can be applied to other thermal geometries (cylinder or sphere) and other known distributions such as the Normal distribution that describe thermocouple location. In addition, expressions for the variance and the probability density function of measured temperature can also be derived and yield further criteria in assessing agreement between theory and experiment.

REFERENCES

Erdogdu, F. 2005. ‘’Mathematical approaches for use of analytical solutions in experimental determination of heat and mass transfer parameter’’, *Journal of Food Engineering*, 68, 233 – 238.

Gordon, C. & Thorne, S. 1990. ‘’Determination of the thermal diffusivity of foods from temperature measurements during cooling’’, *Journal of Food Engineering*, 11, 133 – 145.

Incropera, F.P. & DeWitt, D.P. 1990. *Introduction to Heat Transfer*, John Wiley & Sons, New York, USA

Law, A. M., & Kelton, W. D. 1991. *Simulation modelling and analysis*. McGraw-Hill, New York, USA.

OPTIMIZATION OF DRYING KINETICS OF PANEER WITH LOW PRESSURE SUPERHEATED STEAM USING AN ARTIFICIAL NEURAL NETWORK

Shivamurti Shrivastav
Department of Food processing Technology
A D Patel Institute of Technology
Anand, Gujarat, India
E-mail: shivmurtis@gmail.com

B. K. Kumbhar
Department of Process and Food Engng.
G. B. Pant Univ. of Agril and Tech
Pantnagar
Uttarakhand, India

Amarjeet Kalra
Department of Agril. Engng
Haryana Agril. Univ
Hissar,
Haryana, India

KEYWORDS
Paneer, Superheated steam drying, Low Pressure, Artificial Neural Network, Optimization

ABSTRACT

Paneer is an important dairy product and is used to prepare different culinary dishes. It is highly perishable in nature at ambient conditions and its shelf life is very low. Moreover at high temperature, product develops a sour smell, bitter taste and also being sparsely covered with moulds. Therefore, here is need to develop some preservation technique to enhance the shelf life. Drying can be one of the methods to increase shelf life of paneer. Due to its numerous advantages such as less energy wastage, high heat transfer coefficient, no oxidative changes during drying, no resistance to mass transfer at the surface, higher porosity, Low pressure superheated steam drying (LPSSD) is used as a hybrid drying to dry food products. The neural network model consisted was developed of an input, a hidden and an output layer. The input layer has two nodes, which corresponded to two processing conditions or independent variables: Time of drying and weight changed with corresponding time. The output layer consisted of three neurons or dependent variables, representing the moisture content (%db), drying rate (dm/dt) and moisture ratio (MR). The correlation coefficients were greater than 0.98 in all cases. For all combined data set with superheated steam, the R^2 were found 0.9975, 0.9934 and 0.9983 for moisture content, drying rate and moisture ratio. Whereas For all combined data set without superheated steam, the R^2 were found 0.9991, 0.9846and 0.9991 for moisture content, drying rate and moisture ratio.

INTRODUCTION

Paneer, an acidic coagulated or rennet coagulated dairy product, is highly nutritious in terms of fat and protein content. Its normal shelf-life is 1-2 days at room temperature or 3 days at 10^0C due to high moisture content. Attempts have been made to extend the shelf life of paneer by different drying methods. Low pressure superheated steam drying (LPSSD) is being explored for drying of food materials due to its numerous advantages such as less energy wastage, high heat transfer coefficient, no oxidative changes during drying, no resistance to mass transfer at the surface, higher porosity, recovery of latent heat of evaporation and higher mass transfer rates (**Mujumdar 2006**). LPSSD has been applied to drying of shrimp banana, apples, potatoes, cassavas, carrots (**Mujumdar 2004 a and b, Elustondo 2001**).

Drying phenomena has been studied extensively and mathematical models are developed. Due to their limited application covering the drying kinetics over the entire operating conditions, new methods namely artificial neural network (ANN) is being explored recently with success.

In process control, the main objectives are food safety, high quality and yield at minimal costs. To obtain high quality products, on-line control techniques are required. Most food processes are highly nonlinear, with time varying dynamics, which complicates food automation. However, the recent developments in artificial intelligence based advanced control tools such as neural network (NN) to food processing have opened up novel possibilities for processing industries (**Susan, 1998**).

Artificial neural networks (ANN) are mathematical models which have the capability of relating the input and output parameters, without requiring a prior, knowledge of the relationships between the process parameters. It involves training and testing of ANN models (**Borggard et al, 1992**).

The objective of this work was to develop ANN models for predicting moisture content (%db), drying rate (dm/dt) and moisture ratio (MR). This will also compare the moisture ratio obtained from experiments, drying models and by ANN modeling.

EXPERIMENTAL SETUP

Experimental setup of low pressure superheated steam dryer was developed to conduct the drying experiments. Main components of the experimental setup were steam generator, drying chamber, vacuum pump and data acquisition system with computer. The drying chamber consisted of a box insulated properly with rock wool. Inner dimensions of insulated chamber were 40 x 45 x 45 cm. Two electric heaters of 1.5 kW capacities each were provided on opposite side walls of the drying chamber. The temperature of drying chamber was controlled by a temperature controller

The drying chamber was connected by a pipe from bottom to a chamber in which digital balance was kept. An autoclave was used as a steam generator and a steam reservoir. A steam trap was provided to reduce accumulation of steam condensate in the reservoir. Steam was transported to the drying chamber through a pipe insulated with glass wool. A heating tape, rated

1kW was mounted on steam pipeline to increase the steam temperature to desired level of superheating.

The sample holder was made using thin stainless steel sheet of 15 cm diameter. This was connected to a balance by a thin rod passing through a G.I. pipe. One side of the rod was attached to the sample holder and other side was rested on analytical digital balance. The balance was placed in a smaller chamber. The balance had a weighing capacity of 320g with a least count of 0.001g. The data recorded by this balance was transferred through the serial cable by software. Electronic balance attached with computer allows continuous weighing of the sample.

Chromel - Alumel (K type) thermocouples were installed to measure temperature of superheated steam at inlet of drying chamber, drying chamber and product chamber continuously. These thermocouples were attached to the data logger. Thermocouple signals multiplexed and transferred to the computer through Terminal Software, installed in PC. A vacuum pump was used to create the desired vacuum in the drying chamber. 1 and 1.5 cm-cube paneer size were used to study the kinetics. The experiments were performed at 10, 14 and 18 kPa absolute pressure and 62, 72 and 82^{0}C temperature.

Artificial Neural Network Model

The neural network model consisted of an input, a hidden and an output layer. The input layer has two nodes, which corresponded to two processing conditions or independent variables: Time of drying and weight changed with corresponding time. The output layer consisted of three neurons or dependent variables, representing the moisture content (%db), drying rate (dm/dt) and moisture ratio (MR).

MATLAB-7 software used for Artificial Neural Networks (ANN) modeling and evaluating the different training functions. The networks were simulated based on a multilayer feed forward neural network. This type of network is very powerful in function optimization modeling (**Kerdpiboon, 2006**). The input layer, hidden layers, and output layer structures are shown in Fig. 1. The inputs required for modeling other than drying time and weights were:

Method of computation -Back propagation
Algorithm - Levenberg -Marquardt
The network training - Different size of epochs
Goal - Minimum error
Transfer functions - Hyperbolic tangent, sigmoid transfer function and Linear transfer function

A back-propagation algorithm was used to implement supervised training of the network. During training, weighting functions for the inputs to each ANN were determined, such that the predicted output best matched the actual output from the data set. Weights were randomly assigned at the beginning of the training phase, according to the back-propagation algorithm. A hyperbolic tangent was used as the transfer function in each hidden layer, and a linear transfer function was used in the output layer. Minimization of error was accomplished using the Levenberg – Marquardt (LM) algorithm. By this algorithm tat trains a neural network 10 to 100 faster than the usual gradient descent backpropagation method. It will always compute the approximate Hessian matrix, which has dimensions n-by-n. Training was finished when the mean square error (MSE) converged and was less than 0.001. If the MSE did not go below 0.001, training was completed after 5000 epochs, where an epoch represents one complete sweep through all the data in the training set. The ANN modeling thus obtained for moisture content, moisture ratio and drying rate by combining all drying data for temperatures, pressures and size (Six ANN models)

The inputs included the time of drying and weight changed with time. The output layer consisted of %db, dm/dt and MR. The number of hidden layers and number of neurons in each hidden layer were varied from 3 to 9 (3, 5, 7, or 9). The networks were simulated with the learning rate equal to 0.05.

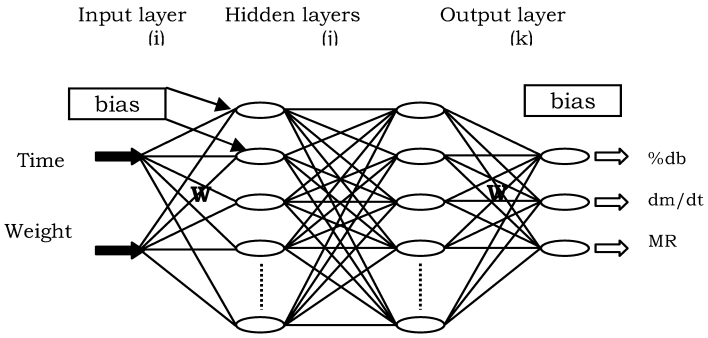

Figuers 1 Theoretical architecture of multilayer neural network for prediction of moisture content dry basis, drying rate and moisture ratio

The optimized configurations from training for each neuron were selected based on neural network predictive performance, which gave the minimum error from the training process. The average mean square error (MAE), standard deviation of MAE (STDA), percentage of relative mean square error (%MRE), and standard deviation of %MRE (STDR) were used to compare the performances of various ANN models, and were calculated as (**Kerdpiboon, 2006 and Torrecilla, 2007**):

$$MAE = \frac{1}{N}\sum_{i=1}^{N} \Delta P_A$$

$$STD_A = \sqrt{\frac{\sum_{i=1}^{N} (\Delta P_A - \overline{\Delta P_A})^2}{N-1}}$$

$$\%MRE = \left(\frac{1}{N}\sum_{i=1}^{N} \Delta P_R\right) \times 100$$

$$STD_R = \sqrt{\frac{\sum_{i=1}^{N} (\Delta P_R - \overline{\Delta P_R})^2}{N-1}}$$

Where

$$\Delta P_A = |P_p - P_E|$$

$$\Delta P_R = |(P_p - P_E)/P_E|$$

Where

P_p = Predicted output (%db, dm/dt, MR)

P_E = Experimantally measured output

RESULTS AND DISCUSSION

The ANN optimization process was performed using a trial and error technique. Both time and weight were used as input in the artificial neural network structure. The data set of inputs and outputs used to train the ANN consisted of individual conditions, combination of temperatures at different conditions, combination of pressure at different conditions, combination of all superheated steam with 1 and 1.5 cm-cube sizes of paneer. Each data set was divided in to two groups, consisting of 50% for training and 50% for testing.

Artificial neural network with between 1 and 2 hidden layers tested and with 3-9 neurons per hidden layer. Each combination of hidden layers and neurons per hidden layer was trained. The result showed that the number of hidden layers, and neurons per hidden layer, that yielded minimum error was different for each drying technique. Table 1 gives the detailed ANN structure for all combined data set with superheated steam and without superheated steam drying. In table 1, the minimum MRE was found with two hidden layers and seven neurons for moisture content dry basis, two hidden layers five neurons for drying rate and two hidden layers and seven neurons for moisture ratio. A large number of hidden layers does no required to lower the error if there are enough number of neurons (**Torrecilla et al., 2007**). The best prediction for most of the data set contained two hidden layers. ANN developed for combined drying data had slightly higher error than individual conditions.

Plots of experimentally determined moisture content, drying rate and moisture ratio versus ANN predicted values for all combined data are shown in figure 2. The correlation coefficients were greater than 0.98 in all cases. For all combined data set with superheated steam, the R^2 were found 0.9975, 0.9934 and 0.9983 for moisture content, drying rate and moisture ratio. Whereas For all combined data set without superheated steam, the R^2 were found 0.9991, 0.9846and 0.9991 for moisture content, drying rate and moisture ratio. In this study the ability to predict moisture content, drying rate and moisture ratio were very good. Studies using regression techniques in analytical models had less predictable than ANN models. While this is perhaps reasonable predictive power, the implementation of the ANN provided even better prediction capability.

CONCLUSION

Artificial Neural Network can be used to predict the drying characteristics of paneer undergoing different drying techniques. The optimal models for combined drying can predict the moisture content, drying rate and moisture ratio with R^2 value greater than .98 offered better prediction than analytical model.

Table 1 Errors in the prediction of drying characteristics with different number of hidden layers and neurons per layer for paneer under going combined 1 and 1.5 cm-cube under low pressure superheated steam drying

Out put	No of hidden layer	No of neurons	MAE	STDA	MRE	STDR	R^2
(%) db	1	3	2.833	2.466	35.907	0.844	0.995
		5	3.287	3.503	14.463	0.223	0.993
		7	3.306	2.364	19.179	0.301	0.991
		9	3.301	2.708	32.432	0.769	0.990
	2	3	2.556	2.269	28.335	0.721	0.991
		5	3.920	3.436	23.833	0.442	0.983
		7	**2.165**	**1.775**	**10.688**	**0.108**	**0.997**
		9	2.844	2.461	35.646	0.827	0.995
dm /dt	1	3	0.068	0.148	26.090	0.493	0.905
		5	0.058	0.145	17.298	0.263	0.902
		7	0.054	0.147	20.492	0.370	0.910
		9	0.069	0.111	38.568	0.782	0.941
	2	3	0.066	0.117	36.801	0.677	0.937
		5	**0.052**	**0.126**	**15.287**	**0.172**	**0.993**
		7	0.060	0.147	17.325	0.195	0.897
		9	0.055	0.135	17.504	0.315	0.916
MR	1	3	0.032	0.028	64.022	2.291	0.995
		5	0.037	0.031	47.427	1.686	0.995
		7	0.022	0.016	15.407	0.375	0.996
		9	0.037	0.029	58.380	2.163	0.989
	2	3	0.023	0.021	36.129	1.580	0.994
		5	0.041	0.035	35.063	1.297	0.983
		7	**0.020**	**0.015**	**13.109**	**0.238**	**0.998**
		9	0.032	0.026	61.167	2.168	0.995

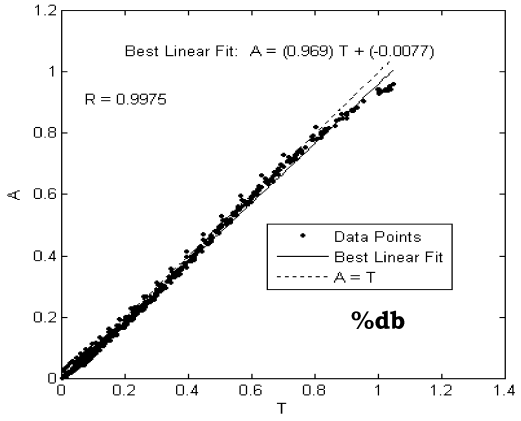

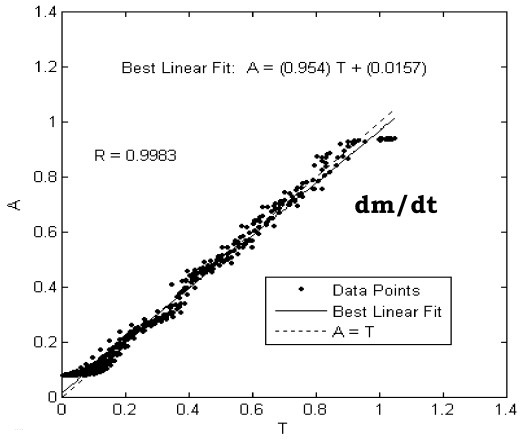

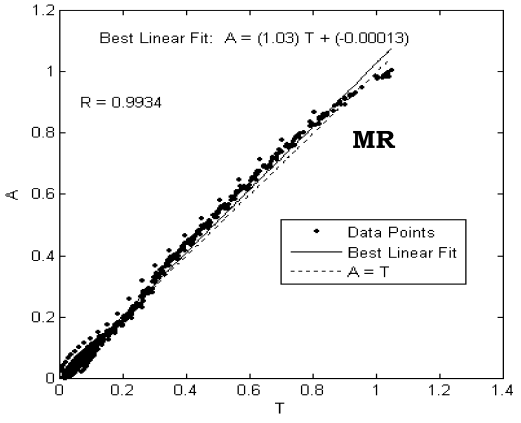

Figures 2 Correlation between predicted and experimental values using the optimal ANN (LPSSD)

REFERENCES

Mujmudar, A. S. 2006. "Some recent developments in drying technologies appropriate for postharvest processing." *Int. J. Postharvest Technol. and Innovation.* 1(1), 76-92.

Mujmudar, A. S. 2004a. "Role of International drying symposium in promoting innovation and global R & D effort in drying technologies." *Proceedings of the Fourteenth Int. Drying Symposium, Brazil.* 101-118.

Mujumdar, A.S. 2004b. "Research and developments in drying: recent trends and future prospects." *Drying Technol.* 22(1-2), 1-26.

Elustondo, D.; M.P. Elustondo; and M.J. Urbicain, 2001. "Mathematical modeling of moisture evaporation from foodstuffs exposed to subatmospheric pressure superheated steam." *J. Food Engng* 49, 15-24.

Susan, L. 1998. "Experts systems-what can they do for the food industry?" *Food Sci. and Technol.* 9, 3-12.

Borggard, C. and H.H. Thodberg, 1992. "Optimal minimal neural interception of spectra." *Anal. Chem.* 64, 545-551.

Kerdpiboon, S.; S.L. Kerr and S. Devahastin, 2006. "Neural network prediction of physical property changes of dried carrot as a function of fractal dimension and moisture content." *Food Research Int.* 39, 1110-1118.

BIOGRAPHY

The author was born in Fatehpur district of Uttar Pradesh, India. He passed his intermediate examination from Govt. Inter College, Fatehpur, Uttar Pradesh. He obtained his B. Tech. (Agricultural Engineering) degree from College of Agricultural Engineering and Technology, Orissa University of Agriculture and Technology, Bhubeneswar, Orissa and M. Tech. with major in Agriculture Process and Food Engineering from College of Technology, Gujarat Agriculture University, Junagadh, Gujarat. He completed his Ph. D. from G. B. Pant University of Agriculture and Technology, Pantnagar, Uttarakhand, India. Author worked as Academic Associate at Indian Institute of Management, Ahemedabad and presently working as Assistant Professor at A D Patel Institute of Technology, Anand, Gujarat. The author is a life member of Indian Society of Technical Education, Association of Food Scientists and Technologist (India) and Associate Member of Institution of Engineers.

SIMULATION TOOLS FOR FOOD ANALYSIS

Low-grade cane sugar crystallization. Study of the effects of operating conditions on the mass of crystal germs produced carried out by design of experiments

Brigitte Grondin-Perez, Michel Benne, Jean-Pierre Chabriat
Faculty of sciences and technology – Reunion Island University
15 ave René Cassin 97715 Sainte Clotilde Cedex
michel.benne@univ-reunion.fr

1. Introduction

At the Bois-Rouge factory, the crystallisation process is carried out using three massecuites scheme, known technically as jets A, B and C. Unlike the A and B sugars, the C sugar is not marketable. It is re-thickened and injected back into the factory circuit. The crystallisation of the third jet is therefore the last stage to allow the extraction of sucrose from the liquid phase. Any sucrose molecule left in liquid form after this last transformation is completely lost to the manufacturer, and so from an economic point of view, this last stage is extremely important.
A current methodology used in sugar industry to exhaust a sucrose solution consist in concentrating the solution to a particular state of super-saturation, sow it with a certain volume of slurry, and then allow their growth to obtain the C crystals.
Numerous works (Bonnecaze (2004)) have shown that the quality of the initial population of seed-crystals has a large impact on the yields from the C crystallisation process.

As part of the optimisation of the third jet crystallisation process at the Bois-Rouge sugar refinery, we have undertaken a study of the seeding phase, using a methodology of design of experiments. Our goal is to evaluate the influence of some parameters defining the operating conditions upon the mass of seed-crystals produced.

2. Study of the seeding phase. Methodology of experiment plans

The study of the seeding phase involves determining the importance of the main factors influencing the quality of the initial seed-crystals population. To measure the influence of the principal parameters which affect this quality, we chose a methodology based on design of experiments. These were carried out following a pilot study in the laboratory, which had the advantage of allowing experiments while varying several parameters. Industrial production constraints mean that these experiments cannot be carried out on site.

2.1 Factors and results of the experiment plans

During the seeding phase, the nuclei introduced into the supersaturated sucrose solution come together into seed-crystals. By considering this initial state, we performed a first study of the seed-crystals population by observing the principal factors likely to affect both their quantity and quality.
Numerous scientific works have investigated the initial seed-crystals population (Clériot (1993), Vaccari and Montovani (1995), Marchal (1989), Pautrat, Genotelle and Mathlouthi (1996), Lin, Siyuan, Bing (1998)). However, most of these studies were carried out on yields from the first jet, i.e. the results of A crystallisation. In the A jet, the quality of the initial population is best described in terms of crystal facies and size distribution: the standard deviation of this distribution should be as small as possible.
Any study of this kind has been lead in the field of C crystallisation

A study carried out in the laboratory consisted in using a methodology of design of experiments to highlight the influence of certain factors on the total mass of seed-crystals larger than 6 µm.
Earlier works (Cleriot, (1993)) have shown that for an optimal seeding of a sugar solution, the choice of seeding point, the granulation characteristics of the seed-germs introduced and the duration of the maturing (or stabilisation) period are all essential.

We set up an experiment plan based on the following three factors:

- F1 : the purity of the initial solution;
- F2 : the conductivity of the solution at the moment of seeding;
- F3 : the mass of slurry used.

The first two factors give information about the initial state when the slurry is added to the solution. The purity of the solution gives an appraisal of the matter involved, and F2 gives more information about the solution's super-saturation.

In order to study the impact of the seed-germs' granulation characteristics on the crystalline mass produced, it is necessary to have some seed samples in which a granulation criterion, such as the size of the micro-crystals, takes at least two different values. However, as measurements of granulation are generally found using statistics based on representative samples, it is practically impossible to guarantee that two samples possess the same granulation characteristics. For these reasons, we chose as criterion the mass of seed-germs introduced, at the expense of a granulation criterion.

The result Y from the plan is the crystalline mass obtained after centrifugation through a sieve which separates the mother-liquor from crystals with a diameter greater than 6 µm. It is therefore a number criterion which was chosen.

The initial solution, the magma, is a mixture of various products, and so its purity in the factory varies greatly. In the laboratory, it is easy to obtain a magma solution with defined purity criteria by mixing products taken on site.

Each experiment depends on the state of super-saturation of the solution. Seeding an under-saturated solution does not produce seed-crystals. Conversely, the labile supersaturated state of a sugar solution can promote primary nucleation, and generate micro-crystals of uncontrollable size. The generation of the initial population of micro-crystals must therefore be carried out while controlling the state of super-saturation in the solution.

In the sugar industry, the sucrose solution's electrical conductivity is used to indicate the level of super-saturation.

At Bois Rouge, by making the assumption that the mass by volume of the seed-germs is constant, the volume to be added for the growing phase is fixed by the vat. To test the impact of this initial volume on the production of seeds larger than 6 µm, we reproduced the operating conditions at Bois Rouge, by working with the same conditions of temperature and reduced pressure. The upper and lower values for each of the factors were chosen according to the different operational ranges used in the manufacturing process.

Table 2.1 below brings together all the experimental upper and lower values for each factor. We chose to test two different operating zones depending on the nature of the products used on site (variation range of the solution's conductivity). Two purity intervals are given because they correspond to different products. The variation in the slurry mass introduced was the same in each case.

	Pte_{PC} (%) Interval 1	Pte_{PC} (%) Interval 2	λ_{sol} (S/cm) Interval 1	λ_{sol} (S/cm) Interval 2	M_{sem} (g)
Level +1	83.8	87.7	550	550	40
Level -1	69.9	53.3	430	500	20

Table 2.1

Pte_{PC} : purity magma - λ_{sol} : conductivity of solution - M_{sem} : Mass of slurry

2.2 Experimental approach

A three factor plan is based on the completion of eight experiments. The experimental approach used to carry out each of these experiments is detailed in Table 2.2:

Phase 1	Introduction of 4l of the product	Purity factor -1/+1
Phase 2	Concentration of the solution	Conductivity -1/+1
Phase 3	Introduction of the slurry	Mass of slurry -1/+1
Phase 4	Maturation of the seed-crystals	Duration : 30 min
Phase 5	Measurement of the crystalline mass obtained after centrifugation	20 hours after seeding

Table 2.2

To guarantee a certain degree of homogeneity, the sampling was carried out on the same day, for each of the products.

Three complete plans were carried out using these samples:

- PE1 and PE3 involve the same products (interval 1 for the factor F1 : purity of magma), which we will list;
- PE2 involves interval 2 of the factor F1.

The ranges of the different factors are summarised in Table 2.3 :

PE1	**Level –1**	Molasses A	430 ($S.cm^{-1}$)	20 (g)
	Level +1	Liquor std	550 ($S.cm^{-1}$)	40 (g)
PE2	**Level -1**	Molasses A	500 ($S.cm^{-1}$)	20 (g)
	Level +1	Liquor std	550 ($S.cm^{-1}$)	40 (g)
PE3	**Level –1**	Molasses A	550 ($S.cm^{-1}$)	20 (g)
	Level +1	Liquor std	600 ($S.cm^{-1}$)	40 (g)

Table 2.3

The result Y of the experiments is the crystalline mass obtained by centrifuging a constant volume of massecuite ($900\,ml$). To describe the interactions between the factors and the response, and between the different factors, it is necessary to estimate the coefficients a_i of a polynomial expression, the first degree form of which is most often used:

$$Y = a_0 + a_1.F1 + a_2.F2 + a_3.F3 + a_{12}.F1.F2 + a_{23}.F2.F3 + a_{13}.F1.F3 + a_{123}.F1.F2.F3 \quad (1)$$

3. Results and future work

The matrix of the effects obtained from the various experiments in plans PE1, PE2 and PE3 is shown in Table 3.1 below:

	F1	F2	F3	PE2	PE1	PE3
Run n° 1	-1	-1	-1	678	474	479
Run n° 2	-1	+1	-1	614	546	410
Run n° 3	-1	-1	+1	694	579	380
Run n° 4	-1	+1	+1	617	325	351
Run n° 5	+1	-1	-1	749	560	460
Run n° 6	+1	+1	-1	710	420	325
Run n° 7	+1	-1	+1	840	493	522
Run n° 8	+1	+1	+1	702	411	405

Table 3.1 : matrix of the effects –Plans PE1, PE2, PE3

3.1. Results of plans PE1 and PE3

When studying the results obtained from PE1 and PE3, the most important problem identified was undoubtedly that of reproducibility. Indeed, the range of values of factor F2 includes a common limit for PE1 and PE3. For this limit, when the two other factors are identical, the runs were therefore carried out in similar conditions. Nevertheless, there is a non-negligible difference in the crystalline masses obtained in these conditions:

Runs	F1	F2	F3	Y_1 (PE1)	Y_2 (PE3)	Y_1-Y_3
E8(PE1)=E7(PE3)	69.9	550	40	411	522	-111
E6(PE1)=E5(PE3)	69.9	550	20	420	460	-40
E4(PE1)=E3(PE3)	83.8	550	40	325	380	-55
E2(PE1)=E1(PE3)	83.8	550	20	546	479	+67

Table 3.2

Further, a complete plan involves experiments spread over about ten days. As the products sampled for these plans were of the same nature, we conclude that the inconsistency in the observed results may be because refrigeration at 4°C is insufficient to stop bacterial activity. This would mean that during the storage period, alcohol fermentation reduced the sucrose concentration in the solutions, changing their purity.

The intermediate plan PE2 allows the analysis to be completed. In this last plan, the eight usual experiments are supplemented by two central points: the levels of each factor are chosen in the middle of each of the operational zones (level 0).

The matrix of the effects obtained and the operating conditions in plan PE4 is given in Table 3.5 below:

	F1	F2	F3	PE2
Run n° 1	-1	-1	-1	678
Run n° 2	-1	+1	-1	614
Run n° 3	-1	-1	+1	694
Run n° 4	-1	+1	+1	617
Run n° 5	+1	-1	-1	749
Run n° 6	+1	+1	-1	710
Run n° 7	+1	-1	+1	840
Run n° 8	+1	+1	+1	702
Central point 1	0	0	0	768
Central point 2	0	0	0	781

Table 3.5

The average effects of each factor are given in the table below:

	Mean effect	F1	F2	F3	Y
E1	-1	-1	-1	-1	678
E2	1	-1	1	-1	614
E3	1	-1	-1	1	694
E4	-1	-1	1	1	617
E5	1	1	-1	-1	749
E6	-1	1	1	-1	710
E7	-1	1	-1	1	840
E8	1	1	1	1	702
Average	-10.75	49.75	-39.75	12.75	

Table 3.6

For PE2, the refrigeration of the products at –18°C justifies the assumption that the purity of the products used did not vary. Indeed, the yield is higher than the crystalline mass produced in the previous runs, which confirms the deterioration of the products at 4°C.
The dominating effects of the initial solution purity and its electrical conductivity at the moment of seeding are shown in the table of mean effects, above. The results of PE2 are consistent with those of PE3.

3.2. Model identified using the results from PE2

To complete the analysis, a polynomial type model (Goupy (2001)), of first degree in each of the factors taken independently, was identified using the results from plan PE2 (see equation 1). The approximation of the parameters was carried out in the usual way, using measured factor-response pairs, and linear regression.

Three first degree models were identified by using the software MODDE. These models take into account the main factors and/or the interactions between these factors. In each case, the form of the model chosen as well as its associated correlation coefficient is given.

		F1	F2	F3	F1F2	F1F3	F2F3	
Model structure	a_0	a_1	a_2	a_3	a_4	a_5	a_6	correlation coefficient
without interactions with central points	715	50	-40	13	0	0	0	0.74
with interactions with central points	715	50	-40	13	-4.5	8	-14	0.77
with interactions without central points	700	50	-40	13	-4.5	8	-14	0.96

Table 3.7

Inspection of the correlation coefficients shows that the model which takes into account the interactions between factors, but not the central points, is the best. This model is given by the following equation:

$$Y = 700 + 50.F1 - 40.F2 + 13.F3 - 4,5.F1.F2 + 8.F1.F3 - 14.F2.F3$$

Inspection of the coefficients a_i in the model confirms that the three factors are significant, and that the most influential are the solution's conductivity and its purity. Among the interactions between factors, only that between the solution's conductivity and the seed-germ mass introduced is significant, although its impact is nonetheless limited.
This model calculates a crystalline mass of 700g when the factors are chosen in the middle of their operational zone. The difference between the model response and measurements is significant for the central points (about 10%). Several hypotheses might explain this phenomenon:

- the first relates to the reproducibility of the results, mentioned above;

- the second relates to the accuracy of the model, unsatisfactory for three reasons;

➡ to facilitate this first approach, the experiment plans were based on three factors, which do not provide a proper phenomenological description of the crystallisation process, which is complex in an impure environment;

➡ as the choice of three factors has been shown to be insufficient, other influential factors should certainly be taken into account, in particular the viscosity of the reactive mixture;

➡ the choice of model structure (first degree) is perhaps too simple to reach a satisfactory level of precision.

4. Conclusion

Our objective is to find the optimal operating conditions for generating an initial population of crystals-seed, with precise characteristics, in order to improve yields from the crystalline growth phase. A first approach which involved using a methodology of experiment plans to identify a linear relationship, allowed us to quantify the impact of three factors on the crystalline mass produced, under certain conditions. However, the model derived exhibits some inaccuracies. In order to improve it, we plan to carry out further experiments which will reveal more central points, while taking into account at least one more factor which affects the crystallisation phenomenon, namely the solution's viscosity.

5. References

Bonnecaze, C.,(2004)
Cristallisation C en sucrerie de canne : modélisation de la pureté liqueur-mère et étude de l'ensemencement
Thèse de Doctorat, Université de La Réunion, La Réunion.

Clériot, J. (1993)
La sucrerie vue au microscope
IAA,(Industrie Agro-Alimentaire).

Goupy, J.,(2001)
Introduction aux plans d'expériences
2nde édition, Industries et Techniques,
série : Conception, Dunod, Paris.

Grondin-Perez, B.,Benne, M., Chabriat, J.P., (2006)
Supervision of C crystallisation in Bois Rouge sugar mill using on-line crystal content estimation using synchronous microwave and refractometric brix measurements, pp 639-645, vol(76),
Journal of Food Engineering.

Lin, L., G. Siyuan, L. Bing,(1998)
Microwave enhancement of sucrose crystal growth
1998, vol. 100, n° 1200, p. : 593-596, International Sugar Journal.

Marchal, P.,(1989)
Génie de la cristallisation – Application à l'acide adipique
Thèse de doctorat, Institut National Polytechnique de Lorraine, Nancy.

Pautrat, C., J. Genotelle, M. Mathlouthi, (1996)
Croissance des cristaux de saccharose en présence d'impuretés macromoléculaires : un moyen de contrôle de la qualité du sucre blanc
In proceedings of the 3ième symposium de Adrew van Hook Association : Sugar Crystallisation.

Vaccari, G., G. Mantovani, (1995)
*La cristallisation du saccharose (*p. 35-78)
dans Le saccharose - propriétés et applications, M. Mathlouthi et P. Reiser-Editions Polytechnica,

Determination of dielectric parameters of frozen materials via reverse technique

S. Curet, O. Rouaud, L. Boillereaux

GEPEA, UMR CNRS 6144, ENITIAA, rue de la Géraudière, BP 82225, 44322 Nantes

INTRODUCTION

Microwave heating is used in various processes of the food industry, as drying, tempering, thawing and heating. Numerous works related in the literature deal with modelling of drying processes [1-3] or heating ones [4,5]. The literature is however more limited concerning thawing. The main problem of microwave thawing comes from the existence of hot spots leading to temperature heterogeneities [6,7]. It constitutes a brake to a larger development of this technology in food industry, despite its great interest in terms of flexibility.

These hot spots are due to resonance phenomena in the frozen phase of foods. These resonances can be observed when the penetration depth is larger than the thickness of the sample to treat. This penetration depth increases when dielectric properties are small, which is thus observed with frozen materials.

In order to develop accurate simulators allowing to improve microwave thawing processes, it is necessary to have a good estimation of the dielectric properties (loss factor and permittivity) especially in the frozen phase. In this study, we propose to determine these parameters using reverse approaches.

MATERIAL AND METHODS

The experimental apparatus is a microwave system (figure 1), supplying a monochromatic wave in the fundamental mode, denoted $TE_{1,0}$, operating at a frequency of 2.45GHz. Microwave energy is transmitted along the z-direction of a rectangular wave guide (section 86mm×43 mm). The sample (84mm×41mm×50 mm) fills the guide. A layer of polystyrene, sufficiently thin (1mm) to neglect its effects on the electric field, is inserted between the walls and the product to limit the heat losses. In the same way, the guide is covered by insulating foam. The sample rests on a polystyrene plate to consider only one convective exchange in the upper surface. To ensure that only a minimal amount of microwave is reflected back to the sample, a water load is fixed at the end of the guide. The incident power at the upper surface of the food sample is measured. The considered sample is a block of tylose made of methylcellulose (Methocel® A 4MFG, DOWChemicals) in which the temperature is measured in three locations using optical fibre sensors (LUXTRON Fluroptic Thermometer, model 790, accurate to ±0.5°C). The tylose under consideration is 50mm thick and is composed of water (86.6%), methyl cellulose (13%) and salt (0.4%). Tylose is widely used as an experimental material in food-related research. Experiments are made in frozen zone with microwave power input fixed at 500W. The initial temperature of sample is approximately -20°C.

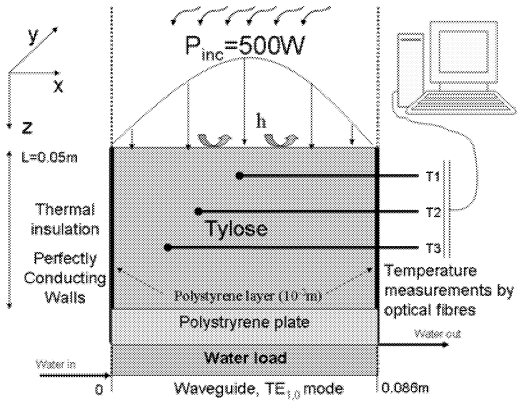

Figure 1. Schema of the experimental apparatus

DESIGN OF THE SIMULATOR

Heat transfer model

In order to analyze the process of heat transport due to microwave heating of a block of tylose, the following assumptions are introduced:

Assumption 1: The product receives the electromagnetic waves by the upper surface.

Assumption 2: The product is homogeneous and isotropic.

Assumption 3: The thermophysical and dielectric properties are temperature dependent.

Assumption 4: The mass transfer is negligible.

Assumption 5: The lateral and lower surfaces of the product are perfectly insulated.

Assumption 6: The initial temperature of the food sample is homogeneous.

Heat transfer is based on the generalised heat equation which depends on thermophysical properties of the product, as follows:

$$\rho Cp_{app}\frac{\partial T}{\partial t} = div.(k\nabla T) + Q_{abs} \quad (1)$$

The effective heat capacity method, that requires a single energy balance equation, has proved to be reliable for studying phase change in multicomponent materials such as food materials [6,8]. It consists in using an effective heat capacity for the entire domain.

Into the general heat equation, Q_{abs} denotes the internal heat generation source term and quantifies the amount of power which is dissipated into the product by dielectric losses. In order to evaluate this source term, the electromagnetic field is solved into the product according to the theory of Maxwell's equations. The governing equations for a propagating electromagnetic wave in differential form are:

$$\nabla \times H = \frac{\partial D}{\partial t} + J = \frac{\partial \varepsilon E}{\partial t} + \sigma E \quad (2)$$

$$\nabla \times E = -\frac{\partial B}{\partial t} = -\frac{\partial \mu H}{\partial t} \quad (3)$$

$$\nabla.D = \nabla.\varepsilon E = \rho_e \quad (4)$$

$$\nabla.B = \nabla.\mu H = 0 \quad (5)$$

with

$$J = \sigma(\omega)E(t), \quad D = \varepsilon(\omega)E(t) \quad \text{and} \quad B = \mu(\omega)H(t)$$

$\varepsilon = \varepsilon' - j\varepsilon''$ is the complex permittivity, ε' is the dielectric constant and ε'' is the dielectric loss factor with $j^2 = -1$. The permeability μ may be represented by $\mu_0 = 4\pi \times 10^{-7}$ H.m^{-1}, the permeability of vacuum [9]. In practice, we limit ourselves to time-variant fields following a harmonic law, with a pulsation $\omega = 2\pi f$, where f is the frequency of the wave.

In our case, the fundamental mode, that is $TE_{1,0}$, is considered. It means that the electric field is in the (xOy) plane with only a component E_y.

In $TE_{1,0}$ mode [10], considering a rectangular guide filled by a homogeneous dielectric, the E_y component of the electric field is straightforwardly obtained from the resolution of Maxwell's equations :

$$E_y = E_0 \sin\left(\frac{\pi x}{a}\right) \quad (6)$$

In this study, we propose to solve the model using COMSOL®, release 3.3, where the resolution of Maxwell equations is coupled to the heat transfer resolution via a finite elements scheme. More details concerning the numerical resolutions can be found in [14].

Into the heat transfer equation, the source term is computed from the knowledge of the local electric field as follows [9]:

$$Q_{abs} = \omega.E_{rms}{}^2.\varepsilon_0.\varepsilon'' \quad (7)$$

This source term depends explicitly of the loss factor, and implicitly of the dielectric permittivity because E_{rms}^2 depends on ε'. In the sequels, we will consider that, on the temperature range considered for the experiments, ε' is constant and ε" is an exponential function of temperature:

$$\varepsilon'' = \alpha \cdot \exp(\beta T) \quad (8)$$

Let us denote p the vector of parameters to estimate using reverse approach:

$$p = \begin{bmatrix} \varepsilon' \\ \alpha \\ \beta \end{bmatrix}.$$

Initial and Boundary conditions

As initial condition, the material is assumed to be at uniform temperature T_0. Convective coefficient h=10W.m^{-2}.K^{-1} is due to natural convective flux at the upper surface of the product. Walls of the wave guide are thermal insulated. Mathematically, the initial and boundary conditions can be written as:

$$\begin{cases} T = T_0 & at\ t = 0,\ \forall x\ \forall z \\ k\dfrac{\partial T}{\partial z} = h(T - T_\infty) & at\ z = 0, \forall x \\ k\dfrac{\partial T}{\partial z} = 0 & at\ x = 0, x = a, \forall z \\ k\dfrac{\partial T}{\partial z} = 0 & at\ z = L, \forall x \end{cases} \quad (9)$$

Walls of the wave guide are perfect electric conductors. Incident electromagnetic wave is applied at the top of the product. Wave reflection between the air medium and the surface of the product is directly computed according to the theory of Maxwell's equations. At the end of the rectangular wave guide, the resulting electromagnetic wave exits the guide without any reflection.
The initial and boundary conditions can be written as:

$$\begin{cases} E_y = E_0 \sin\left(\dfrac{\pi x}{a}\right) & at\ z = 0, \forall x \\ E_y = 0 & at\ x = 0, x = a, \forall z \end{cases} \quad (10)$$

REVERSE APPROACH

Let us denote Y the observation vector, composed by the measurements obtained from the 3 optical fibres as illustrated on figures 1 and 2:

$$Y = {}^t\left[T_1 \quad T_2 \quad T_3\right] \quad (11)$$

The observations are done at regular sampling period. Let us denote Y_{exp} the observations realized on the whole experiment time, from t_{init} to t_{final}:

$$Y_{\exp} = {}^t\left[Y(t_{init}) \quad Y(t_{init} + t_s) \quad Y(t_{init} + 2t_s) \quad \cdots \quad Y(t_{final})\right]$$

Y_{model} is the corresponding values of temperatures T_1 to T_3 issued from the simulator.

Let us denote p_{opt} the optimal parameters vector such as:

$$p_{opt} = \arg\min J(p) \quad (12)$$

where

$$J(p) = {}^t\left[Y_{\exp} - Y_{\mathrm{mod}el}\right] \cdot \left[Y_{\exp} - Y_{\mathrm{mod}el}\right] \quad (13)$$

We propose to estimate p_{opt} using the well-known Levenberg-Marquardt methodology [11], which is implemented in Matlab®. Due to the strong non linearity of the model, the gradient of the criterion is estimated during optimization procedure via finite differences. The routine implemented in Matlab® supplies an estimation of the Hessian at the optimum, but the quality of this estimation is highly bound to the consistency of the algorithm. For this reason, it is proposed here to compute the Hessian at the optimum with the following approximation:

$$\nabla^2 J(p_{opt}) \approx {}^t\left[\frac{\partial Y_{\mathrm{mod}el}}{\partial p}\right] \cdot \left[\frac{\partial Y_{\mathrm{mod}el}}{\partial p}\right] \quad (14)$$

To obtain the Hessian matrix, small variations δp (about 1%) can be applied on the 3 parameters of p to compute

$$\left[\frac{\partial Y_{\mathrm{mod}el}}{\partial p}\right] \approx \frac{\Delta Y_{\mathrm{mod}el}}{\delta p} \quad (15)$$

The knowledge of the Hessian at the optimum allows computing a standard deviation for each estimated parameter, provided that the standard deviation of the measurements is known.
For the i^{th} estimated parameter, it can be calculated as follows [12]:

$$\sigma_i = \sigma_{\exp} \sqrt{\frac{\det\left[\nabla^2_{ii} J(p_{opt})\right]}{\det\left[\nabla^2 J(p_{opt})\right]}} \quad (16)$$

$\sigma_{\exp}$ is the standard deviation of the experimental measurements, and $\nabla^2_{ii} J(p_{opt})$ is the Hessian matrix deprived of the i^{th} line and i^{th} column.
This expression is equivalent to compute the covariance matrix $\left[\nabla^2 J(p_{opt})\right]^{-1}$ and to consider the square roots of its diagonal terms multiplied weighted with $\sigma_{\exp}$.

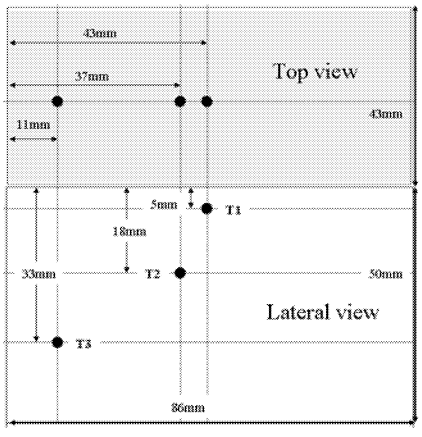

Figure 2. locations of the experimental measurements

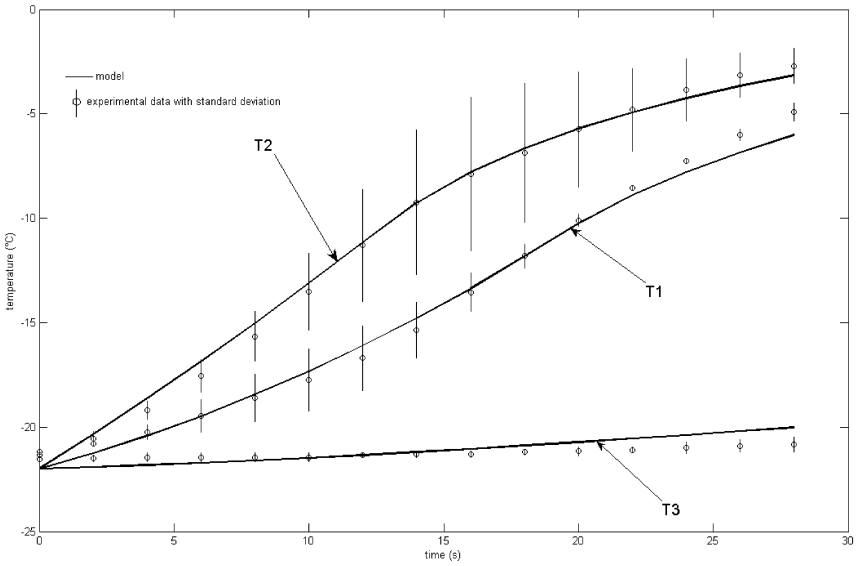

Figure 3. Experimental and model temperatures with optimal parameters. P_{inc} = 500 W

EXPERIMENTAL RESULTS

In this study, we have proceeded to 10 experiments in similar conditions:

- initial temperature close to -21°C,
- microwave power of 500 W,
- optical fibres located at the same positions, as illustrated on figure 2.

However, optical fibres are particularly difficult to introduce into the frozen product with a good accuracy. The consequence is an important sensitivity of the temperature measurements, especially at the neighbourhood of resonance spots. For this reason, on figure 3 are represented the mean values of temperatures (circles) and their respective standard deviations (vertical bar).

Considering all the experiments, the standard deviation of the output vector Y has been established: $\sigma_m = 0.85$

During the optimization procedure, the mean values of experimental temperatures have been considered. The optimization has been repeated using several set of initial parameters in order to avoid local minima.

The optimal parameters obtained are:

$$p_{opt} = \begin{bmatrix} 5.469 \\ 3.88 \cdot 10^{-9} \\ 0.072 \end{bmatrix}$$

The temperatures T_1 to T_3 issued from the model with p_{opt} are illustrated by continuous lines on figure 3.

It is now proposed to evaluate the relevance of the methodology by comparing with experimental results published in [13], with the same product, but in different experimental conditions:

- microwave power of 1000 W
- optical fibres located at different positions, as illustrated on figure 4.

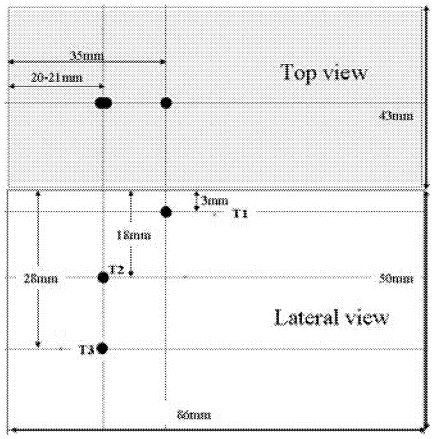

Figure 4. locations of the experimental measurements. From [13]

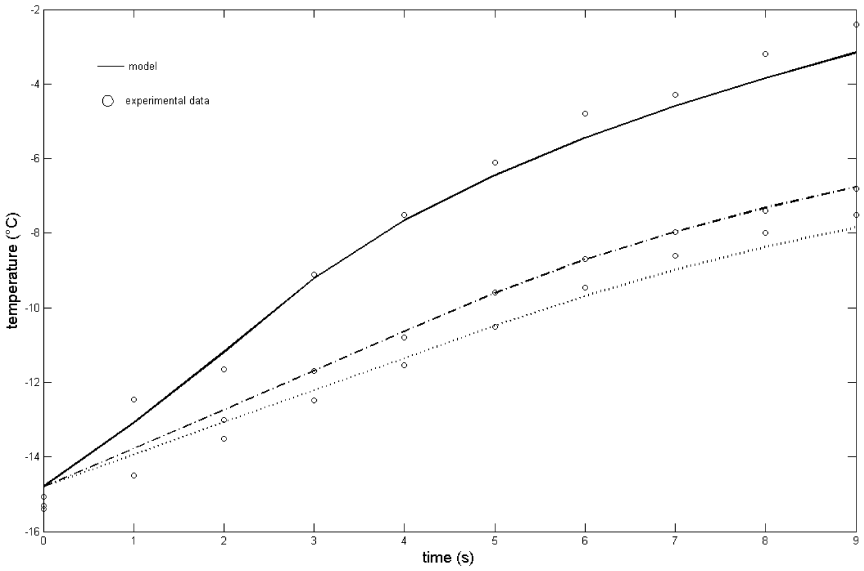

Figure 5. Experimental and model temperatures with optimal parameters. P_{inc} = 1000 W. From [13]

Concerning the minimization procedure, the estimation of the Hessian at the optimum leads to:

$$\nabla^2 J(p_{opt}) = \begin{bmatrix} 7.2\cdot10^{2} & 2.29\cdot10^{11} & 2.34\cdot10^{5} \\ 2.29\cdot10^{10} & 1.05\cdot10^{20} & 1.03\cdot10^{14} \\ 2.34\cdot10^{5} & 1.03\cdot10^{14} & 1.03\cdot10^{8} \end{bmatrix}$$

Finally, equation (16) allows evaluating the standard deviation of each parameter:

$$\sigma_1 = 0.07; \sigma_2 = 0.93\cdot10^{-9}; \sigma_3 = 0.001$$

These standard deviations show that, despite a large uncertainty on temperature measurements due to problems of repeatability, the dielectric permittivity can be estimated with a very good accuracy. Indeed, it can be noticed that $\sigma_1 << \varepsilon'_{opt}$

On the contrary, the loss factor, obtained with equation (8) with T in Kelvin, is estimated with a large uncertainty, as illustrated on figure 6.

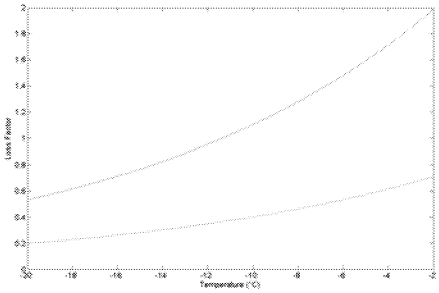

Figure 6. Uncertainty on estimated loss factor

Some general indications can be deduced from these experiments. It appears that, as illustrated on figure 3, a measurement at the neighbourhood of a resonance point leads to a large standard deviation, due to the large sensitivity to the position of the sensor. Nevertheless, such a measurement is particularly sensitive to the electric field distribution, and thus allows evaluating with a good accuracy the dielectric permittivity, whose electric field depends directly.
On the contrary, this measurement uncertainty leads to a very bad estimation of the loss factor.

A good recommendation to correctly estimate the dielectric properties would be to proceed in two steps: (i) estimation of the vector parameters p with measurements located close to the resonance points (the resonance points are not a priori known, and a try-and-error procedure is necessary), (ii) adjustment of the loss factor with measurements effected far from the resonance points, with a small uncertainty on experimental data.

CONCLUSION

In this paper, we have proposed to estimate via reverse techniques the dielectric properties of frozen material. The approach presented allows first to estimate loss factor and permittivity, but also to evaluate standard deviations for the estimated parameters.
A set of experiments have been used for the minimization procedure and the standard deviations evaluation. The obtained optimal parameters have

been implemented in a simulator. Temperatures issued from this simulator have been compared with experimental data issued from works previously published and in different conditions.
The results obtained have shown a good adequacy between model and experiment.
The computation of standard deviations for the estimated properties has highlighted the difficulty to estimate the loss factor with a good accuracy, while the dielectric permittivity can be evaluated with a small uncertainty.
Finally, some recommendations to evaluate dielectric properties of frozen material (that is, with the presence of resonant mode), have been proposed.

REFERENCES

[1] E.C.M. Sanga, A.S. Mujumdar, and G.S.V. Raghavan, Simulation of convection-microwave drying for a shrinking material, *Chem. Eng. Process.*, 41 (6) (2002) 487-499.

[2] H. Feng, Analysis of microwave assisted fluidized-bed drying of particulate product with a simplified heat and mass transfer model, *Int. Commun. Heat Mass*, 29 (8) (2002) 1021-1028.

[3] P. Salagnac, P. Glouannec, and D. Lecharpentier, Numerical modeling of heat and mass transfer in porous medium during combined hot air, infrared and microwaves drying, *Int. J. Heat Mass Tran.*, 47 (2004) 4479-4489.

[4] V.R. Romano, F. Marra, and U. Tammaro, Modelling of microwave heating of foodstuff: study on the influence of sample dimensions with a FEM approach, *J. Food Eng.*, 71 (3) (2005) 233-241.

[5] P. Rattanadecho, The simulation of microwave heating of wood using a rectangular wave guide: Influence of frequency and sample size, *Chem. Eng. Sci.*, 61 (14) (2006) 4798-4811.

[6] B.J. Taher and M.M. Farid, Cyclic microwave thawing of frozen meat: experimental and theoretical investigation, *Chem. Eng. Process.*, 40 (4) (2001) 379-389.

[7] C.M. Liu, Q.Z. Wang, and N. Sakai, Power an Temperature distribution during microwave thawing, simulated by using Maxwell's equations and Lambert's law, *Int. J. Food Sci. Tech.*, 40 (2005) 9-21.

[8] T. Basak and K.G. Ayappa, Analysis of Microwave Thawing of Slabs with Effective Heat Capacity Method, *AICHE J.*, 43 (1997) 1662-1674.

[9] J.E. Lanz, A numerical model of thermal effects in a microwave irradiated catalyst bed, Virginia Polytechnic Institute and State University, Blacksburg, Virginia, 1998, 113.

[10] L. Outifa, Contribution au génie de l'élaboration par micro-ondes de matériaux composites à matrice polymère de dimensions supérieures à la longueur d'onde, Université Pierre et Marie Curie, Paris, 1992, 190.

[11] D.W. Marquardt, An algorithm for least-squares estimation of non-linear parameters, *Journal of the Society for Industrial and Applied Mathematics*, 11 (2) (1963) 431-441.

[12] W.H. Press, B.P. Flannery, S.A. Teukolsky, and W.T. Vetterling, *Numerical Recipes the art of scientific computing*, Cambridge University Press, (1988).

[13] E. Akkari, S. Chevallier and L. Boillereaux, A 2D non-linear "grey-box" model dedicated to microwave thawing: theretical and experimental investigation, *Computers and Chemical Engineering*, 30 (2) (2005) 321-328.

[14] Curet S., Rouaud O., and Boillereaux L., Microwave tempering and heating in a single-mode cavity: Numerical and experimental investigations, Chemical Engineering and Processing: Process Intensification, In Press, Corrected Proof.

MODELLING AND SIMULATION IN FOOD SCIENCES AND FOOD ENGINEERING

MODELLING AND SIMULATION OF BAKERY PRODUCTION LINES FOR PROCESS ANALYSIS AND OPTIMIZATION

Walid Hussein, Florian Hecker, Martin Mitzscherling, Thomas Becker
FG Prozessanalytik und Getreidetechnologie, Universität Hohenheim
Garbenstraße 23, D-70599 Stuttgart, Germany
E-mail: {whussein|heckerfl|mitzsche|tb}@uni-hohenheim.de

KEYWORDS
Computer-aided analysis, Decision support systems, Model design, Optimization, Performance analysis.

ABSTRACT

Most bakeries work on a suboptimal level concerning utilization of devices, energy consumption and staff allocation. That results in "bottle-necks", operation problems, and not achieving the best possible profits. In order to detect these suboptimal processes, it is advantageous to use virtual models. Once created, these models behave like the real system. Thus, they will provide a possibility to predict the changes that may occur to the real production, if the specifications of the production elements are changed. Furthermore, the models can provide a very detailed look on the production flows, which helps to find and eliminate inefficient production schemes and "bottle-necks". Therefore, they provide a powerful tool for production planning.

1. INTRODUCTION

Although there are many software programs which are built for simulation of the industrial processes, such like SIMBAX, SIMPLORER, DELMIA, FLEXSIM, and ARENA, applications of modelling and simulation in baking production processes are rare. (Kelton 2004) presented the concepts and methods of simulation using Arena as a carrier to help the modeller reach the ability to carry out effective simulation modelling. Arena is based on the SIMAN modelling language, and has an object-oriented design and the ability to be tailored to any application area. Some simulation examples at which Arena is successfully implemented are contact centers, auto manufacturing plant, bank facilities, and airport operations. (Balci 1990; and Banks 1999) focused on verification and validation of the model as the most important element. Their aim was to certify the model's accuracy when used to predict the performance of the real-world system that it represents, or to predict the difference in performance between two scenarios or two model configurations. (Shannon 1998) cited the "40-20-40 Rule". This rule states that 40 percent of the effort and time in a project should be devoted to the understanding of the problem, goals, boundaries and collecting data. The next 20 percent is to the formulation of the model in an appropriate simulation language, and the remaining 40 percent to the verification, validation and implementation. (Greasley 2003) noted that simulation is best suited to systems that do reach equilibrium, meaning that the stability of the process needs to be considered before simulation is used. The author also mentioned the importance of the visual animated display as a communication tool to facilitate discussion and development of new ideas. Furthermore, (Goldsmann 1992) presented a reasonable proposal to analyze the simulation results. Obviously, all the previously mentioned simulation software, modelling techniques and simulation analysis algorithms, may be applied to the case of bakery production lines. To our knowledge, the simulation as an effective tool for the production planning and management is still not commonly implemented in bakeries, though.
This paper displays the current research on modelling and simulation of baking processes, with the solution of the processing problems and optimization of the production plans. A procedure combining elements of Banks and Shannon would be used in this study. In this study, we choose the production line of a small bakery that produces ten kinds of products as a working example, and its baking processes are modelled using Arena. The modelled processes are connected to figure out the proposed production line. The production line is simulated to validate the process inputs/outputs with respect to the real bakery production line's data. Once the validation is performed successfully, the analysis of the simulation data is possible, and the possibilities to optimise the process are investigated.

2. MATERIAL AND METHOD

To model the production line and obtain efficient processes simulation and consequently processes optimization, the procedure is initiated by collecting the bakery data. This data is collected for one shift period which starts at 1:00 and ends at 7:10. The next step is to formulate the model and simulate it, followed by validation of the simulation results with respect to the real data, after which these results are used for analysis and optimization purposes.

2.1 Production Line Data

The production line data includes the bakery products, the required ingredients, the utilized devices (Table 1), and the workers responsibilities (Table 2).

Table 1: The utilized devices in the bakery production line.

Device Name	No. of Items
Mixer	2
Dough Divider	1
Forming Machine (Depositor)	1
Dough Retarder (Fermentation Interruption)	1
Dough Proofer	2
Rack Oven	1
Tunnel Oven	1

The number of workers on the workbench (to form the dough) is three, one of them is also charged to mix the ingredients. Thus, during the mixing period there will be only two bench workers. One worker is required to transport the products between baking processes and another worker for the final products' packaging.

Table 2: The workers allocation, numbers and salaries during one shift period.

Worker Task	No.	Worker Salary (per hour)
Dough Forming on Bench	2	x
Dough Mixing and Dough Forming Assistance	1	1.1 * x
Products Transportation among Devices	1	0.2 * x
Packaging	1	0.5 * x

As shown in Figure 1, the production plan clarifies the processes that each product will go through on the production line during the shift period, starting from the dough mixing process up to the products shipping process. Two products (Multigrain rolls and poppy seed rolls) terminate their processing path at "Dough Retarder", to be baked in the following shift period.

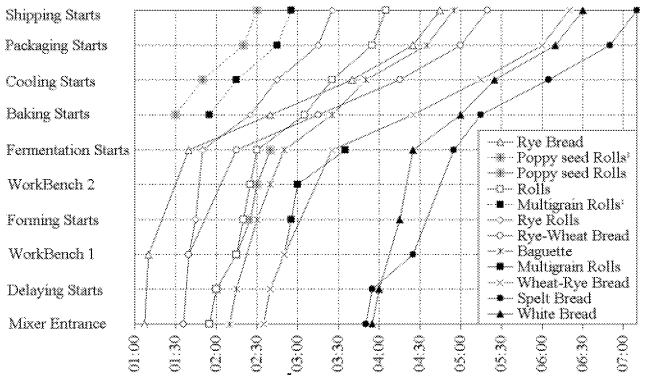

Figure 1: The time plan for one shift period explains the stages that products will follow on the production line.

2.2 Production Line Modelling And Simulation

Arena is an advanced software program that provides an interactive environment for graphically animating, verifying and analyzing simulation models. Within Arena's building area, the bakery production line model is generated using modules. Each module is programmed to represent a certain production line process. For example: the "Tunnel Oven" module (in Fig. 2) contains all required information about the baking process in the tunnel oven. In addition, some attributes are assigned in the beginning of the model as properties attached to the specified product. Such like "Rye Bread.Baking Period" which is an attribute that refers to the baking time necessary. Some decision modules (e.g. Ovens Distributer) are also used to spread out the products to their consequent process units (modules). Figure 3 is a screen shot of a production line simulation, illustrating the flow of products along production devices.

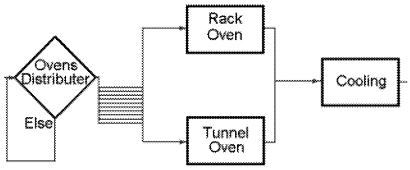

Figure 2: Production line modelling (distribution of products to ovens)

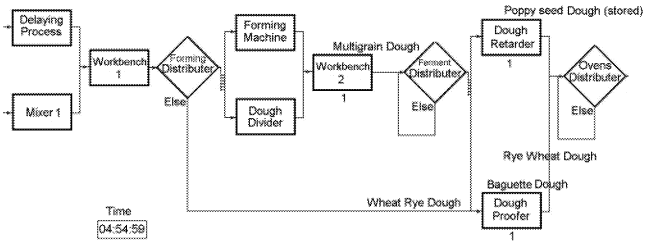

Figure 3: A capture of a part of the production line during simulation

3. RESULTS OF THE SIMULATION

Once the simulation results are validated with the real production line data, we can rely on them to analyze and optimize the production line processes. Figure 4 shows some of the simulation results. The rack oven (Fig. 4(b)) is idle for 55 minutes out of its 185 total working minutes (it is shut down from 4:00 up to 4:50), totally this wastes about 30% of its energy. "Tunnel Oven", "Dough Retarder" and "Dough Proofer" can be occupied with more than one product at the same time. Instead, the tunnel oven contains only one product for 170 minutes out of its 205 total working minutes (Fig. 4(c)). Meanwhile, the dough proofer

contains only one product for 125 minutes out of its 215 total working minutes. Moreover, workbench schedule (Fig. 4(d)) places its workers free for 50 minutes in the middle of the shift period, which is a quite long break compared to their 174 total actual working minutes. Finally, the "Multigrain Rolls" dough waits for 25 minutes before being processed in the "WorkBench 2", after being formed in "WorkBench 1" and "Dividing Machine". This waiting period is too long for a pre-formed dough.

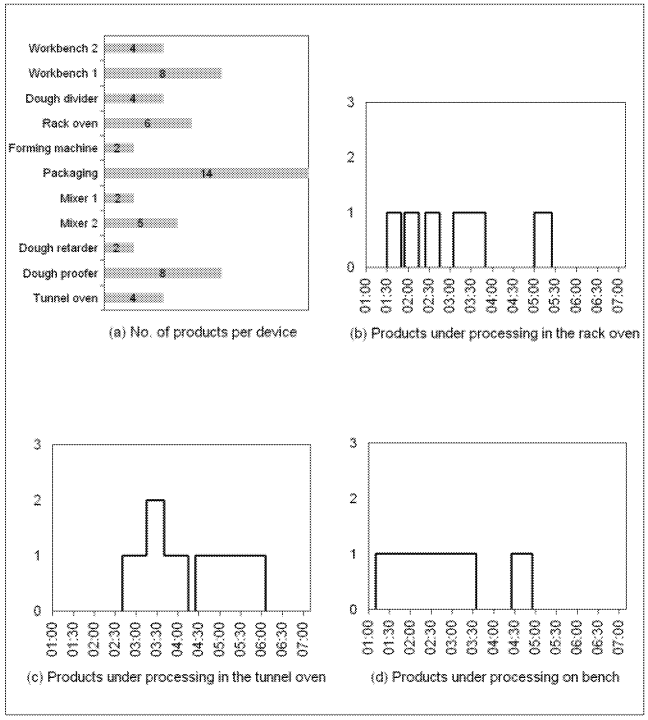

Figure 4: Simulation results for some production line devices utilization

4. PRODUCTION LINE OPTIMIZATION

The above observations imply that the real production line is operated with a suboptimal production plan, and it is preferable to design a more effective production plan that reduces the wasted times and the wasted energy. Using the production line model, it is simple to modify the production plan, and instantaneously observe the responses on the simulation results. After some iteration, we reach a more qualified production plan as in Figure 5.

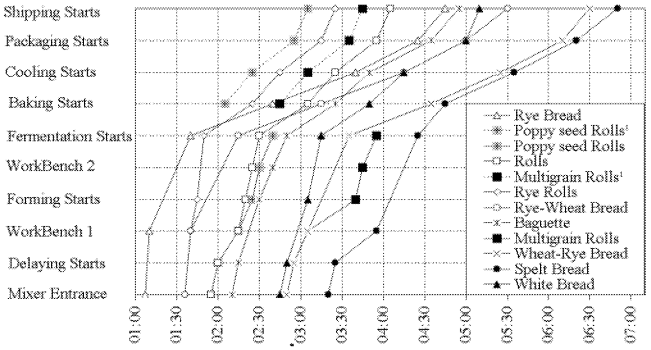

Figure 5: The optimized time plan for one shift period explains the stages that products will follow on the optimized production line.

By rescheduling the production plan of some products (Fig. 6(a)), the idle utilization time gaps of "Rack Oven" are removed, and it is fully occupied through its 130 working minutes.

As for the bench workers schedule, we can reorganize their break to start at 2:50 for 15 minutes, and continue working for 35 minutes. Then they are given another break for 5 minutes, and continue working for the last 40 minutes. This is applied in Figure 6(b) through rescheduling some more products.

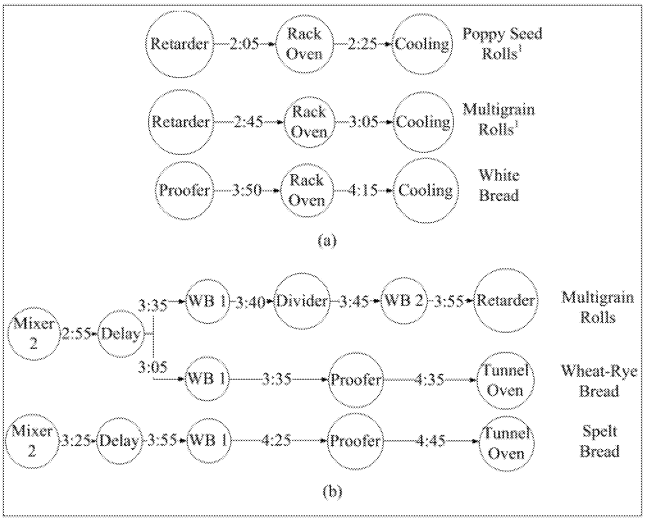

Figure 6: The new, optimized schedule of some products

Rescheduling of those products' production plan will also decrease the working time of the "Tunnel Oven" and "Dough Proofer". This is achieved by increasing the rate of their processing products per time, to be more than one when applicable. Additionally, "Multigrain rolls" will be no longer delayed before being processed in "WorkBench 2".

5. CONCLUSION

Simulation of the Bakery production line presents a good opportunity to optimize the processes and save the energy consumed of the production devices. Furthermore decreasing the working period of the workers on the production line, saves extra salary, or at least will make the workers free for other bakery tasks. Figure 7 shows a comparison in devices utilization and workers allocation, between the real production line and the optimized one.

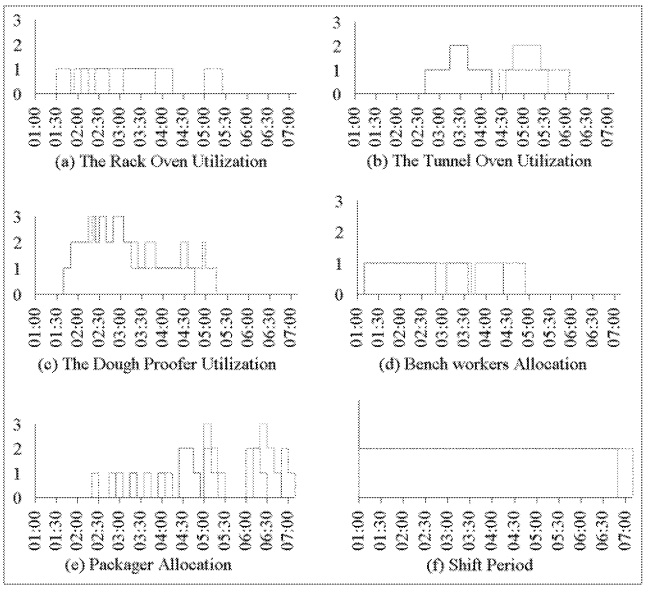

Figure 7: Comparison in resources management before optimization (dotted line) and after optimization (solid line)

From (Fig. 7(a, b and c)) the energy consumptions of "Rack Oven", "Tunnel Oven" and "Dough Proofer" are reduced by 30%, 15% and 14%, respectively. On the other hand, Fig. 7(d and e) show that the total working times of the bench and packaging workers are reduced by 30 and 55 minutes, respectively. The saved workers time can be fulfilled in other tasks or saving 13% of the bench workers salary and 19% of the packaging worker salary.

Finally, the packaging process terminates at 6:50 rather than 7:10, reducing the total shift period by 20 minutes, and the products are ready for shipping at an earlier time. (Table 3) summarizes the optimization results in comparison to the actual results.

Table 3: Comparison in the working times (in minutes) before and after optimization. E_2, S_2 and T_2 symbolize energy consumption, workers salary and shift period after optimization, respectively. E_1, S_1 and $T_1$are for the case before optimization.

Production Line Item	Real Plan	Optimized Plan	Conclusion
The Rack Oven	185	130	$E_2 = 0.70\ E_1$
The Tunnel Oven	205	175	$E_2 = 0.85\ E_1$
The Dough Proofer	215	185	$E_2 = 0.86\ E_1$
Bench Workers	225	195	$S_2 = 0.87\ S_1$
Packager	290	235	$S_2 = 0.81\ S_1$
Shift Period	370	350	$T_2 = 0.95\ T_1$

6. FURTHER IMPLICATIONS

The upcoming step to this research is to create a generalized simulation and optimization tool for bakery production lines with an implemented user friendly graphical interface (GUI). This tool will allow the user to define and save the production line data, simulate the generated production line model, analyze and optimize the simulation results.

7. REFERENCES

Balci, O., (1990), "Guidelines for Successful Simulation studies", *Proceeding of the 1990 Winter simulation Conference*, O. Balci et al. (eds.), pp. 25-32.

Banks, "Introduction to Simulation", in *Proceedings of the 1999 Winter Simulation Conference,* Phoenix, Arizona, December 5 – 8, www.informs-cs.org/wscpapers.html.

Goldsmann, D., (1992), "Simulation Output Analysis", *Proceedings of the 1992 Winter Simulation Conference*, J. J. Swain et al. (eds.), pp. 97-103.

Greasley, "Using Business-Process Simulation within a Business Process Reengineering Approach", *Business Process Management Journal,* Vol. 9 (2003), No. 4, 408-420.

Kelton, R. P. Sadowski and D. T. Sturrock, (2004), "*Simulation with Arena"*, 3rd ed., McGraw-Hill, New York, NY.

Shannon, "Introduction to the Art and Science of Simulation", in *Proceedings of the 1998 Winter Simulation Conference,* Washington, D.C., December 13 – 16, www.informscs.org/wscpapers.html.

SANDWICH BREAD COOLING

Jean-Yves Monteau
GEPEA, UMR CNRS 6144
École Nationale d'Ingénieurs des Techniques des Industries Agricoles et Alimentaires
rue de la Géraudière, B.P. 82225, 44322 Nantes cedex 3, France
E-mail: monteau@enitiaa-nantes.fr

KEYWORDS
Sandwich bread, Cooling, Model

ABSTRACT

Post baking bread cooling was not very studied until now. Nevertheless the time required is not insignificant for the baking industry, and this phase of processes induces mass losses. The objectives of the work presented here are i) to determine the effects of ambient conditions and of the nature of cooling, natural or forced convection, on the water loss and the cooling time, and ii) to define optimal conditions for the sandwich bread cooling. A model validated in preceding work was used. Various ambient temperature and humidity values are used, as well in natural convection as in forced convection. On the surface the respective weight of convection, radiation and evaporation is studied as well. Radiation is the heat transfer mode the most influent on the cooling time and the water loss in natural convection. In forced convection, the thermal convection is the most influent. Results show that the water loss is very dependant of the cooling time: the lower the cooling time, the lower the water loss. Optimal cooling would be obtained with forced convection, low ambient temperature value and humid ambiance.

INTRODUCTION

In industry, sandwich bread cooling is generally achieved in natural convection without special cares about ambient conditions, temperature and humidity. That involves various cooling times, more or less significant water losses and thus variable quality.

Among the several cooling techniques, vacuum cooling was applied on bakery products (McDonald and Sun 2000). In particular, use of modulated vacuum cooler (MVC) allows to drastically speed up cooling (30 s to 5 min instead of 1 to 3 h), but with an increased water loss. This method presents numerous advantages for industry but induces a certain loss of product aroma. A patent was registered by Allied Bakeries Ltd (Anonymous 1996) for vacuum cooling of bakery products with sprayed liquid, preferably sterile water, to compensate water loss.

Many studies can be found about bread baking. On the other hand very few searchers were interested in the cooling. Nevertheless works of Grenier et al. (2002) can be quoted: sandwich bread cooling was studied, after turning out of the mould, in forced convection with an air velocity equal to $1\,\mathrm{m\,s^{-1}}$. Increase of ambient temperature increased cooling time but reduced water loss. Cooling rate was decreasing. An intense evaporation-condensation in the crumb was proposed as an explanation for this varying cooling rate.

Le Bail et al. (2005) used an experimental design to study the impact of selected parameters on the crust scaling for the frozen part-baked bread after final baking. The selected parameters were ambient air humidity during phases of fermentation, partial baking and post-baking cooling, and core temperature before freezing. Air humidity during the first post-baking cooling is the most influent parameter. Cooling must be achieved in humid conditions to reduce scaling.

Hamdami et al. (2004) studied cooling of frozen part-baked bread from partial baking to freezing. At surface, in the first moments, the local water content is decreased by an intense evaporation, so that there is not freezing. Then, there is surface rehydration by water diffusion from the interior of the product. Except the zone close to surface, local water content is homogenous in the product. Surface temperature decreases quickly at negative values, whereas, inside the product, temperature presents a freezing plateau.

Technological progress gives to researchers powerful analysis tools: Lucas et al. (2005a;b) studied, using MRI, the cooling and freezing phases of part-baked bread. The porosity, i.e. the crumb proportion, and the local water content are the main sources of the signal variations during the cooling phase. The effect of temperature is of the same order that the noise impact to the MRI signal and might be ignored. The signal variation during the cooling phase was considered mainly due to the porosity change rather than the local water content change.

Some authors quoted previously (Grenier et al. 2002, Hamdami et al. 2004) developed simulators for the needs of their works. About commercial software designed for the study of the bakery processes, BAKTIX can be mentioned (Van Der Sluis 1993). This software is designed for the cooling and the freezing phases simulation of bakery products. The temperature and moisture distribution inside the product are computed. The software is based on the finite elements method. A ready to use library of models is supplied. The software allows to study heat and mass transfers for irregularly shaped products.

The works presented here use an heat and mass transfers model for the cooling phase of the sandwich bread. To use a simulator perfectly suited to our product and allowing to modify the equations in accordance with our needs, we developed our own model. The variations of the temperature and local water content in the product, and thus the cooling time and the water loss can be studied in natural or forced convection, and in relation with the ambient temperature and humidity values. The objectives of the work were i) to conclude about the impact of these parameters and ii) to deduce information to optimize the cooling phase, i.e. to minimize the cooling time and the water loss.

MODEL

The model was presented in (Monteau 2008) and was used to model, using inverse method, the variation of the thermal conductivity versus the temperature and the local water content values in any place of the product. This 2D-model was designed to compute the temperature and local water content distribution at any time as well as the water loss. The computations are for half a slice of sandwich bread such as drawn on Figure 1. The model was validated in experiments by cooling sandwich bread, after turning out of mould, in a climatic chamber Vötsch VC 7018 (Vötsch, Reiskirchen-Lindenstrath, Germany) in forced convection with an air velocity value equal to $2\,\mathrm{m\,s^{-1}}$ on average. In the model, the heat and mass convection coefficients were computed for this condition for the forced convection case. The model of the system is based on the Fourier's second law for the heat transfer and the Fick's second law for the mass transfer.

The surface boundary condition takes into account the transfers by convection, radiation, and evaporation.

The evaporation flow is integrated on surface and in time to compute the mass loss.

The ambient parameters, temperature and relative humidity, are equal to 20 °C and 0.5 if not specified in the runs of the simulator.

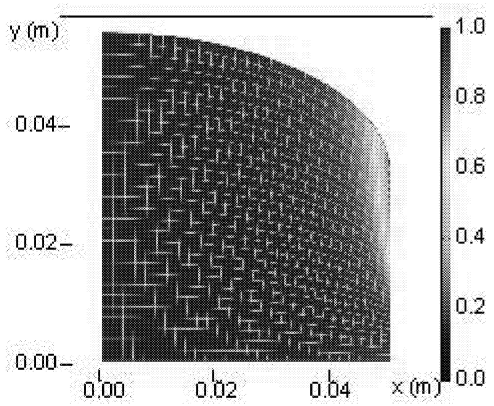

Figure 1: Geometry and mesh. The colours are for the mesh quality and are linked to a number between 0 and 1 (0 for the worst quality and 1 for the best one)

The initial conditions are homogeneous temperature 96 °C and local water content 0.762 kg water/kg dm.

The model was implemented with Comsol 3.3a. The mesh used is tetrahedral 30×28 (Figure 1).

MODEL EXPLOITATION

The model was used to compare the cooling time and the water loss in relation with the cooling conditions: ambient temperature and humidity, natural or forced convection. In simulation, to suppress transfer terms in the boundary conditions is easy. So the impact of the radiation, the thermal convection and the evaporation on the cooling time and the water loss was studied.

The cooling phase was regarded as finished when the core temperature inside the product reached 25 °C.

The first runs of the simulator were intended for the comparison of the impact of the natural convection and of the forced convection at standard ambient conditions 20 °C et 0.5 relative humidity.

A second series of runs were to judge the influence of the ambient temperature ranging from 5 to 20 °C on the cooling time and the water loss, as well in natural convection as in forced convection, the relative humidity being fixed at 0.5. In the same way runs were achieved with an ambient temperature value equal to 20 °C and a scanning for the relative humidity from 0 to 1.

Lastly the impact of the three modes of transfer at sur-

face on the cooling time and the water loss was investigated.

RESULTS AND DISCUSSION

In natural convection the cooling time was 5279 s. In forced confection it was 4467 s. Thus the forced convection decreases the cooling time by 15.4 % because of the higher heat transfer convection coefficient. The change of the water loss during the cooling is shown on the Figure 2 for the natural and the forced convection. The water loss is equal to 4.47 g in natural convection and to 4.13 g in forced convection, i.e. a decrease equal to 7.6 % between the two modes. These values are respectively equal to 1.44 % and 1.33 % of the initial mass. The two lines are practically superimposed, which means that the evaporation flow is the same in natural and in forced convection. Nevertheless, in the ten first seconds, this flow is much more important in forced convection than in natural convection (Figure 3), and the water loss too. The flow decreases rapidly in forced convection after the ten first seconds, and more slowly in natural convection, which leads to loss water appreciably equal as of 30 s. The diffusion inside the product is the factor limiting the evaporation. For the whole of the cooling, the water loss is lower in forced convection because the cooling is finished earlier.

On the Figures 4 and 5 are shown the cooling time and the water loss in natural and in forced convection for ambient temperature values equal to 5, 10, 15 and 20 °C with a relative humidity value equal to 0.5.

For all the values of the ambient temperature, the cooling time and the water loss are greater in natural convection than in forced convection, which extends the results obtained for the ambient temperature value equal to 20 °C. The saving of time and the decrease of water loss obtained in forced convection compared to the natural convection is practically the same whatever the ambient temperature. On average, they are respectively equal to 13.9 % and to 6.75 %. The increase in the cooling time and in the water loss obey to an exponential law.

On the Figures 6 and 7 are shown the changes in the cooling time and in the water loss in natural and in forced convection for ambient relative humidity values ranging from 0 to 1. The cooling time is practically the same for relative humidity values from 0 to 0.8. For the range 0.8 to 1, it seems to increase. For these runs, the forced convection decreases the cooling time on average of 14.2 % compared to the natural convection.

On the other hand the water loss is quite dependant of the relative humidity. The water loss decreases when the relative humidity increases. The water

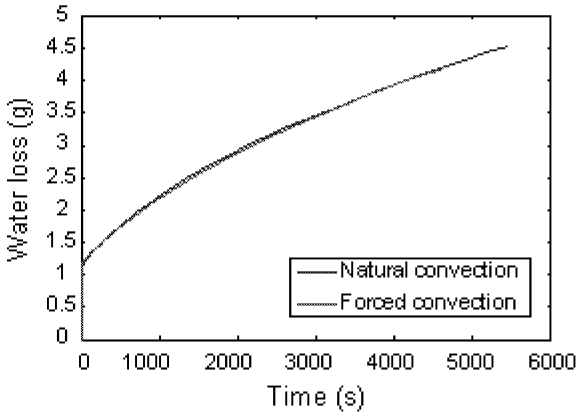

Figure 2: Water loss change in natural and forced convection

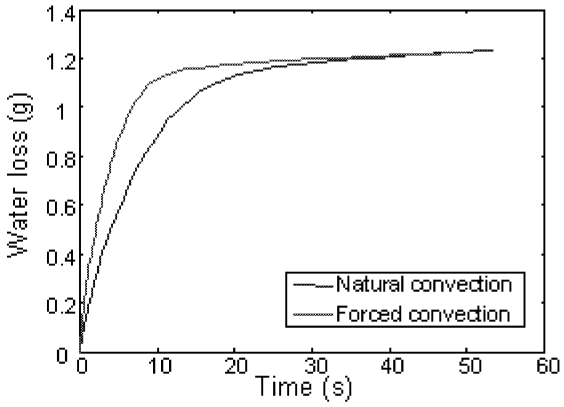

Figure 3: Water loss change in natural and forced convection for the 50 first seconds

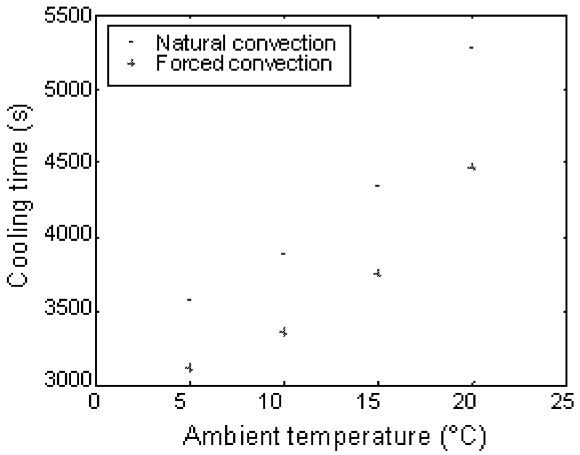

Figure 4: Cooling time versus ambient temperature

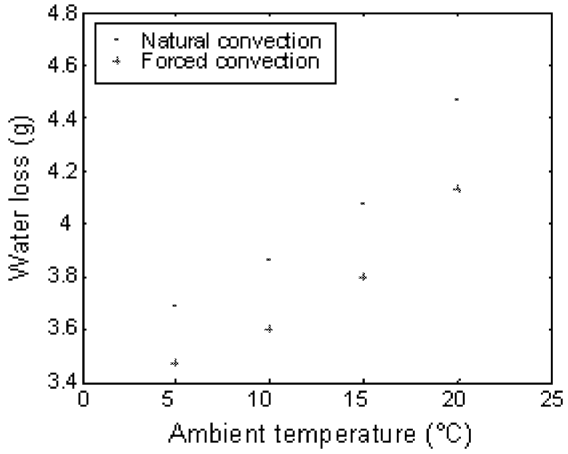

Figure 5: Water loss versus ambient temperature

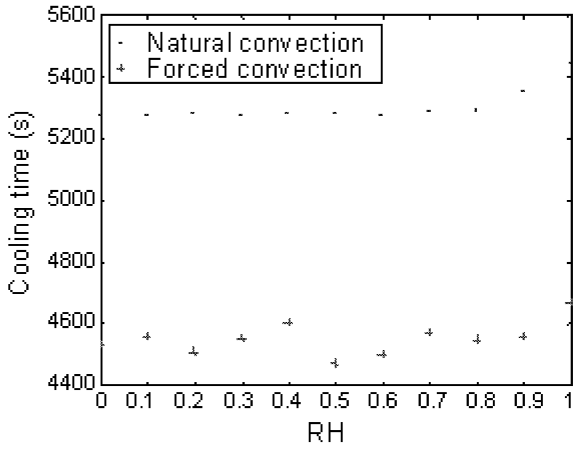

Figure 6: Cooling time versus relative humidity

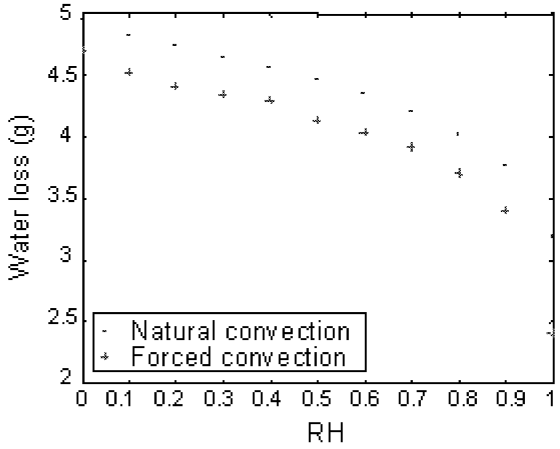

Figure 7: Water loss versus relative humidity

loss decreases drastically when the relative humidity approaches 1. Nevertheless water loss is never equal to 0, even when ambient air is saturated in water vapour, because of the temperature value greater on the bread surface than in the ambient air, which gives evaporation. For these runs, the forced convection decreases on average the water loss of 8.7 % compared to the natural convection.

In the tables 1 and 2, the influence of the three modes of heat transfer at the bread surface, convection, radiation and evaporation, once the process finished, i.e. when the core temperature reaches 25 °C, can be compared.

Table 1: Influence of the Three Modes of Heat Transfer at Surface on the Cooling Time and the Water Loss in Natural Convection

	t_r (s)	p (g)
With the three modes	5279	4.47
Without radiation	7061 (+33.7 %)	5.24 (+17.22 %)
Without evaporation	5599 (+6.06 %)	0
Without thermal convection	6849 (+29.7 %)	5.149 (+15.2 %)

The percentages are given compared to the case with the three modes

Table 2: Influence of the Three Modes of Heat Transfer at Surface on the Cooling Time and the Water Loss in Forced Convection

	t_r (s)	p (g)
With the three modes	4467	4.13
Without radiation	4924 (+10.2 %)	4.349 (+5.3 %)
Without evaporation	4772 (+6.8 %)	0
Without thermal convection	6854 (+53.4 %)	5.201 (+25.9 %)

The percentages are given compared to the case with the three modes

In natural convection, the radiation is the most influent of the mode of transfer on the cooling time, since the suppression of this mode increases the most the cooling time. Then it is the thermal convection by far before the evaporation. In forced convection the most influent is the thermal convection, then it is the radiation and finally the evaporation. In natural convection, the water

loss is a little more significant if the radiation is suppressed than if the thermal convection is suppressed. In forced convection the inverse is observed: the suppression of the thermal convection increases the losses of 25.9 % and the suppression of the radiation increases them only by 5.3 %. Obviously the suppression of the evaporation suppresses the losses. To conclude, as well for the cooling time as for the losses, the radiation is the most important mode in natural convection, and the thermal convection in forced convection. The evaporation is the less significant mode on the cooling time but is the real physical cause of the losses.

CONCLUSION

A post-baking cooling model of sandwich bread was developed. The runs revealed that the water loss is very dependant of the cooling time. The forced convection speeds up the cooling and in this way decreases the water loss. The cooling time and thus the water loss increases following an exponential law when the ambient temperature increases. The ambient relative humidity has not a real impact on the cooling time, but when is near the saturation, allows to minimize the water loss.

The comparative study on the impact of the radiation, of the thermal convection and of the evaporation shows than in natural convection the radiation is the most influent factor and than in forced convection it is the thermal convection. In any cases the evaporation has a low influence on the cooling time.

The whole of these results points out than in practice to decrease the cooling time and the water loss, the product has to be cooled down in forced convection, at the lowest possible temperature, and in saturated atmosphere. These ambient conditions would involve an energy cost, whereas, actually, the cooling is usually carried out without control of these ambient conditions and thus without energy cost. A continuation of this work could be a study about this energy cost and the search for its minimization.

REFERENCES

Anonymous, 1996. *Cooling baked products : Sloan, R. (Allied Bakeries, Ltd, Staines, UK TW18 4BA) UK Patent Application GB 2 290 449 A. Trends in Food Science & Technology*, 7, no. 10, 339–361.

Grenier A.; Monteau J.Y.; and Hayert M., 2002. *Effect of external conditions on the rate of post-baking chilling of bread. Journal of Food Engineering*, 55, no. 1, 19–24.

Hamdami N.; Monteau J.Y.; and Le Bail A., 2004. *Heat and mass transfer in par-baked bread during freezing. Food Research International*, 37, no. 5, 477–478.

Le Bail A.; Monteau J.Y.; Margerie F.; Lucas T.; Chargelegue A.; and Reverdy Y., 2005. *Impact of selected process parameters on crust flaking of frozen partly baked bread. Journal of Food Engineering*, 69, no. 4, 503–509.

Lucas T.; Le Ray D.; and Davenel A., 2005a. *Chilling and freezing of part-baked bread. Part I: An MRI signal analysis. Journal of Food Engineering*, 70, no. 2, 139–149.

Lucas T.; Quellec S.; Le Bail A.; and Davenel A., 2005b. *Chilling and freezing of part-baked bread. Part II: Experimental assessment of water phase changes and structure collapse. Journal of Food Engineering*, 70, no. 2, 151–164.

McDonald K. and Sun D.W., 2000. *Vacuum cooling technology for the food processing industry: a review. Journal of Food Engineering*, 45, no. 2, 55–65.

Monteau J.Y., 2008. *Estimation of thermal conductivity of sandwich bread using an inverse method. Journal of Food Engineering*, 85, no. 1, 132–140.

Van Der Sluis S.M., 1993. *Cooling and freezing simulation of bakery products.* In *Proc. IIR Meeting Comm. B1, B2, D1, D2/3.*

Effect of temperature and relative humidity on the respiration rate (RR) and transpiration rate (TR) of *Agaricus bisporus*

Leixuri Aguirre
Jesus M. Frias
Catherine Barry-Ryan
Antoine Clement
Dublin Institute of Technology
Cathal Burgha Street
Dublin 1, Ireland
Leixuri.Aguirre@dit.ie

Helen Grogan

Teagasc Kinsealy R & D Centre,
Malahide Road
Dublin 17, Ireland

ABSTRACT

Stored or packaged mushrooms have a very high metabolic activity, consuming O_2, producing CO_2 and water as a result of their respiratory metabolism. A closed system methodology was employed to measure the O_2, CO_2 respiration rate (RR) and the transpiration rate (TR) of mushrooms. The effect of storage temperature and the change of RR and TR during storage time were studied. After careful examination of the data of RR & TR on the mushrooms during storage, a linear model (for the O_2 and CO_2 RR) and a Weibull model (for the TR of O_2 and CO_2) were proposed to describe the primary model. Both RR & TR were dependent on the temperature of storage. The O_2 and CO_2 RR were found to have a significant linear increase with storage time. This pointed to the need to adjust storage conditions for these dynamic changes. The variability of the RR was also dependent on temperature indicating that the use of low storage temperatures is more beneficial in terms of having a homogeneous product than to slow the metabolic activity. An optimal temperature for minimise weight losses by transpiration was found at 6.4ºC.

KEYWORDS Modelling, respiration, mushrooms

INTRODUCTION

Fresh products stored or packaged remain metabolically active, consuming oxygen (O_2) and producing carbon dioxide (CO_2) and water as a result of their respiratory metabolism. The respiration rate (RR) is the O_2 consumption rate or the CO_2 production rate. The transpiration rate (TR) is the process in which the mushroom tissues give off water vapour to the atmosphere, as an essential physiological process.

Fresh produce continues to lose water after harvest, but unlike the growing plant it can no longer replace lost water from the soil. The loss of water from fresh products after harvest is an important problem for the food industry and agriculture, causing shrinkage and weight loss. When the harvested produce losses 5-10 % of its fresh weight, normally it becomes unusable (Mahajan *et al.*, 2008). To extend the shelf life of produce, its rate of water loss must be kept as low as possible. *Agaricus bisporus* is one of the most perishable products and usually its shelf life is 1-3 days at room temperature, weight loss being one of the principal problems.

Vegetable respiration and transpiration rates are essential measures of packaging vegetable, and if not taken into account, may lead to a total consumption of the oxygen with in the package, producing anaerobic processes and resulting in a fermented product that will lack the quality of the fresh product. Transpiration of water will induce condensation of water on the surface of product and the packaging film, slowing down the gas transfer through the packaging film and providing media for microbial growth.

There are several methods of measuring the respiration and the transpiration rate of a vegetable, and the easiest one to implement is the closed system method (Fonseca et al., 2002).

The aim of this study is i) to determine the density of the mushrooms in order to ii) determine the RR and the effects of the storage on the RR and iii) the TR during the storage under controlled environmental conditions.

MATERIALS AND METHODS

In order to estimate the volume filled by the mushrooms in the closed system, their bulk density was determined following the methodology of Fonseca (2002).

Determination of the respiration rate

A closed system methodology was employed to measure the RR of mushrooms and to see the effect of storage temperature and packaging atmosphere on the RR and TR of mushrooms.

The system was closed with the lid of the container and the concentration of O_2 and CO_2 was measured. Three repetitions were measured each time using the MAP test 4000 (MAP test 4000, AGB scientific ltd, Dublin).

In order to determine the RR the concentration of O_2 and CO_2 were measured every 20-30 minutes. Each respirometer with mushrooms was stored from three to ten days.

To avoid O_2 depletion and excessive CO_2 production that may affect the RR, the system was reset every time the percentage of CO_2 reached 5 %. To reset the system, the lid was opened for one hour in order to get the initial conditions (atmospheric air). The experiment was carried out at 3 different temperatures (4, 15 and 22 °C).

Determination of the transpiration rate

In order to study the TR the mushrooms were stored in a closed systems at 3 different temperatures (5, 15 and 21 °C) and the relative humidity was measured using data loggers (Testo 175-H2, Eurolec Instrumentation Ltd, Ireland).

The container was opened once condensation appeared; which meant that the atmosphere inside the

container had reached saturation (100 % RH). Containers were drained and mushrooms and data loggers were spread on a grid, at the experimental temperature. This allowed the condensed water and the mushrooms to return to their original conditions. Dry containers were used and the same mushrooms were weighed and a new experiment at the same temperature was performed.

RESULTS AND DISCUSSION

Respiration Rate

Figure 1 shows that mushrooms have a constant RR: the slopes of the O_2 consumption and CO_2 production (ml gas/g mushroom) versus time were straight lines and a linear model was used.

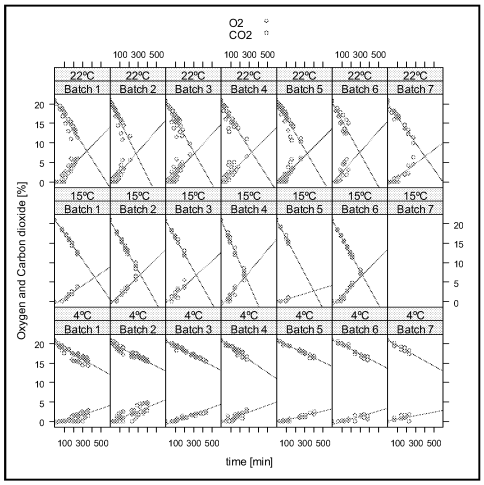

Figure 1 Kinetics Of The Gas Change For Mushrooms In a Closed System Respirometer, For Each Temperature Over Time. The Temperature Of The Experiment (Green) And The Batch Number (Orange) Are Indicated

Figure 1 also shows the gas consumption in each closed system respirometer for each temperature. All initial CO_2 readings started at 0, due to the limits of the detector. Figure 2 shows that temperature has an important effect on the RR. The RR decreased when the temperature was reduced. At the same time the variability increased when the temperature was increased.

Figure 2 also shows the O_2 consumption rate at each temperature, which was constant at low temperatures, lower than ~0.05 mg O_2/g of mushroom per minute, proving that storage time does not have an effect on the O_2 consumption velocity at low temperatures. The small perturbations on the initial O_2 content and on the O_2 consumption velocity were due to batch-to-batch variability and experiment to experiment variability. These perturbations could be expressed as random effects belonging to a normal distribution with an average zero on the intercept and the slope of the linear model. In the case of 15 ˚C and 22 ˚C the O_2 consumption rate increased during storage. At 15 ˚C the initial O_2 consumption rate was ~0.12 mg O_2/g of mushroom per minute and increased to ~0.21 mg O_2/g of mushroom per minute. In the case of 22 ˚C, the increased O_2 consumption rate was higher and starts at ~0.15 mg O_2/g of mushroom per minute and finished in ~0.31 mg O_2/g of mushroom per minute which was more than 6 times higher that at 4 ˚C.

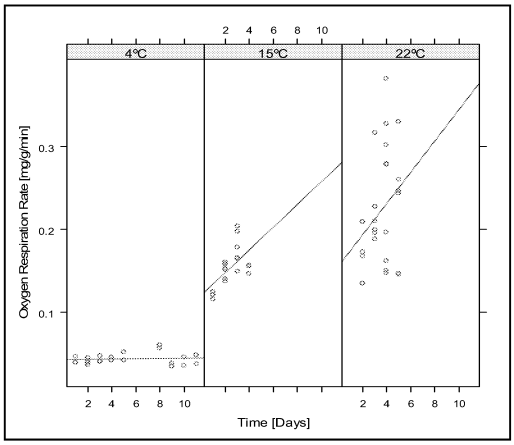

Figure 2 Effect Of The Storage Day On The O_2 Consumption Rate For Each Temperature.

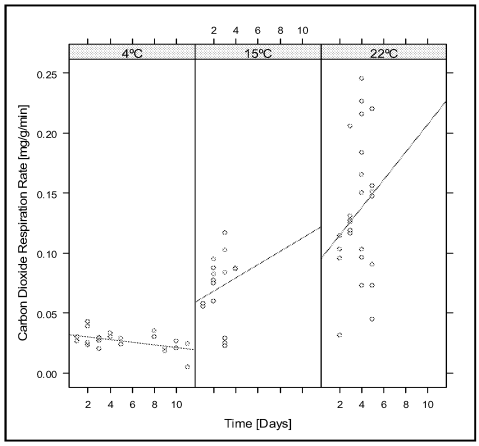

Figure 3 Effect Of Storage Time On The CO_2 Production Rate For Each Temperature.

Figure 3 showed that the CO_2 production rate was almost constant for low temperatures and lower than ~0.04 mg CO_2/g of mushroom per minute, proving that the storage time did not have an effect on the CO_2 production velocity at low temperatures. In the case of 15 ˚C and 22 ˚C the CO_2 production velocity increased during storage. At 15 ˚C the initial CO_2 production velocity is ~0.06 mg CO_2/g of mushroom per minute and increased to ~0.12 mg CO_2/g of mushroom per minute. In the case of 22 ˚C, the increase of the CO_2 production velocity was higher and starts at ~0.09 mg CO_2/g of mushroom per minute and finished at ~0.25 mg CO_2/g of mushroom per minute which was more than 6 times higher than at 4 ˚C.

Modelling

After analyses of the Figures 2, 3 and 4, linear mixed models were used to build the model of the RT:

$$O_2t \sim time + time{:}\ temp\ (T) + time{:}\ temp\ (T){:}\ day \quad (1)$$

$$CO2t \sim time + time{:}\ temp\ (T) + time{:}\ temp\ (T){:}\ day \quad (2)$$

Where O_2t were the mg of O_2 per gram of mushrooms at 0°C, time was the storage time, time: temperature (T) was the dependence of the temperature during the storage time and time: temperature: day is the dependence of the temperature on the storage time. For Equation 2, CO_2t was the mg of CO_2 per gram of mushrooms at 0°C, time was the storage time, time: temperature (T) was the dependence of the temperature during the storage time and time: temperature: day is the dependence of the temperature on the storage time.

To adjust the models, the coefficients were required. A linear mixed-effects model fit by REML was done to check if it fitted well with the values and if the effects were still significant. The final models were:

Table 1 Linear Mixed Model Used For The O_2 Consumption. All Linear Effects Significant ($p<0.05$). Standard Errors For Fixed Effects and Confidence Intervals For Random Effects Are Indicated in Subscripts.

Parameter	**Estimate**
(Intercept)	84 $_{(3.7)}$
time	-0.007 $_{(0.002)}$
time: temperature	-0.01 $_{(0.0004)}$
Variability between batches	
$\sigma_{\text{Intercept}}$	30 $_{[25.3\text{-}35.8]}$
$\sigma_{\text{Temperature}}$	0.002 $_{[0.002\text{-}0.003]}$
Residual	1.1

The O_2 consumption rate was only affected by temperature and not by the storage time (p-value > 0.05). The variability at the beginning of the experiment is 30% and the variability on the slope is 0.002.

Table 2 Linear Mixed Model Used For The CO_2 Production. All Linear Effects Significant ($p<0.05$).

Parameter	**Estimate**
(Intercept)	-2.6 $_{(0.28)}$
time	0.0097 $_{(0.003)}$
time: temperature	0.005 $_{(0.0004)}$
Variability between batches	
$\sigma_{\text{Intercept}}$	1.46 $_{[0.96\text{-}2.22]}$
$\sigma_{\text{Temperature}}$	0.001 $_{[0.0014\text{-}0.0023]}$
Residual	2.7

The CO_2 production velocity was affected by temperature ($p<0.05$). The variability at the beginning of the experiment was 1.46 % and the variability on the slope is 0.001.

This experiment showed that the RR, O_2 and CO_2, was dependent on the temperature. Mushroom RR, was lower at low temperatures than at high temperatures. Thus, metabolic reactions would be slowed down with low temperatures. These results are in agreement with the results of RR obtained by Tiehua et al. (2007), Alique *et al*. (2005) and Jacxsens *et al.* (2001) who reported that storage temperatures dominated the respiration rate of fresh produce. Varoquaux et *al*. (1999) reported that the RR increased when the storage temperature was increased for mushroom *Agaricus bisporus* (1999). Day (2001) and McLaughlin & Pitt (1999) proved that control of the RR was very important and lowering the respiration rate could extend the shelf life and preserve the quality of products.

The difference in RR between batches of mushrooms might be due to the difference of maturity and product heterogeneity. Cliffe-Brynes & O'Beirne (2007) Tiehua *et al*. (2007), Alique *et al*. (2005), Jacxsens *et al.* (2001) and Varoquaux et *al*. (1999) analysed the RR at the exact moment that postharvest starts and in this study the mushrooms are form a local market and the analysis started a day after harvest.

The time of storage had an effect on the RR, linked with the temperature, even though it was not proved statistically for the O_2 consumption. The RR increased with time of storage and with the temperature. The variability, as well, was very important between batches and between experiments; and this variability increased with the temperature.

The mathematical models which were built described the kinetics of the O_2 and the CO_2 respiration rate. Thus, it was possible to determine the RR at given temperatures and storage times in order to choose MAP parameters. It could be concluded that the time of storage did not affect the metabolism of the mushrooms at low temperatures (4 °C) but would have an effect at high temperature (15 and 22 °C).

Transpiration Rate

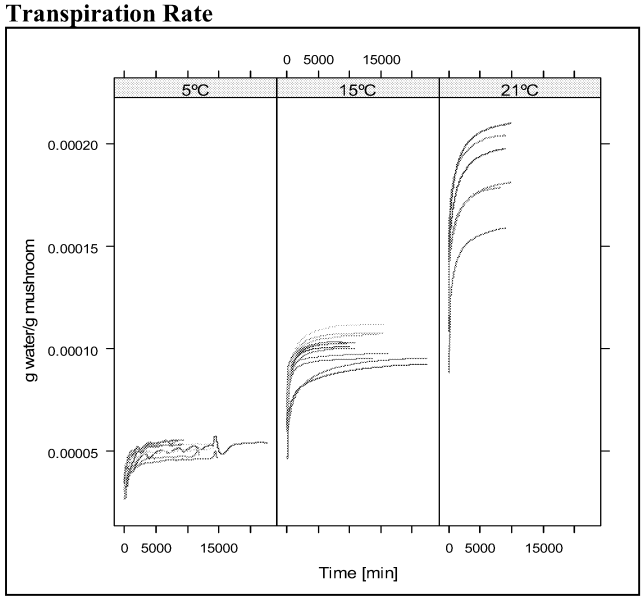

Figure 4 Water Production Per Gram Of Mushrooms For Experiments At Different Temperatures. The Colour Lines Indicate Each Batch.

The TR was estimated, in gram of water per gram of mushroom, using the relative humidity, the temperature, the free volume and the weight of the mushrooms. Equations describing the physical properties of moist air were used, and finally arrived at Equation 3 and 4:

The TR kinetics were not linear (Figure 5), the effect of parameters such as temperature and storage time could not be analyzed with the experimental values; a non-linear model was needed to describe the kinetics.

However, the effect of the temperature was very significant. The TR increased with temperature. Figure 4 shows the variability inside batches and how this variability increased with the temperature.

Model building

The dynamic evolution of the TR looked like a growth curve. The most suitable model found for this kind of dynamic was the Weibull model:

$$Wpg \sim Asym - Drop \times e^{-e^{lrc} t^{pwr}} \quad (3)$$

with

$$\begin{aligned} Asym &\sim T + T^2 \\ Drop &\sim T + T^2 \\ lrc &\sim T \\ pwr &\sim 1 \end{aligned} \quad (4)$$

Where Wpg: transpiration rate (g water / g mushrooms), t: time (s), Asym was the numeric parameter representing the horizontal asymptote on the right side, Drop was the numeric parameter representing the change from "Asym" to the "Wpg" intercept, lrc was the numeric parameter representing the natural logarithm of the rate constant, pwr was the numeric parameter representing the power to which "t" is raised. In conclusion, the final TR model is in Table 3.

Table 3 Weibull Model Used For The TR. All Effects Significant ($p<0.05$). Standard Errors For Fixed Effects and Confidence Intervals For Random Effects Are Indicated in Subscripts.

	Estimate
Asym	$7.7e\text{-}05_{(8.2e\text{-}06)} - 8e\text{-}06_{(1.6e\text{-}06)} * T + 6.3e\text{-}07_{(1.1e\text{-}07)} * T^2$
Drop	$3.06e\text{-}05_{(6.1e\text{-}06)} - 3e\text{-}06_{(1.0e\text{-}07)} * T + 1.0e\text{-}07_{(1.0e\text{-}08)} * T^2$
lrc	$-4.461102_{(0.3546748)} + 0.057763_{(0.0243699)} * T$
pwr	$0.548189_{(0.0229818)}$
Variability between batches	
$\sigma_{Intercept}$	9.45e-06 [7.3e-06-1.2e-05]
σ_{Drop}	7.72e-06 [5.8e-06-1.01e-05]
σ_{lrc}	0.75 [0.54-1.03]
σ_{pwr}	0.117 [0.088-0.16]

This model showed that all the effects are significant ($p> 0.05$) and there was a quadratic effect of the temperature, so with the derivative of the time it was possible to find a minimum or maximum for the Drop. In this case a minimum was found, that means the point of minimum TR, at 6.4 ˚C (Figure 5).

This experiment showed the TR of mushrooms (gram of water per gram of mushrooms) in a closed system at different temperatures as a function of time. The behaviour of the TR function of time was in all the cases the same: a quick increase and then an asymptotic stabilization. In fact, there was a difference of water potential between the mushrooms and the atmosphere inside the system, and this product released water until a balance was achieved. The lack of external cuticle in mushrooms to protect them from water loss and the fact that they are composed mainly of water are key contributing factors in their transpiration rate.

It could also be seen that there was a big variability inside experiments, due to the non-homogeneity of the mushrooms and their sensitivity to environmental factors. The variability increased with temperature (Figure 5). The experiment showed that variability at 22 ˚C is ten times bigger than variability at 4 ˚C.

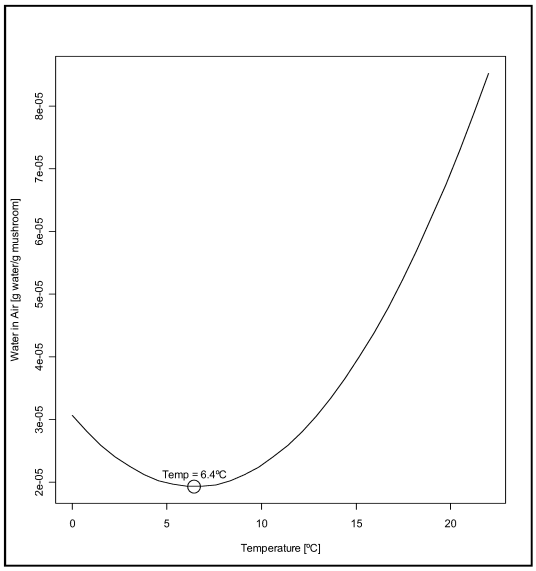

Figure 5 Temperature Point Where The TR Of Rhe Mushrooms Is Minimised.

The effect of the temperature was significant, as shown previously in the model building. The TR increased with the temperature, the asymptotic value stabilizing at higher TR when the temperature got more and more significant. This effect might be explained by the mushroom's metabolism which would be slowed down at low temperatures, but also by the saturated vapour pressure which was higher at high temperature. Therefore, low temperatures were better to prevent weight loss.

The model built described the kinetics of the TR on a function of time and temperature in a closed system. So, at

given temperatures and times, the amount of water produced per gram of mushroom could be determined. The asymptotic value was the most important because it represented the TR at equilibrium. In MAP, this value might be used to determine the quantity of water per gram of mushroom to be maintained as a guide to producers to avoid water loss and condensation in packs (risk of microbial spoilage).

CONCLUSIONS

The study showed that the respiration rate, O_2 consumption and CO_2 production was dependent on the temperature of storage. Respiration rate of the mushrooms increased, when the temperature was increased and the variability in the respiration also increased with the temperature.

The O_2 consumption and CO_2 production at low temperatures were constant, and storage time did not have a significant effect.

Transpiration rate was affected by the temperature. Transpiration rate decreased when the temperature was decreased. This effect could be explained by the mushroom metabolism which would be slowed down at low temperatures, but as well by the saturation vapour pressure which was higher at high temperatures. The results showed the variability inside batches increased with temperature. The study found that the transpiration rate was minimized at 6.4 ˚C.

FUTURE WORK

Possible extensions of this work would involve a more detailed experimental plan, with a larger number of temperatures and to study if significant effects can be found for both respiration coefficients O_2 and CO_2 . A detailed study of the respiration quotient would provide for a better insight on possible metabolic deviations.

REFERENCES

Alique, R. & De la Plaza, J. L. (1993). Tecnologías post-cosecha del champiñón cultivado. I Jornadas Técnicas del champiñón y otros hongos comestibles en Castilla- La Mancha, 85-94. Motilla del Palancar, Cuenca, Spain.

Fonseca, S.C., Oliveira, F.A.R. & Brecht, J.K. (2002) Modelling respiration rate of fresh fruits and vegetables for modified atmosphere packages: a review. Journal of Food Engineering, 52, 99–119.

Jacxsens, L., Devlieghere, F., Van Der Steen, C. & Debevere, J. (2001). Effect of high oxygen modified atmosphere packaging on microbial growth and sensorial qualities of fresh-cut produce. International Journal of Food Microbiology, 71, 197-210.

Mahajan, P.V., Oliveira, F.A.R. & Macedo, I. (2008). Effect of temperature and humidity on the transpiration rate of the whole mushrooms. Journal of Food Engineering, 84, 281-288.

Pinheiro, J. C. & Bates, D. M. Mixed-Effects Models in S and S-PLUS'. ISBN 0-387-98957-9, 2000.

Tiehua, L., Min, Z. & Shaojin W. (2007). Effects of temperature on Agrocybe chaxingu quality stored in modified atmosphere packages with silicon gum film windows. Food Science and Technology, doi:10.1016/j.lwt.2007.07.013

Varoquaux, P., Gouble, B., Barron, C. & Yildiz, F. (1999). Respiratory parameters and sugar catabolism of mushroom (Agaricus bisporus Lange). Postharvest Biology and Technology, 16, 51-61.

McLaughlin, N.B. & Pitt, R.E. (1984). Failure characteristics of apple tissue under cyclic loading. Transactions of the ASAE, 27(1), 311–320.

BIOGRAPHY

LEIXURI AGUIRRE obtained a Dip in Nutrition and Dietetics and a BSc in Food Science and Technology from the Pharmacy Faculty of Basque Country University. She entered the PhD register of the the School of Food Science and Environmental Health of the Dublin Institute of Technology in 2004. Her research interests are in the area of image analysis of food products, mathematical modeling in food considering variation, mushrooms and quality parameters.

JESUS M. FRIAS Dr Frías's BSc is in Food Science and Technology from the Pharmacy Faculty of Basque Country University and his PhD is in Biotechnology from the ESBUCP (Portugal). He joined the School of Food Science and Environmental Health of the Dublin Institute of Technology as a lecturer in Food Chemical Analysis and presently works as the (Acting) Head of the Food Science Department of the School. His research interests are in the areas of Mathematical modelling of food kinetic phenomena, Fruit and vegetable technology; product natural variability and shelf life modeling, Vitamin stability, Drying technologies and mechanical stress during dehydration.

CATHERINE BARRY-RYAN received her BSc (Hons) from the National University of Ireland Dublin in Industrial Microbiology and PhD in Food Technology from the University of Limerick for work on processing and packaging of ready-to-eat products. She worked as a Research Fellow (Food Research Centre) with Lecturing (BSc in Food Technology) at the University of Limerick. Her research interests are in modified atmosphere packaging and post harvest treatment of fruit and vegetables as well as the development of functional food. She is currently a senior lecturer in Food Product Development in Dublin Institute of Technology.

HELEN GROGAN graduated from UCD, Dublin in 1992 with a PhD in Mycology. Dr. Grogan joined Teagasc in October 2005 as a Senior Research Officer with responsibility for the mushroom research program and providing plant pathology diagnostics to the Teagasc Horticulture Advisory Service. Prior to this she worked for 14 years at Warwick HRI, University of Warwick, as a Research Leader in Applied Mushroom Pathology. She has extensive research experience in the epidemiology and control of mushroom diseases. She also has worked on the dynamics of fungicide persistence in mushroom casing, fungicide efficacy, and resistance of pathogens to fungicides.

ANTOINE CLEMENT is an undergraduate student from the food engineering course at the AgroParisTech (Paris, France) doing an ERASMUS exchange at the School of Food Science and Environmental Health of the Dublin Institute of Technology.

Time to Failure and Time to Repair Profiles Identification

Giuseppe Perrica, Cesare Fantuzzi, Andrea Grassi,
Gabriele Goldoni and Federico Raimondi*

April 30, 2008

Abstract

This paper covers with the identification of real statistical distribution of time to failure (TTF) and time to repair (TTR) of a manufacturing production line. A formal procedure to obtain TTF and TTR profile distributions (location, scale and shape parameters) has been defined. The procedure processes redundant and corrupted signals logged from control systems of the manufacturing machines during operative phases (i.e. alarms and process data).

We define a formal algorithm to filter the data and establish the qualitative and quantitative characteristics for reliability applications. This procedure has been applied to data acquired from a Tetra Pak packaging line. The resulting TTF and TTR profiles have been used to define statistical failure and restoration input in simulation campaigns of packaging line.

Introduction

Simulation is a tool for supporting the analyst in the design and assessment process allowing the experimentation and understanding of ideas and insights into effects in a virtual world, and can produce a reduction in development costs. Manufacturing simulation has been one of the primary application areas of simulation technology. It has been widely used to improve and validate a wide range of manufacturing systems designs [1, 2].

To carry out helpful simulation studies we need a realistic system model and to specify correctly probability inputs such as machines failure and repair statistical distribution. The simulations probability inputs are obtained by processing data acquired from machines data captured from the system.

To specify simulation inputs, we can collect data using one of the following approaches [1]:

- Stored data is used directly in the simulation, individual data fed into model, based on time stamp: *traced-driven approach.*
- The data is used to create an *empirical distribution* functions.

Inferential statistics comprises the use of statistics to make inferences concerning some unknown aspect of a population, comparison of different scenarios is a very common use of these techniques in simulation applications. For this reason, the correctness of input data is crucial to guarantee the accuracy of simulation results and conclusions [3].

Usually *logger systems* are integrated in manufacturing sites, in particular production lines; they are tools for collecting and loading real time events and manufacturing parameters, useful for performances analysis but not for reliability applications [4, 5, 6, 7].

Generally, simulation studies assume that the system failure and repair times follow a particular statistical distribution (i.e. exponential, weibull or normal distribution) based on field practical considerations and theory studies without any systematic approach [8, 15, 16].

On the other hand, in literature there are many examples that provide guidelines to develop a production line database, especially in semiconductor field. But there are not many works that lead the practitioners to follow a helpful procedure to obtain realistic and useful inputs for a simulation study from all the logged data [10].

The focus of the present work is to suggest a procedure for this gap. The main contribution of this paper will be to establish a general methodology that makes it possible to obtain a minimal data structure for failure and repair statistical process characterization, starting from a complex and unsuitable mass of recorded data. This procedure has been applied to the simulation of a packaging line from Tetra Pak.

In section 1, common data structure and data collection systems are presented and discussed, in section 2

*Giuseppe Perrica, Cesare Fantuzzi and Andrea Grassi are with *Dipartimento di Scienze e Metodi dell'Ingegneria, Università di Modena e Reggio Emilia, Via Amendola, 2 (Pad. Morselli) – 42100 Reggio Emilia (Italy).*
`<name.surname>@unimore.it`
Gabriele Goldoni and Federico Raimondi are with *Tetra Pak Packaging Solutions, Via Delfini, 1 – 41100 Modena (Italy).*

simulation input profile detection is presented and described. Finally, in section 3, methodology application is discussed.

1 Data Structure and Collection

In this section, typical available data structures are presented and an example is reported: the Monitoring System of Tetra Pak (MS).

Input data collection is one of the key areas in simulation. The quality of simulation output data and consequently simulation derived conclusions are directly dependent on the accuracy and reliability of the input data. This mainly depends on how and what data is collected and is generally recognized as one of the major hurdles of simulation projects. It is typical to collect and store transactional data about manufacturing parameters of the whole production cycle in real time; for these purposes support tools for data collection and analysis have been developed. A manufacturing logger system may be linked to other databases, and a data warehouse may be needed for an intermediate integration of the necessary information. Subsequently, one or more data tables can be created from the raw transactional information for analysis. A typical table can contain rows for each operation, each physical resource (i.e. equipments or operators), each operation phase (i.e. maintenance, cleaning, production, etc.) and each entity (i.e. packaging material or product) involved in production cycle. Each row can have information to identify the resource, the current operation, the production route, the time in to the actual operation, the time out from the previous operation, and the entities involved in the particular operation with their parameters (i.e. equipment speed or acceleration) and much more, according to the particular production line. There can also be variables describing the production rate, the product type and the product losses.

The variety and volume of data to be collected is directly determined by the complexity of the system under investigation. There can be hundreds of rows of data for each phase, split in several columns, describing how an individual entity moves through the line. The amount of data grows when we refer to manufacturing lines characterized by short and numerous stops followed by restarts, such as food packaging lines. A typical logger system also records events outside the production phase, for example preparation and maintenance times in historical way.

All logged data can be tabulated by chronological order and can be organized hierarchically. As each operation is time stamped, one of the first processing data steps is to convert the time stamps into meaningful measures, suitable for the particular scope (i.e. performance measurements, statistical analysis, reliability parameters, etc.) [6, 8, 10].

This is where the gap between theories proposed by literature and practical approaches becomes evident.

The Monitoring System tool of Tetra Pak production lines, is an example of a typical logger system. It is a tool that stores many events about the manufacturing process. Parameters such as: product packages, machine alarms, production waste, production shift management, operators' actions, etc. are stored. All these events are useful for generating graphics and reports, suitable for performance indicators, advanced operator assistance, control measures and diagnostic performance. Every stored event includes: date/time, shift, event code, event description, waste packages, alarm source and manual operator actions, as shown in Table 1.

Date	Start Time	Event Code	Event Description	Duration	Packages	Info Event
31/10/07	00:13:45	10300701	STEP ZERO	1:57:34	0	*NA*
31/10/07	00:13:45	10301120	Preparation	0:00:00	0	*NA*
31/10/07	00:13:45	10301209	TBA 1000Sq	1:57:34	0	*NA*
31/10/07	00:13:45	10330117	Alarm Drying	1:57:34	0	*NA*
31/10/07	00:13:45	10330167	Alarm Aseptic	1:57:34	0	*NA*
31/10/07	08:45:45	10300712	PRODUCTION	1:10:55	0	*NA*
31/10/07	08:17:01	10338195	Waste TS	0:04:00	68	*NA*

Table 1: An example of a MS report *(NA: not available)*

2 Statistical Profile Detection Procedure

In deeper detail, the data structure is composed of: *Production Time* (PT), *Down Times* (DT), *Idle Times* (IT) and time outside the production phase with the respective durations [11], as shown in Table 2.

Machine: **Packaging Machine** Date: **31.10.2007**	
Machine State	**Time Duration**
PT	1:45:12
DT	0:26:30
IT	0:50:44
PT	1:57:34
IT	0:11:22
Outside Production Phase	4:16:41

Table 2: Minimal data structure

If we are analyzing TTFs we can find them inside the PT, the time during which the equipment is performing

a primary required function. (i.e. producing product or filled packages for Tetra Pak lines). Equipment stop times can be classified in two categories: stops caused by the equipment itself and stops caused by its interaction with other machines of the production line, called DTs and ITs respectively; the first ones are useful if we are investigating TTR distribution. All this time refers to the poduction phase of production line [11].

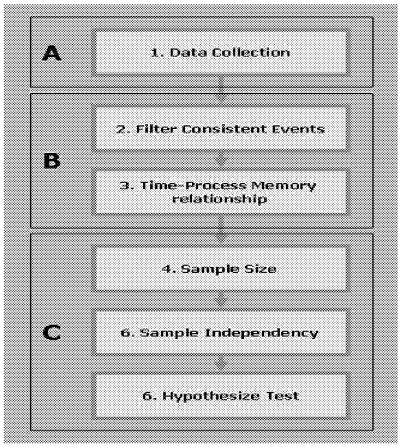

Figure 1: Methodological approach flow chart

As shown in Figure 1, our methodological approach consists of the following steps:

1 – Data collection: The first step is to establish homogeneous conditions to collect data. It is not possible to draw correct conclusions about hypothesized profile distribution if we collect data from different operational scenarios [1].

2 – Filtering procedure: Any filtering procedure is focused on a suitable scope, for this reason, before starting this phase we have to put these questions '*What have we to pointing out?*', '*What are relevant events for these study?*', '*What events have we to not consider?*'. We would identify a correct distribution profile for TTR and TTF that might be useful and realistic for the simulation study, these times must describe the standard equipment behaviour [13].

2.1 – Record selection: Only record data sets that have complete information from each operation from process start to finish should be considered. Data sets not having complete information should be eliminated because incomplete data may lead to incorrect conclusions without considering each step of the process [12].

2.2 – Artefacts removal: We have to neglect events that refer to unusual working conditions. Test or engineering additional times (i.e. some logger systems add to record data factitious DTs in order to time-quantify product losses) are eliminated because these "events" do not refer to a normal production operations of the global equipment. They are logged but do not reflect the true machine behaviour. We also have to individuate and remove all the DTs caused by operators' misfires: i.e. after a machine fault, if an operator commands a manual restart without solving the problem source, the logger system registers a short TTF because the machine state goes 'down' immediately. It is suggested not to consider this TTF in the profile distribution calculation, because this data does not reflect any working operations usually performed by the equipment. It may have been caused by an incorrect problem solving procedure on the part of the operator. Other possible causes of artefacts are represented by testing and training phases [6, 15].

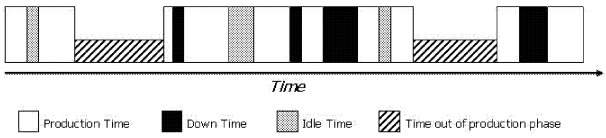

Figure 2: Time–distribution events

3 – Consider time intervals relating to "process memory": As a rule of thumb it may be considered that a machine loses the memory of its "*history*" when it is working in out of production phase. Machine cooling, ordinary and extraordinary maintenance, cleaning parts, mechanical and software updates, are some of the reasons that justify our hypothesis. Instead ITs are time intervals in which the equipment is not in a production state for external reasons and, at the same time, no "*memory*" is lost because the machine remains in the production phase. Based on the previous reason we can hide ITs and can sum two production time intervals separated by an idle times. It is suggested that it is incorrect to consider these two times separately because no actual machine failure has happened. On the contrary, we cannot sum two PTs separated by every event that refers to out of production phase. I.e. referring to Figure 2, we have to consider the third white block as PT without summing the second one that will be neglected because its duration is determined, not by a failure, but by the end of planning production. Instead we have to sum the duration of fourth and fifth white blocks, as a single event. The global effect of the previous consideration is to change the TTF and TTR profile distribution that can only be obtained from raw logged data.

The following steps refer to statistical inferential test:

4 – Choose an appropriate sample size: Before performing a statistical test, it is suggested to extract an opportune sample from filtered data. The choice of its size is led by the following considerations: collecting at least 200 observations on the random phenomenon of interest it is possible to discriminate between two candidate distributions. In general, the benefit produced by an increase in the sample size from 200 to 300 is higher

than an increased sample size from 100 to 200, etc. On the other hand, a more extensive sample size introduces fitting problems: by improving the sample size, it is possible that no well-know probability distribution fits the available data set. For these reasons, it is suggested that 230 observations is an appropriate compromise[9].

5 – Sample independency: Sample independency verification is required before determining the best model for data collected. If this assumption is unsatisfied inferential statistical techniques may not be used or their conclusions can be misleading. With this in mind, a scatter diagram of sample $\{X_i\}$ could be used. A scatter diagram is a plot of pairs (X_i, X_{i+1}). If samples are independent, we expect the points (X_i, X_{i+1}) randomly distributed in the first quadrant of the Cartesian plane. Instead, if the X_i's are correlated, they aligned themselves [1, 2, 12].

6 – Perform hypothesis tests: At this point a hypothesis test can be performed, in deeper detail using the null hypothesis: observed data are independent samples extracted from a theoretical distribution. Performing a hypothesis test, two types of errors can be observed. If one rejects the null hypothesis when in fact it is true, this is called a Type I error (α); its value is under control (usually $\alpha \leq 0.05$). If one fails to reject the null hypothesis when it is false, this is called a Type II error. For a fixed level α and sample size n, the probability of Type II error (β), depends on what distribution is actually true (as compared to the hypothesized distribution), and may be unknown. We call (1-β) the power test and it is equal to the probability of rejecting the null hypothesis when it is false. Clearly, a test with high power is desired.

It is important to emphasize that failure to reject the null hypothesis (observed data are independent samples of the theoretical distribution) doesn't mean that it is true. Defining *p-value* like the smallest level of significance (α) that leads to rejection of the null hypothesis, the more *p-value* is large, the more the fitting is good *(consrevative approach)*. There are definitely situations for which no theoretical distribution will provide an adequate fit for the observed data. In these cases it is recommended to use an empirical distribution [1, 9, 12, 14].

3 Methodology Application

In this section, previous methodology has been applied to data referring to the filler machine of a Tetra Pak production line for TTF distribution profile identification.

Investigation based on MS data coming from different customer sites that respect the following requisites:

- Machine: TP Packaging Machine
- Product: Juice
- Production rate: 8000p/h
- Package 200s

Non homogeneous operational conditions are: number of operators and line layout. Only complete data from the whole amount of information are considered, on the basis we have stated above. Before artefact removing procedures, we elaborate MS records (see Table 1) to obtain minimal data structure composed by TTFs and TTRs durations (see Table 2). For these purpose we have developed a suitable software tool, which also provides time intervals relating to the process memory, as described in the previous section.

The next step is artefacts filtering. The implemented tool provides some rules, lead by practical consideration and specialists guidelines: i.e. it can be assumed that a testing phase is happening if weekly production time is less than twenty hours. Another example of artefact is represented by operator misfires, i.e. we cannot consider records that present a lot of the same alarm repetition spaced out by zero seconds TTFs. It could be the situation where the equipment is restarted without solving the particular machine problem.

It should be stressed that this phase needs accurate and detailed line knowledge and should be conducted under machine specialist counselling. After the filtering phase, 230 observations have been chosen and sample independence has been verified through a scatter plot, results are shown in Figure 3:

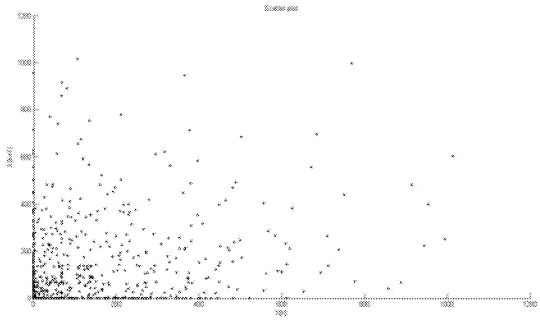

Figure 3: Scatter plot for the considered data–set

Figure 4 shows the Frequency comparison plot which displays two histograms of two data sets (a theoretical distribution and a empiric distribution) on the same graph. Similarity of the two histograms proves that the selected model provides a good fit for the observed data. Gamma-distribution represents the best probability distribution for collected TTFs. Fitted distribution can be characterized by three parameters: scale, location and shape; referring to Figure 4 they are 0, 24.881 and 0.31 respectively. A shape parameter <1 implies that the TTF rate is not constant with a tendency for more early

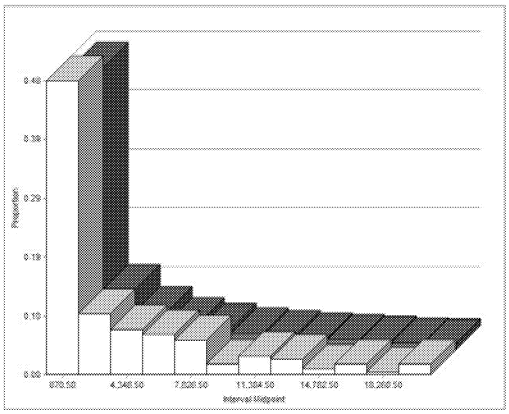

Figure 4: Frequency comparison plot of normalized histograms *(TTFs are reported in seconds)*

failures [14]; this is confirmed by the histograms shown in Figure 4.

The Distribution-Function-Differences Plots are displayed in Figure 5 and Figure 6: the differences have been calculated between the theoretical gamma-distribution and collected data. Small vertical differences (errors) suggest that this model provides a good fit.

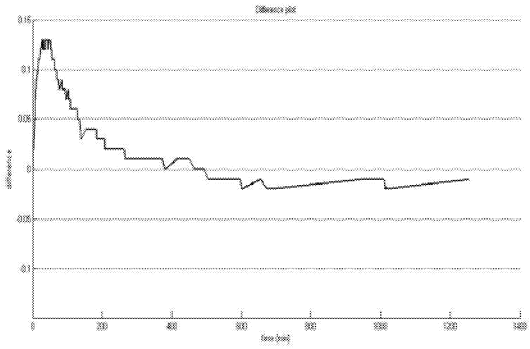

Figure 5: Distribution–Function-Differences *(Used data come directly from the logger system)*

Referring to Figure 5, used data comes from the logger system directly. After the presented methodology application, the same data set has been used for plotting Figure 6. Error trend is similar: the goodness of fit presents the main difference for a small values of TTF and decreases for increasing values. The benefit on the fitting introduced by the proposed methodology can be seen; in fact the difference between the theoretical hypothesized distribution and observed data is reduced . The main difference can be observed among small observations: TTFs shorter than 1 hour (typical maximum value for TTF is more than 16 hours). TTFs which are separated by "*erasing memory events*" are no longer merged; hence the number of long TTFs is also reduced (see Table 3 and Figures 5 and 6).

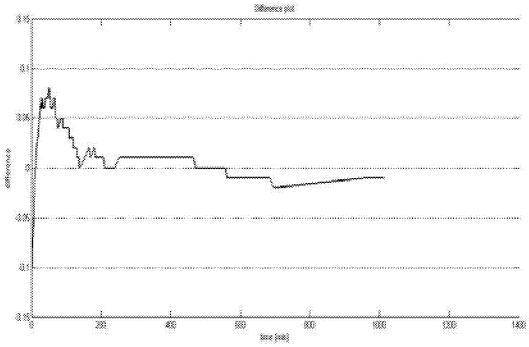

Figure 6: Distribution–Function-Differences *(Used data are processed by the proposed methodology)*

Moreover, performing several tests with different samples coming from the same process, the hypothesized theoretical distributions are always gamma type. On the contrary, using data without the application of any filtering procedure, results in fitted distributions that are not always of the same type. They can be gamma, lognormal, weibull or others according to the particular data sample.

	Raw Data	**Filtered Data**
Observed Data	230	230
Minimum observation (*seconds*)	0	1
Maximum observation (*hours*)	20.91	16.91
Mean (*minutes*)	114	109
Median (*minutes*)	21.85	33.4
Standard devaition (*minutes*)	1.11	0.96
Absolute error mean (*seconds*)	0.0548	0.0465
Error standard deviation by theoretical distribution (*seconds*)	0.06	0.05

Table 3: Data summary comparison

In order to establish methodology efficiency on parameters estimation by inferential statistic tests, four investigations on different sample set have been treated. In Table 4 Shape and Scale parameters are reported for raw^I and $treated^{II}$ samples referring to the same time period.

This data is used to compute a confidence interval and perform a hypothesis test on the difference between two sample means. The difference between shapes and scales means, are 0.15 and 24240 respectively. The results shown in Table 4 prove that the methodology introduced is able to discriminate parameter differences

with a power test of more than 93%, thus confirming methodology effects on fitting theoretical distributions from collected data.

Shape – I	**Scale – I**	**Shape – II**	**Scale – II**
0.238	8489	0.311	6596
0.157	43496	0.263	24881
0.123	79950	0.397	26232
0.201	34380	0.362	11647
mean	*mean*	*mean*	*mean*
0.18	41579	0.33	17339

Table 4: Estimated parameters: raw data *(I)* and treated data *(II)*

Conclusions

To achieve helpful and realistic results in a simulation study it is fundamental to specify correct and realistic TTF and TTR distribution profiles. Starting with data collected from a typical industrial logger system, this paper provides guidelines to obtain, when it is possible, a theoretical distribution that represents a good fit of observed data.

Methodology application effects on collected data are evident, like those confirmed by high values from the power of hypothesised tests to compute a confidence interval of the difference between two population means. Moreover, long TTFs are reduced as a consequence of process memory considerations.

The benefits on simulation results applying the proposed procedure on the observed data are represented by the fact that obtained TTF and TTR distributions are more realistic than raw data, also because they are referred to a normal machine behaviour and memory characteristics, as a consequence, simulation runs have more truthful inputs. Theoretical fitted distribution is no longer dependent on the considered data set, thus confirming the goodness of fitting is improved, as shown by the distribution differences plots and that the fitting error is reduced. During a simulation study, all these considerations imply that we can benefit from all advantages of theoretical probability inputs without making appreciable mistakes.

Acknowledgements

The authors would like to thank Michele Modelli, Stefano Gallerani and Robert Nevin for their cooperation and acknowledge the support of Tetra Pak Packaging Solutions.

References

[1] A.M. Law, W.D. Kelton, *Simulation Modeling and Analysis*, Third edition, McGraw Hill, 2000.

[2] T.J. Banks, J.S. Carson, B.L. Nelson, D.M. Nicol, *Discrete-Event System Simulation*, Fourth edition, Prentice Hall, 2005.

[3] T. Perera, K. Liyanage, *Methodology for rapid identification and collection of input data in the simulation of manufacturing system*, Simulation Pratice and Theory, Vol. 7/7, 2000.

[4] R.W. Bagshaw and S.T. Newman, *Structured approach to the design of a production data analysis facility. Part 1: Conceptual design and information requirements*, International Journal of Production Research, 2001.

[5] M.J. Beach, A.C. Jones, *An integrated manufacturing data management system*, Electronic Manufacturing Technology Symposium, Proceedings of the IEEE, 1990.

[6] T. Perera, K. Liyanage, *IDEF based methodology for rapid data collection*, Integrated Manufacturing Systems, Volume 12/3, Science Direct, 2001.

[7] R.W. Foster, J.E. Kester, *Some considerations for data gathering for simulation data bases*, Aerospace and Electronics Conference, Proceedings of the IEEE, 1990.

[8] C. Bunea, T.A. Mazzuchi, S.Sarkani, *Application of modern reliability database techniques to military system data*, Reliability Engineering & System Safety, Volume 93/1, Science Direct, 2008.

[9] R.A. Johnson, *Miller and Freund's probability and statistics for engineers*, Seventh Edition, Prentice-Hall, 2005.

[10] P. Backus. M. Janakiram, S. Mowzoon, C. Runger, A. Bhargava, *Factory cycle-time prediction with a data-mining approach*, IEEE Transaction on Semiconductor Manufacturing, Vol.19/2, 2006.

[11] L.V. Utkin, *Imprecise reliability of cold standby systems*, International Journal of Quality & Reliability Management, Vol. 20/6, 2003.

[12] D.C. Montgomery, G.C. Runger, *Applied Statistics and Probability for Engineers*, Fourth edition, John Wiley & Sons, 2007.

[13] R.D. Christie, *Statistical Classification of Major Reliability Event Days in Distribution Systems*, IEEE Power Engineering Society Transmission and Distribution, 2001.

[14] M. Evans, N. Hastings, and B. Peacock, *Statistical Distributions*, Third Edition, John Wiley & Sons, 2000.

[15] B.S. Dhillon, N. Yang, *Probabilistic analysis of a maintainable system with human error*, Journal of Quality in Maintenance Engineering, Vol. 1/2, 1995.

[16] P.L. Hall, J.E. Strutt, *Probabilistic physics-of-failure models for component reliabilities using Monte Carlo simulation and weibull analysis: a parametric study*, Reliability Engineering & System Safety, Volume 80, Science Direct, 2003.

EXPANSION OF THE WHOLE WHEAT FLOUR EXTRUSION

Hongyuan Cheng and Alan Friis
Food Production Engineering, National Food Institute
Technical University of Denmark
Søltofts Plads, Building 227, DK-2800, Lyngby, Denmark
E-mail: hyc@bio.dtu.dk

KEYWORDS
Expansion, Extrusion, whole wheat flour, modelling.

ABSTRACT

A new model framework is proposed to describe the expansion of extrudates with extruder operating conditions based on dimensional analysis principle. The Buckingham pi dimensional analysis method is applied to form the basic structure of the model from extrusion process operational parameters. Using the Central Composite Design (CCD) method, whole wheat flour was processed in a twin-screw extruder with 16 trials. The proposed model can well correlate the expansion of the 16 trials using 3 regression parameters. The average deviation of the correlation is 5.9%.

INTRODUCTION

Diets with high amounts of whole grains may help achieve significant weight loss, and also reduce the risk of chronic diseases such as diabetes and cardiovascular disease. Epidemiological studies have shown that increased intakes of whole grain products are associated with reduced risks of diabetes mellitus, hypertension, and cardiovascular disease (Jones, 2000, Slavin, 2004, Katcher et al. 2008). However, most cereal products available in Europe and the United States are produced from highly refined grains, which lead to the loss of many potentially beneficial micronutrients, antioxidants, minerals, phytochemicals, and fiber. Subsequently, the consumption of whole grain is far less than the three servings on a daily basis as suggested by the food pyramid of the United States Department of Agriculture (Slavin, 2004). Whole grain breakfast cereals might contribute to satisfy the recommended daily intake, since they fit to the increasingly fast-paced nature of consumer lifestyles. Breakfast cereals are convenient to prepare and easily consumed. In addition, they appeal to consumers of all income levels (Jones, 2000)

Extrusion cooking has become a well-established industrial technology by offering continuous and flexible processes which allow producing breakfast cereals with diverse textures and shapes and ultimately reducing the costs of the final products. The extrusion cooking process can be analyzed in terms of operational parameters, system and product characteristics. By changing the operational parameters it is possible to influence the time-temperature-shear history of the grain flour in the extruder. System parameters such as specific mechanical energy (*SME*) are generally used to describe the time-temperature-shear history, which affects the extent of biopolymer modification and finally the expansion and texture of extruded products. Although starch is known to be the key biopolymer in extrusion cooking, other ingredients of cereal-based food systems such as proteins, fat or fiber also influence the system and product characteristics, e.g. by competing with starch for water (Moraru and Kokini, 2003). Due to these compositional and structural complexities of the raw material as well as the large number of operational parameters involved in the extrusion process, obtaining the desired extrudate properties, e.g. optimal expansion and texture, is a challenging task and often depends on trial and error experience. The empirical experience is often valid only for the specific extrusion equipment that has been used to generate the good operation conditions.

In practical food industrial applications, one often needs to run some trials in a pilot extrusion process in a new food product development stage. Through the trials, a set of specific operating parameters can be established for the new recipe material extrusion. The procedure sometimes is out of control in the time or raw materials cost frame. In this work, we present an engineering procedure to find out the suitable process parameters to reach correct expansion for whole wheat flour extrusion in a pilot plant, which includes experimental design and process parameter correlation.

EXTRUSION EXPERIMENTS DESIGN

The extrusion experiments design was setup by a traditional way. With considering the extruder limitation, a Central Composite Design (CCD) (Esbensen, 2000) was used in the study, which was based on five levels of three variables (Table 1). The independent extrusion variables considered were barrel temperature in different zones, feed water content and screw speed. All other parameters were kept constant. Operating ranges and five standardized levels were established by preliminary study of each variable. According to the CCD, the experimental plan comprised 15 trials (8 factorial points, 6 axial points and 1 central point).

Table 1 Coded levels for the central composite design

Variables	Levels				
	$-\alpha$	**-1**	**0**	**1**	**$+\alpha$**
T_5, °C	101	111	125	139	149
X_w, %	9.2	10.5	12.5	14.5	15.8
N_s, rpm	208	245	300	355	393

In Table 1, T_5 is the temperature of zone 5 (closest zone to die), °C, X_w is the water content, weight percent, %, N_s is the screw speed, rpm, α equals to 1.682.

In the investigation, the extrudate expansion was set as the objective of the extrusion process operation. Through the experiments, it was expected to develop a quantitative correlation for extrudate expansion and extrusion operating conditions. With the help of the correlation model, the number of runs could be reduced for a similar recipe food extrusion using the whole wheat flour.

EXTRUSION EXPERIMENTS

Whole wheat grain was milled to obtain the whole wheat flour. The whole wheat flour was processed in a Werner & Pfleiderer Continua 37 co-rotating twin-screw extruder. The CCD table, i.e. Table 1, was used to set up 15 experimental runs. First, 15 trials were carried out to search the optimal extrusion conditions for maximum expansion. After the 15 trials, one more run was carried out to obtain the maximum expansion. The last trial conditions were estimated from the response surface methodology. The trial capacity was in 22-27kg/hr levels. In the experimental work, the wheat flour, water and additives are directly fed into extruder without pre-mixing. The extrudates were dried at 110°C for about 10 minutes in a continuous processing oven. The extrudate bulk density was measured during the extrusion operations using weight method for 1 liter extrudates.

MODEL CONSTRUCTION

In decades, many investigations have been carried out for the relationship between extrudate expansion and operating conditions (Alvarez-Martinez, et al. 1988, Cai and Diosady, 1993, Moraru and Kokini, 2003). As the food market is very volatile, food producers have to change their recipe all the time. Sometimes the maximum expansion is the target. In other cases, mild extrusion conditions are expected in order to improve the nutritional quality of products (Singh et al. 2007). A quantitative correlation for the extrudate expansion and operating condition will significant benefit the food extrusion applications.

In these correlations and models, some are based on empirical regression from operating conditions (Ding, et al. 2006). Others use the models from a sort of theories or mechanisms (Fan and Mitchell, 1994). In the empirical regressions, a model is often constructed with linear and quadratic terms according the statistical significant for a specific extrusion process. This kind of model construction normally results in many regression coefficients to be determined from experimental data. No doubt, the empirical equation has played an important role in extrusion product development. However, sometimes the empirical models contain many operating parameters and product properties. The uncertainty of the measurement of the product properties could be very diverse. Thus, the uncertainty can transfer into the empirical correlation model. The mechanism model has a solid theoretic background and is the direction to develop a model to describe the extrusion process operation. However, the mechanism-based model often needs accurate food fluids physical property correlations to support its prediction and estimation for the extrusion process behaviors. Because the food fluids belong to non-Newtonian fluid and have very complicated behaviors, the development of a precise physical property calculation model for such food fluid is very difficult.

In this work, a dimensional analysis based model is proposed to correlate the extrudate expansion and extruder operating conditions. Dimensional analysis method is a classical way in industrial applications to setup a model. In the applications of fluid mechanics and fluid heat transfer, the dimensional analysis method has obtained tremendous successful achievements. However, this method is seldom used to setup the correlation between extrudate expansion and extrusion operating parameters.

Extrudate expansion is a reflection of extrusion equipment design and process operation conditions. The equipment design may include different pre-mixing methods, various screw structures, die design, etc. Because the process operation conditions are the adjustable process control parameters for an existing production line, we will only study the correlation between process operation conditions and extrudate expansion in this work. In an extrusion process, many process parameters have influence on the extrudate expansion, e.g. different zone temperatures, die temperature and pressure, process capacity, screw speed, torque, water content, fluid viscosity, specific mechanical energy, etc. Many researchers have used different methods to correlate the process parameters with extrudate expansion (bulk density) and achieved their successes. In this work, the dimensional analysis method will be applied to analysis and correlate these parameters.

Historically, the dimensional analysis methods include the Rayleigh method and the Buckingham pi method (Buckingham, 1914, Rayleigh, 1915, Perry and Green, 1999). In this work, the Buckingham pi method is applied to construct a model. For an extrusion process, we can find out a set of key variables and their dimensions in the engineering system as below:

T_0, T_d=temperature, T
F_T, F_w=flowrate, mass/time, M/t
N_s=screw speed, 1/time, $1/t$
τ=torque, force·length $F{\cdot}L$
P_d =die pressure, force/length^2 F/L^2
$\overline{\rho}_B$ =density, mass/volume, M/L^3

Here, the units T, M, t, F and L respectively represent temperature, mass, time, force and length. Among the variables, $\overline{\rho}_B$ is the bulk density of extrudates, g/liter, F_w is the water flowrate added into the extruder, kg/hr, F_T is the total flowrate of all feed materials (wheat flour, water and additives), kg/hr, T_d is the die temperature, °C, T_0 is the room temperature (25°C), which is also the raw material initial temperature, P_d is the die pressure, bar, τ is the torque, Nm, N_s is the screw speed, rpm.

From the key extrusion process parameters, a variable and units matrix is formed as shown in Table 2.

Table 2 Selected variables and units matrix

Unit	T_0	T_d	F_T	F_w	N_s	P_d	τ	$\overline{\rho}_B$

T	1	1	0	0	0	0	0	0
M	0	0	1	1	0	0	0	1
t	0	0	-1	-1	-1	0	0	0
F	0	0	0	0	0	1	1	0
L	0	0	0	0	0	-2	1	-3

In the formation of Table 2, we assume that the fluid density just before flash-out from die linearly proportions to the bulk density.

Through calculation, it can be found out that the rank of the matrix shown in Table 2 is 5. The physical variables in Table 2 are 8. From the Buckingham pi theorem, three dimensionless groups can be established from the matrix, which are given as follows:

$$\frac{P_d \cdot F_T}{\overline{\rho}_B \cdot \tau \cdot N_s}, \quad \frac{F_w}{F_T}, \quad \frac{T_d}{T_0}$$

In the studied extrusions process, the term F_w/F_T represents the water content of processing materials. The term T_d/T_0 is the temperature changes of processing materials from its initial condition to the vicinity of flash-out from extruder. The term $\frac{P_d \cdot F_T}{\overline{\rho}_B \cdot \tau \cdot N_s}$ represents the energy added into the processing materials. In fact, the term $\tau \cdot N_s/F_T$ reflects the widely used specific mechanical energy (SME). From the three dimensionless groups, different model expressions can be constructed. In this work, a model is obtained as

$$\overline{\rho}_B = K(X_W)^{\alpha}\left(\frac{T_d}{T_0}\right)^{\beta}\left(\frac{P_d \cdot F_T}{\tau \cdot N_s}\right) \qquad (1)$$

where $\overline{\rho}_B$ is the bulk density of extrudates, g/liter, X_w is the water content of feed material and equals to F_w/F_T, weight fraction. K, α and β are the model coefficients, which need to be determined from experimental data.

From the equation (1), it can be seen that the equation lacks of physical properties of food fluids. Thus it is only suitable to the specific whole wheat flour extrusion. However, the equation is simple and contains only correlation coefficients. The simple format model meets the engineering applications.

Using the data from the 16 runs for whole wheat flour extrusion, the model coefficients are determined as shown in Table 3. The average absolute deviation (AAD) of the model correlation with experimental bulk density data is 5.9%, where AAD is calculated as.

$$\text{AAD} = \frac{1}{n}\sum_n \left[\frac{\overline{\rho}_B^{\text{exp}} - \overline{\rho}_B^{\text{cal}}}{\overline{\rho}_B^{\text{exp}}}\right]\% \qquad (2)$$

In equation (2), n is the number of experimental runs. The model correlation results for the extrudate bulk density are shown in Figure 1. The estimation error distribution of the model for extrudate bulk density is shown in Figure 2. As shown in Figure 2, the bulk density estimation errors are evenly distributed.

Table 3 Coefficients of equation (1)

Coefficient	K	α	β
Value	13508	0.7774	-0.2882

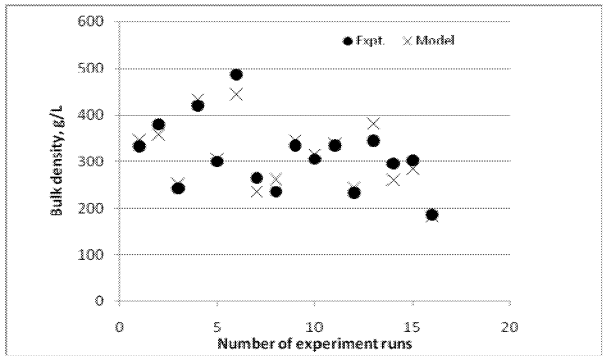

Figure 1: Correlation results of bulk density at different runs

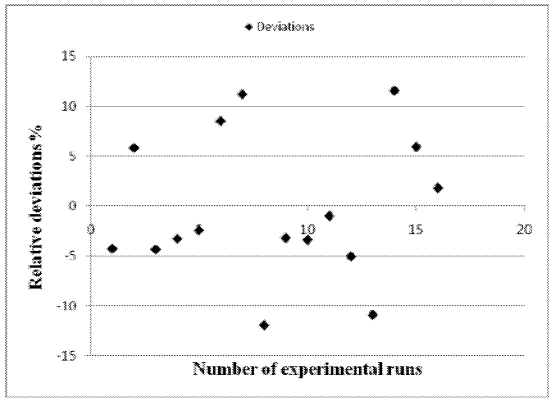

Figure 2: Relative deviations of equation (1) in correlation with bulk density and extusion operating conditions

In Figure 2, the relative deviation (R_d) is calculated as

$$R_d = \frac{\overline{\rho}_B^{\text{exp}} - \overline{\rho}_B^{\text{cal}}}{\overline{\rho}_B^{\text{exp}}}\% \qquad (3)$$

DISCUSSIONS AND CONCLUSIONS

In engineering applications, a simple and reliable model often can help engineers to reach an optimal solution through observing the interactions of different operational parameters. In this work, the model construction is based on the engineering principle. A dimensional analysis method is used to build a model with the key process parameters. From the model one can quantitatively estimate the extrudate bulk density changes with different control parameters and the interactions of these parameters.

The model estimation results show that the proposed can successfully represent the extrudate bulk density in different extruder operating conditions. The average absolute deviation in the estimation of extrudate bulk density is 5.9%.

ACKNOWLEDGMENTS

We acknowledge Hanne T. Pedersen, Jørgen Busk from Danish Technological Institute and Danish Technological Institute for providing its pilot plant, raw materials and technical support in this research work.

REFERENCES

Alvarez-Martinez, L.; K. P. Kndury and J. M. Harper 1988. “A general model for expansion of extruded products.” *Journal of Food Science*, 53, 609-615

Cai, W. and L. L. Diosady. 1993. “Modeling of expansion and water solubility index of wheat starch during extrusion cooking” *Acta Alimentaria*, 22, 181-92.

Buckingham, E. 1914. “On physically similar systems; illustrations of the use of dimensional equations". *Phys. Rev*. 4: 345-376.

Ding, Q.-B.; P. Ainsworth; A. Plunkett; G. Tucker and H. Marson. 2006. “The effect of extrusion conditions on the functional and physical properties of wheat-based expanded snacks”. *Journal of Food Engineering*, 73, 142-148.

Esbensen, K.H. 2000, “Multivariate Data Analysis-in Practice” 4th Ed. CAMO ASA, Oslo, Norway

Fan, J.; J.R. Mitchell; J. M. V. Blanshard. 1994. “A computer simulation of the dynamics of bubble growth and shrinkage during extrudate expansion”. *Journal of Food Engineering*, 23, 337-356.

Jones, J. M., 2000. “Cereal nutrition”. In: Fast, R. B.; Caldwell, E. F.: Breakfast Cereals and how they are made. St. Paul: American Association of Cereal Chemists. p.411-442.

Katcher, H. I.; R.S. Legro; A.R. Kunselman; P.J. Gillies; L.M. Demers; D.M. Bagshaw and P.M. Kris-Etherton. 2008. “The effects of a whole grain-enriched hypocaloric diet on cardiovascular disease risk factors in men and women with metabolic syndrome”. *American Journal of Clinical Nutrition*, 87, 79-90.

Moraru, C. I. and J.L. Kokini. 2003 “Nucleation and expansion during extrusion and microwave heating of cereal foods”. *Comprehensive Reviews in Food Science and Food Safety*, 2, 120-138.

Perry, R.H and D. W. Green. 1999. *Perry’s Chemical Engineers Handbook*, 7th Ed. McGraw-Hill, New York, p.3-89 to 3-90

Rayleigh, 1915. “The principle of similitude”. Nature, 95, 66-68.

Singh, S.; S. Gamlath and L. Wakeling. 2007. “Nutritional Aspects of Food Extrusion: a Review” *International Journal of Food Science and Technology*, 42, 916-929.

Slavin, J. 2004. “Whole grains and human health”. *Nutrition Research Review*, 17, 99-110.

RISK ASSESSMENT MODELLING IN FOOD AND BIOTECHNOLOGY

A META-ANALYSIS STUDY OF THE EFFECT OF CHILLING ON PREVALENCE OF *SALMONELLA* SPP. ON PIG CARCASSES

D. Bergin, U. Gonzales-Barron, F. Butler,
Biosystems Engineering, UCD School of Agriculture, Food Science and Veterinary Medicine,
University College Dublin,
Earlsfort Terrace,
Dublin 2, Ireland,
E-mail: donal.bergin@ucd.ie

KEYWORDS
Meta-analysis, prevalence, *Salmonella*, pork, pig carcass, chilling..

ABSTRACT
Meta-analysis, a body of statistical techniques to systematically synthesise findings from individual studies in order to produce more precise estimates of the effects of particular interventions (treatments) and to obtain a better understanding of the factors originating differences among studies. Because of the systematic and methodical approach of meta-analysis (i.e., individual studies are weighed according to precision) and its reliance on actual data, the output distribution of the relative risk effect size merits consideration for inclusion in the chilling stage of quantitative risk assessments modelling the prevalence of this pathogen along the pork production chain. This is so that policy-makers and decision-makers can access reliable and concise information on effectiveness of interventions to control and prevent food borne illnesses in humans. The objective of this work was to demonstrate the applicability of a parametric approach of meta-analysis to the specific study of the effect of chilling during pork processing on *Salmonella* prevalence on pig carcasses. Two measures of effect size or parameterisations for binary outcomes (relative risk and risk difference) were utilised to perform separate meta-analyses. Both meta-analyses confirmed that the chilling operation has a significant beneficial effect ($P<0.001$) for the reduction in *Salmonella* prevalence on pig carcasses.

INTRODUCTION

Meta-analysis refers to 'the statistical analysis of a large collection of results from individual studies, such as experimental studies, opinion surveys and casual models, for the purpose of integrating the findings' (Glass, 1976).

Yates and Cochran (1938) were the first to conduct what can be thought of a primitive form of synthesising research by systematically combining estimates from different agricultural experiments. However, the introduction of a sole name for this collection of techniques ('meta-analysis' as coined by_techniques ('meta-analysis' as coined by Glass (1976)) appears to have led to an upsurge in the development and application (Whitehead, 2002). The main aim of this demonstration study was to introduce a traditional parametric approach of meta-analysis (which is widely used in meta-analysis of clinical trials) with the purpose of synthesising findings of prevalence studies of pathogens within the food processing chain. Specifically, this study aimed (i) to investigate whether there is support in the sampled population of studies for the causal inference that the chilling stage within pork production had a statistically-significant decreasing effect on *Salmonella* prevalence of pig carcasses; and if so, (ii) to estimate the overall effect of the chilling operation on the studied outcome

METHODOLOGY

As with any statistical analysis, meta-analysis begins with a focused study question. When framing precise questions, three important facets are to be considered: population, intervention or treatment and outcome. The problem statement in this study was the estimation of the overall effect of chilling on the *Salmonella* prevalence of pig carcasses during pork production. The *population* is specified as eviscerated pig carcasses post-meat inspection in slaughterhouses. In this case, the *intervention* or *treatment* is represented by the chilling stage during pork processing, which includes cooling and posterior cold storage (18-24 hours) at ~5°C. The measured *outcome* is the presence of *Salmonella* spp. on the pig carcass surface.

Therefore a database of studies must be screened to certain criteria. The resultant data of interest from the ten individual studies are compiled in Table 1. The data of interest from the ten individual studies are compiled in Table 1. The effect size (θ) refers to the degree to which the hypothetical phenomenon (i.e, decrease in *Salmonella* prevalence due to chilling) is present in the population (i.e, pig carcasses during processing at slaughterhouses). The outcome data are available on n_T pig carcasses in the post-chilling group (treated group) and n_C pig carcasses in the pre-chilling group (control group). The numbers of successes (*Salmonella*-positive carcasses) and failures (*Salmonella*-negative carcasses) in the post-chilling group are given by s_T and f_T, respectively, and in the pre-chilling group by s_C and f_C, respectively. The methodology for paramative *fixed effect* and *random effect* meta-analysis was formulated from

Whitehead (2002). A *fixed-effect* method makes the strong assumption that each study is estimating the same underlying effect size or treatment difference, with a random error that stems only from a chance factor associated with subject-level sampling error (Table 1).

Table 1. Occurrence of *Salmonella*-contaminated pig carcasses before and after chilling as detected in individual studies

Study number	Study reference	Pre-chilling (control)			Post-chilling (treatment)		
		s_C	f_C	n_C	s_T	f_T	n_T
1	Oosterom et al. (1985)	27	183	210	12	198	210
2	Saide et al. (1995)	3	267	270	1	269	270
3	Davies et al. (1999)	7	18	25	3	22	25
4	UCD study (2000)*	3	160	163	1	162	163
5	Quirke et al. (2001)	6	413	419	1	418	419
6	Booteldoorn et al. (2003)	138	232	370	12	63	75
7	Bouvet et al. (2003)	7	113	120	3	117	120
8	Lima et al. (2004)	5	25	30	4	26	30
9	Alban et al. (2005)	6	94	100	4	96	100
10	Teagasc study (2007)**	18	153	171	5	156	161

* Non-published studies from University College Dublin

** Article in preparation, Teagasc

However it is unusual if all studies being meta-analysed produced similar effect size estimates. Essentially, *a random-effects* model relaxes the assumption that each study is estimating exactly the same underlying effect size, and instead includes another random component by assuming that the true effect size in each study is itself a realisation of a random variable (Table 2). To account for the between-study variability, a random-effects meta-analysis was performed, and the standard error and weight values of individual studies were recalculated (Table 3)

RESULTS AND DISCUSSION

Both meta-analyses confirmed that the chilling operation has a significant beneficial effect (P<0.001) for the reduction in *Salmonella* prevalence on pig carcasses. The selection of an appropriate effect size parameterisation is a crucial stage as it highly affects the resulting meta-analysis. For instance, because risk difference is a parameter sensitive to the differences in carcass swab areas and *Salmonella* detection methods varying across studies, its meta-analysis highly reflected this heterogeneity (P<0.001)

Table 2. Fixed-effects meta-analysis for the effect size parameterisation of 'log relative risk' of *Salmonella* presence on pig carcass after chilling in relation to control (before chilling)

Study number	Effect size (θ_i)	Standard error ($se(\theta_i)$)	Relative weight (ω_i)
1	-0.811	0.333	9.021
2	-1.098	1.151	0.754
3	-0.847	0.629	2.524
4	-1.098	1.149	0.757
5	-1.792	1.078	0.861
6	-0.846	0.273	13.42
7	-0.847	0.678	2.176
8	-0.223	0.619	2.609
9	-0.405	0.629	2.521
10	-1.211	0.493	4.107
U = 27.213; (1 df) p<0.001			
Q = 2.953; (9 df) p=0.966			
Overall effect θ: -0.838			
Standard error of overall effect $se(\theta)$: 0.161			

Table 3. Fixed-effects and random-effects meta-analysis for the effect size parameterisation of 'difference in probability' of *Salmonella* presence between chilled pig carcasses and pre-chilled pig carcasses

Study number	Effect size (θ_i)	Fixed effects		Random effects	
		Standard error ($se(\theta_i)$)	Relative weight (ω_i)	Standard error ($se^*(\theta_i)$)	Relative weight (ω_i*)
1	-0.071	0.028	1265.7	0.036	766.2
2	-0.007	0.007	18395	0.024	1755.9
3	-0.160	0.111	81.38	0.113	78.10
4	-0.012	0.012	6745.7	0.026	1507.4
5	-0.012	0.006	25400	0.024	1803.4
6	-0.213	0.049	412.5	0.054	340.2
7	-0.033	0.026	1513.1	0.034	850.3
8	-0.033	0.092	117.9	0.095	111.2
9	-0.020	0.031	1054.8	0.038	683.5
10	-0.074	0.027	1355.6	0.035	798.2
U = 14.042; p<0.001		Overall effect θ: -0.0158		Overall effect θ*: -0.0342	
Q = 28.551; p<0.001		St. error $se(\theta)$: 0.0042		St. error $se(\theta^*)$: 0.0107	
τ^2=0.000515					

In meta-analysis a visual representation of the analysis is called a 'forest plot'. Forest plots use point estimates of the individual studies along with their confidence intervals and may help to reveal discernable patterns in the data among studies. This plot highlights the variability in the estimates and in the precisions between studies. The marker size illustrates the contribution of each study to the overall effect estimate. A visual examination of the forest plot shown in Figures 1 and 2, gives an idea of the small level of discrepancy among studies

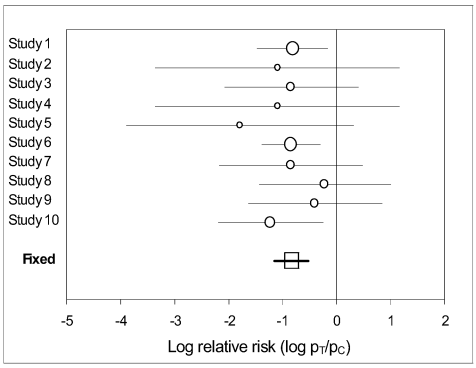

Figure 1. Log relative risk of *Salmonella* presence on pig carcass after chilling (p_T) relative to control (p_C, before chilling). Individual study estimates and overall fixed effects are presented with 95% CI. The circular marker size represents relative weight (ω_i) given to individual studies

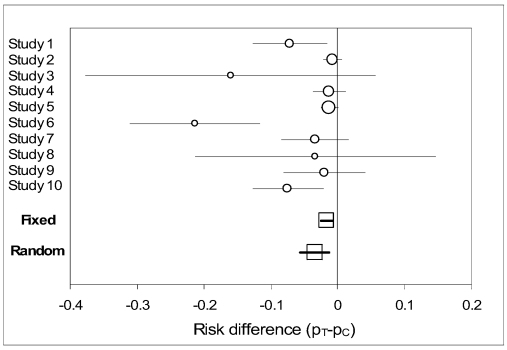

Figure 2. Difference in probability of *Salmonella* presence between chilled pig carcasses (p_T) and pre-chilled pig carcasses (p_C). Individual study estimates and overall fixed and random effects estimates are presented, with 95% CI. The circular marker size represents relative weight corrected for random effects (ω_i^*) given to individual studies

Conclusions

This demonstration study showed how individual studies of a pathogen's prevalence in a relevant stage within the food processing chain can be systematically summarised by means of a traditional parametric approach of meta-analysis.. Also, it has been demonstrated that the effect size parameterisation is an important issue affecting the resulting meta-analysis. For binary outcomes, the effect size measure of relative risk was more adequate than the risk difference, as its meta-analysis, less influenced by the diverse sources of variability among studies, led to a fixed-effects solution, which is more suitable for a meta-analysis based on a small number of individual studies. The parameterisation of relative risk is appropriate from the point of view of risk assessment, as its more precise outcome distribution (reduced uncertainty) of prevalence reduction during chilling can be readily inserted into a quantitative risk assessment modelling *Salmonella* presence along the diverse stages of the pork production process.

Acknowledgements

Safefood, The Food Safety Promotion Board and the Food Institutional Research Measure (FIRM) administered by the Irish
Department of Agriculture and Food are acknowledged for funding this project.

REFERENCES

Botteldorm, N., Heyndrickx, M., Rijens, N., Grijspeerdt, K. and Herman, L. 2002. "Salmonella on pig carcasses: positive pigs and cross contamination in the slaughterhouse". Journal of Applied Microbiology 2003, 95, 891-903.

Davies, R.H., McLaren, I.M. and Bedford, S. (1999)" Distribution of Salmonella contamination in two pig abattoirs~". In Proceedings of the 3rd International Symposium on the Epidemiology and Control of Salmonella in Pork pp. 267–272. Washington DC, USA.

Alban, L., and Stark, K. D. C. 2005. "Where should the effort be put to reduce the *Salmonella* prevalence in the slaughtered swine carcass effectively?". Preventive Veterinary Medicine, 68: 63-79.

Bouvet, J., Bavai, C., Rossel, R., Le Roux, A., Montet, M. P., Mazuy, C., and Vernozy-Rozand, C. 2003. "Evolution of pig carcass and slaughterhouse environment contamination by *Salmonella"*. Revue de Medecine Veterinaire, 154(12): 775-779.

Cochran, W. G. 1954."The combination of estimates from different experiments". Biometrics, 10:101-129.

Glass, G. V. 1976. "Primary, secondary and meta-analysis of research". Educational Researcher, 5 (1, 3): 3-8.

Lima, E. S., Pinto, P. S., Santos, J. L., Vanetti, M. C., Bevilacqua, P. D., Almeida, L. P., Pinto, M. S., and Dias, F. S. 2004. Isolamento de *Salmonella* sp. e *Staphylococcus aureus* no proceso do abate suíno como subsídio ao sistema de análise de perigos e pontos críticos de controle – APPCC. Pesquisa Veterinária Brasileira, 24(4): 185-190. (In Portuguese)

Oosterom, J., Dekker, R., de Wilde, G. J. A., van Kempen-de Troye, F., and Engels, G. B. 1985. "Prevalence of *Campylobacter jejuni* and *Salmonella* during pig slaughtering". The Veterinary Quarterly, 7(1): 31-34.

Quirke, A. M., Leonard, N., Kelly, G., Egan, J., Lynch, P. B., Rowe, T., and Quinn, P. J. 2001. "Prevalence of *Salmonella* serotypes on pig carcasses from high- and low-risk herds slaughtered in three abattoirs". Berlin Munich Tierarztlung und Wissenschaft, 114: 360-362.

Saide-Albornoz, J., Knipe, C. L., Murano, E. A., and Beran, G. W. 1995. "Contamination of pork carcasses during slaughter, fabrication and chilled storage". Journal of Food Protection, 58(9): 993-997.

Whitehead, A. 2002. "Meta-analysis of controlled clinical trials". John Wiley & Sons, West Sussex, England. 319p.

Yates, F., and Cochran, W. G. 1938. "The analysis of groups of experiments". Journal of Agricultural Science, 28(1): 556-580.

A PRELIMINARY SIMULATION MODEL FOR THE PREVALENCE OF *SALMONELLA* spp. DURING PORK PROCESSING IN IRELAND

Ursula Gonzales Barron
Francis Butler
Donal Bergin

School of Agriculture, Food Science and Veterinary Medicine
University College Dublin
Belfield, Dublin 4. Ireland

Sharon Duggan
Deirdre Prendergast
Geraldine Duffy

Food Safety Department

Ashtown Food Research Centre
Dublin 15. Ireland

E-mail: ursula.gonzalesbarron@ucd.ie

KEYWORDS
Pig carcass, pork, prevalence, risk assessment, model, *Salmonella*.

ABSTRACT

Slaughter pigs carrying *Salmonella* are a considerable risk for contamination of the ultimate meat and meat products. As part of a programme to develop a quantitative risk assessment model for *Salmonella* on pork in the Republic of Ireland, this study aimed to estimate the occurrence of *Salmonella* on pig carcasses and pork joints. As a strong association between the proportion of animals carrying *Salmonella* and the proportion of contaminated carcasses at the end of the slaughter line has been observed by numerous researchers; this investigation brought together the results of several relevant studies in order to model a relationship between *Salmonella* prevalence in pigs' caeca and *Salmonella* prevalence on carcasses post-evisceration. The model estimated the *Salmonella* prevalence in pork joints from Irish boning halls to be on average 3.9% (95% CI 1.6-8.2%), and was validated by the results of a large survey (n=720) of *Salmonella* in pork joints (mean 3.3%; 95% CI 2.0-4.6%) carried out in four commercial pork abattoirs as part of this research project. Sensitivity analysis reinforced the importance of final rinsing and chilling as critical points that are very efficient at reducing considerably the occurrence of *Salmonella* on the final product.

INTRODUCTION

Foodborne salmonellosis is a major public health issue in all countries and requires concerted efforts to prevent and control the pathogen in the food supply. In Ireland, *Salmonella enterica* continues to be an extremely significant cause of gastroenteritis, despite a decrease in the number of infections due to salmonellosis in 2005 (357 reported cases) compared to 2004 (419 reported cases) (Anonymous 2005a).

Pork is one of the main sources for human salmonellosis being the source of approximately 5-30% of the human cases in industrialised countries (Hald et al. 2004). The primary source of *Salmonella* infection in swine production, and in the whole food production chain, is the *Salmonella*-infected food-producing animal. In the slaughter process, Botteldoorn et al. (2003) and Berends et al. (1997) estimated that contamination of 30% of *Salmonella*-positive finished carcasses arises from cross-contamination of other infected pigs in the slaughterhouse, and that up to 70% by contamination from the carrier animals themselves. It has been observed by numerous researchers (Vieira-Pinto et al. 2005; Sorensen et al. 2004; Botteldoorn et al. 2003; Quirke et al. 2001; Davies et al. 1999; Berends et al. 1998; Morgan et al. 1987; Oosterom et al. 1985; among others) that there is a strong association between the proportion of animals carrying or excreting *Salmonella* and the proportion of contaminated carcasses at the end of the slaughter line.

This preliminary study aimed to estimate the prevalence of *Salmonella* on pig carcasses and pork joints produced in Ireland using quantitative risk assessment techniques. To this effect, the results of a number of published studies were brought together in order to model a relationship between *Salmonella* prevalence in pigs' caecal contents and *Salmonella* prevalence on carcasses after evisceration, for pig batches entering the abattoir. The following processing stages (splitting and trimming, final washing, chilling and jointing) were modelled using a series of published articles and Irish prevalence surveys. A parallel study on the incidence of *Salmonella* on pork oyster cuts (n=720) produced in the boning halls of commercial pork abattoirs of Ireland was performed in order to validate the model's prevalence output.

METHODOLOGY

Salmonella prevalence in caecal contents of slaughter pigs

The main input parameter of this model was the *Salmonella* prevalence in pigs' caecal contents in Ireland. This distribution was obtained by pooling the results of one non-published study, two scientific articles and the findings of a tracking study of *Salmonella* contamination in pigs from farm to primal cut stage, completed recently as part of this project (Table 1), on the basis that all these studies were

conducted in Ireland and that the microbiological methods for determining *Salmonella* were comparable. The uncertainty about the prevalence of *Salmonella* in the caecal contents of Irish pigs (*Pc*) was modelled using a beta distribution.

$$Pc = Beta(242+1, 1098-242+1)$$

Table 1: Sources of Information of Prevalence of *Salmonella* in Caecal Contents of Pigs in Ireland

Source	Total samples	Positive samples
Tracking study (2006-2007) As part of this project	193	87
Casey et al. (2004)	15	9
Quirke et al. (2001)	419	61
UCD study * (1999-2000)	471	85
Pooled data	1098	242

* Non-published results from University College Dublin, Ireland

Estimation of prevalence of *Salmonella* on eviscerated pigs

A regression analysis between *Salmonella* prevalence in pigs' caecal contents (*Pc*) and *Salmonella* prevalence after evisceration (*Pev*), was performed using data points obtained from seven sources of comparable sampling methodology (six published articles and the tracking study mentioned above, as listed in Table 2). Using classical statistics (Vose 2000), uncertainty was added to the gradient '*m*', the intercept '*c*' of the relationship between the proportion of *Salmonella*-positive caecal samples (*x*) and the proportion of *Salmonella*-positive pig carcasses after evisceration (*y*), and the standard deviation 'σ' of the additional unexplained variation. Thus, the variability of *Pev* was calculated as,

$$Pev = Normal(mPc + c, \sigma) \qquad (1)$$

Contamination factor for splitting and trimming

Cross contamination of *Salmonella* from the splitting machine to the carcass may occur, as implied by Hald et al. (2003), Botteldoorn et al. (2003) and Swanenburg et al. (2001), who reported *Salmonella* contamination on splitting machines in 10 to 33% of the sampling visits to abattoirs. In a simulation model of prevalence of *Salmonella* infection during the production process from live pig on the farm to the final carcass (Alban and Stark 2005), the cross contamination during handling (splitting and trimming) was represented by a triangular distribution based on the authors' best guess. This model produced a prevalence increase of 16% due to handling, from an estimate prevalence of 0.05 after evisceration to an estimate prevalence of 0.058 after splitting and trimming. A higher level of cross-contamination was reported by Davies et al. (1999) where splitting increased *Salmonella* prevalence in 50% (from a prevalence of 0.1333 after evisceration to 0.20 post splitting). In this study, the contamination factor (*Csp*) for splitting and trimming was modelled as a triangular distribution with a minimum value of 0 (no cross-contamination), a mode of 0.16 and a maximum value of 0.50. Assuming that the average cross-contamination of *Salmonella* during splitting and trimming in Irish abattoirs was comparable to the one simulated for Danish abattoirs, and that the findings of Davies et al. (1999) represented the worst-case scenario, the *Salmonella* prevalence on carcasses after splitting and trimming (*Psp*) was calculated as,

$$Csp = Triangle(0, 0.16, 0.50)$$

$$Psp = (1 + Csp) \times Pev$$

Table 2: Data Sources for Regression Analysis to estimate *Salmonella* Prevalence on Eviscerated Carcasses

Source	Proportion of *Salmonella*-positive caecal samples (*x*)	Proportion of *Salmonella*-positive eviscerated carcasses (*y*)
Tracking study (2006-2007) As part of this project	87/193	29/191
Sorensen et al. (2004)	216/1658	159/1665
Kranker et al. (2003)	22/122	6/117
Quirke et al. (2001)	61/419	42/419
Davies et al. (1999)	256/2205	155/2211
Morgan et al. (1987)	71/149	41/150
Morgan et al. (1987)	35/145	19/148
Morgan et al. (1987)	28/151	14/150
Oosterom et al. (1985)	44/210	27/210

Reduction factor for final washing

Previous to chilling, pig carcasses are subject to a final rinse with chlorinated water in order to decrease bacterial and Enterobacteriaceae counts. In Irish abattoirs, the carcass wash water is chlorinated to a residual chlorine level of 0.3-0.5 ppm, and the water pressure is approximately 7-8 bar. Assuming that the average level of *Salmonella* decontamination for final washing achieved in a common Irish abattoir can be closely approached by the UK data from Davies et al. (1999) – combining the results from the two abattoirs, *Salmonella* positive samples before final rinsing were 15 out of 75, and positive samples at the entrance to chiller were 9 out of 79 – a reduction factor for final washing (*Rw*) could be modelled from these data. The prevalence of *Salmonella* on pig carcasses after washing (*Pw*) was, therefore, the multiplication of the reduction factor for washing (*Rw*) by the prevalence of *Salmonella* on pig carcasses after splitting and trimming (*Psp*).

$$Rw = \frac{Beta(9+1, 79-9+1)}{Beta(15+1, 75-15+1)}$$

Reduction factor for chilling

A reduction effect of chilling on the recovery of *Salmonella* from pork carcasses has been observed by several researchers. Data on *Salmonella* prevalence on pig carcasses before chilling and after chilling (~5°C, 18-24 h) were taken from seven published studies (Lima et al. 2004; Botteldoorn

et al. 2003; Bouvet et al. 2003; Quirke et al. 2001; Davies et al. 1999; Saide-Albornoz et al. 1995; Oosterom et al. 1985), and two non-published studies (Tracking study 2006-2007; and UCD study 1999-2000). A distribution of the overall relative risk for chilling (*Rch*), a measure of effect size of the chilling operation defined as the probability of encountering *Salmonella*-positive carcasses after chilling relative to the probability of encountering *Salmonella*-positive carcasses before chilling, was estimated using a parametric fixed-effects meta-analysis technique (a detailed explanation is given in Bergin et al. (2008)).

$$Rch = e^{Normal(-0.868, 0.166)}$$

$$Pch = Rch \times Pw$$

Contamination factor in boning halls

Berends et al. (1998) estimated that the contribution of inadequate cleaning and disinfection on any given day is about 9-13% with respect to all contamination that occurs during a full working day. In other words, when *Salmonella*-positive carcasses are being processed, up to ~90% of all cross contamination during cutting is unavoidable, and the remaining ~10% results from *Salmonella*-positive carcasses being processed earlier that day while cleaning and disinfection had been inadequate. In a survey of *Salmonella* contamination in boning halls (carried out in four Irish abattoirs), *Salmonella* in conveyor belts was detected in 2 out of 9 visits (22%). Thus, assuming that cleaning and disinfection is carried out 2-4 times a day (*Np*) (Berends et al. 1998), the probability that cleaning and disinfection is carried out incorrectly at least once a day (p_{icd}) was calculated as,

$$p_{icd} = 1 - (1 - Uniform(0\ ,\ 0.22))^{Np}$$

$$Np = Discrete(\{2,3,4\}, \{1,1,1\})$$

and, considering the contribution of inadequate cleaning and disinfection (9-13%) to the final prevalence, the increase in *Salmonella* prevalence during jointing (C*j*) is,

$$Cj = p_{icd} \times Uniform(0.09\ ,\ 0.13)$$

Therefore, the prevalence of *Salmonella* in pork joints (*Pj*), which is the ultimate model output, was estimated as,

$$Pj = Pch \times (1 + Cj)$$

Model validation

In order to assess its predictability, the model was validated using the results of an extensive survey of *Salmonella* prevalence in pork joints produced in the boning halls of four representative Irish abattoirs. The survey, carried out over 12 visits, revealed 24 positive samples out of 720 (3.3%). The model was developed in Microsoft Excel using the @Risk add-in (Industrial Edition version 4.5.2, Palisade, NY), and run for 10 000 iterations using Latin Hypercube sampling.

RESULTS AND DISCUSSION

The pool of Irish surveys on *Salmonella* prevalence in caecal contents of pigs (Table 1) led to an estimate of 0.22 (95% CI: 0.20-0.25; Table 3). At individual pig level at slaughterhouse, the *Salmonella* prevalence of pigs in Europe has been reported to vary widely (3-40%). The relatively high estimate rate of *Salmonella* present in caeca of slaughter pigs in Ireland appears to be common in other countries such as UK and France. Whereas in a UK national survey of 34 pig abattoirs in England, Scotland and Wales (Davies et al. 2004), 23% (578/2509) of the caecal samples were *Salmonella* positive; Beloeil et al. (2004), sampling from 18 French slaughterhouses, found that 24.8% (256/1030) of caecal samples tested positive for *Salmonella*. However, other studies have reported significantly lower *Salmonella* prevalence in caeca. Some of these differences may be related to the presence and severity of application of national programmes for *Salmonella* control at farm level. These programmes appear to be effective, producing much lower incidences of *Salmonella* in finished pigs being dispatched for slaughter. For instance, while Letellier et al. (1999), sampling from 6 slaughterhouses in Canada, found that 5.2% (74/1420) of pigs coming from 223 herds carried *Salmonella* in caecal contents; a national survey carried out in Denmark after the Danish National *Salmonella* Control Policy had been operating for 4 years, identified *Salmonella* in 3.4% (612/17987) of the caecal content samples (Christensen et al. 1999).

Table 3: Mean, Standard Deviation and Confidence Intervals (95% CI) for the Model's Prevalence Values

Prevalence	Mean (Standard deviation)	95% CI
Caecal (Pc)	0.221 (0.0125)	[0.197 0.246]
After evisceration (Pev)	0.114 (0.0052)	[0.104 0.125]
After splitting (Psp)	0.140 (0.0134)	[0.117 0.168]
After washing (Pw)	0.086 (0.0345)	[0.037 0.171]
After chilling (Pch)	0.034 (0.0214)	[0.010 0.090]
After jointing (Pj)	0.039 (0.0170)	[0.016 0.082]

Figure 1 illustrates the role of uncertainty about the regression parameters (Eq. 1) for the estimation of *Salmonella* prevalence on eviscerated pig carcasses. Each thin line represents the variability in *Pev* determined from the particular sampled values of '*m*' and '*c*', and the bold line represents the averaged effect of uncertainty and variability. The model output of *Salmonella* prevalence after evisceration (11.4%; Table 3) was numerically close to the results of Pearce et al. (2004) who recovered 10% (2/20) positive swabs after evisceration from an Irish slaughterhouse. The prevalence of *Salmonella* on pig carcasses after splitting and trimming was estimated to be on average 14%. A comparable proportion of positive swabs after splitting and trimming was recovered from a large

abattoir in the UK (14% (7/50); Davies et al. 1999), while a higher proportion of 16.7% (5/30) of carcasses tested positive for *Salmonella* after splitting in a large abattoir in Brazil (Lima et al. 2004).

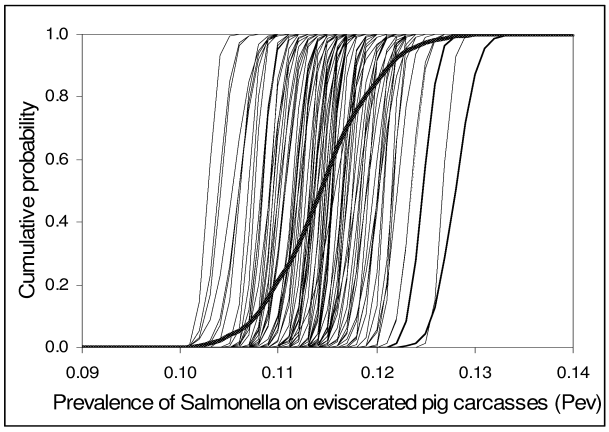

Figure 1: Cumulative Probability Distribution for Prevalence of *Salmonella* on Pig Carcasses after Evisceration

In this simulation study, the final rinsing of carcasses with pressurised chlorinated water was estimated to reduce significantly the *Salmonella* prevalence on carcasses in 38%. Quirke et al. (2001) observed that final washing decreased the *Salmonella* prevalence in 55% on those carcasses originated from pigs belonging to low-risk herds. Notice that, although this is a relevant Irish data source, it was not used for the model as carcasses were not sampled randomly in that trial but according to their herd status category. Thus, at the end of the slaughter line, before chilling, the *Salmonella* prevalence on carcasses of Irish abattoirs was estimated to be ~8.6% (Table 3). Although figures are not directly comparable since detection methods are not fully harmonised among countries, the presence of *Salmonella* on finished pig carcasses (pre-chilling) in European slaughterhouses seems to be variable. Higher values of prevalence (11-37%) have been reported in several Belgian abattoirs (Korsak et al. 2003; Botteldoorn et al. 2003; Korsak et al. 1998). In contrast, from seven slaughterhouses in four western European countries, *Salmonella* was isolated from only 3.8% (62/1623) of the finished carcasses ranging from 1-8% among slaughterhouses (Hald et al. 2003). A larger study carried out in seven large German abattoirs – all located in different states – reported that about 4.7% (564/11942) of the carcass swabs were *Salmonella* positive (Kasbohrer et al. 2000). Similarly, a UK national survey, sampling from 34 pig abattoirs in England, Scotland and Wales, found a proportion of 5.3% (134/2509) *Salmonella*-contaminated carcasses at the end of the slaughter line (Davies et al. 2004).

This model utilised the results of a meta-analysis – applied to a series of previous findings on the effect of chilling – which accounted for the differences among reduction ratios of *Salmonella* prevalence, originating from differences in chilling parameters such as air speed, air flow, relative humidity, temperature profiles for individual carcasses and carcass spacing, as well as microbiological culture methods. This simulation estimated a prevalence of *Salmonella* on chilled pig carcasses of 3.4% (Table 3). This value is equivalent to the results of Bouvet et al. (2003), who sampling carcasses after chilling from three French slaughterhouses, found that 3.3% (6/182) of the carcass swabs were *Salmonella* positive. Within the 95% CI estimated from this simulation (1-9%), also lie the prevalence of 5.7% (12/210) found by Oosterom et al. (1985) and the prevalence of 1.4% (3/213) found by Swanenburg et al. (2001), both from Dutch slaughterhouses.

The cross-contamination factor for jointing (*Cj*) increased the *Salmonella* prevalence to 3.9% (95% CI of 1.6 – 8.2%; Table 3). The shape of the output distribution for the prevalence of *Salmonella* in pork joints produced in Irish boning halls is shown in Figure 2 ('Regressional model'). For reference, the output distribution of a previous simulation model developed by the authors (Gonzales Barron et al. 2007) is also shown in Figure 2. This model ('Stage-by-stage') estimated the *Salmonella* prevalence in pork joints without the use of regression analysis and meta-analysis, but instead by following the changes in *Salmonella* occurrence along each of the pig slaughter process (including scalding, hair removal operations, evisceration, splitting and trimming, final washing, chilling and jointing). The output distribution of the 'regressional' model, in contrast to the 'stage-by-stage' model, was shifted to the right and had a much shorter right tail.

For validation, a sample of 720 pork oyster cuts from the boning halls of four commercial pig abattoirs was analysed for the presence of *Salmonella*. This survey detected a prevalence of 3.33% (24/720) with a 95% CI of 2.02 to 4.64%. The mean values for the simulation (3.9%) and the survey were similar, although the simulated distribution was considerably wide and skewed ('Regressional model' in Figure 2). In support to the distribution shape found by simulation, a key finding from the validation survey was the substantial variation in the prevalence of *Salmonella* on the different days, either morning or afternoon, ranging from 0 to 6.6%. Additionally, according to a zoonoses monitoring survey in Ireland (Anonymous 2005b), the estimated prevalence of *Salmonella* in fresh pork meat at processing plants was on average 1.8% (51/2841).

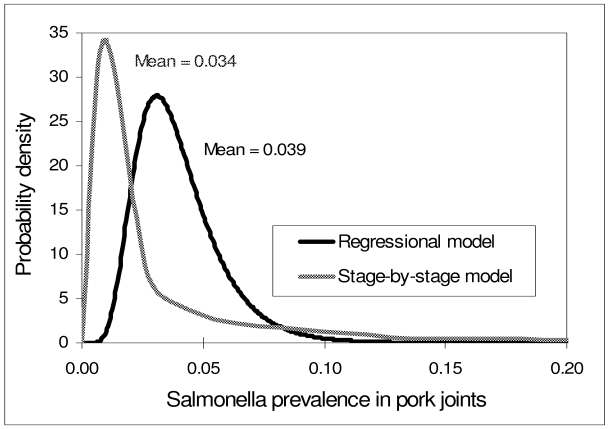

Figure 2: Distribution of *Salmonella* Prevalence in Pork Joints in Ireland as an output of the Regressional Model in contrast to a previously-developed Stage-by-Stage Model

In an attempt to identify the key parameters that have more influence on the model's output, a sensitivity analysis was performed. The sensitivity of the prevalence of *Salmonella* in pork joints to input values was measured by rank correlation, whereby the higher the correlation between the input and the output, the more significant the input is in determining the output's value. The sensitivity analysis showed that the inputs having the greatest impact on *Salmonella* prevalence were the reduction at washing (*Rw*) and the reduction at chilling (*Rch*) (Figure 3). Thus, other model inputs, different from the *Salmonella* prevalence in caecal contents (*Pc*), had stronger influence on the final prevalence on pork joints, which reassuringly implies that subsequent processing stages, when properly performed, can play a significant role in reducing (washing and chilling) and controlling (splitting) the total carcass contamination in the abattoir. Such observations led to the reaffirmation that chilling (as previously proposed by Bolton et al. (2002)) and final washing (as shown by Saide-Albornoz et al. (1995) and Quirke et al. (2001)), should be regarded as critical points in the slaughter process since they all are very efficient at reducing significantly the prevalence of *Salmonella* on the final product.

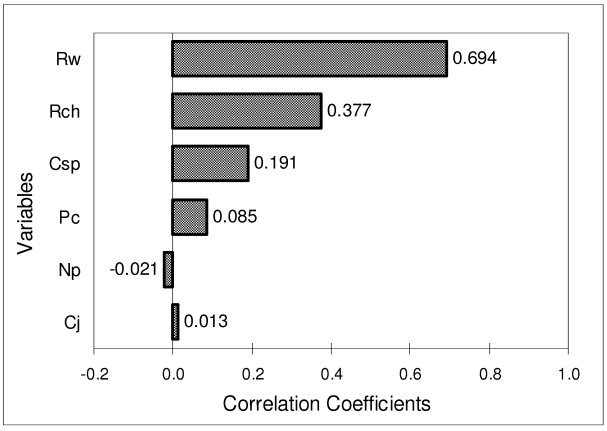

Figure 3: Sensitivity of the Prevalence of *Salmonella* in Pork Joints to the Uncertainty of Individual Variables

A mathematical model is as good as the data it is fed with and, for a more accurate risk assessment model, further research is necessary. Due to unavailable data from lack of research in certain areas, the main simplifying assumption made in order to develop this model was the correlation between the proportion of pigs carrying *Salmonella* in their caeca and the proportion of *Salmonella*-positive carcasses post-evisceration. Nevertheless, given the good agreement between the model prediction of *Salmonella* prevalence on pork joints, and the results of a parallel surveillance study, it can be said that this preliminary model, integrating input distributions justified by relevant research and surveys, approximates well the reality of Irish pig abattoirs.

CONCLUSIONS

A risk assessment model that estimates the prevalence of *Salmonella* on pig carcasses and pork joints was developed on the simplifying assumption that the occurrence of *Salmonella*-infected carcasses post-evisceration is proportional to the total contamination introduced by the carrier animals themselves entering the slaughterline. The model output for the *Salmonella* prevalence on pork joints produced in boning halls was successfully validated with the results of an extensive survey carried out in four representative Irish abattoirs. While the model predicted a proportion of *Salmonella*-contaminated pork joints of 3.9%, the survey detected *Salmonella* in 3.3% (24/720) of the pork oyster cuts. The sensitivity analysis showed that the stages of final washing and chilling had strong impact on the prevalence of *Salmonella* on pork joints, meaning that these subsequent processing stages are critical as a means of significantly improving the microbiological quality of pork.

ACKNOWLEDGEMENTS

The authors wish to acknowledge *Safe*food, The Food Safety Promotion Board and the Food Institutional Research Measure (FIRM) administered by the Irish Department of Agriculture and Food. The authors also wish to acknowledge the partial financial support of QPORKCHAINS, an EU 6th Framework project.

REFERENCES

Alban, L., and K. D. C. Stark. 2005. "Where should the effort be put to reduce the Salmonella prevalence in the slaughtered swine carcass effectively?" *Preventive Veterinary Medicine* 68, 63-79.

Anonymous. 2005a. *Annual Report of the Health Protection Surveillance Centre of Ireland*. HPSC, Ireland. ISSN 1649-0436. Available from: http://www.ndsc.ie/hpsc/AboutHPSC/AnnualReports/File,2141,en.pdf

Anonymous. 2005b. *The community summary report on "trends and sources of zoonoses and zoonotic agents in humans, antimicrobial resistence and foodborne outbreaks in the European Union in 2005"*. The EFSA Journal, 94. Available from: http://www.efsa.europa.eu/etc/medialib/efsa/science/monitoring_zoonoses/reports/zoonoses_report_2005.Par.0001.File.dat/Zoonoses_report_2005.pdf

Beloeil, P. A., C. Chauvin, K. Proux, F. Madec, P. Fravalo and A. Aliom. 2004. "Impact of the Salmonella status of market-age pigs and the pre-slaughter process process on Salmonella caecal contamination at slaughter". *Veterinary Research* 35, 513-530.

Berends, B. R., F. Van Knapen, D. A. A. Mossel, S. A. Burt and J. M. A. Snijders. 1998. "Salmonella spp. on pork at cutting plants and at the retail level and the influence of particular risk factors". *International Journal of Food Microbiology* 44, 207-217.

Berends, B. R., F. Van Knapen, J. M. A. Snijders and D. A. A. Mossel. 1997. "Identification and quantification of risk factors regarding Salmonella spp. on pork carcasses". *International Journal of Food Microbiology* 36, 199-206.

Bergin, D., U. Gonzales Barron and F. Butler. 2008. "A meta-analysis study of the effect of chilling on prevalence of Salmonella spp. on pig carcasses". *Journal of Food Protection* (submitted).

Bolton, D. J., R. A. Pearce, J. J. Sheridan, I. S. Blair, D. A. McDowell and D. Harrington. 2002. "Washing and chilling as critical control points in pork slaughter hazard analysis and critical control point (HACCP) systems". *Journal of Applied Microbiology* 92, 893-902.

Bouvet, J., C. Bavai, R. Rossel, A. Le Roux, M. P. Montet, C. Mazuy and C. Vernozy-Rozand. 2003. "Evolution of pig

carcass and slaughterhouse environment contamination by Salmonella". *Revue de Medicine Veterinaire* 154, No.12, 775-779.

Botteldoorn, N., M. Heyndrickx, N. Rijpens, K. Grijspeerdt and L. Herman. 2003. "Salmonella on pig carcasses: positive pigs and cross contamination in the slaughterhouse". *Journal of Applied Microbiology* 95, 891-903.

Casey, P. G., D. Butler, G. E. Gardiner, M. Tangney, P. Simpson, P. G. Lawlor, C. Stanton, R. P. Ross, C. Hill and G. F. Fitzgerald. 2004. "Salmonella carriage in an Irish pig herd: correlation between serological and bacteriological detection methods". *Journal of Food Protection* 67, No. 12, 2797-2800.

Christensen, J., D. L. Baggessen, V. Soerensen and B. Svensmark. 1999. "Salmonella level of Danish swine herds based on serological examination of meat-juice samples and Salmonella occurrence measured by bacteriological follow-up". *Preventive Veterinary Medicine* 40, 277-292.

Davies, R. H., I. M. McLaren and S. Bedford. 1999. "Distribution of Salmonella contamination in two pig abattoirs". In: *Proceedings of the 3rd International Symposium on the Epidemiology and Control of Salmonella in Pork* (Washington, Aug. 4-7). 267-272 p.

Davies, R. H., R. Dalziel, J. C. Gibbens, J. W. Wilesmith, M. B. Ryan, S. J. Evans, C. Byrne, G. A. Paiba, S. J. S. Pascoe and C. J. Teale. 2004. "National survey for Salmonella in pigs, cattle and sheep at slaughter in Great Britain (1999-2000)". *Journal of Applied Microbiology* 96, 750-760.

Gonzales Barron, U., D. Bergin, F. Butler, D. Prendergast, S. Duggan and G. Duffy. 2007. "A preliminary risk assessment of prevalence of Salmonella spp. during pork processing in the Republic of Ireland". In *Proceedings of the 5th International Conference Predictive Modelling in Food* (Athens, Sep. 16-19). APM897.

Hald, T., A. Wingstrand, M. Swanenburg, A. von Altrock and B. M. Thorberg. 2003. "The occurrence and epidemiology of Salmonella in European pig slaughterhouses". *Epidemiology and Infection* 131, 1187-1203.

Hald, T., D. Vose, H. Wegener and T. Koupeev. 2004. "A Bayesian approach to quantify the contribution of animal-food sources to human salmonellosis". *Risk Analysis* 24, No. 1, 255-269.

Kasbohrer, A., D. Protz, R. Helmuth, K. Nockler, T. Blaha, F. Conraths and L. Geue. 2000. "Salmonella in slaughter pigs of German origin: an epidemiological study". *European Journal of Epidemiology* 16, 141-146.

Korsak, N., G. Daube, Y. Ghafir, A. Chahed, S. Jolly and H. Vindevogel. 1998. "An efficient sampling technique used to detect four foodborne pathogens on pork and beef carcasses in nine Belgian abattoirs". *Journal of Food Protection* 61, 535-541.

Korsak, N., B. Jacob, B. Groven, G. Etienne, B. China, Y. Ghafir and G. Daube. 2003. "Salmonella contamination of pigs and pork in an integrated pig production system". *Journal of Food Protection* 66, No. 7, 1126-1133.

Kranker, S., L. Alban, J. Boes and J. Dahl. 2003. "Longitudinal study of Salmonella enterica serotype Typhimurium infection in three Danish farrow-to-finish swine herds". *Journal of Clinical Microbiology* 41, No. 6., 2282-2288.

Letellier, A., S. Messier and S. Quessy. 1999. "Prevalence of Salmonella spp. and Yersinia enterocolitica in finishing swine at Canadian abattoirs". *Journal of Food Protection* 62, No. 1, 22-25.

Lima, E. S., P. S. Pinto, J. L. Santos, M. C. Vanetti, P. D. Bevilacqua, L. P. Almeida, M. S. Pinto and F. S. Dias. 2004. "Isolamento de Salmonella sp. e Staphylococcus aureus no proceso do abate suíno como subsídio ao sistema de análise de perigos e pontos críticos de controle – APPCC". *Pesquisa Veterinária Brasileira* 24, No. 4, 185-190. (In Portuguese).

Morgan, I. R., F. L. Krautil and J. A. Craven. 1987. "Effect of time in lairage on caecal and carcass Salmonella contamination of slaughter pigs". *Epidemiology and Infection* 98, 323-330.

Oosterom, J., R. Dekker, G. J. A. de Wilde, F. van Kempen-de Troye and G. B. Engels. 1985. "Prevalence of Campylobacter jejuni and Salmonella during pig slaughtering". *The Veterinary Quarterly* 7, No. 1, 31-34.

Pearce, R. A., D. J. Bolton, J. J. Sheridan, D. A. McDowell, I. S. Blair and D. Harrington. 2004. "Studies to determine the critical control points in pork slaughter hazard analysis and critical control point systems". *International Journal of Food Microbiology* 90, 331-339.

Quirke, A. M., N. Leonard, G. Kelly, J. Egan, P. B. Lynch, T. Rowe and P. J. Quinn. 2001. "Prevalence of Salmonella serotypes on pig carcasses from high- and low-risk herds slaughtered in three abattoirs". *Berlin Munich Tierarztlung und Wissenschaft* 114, 360-362.

Saide-Albornoz, J., C. L. Knipe, E. A. Murano and G. W. Beran. 1995. "Contamination of pork carcasses during slaughter, fabrication and chilled storage". *Journal of Food Protection* 58, No. 9, 993-997.

Sorensen, L. L., L. Alban, B. Nielsen and J. Dahl. 2004. "The correlation between Salmonella serology and isolation of Salmonella in Danish pigs at slaughter". *Veterinary Microbiology* 101, 131-141.

Swanenburg, M., H. A. P. Urlings, J. M. A. Snijders, D. A. Keuzenkamp and F. van Knapen. 2001. "Salmonella in slaughter pigs: prevalence, serotypes and critical control points during slaughter in two slaughterhouses". *International Journal of Food Microbiology* 70, 243-254.

Vieira-Pinto, M., P. Temudo and C. Martins. 2005. "Occurrence of Salmonella in the ileum, ileocolic lymph nodes, tonsils, mandibular lymph nodes and carcasses of pigs slaughtered for consumption". *Journal of Veterinary Medicine* B52, 476-481.

Vose, D. 2000. *Risk Analysis: a Quantitative Guide*. 2nd Ed. J. Wiley. Chichester, England.

A COMPARISON OF DETERMINISTIC AND STOCHASTIC EPIDEMIC MODELS FOR THE RISK ASSESSMENT OF SALMONELLA AT THE PREHARVEST LEVEL OF PORK PRODUCTION

Ilias Soumpasis
Francis Butler

School of Agriculture, Food Science and Veterinary Medicine
University College Dublin
Belfield, Dublin 4, Ireland
E-mail: {ilias.soumpasis|f.butler}@ucd.ie

KEYWORDS
Farm, Pig, Risk Assessment, Salmonella, Simulation

ABSTRACT

For the last years there has been an increasing interest in microbial food safety and some efforts have been put into modelling Salmonella Typhimurium at the preharvest part of the pig food chain, the farm. Transmission of S. Typhimurium at the farm level is a dynamic process and a good approach is to model it using epidemic models. In this paper we use two different types of model to describe the dynamics of S. Typhimurium at farm, one deterministic and one stochastic and try to validate we aim to validate them using the results of an experimental infection. The results of each of the modelling techniques are discussed and compared. Deterministic models are used for modelling infectious diseases at big populations while at pig farm and pen level stochastic models seem to be more appropriate. Demographic event-driven stochasticity gives variation to the results and seems to explain the actual fluctuations of Salmonella prevalence of batches of pigs from the same farms arriving to slaughterhouse. The need for systematic sampling at slaughterhouse or farm level is drawn and future work towards enrichment of the models in order to predict most common real life scenarios is proposed.

INTRODUCTION

For the last years there has been an increasing interest in food-born diseases and much of the research effort is directed towards the assurance of food safety. Salmonella *enteritis* serovar Typhimurium (S. Typhimurium) is considered the second most commonly human isolated serovar and it is the most commonly isolated serovar from pigs (Hill et al., 2007). Thus there were already some efforts to model the transmission of S. Typhimurium in grower-finishing pig-farms either using differential equations (Ivanek et al. 2004; Hill et al. 2007) or using a discrete time stochastic state-transition approach as a part of a holistic farm-to-fork model (van der Gaag et al. 2004). The pork supply chain can be divided into four parts: consumption (consumer stage), processing and retail (boning through retail stages), harvest (transporting finishing pigs through the slaughtering stages) and preharvest (breeding through finishing stages) (van der Gaag and Huirne, 2002). Different parts of the chain are governed by different dynamics, thus they should be modelled with different techniques. Previous studies (van der Gaag and Huirne 2002; Alban and Stärk 2005) indicated that the preharvest stage is of great importance in controlling the prevalence and the population of S. Typhimurium at the final product.

The main effort of this paper is to demonstrate a way of exploring the dynamics of S. Typhimurium in pig farms and identify gaps of knowledge. Understanding the way S. Typhimurium transmits in the farm and from farm to farm will provide the ability to calculate an estimate of the prevalence at a national level and to propose ways of controlling it. Therefore, we will present two different approaches for modelling S. Typhimurium dynamics in pig farms, a deterministic and a stochastic one, and make a comparison of the results. Moreover we will try to show why the stochastic method seems more appropriate in the case of pig farms and answer to questions addressed by the academic community about the source of the actual fluctuations of Salmonella prevalence of batches of pigs from the same farm. We will not go too far into the parameterization of the models, but we will use simple inputs already published or used in the literature, because otherwise it would be out of the scope of this paper.

The model was written in Python programming language v.2.5.1 (van Rossum 2007) using scipy/numpy libraries (Jones et al. 2001) for numerical calculations and solution of the differential equations and matplotlib/pylab libraries (Hunter 2007) for plotting. The algorithm for the solution of the differential equations uses lsoda from the FORTRAN library odepack (Hindmarsh 1983; Petzold 1983).

THE DETERMINISTIC EPIDEMIC MODEL

The main objective of this work is to produce realistic and reliable model using parameters from experimental infections. In order to validate the models the results of the Nielsen et al. (1995) were used. Following the work of Kermack and McKendrick (1927) we will try to make a dynamic epidemic model that is consisted from seven classes and is a set of seven ordinary differential equations. The main model should be a four class SEIR (Susceptible - Exposed - Infectious - Recovered) model. However in the experiment made by Nielsen et al. (1995) there was already an experimental infection with a highly infectious dose; thus we can not consider that we start with a susceptible class (there are no susceptible animals at day 0). Moreover, it is clear that recovered pigs lose their immunity after a period of time and they can become susceptible again. The immunity a pig can earn from the infection of S. Typhimurium is not lifelong and the resistance to disease rests primarily on cell-

mediated immunity; this is one of the reasons a vaccination seems to not have any positive results (Straw et al.2006 p.751). It is argued that pigs already infected once can have different response as shorter infectious periods (due to faster seroconversion) or prolonged recovered periods (antibodies are circulating for more time) (van der Gaag and Huirne 2002; van der Gaag et al. 2004). So it is a good idea reinfected animals to be modelled as separate classes as second generation (2G) because of the different parameters that maybe used. Our model is consisted of the following seven classes:

- Exposed (E)
- Infectious (I)
- Recovered (R)
- Susceptible (S)
- Exposed 2G (E1)
- Infectious 2G (I1)
- Recovered 2G (R1)

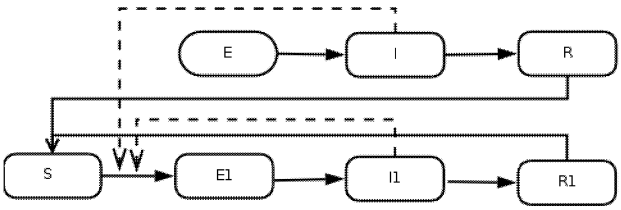

Figure 1: Classes of the model

The total number of pigs (N) is 37, the same as the total number of the field experiment (Nielsen et al. 1995). At time 0 all classes have 0 animals except of the Exposed (E) which has 37 animals. Figure 1 illustrates the movement from class to class (solid lines) and also the influence of classes I and I1 to the rate of movement from class S to E1. Although S. Typhimurium is known to be transmitted through faeces, meaning that a new class describing the survival of the microbe in the environment might be added, it does not seem to be needed, possibly because of the cleaning procedures and the design of the experiment. It is safe to assume that for the time step of one day, S. Typhimurium population in the environment drops below a critical level for infection. The equations of the model are:

$$
\begin{aligned}
dE/dt &= -\,sigma * E \\
dI/dt &= sigma * E - gamma * I \\
dR/dt &= gamma * I - kapa * R \\
dS/dt &= kapa * (R + R1) - beta * S * (I + I1) / N \\
dE1/dt &= beta * S * (I + I1) / N - sigma * E1 \\
dI1/dt &= sigma * E1 - gamma2 * I1 \\
dR1/dt &= gamma2 * I1 - kapa * R1
\end{aligned}
\qquad (1)
$$

The parameters sigma, gamma, gamma2 and kapa are the rates at which pigs are moving from one class to the next and they were calculated from Fedorka-Cray et al. (1994), Wood et al. (1989) and Nielsen et al. (1995). These rates correspond to the inverse of period of the time that a pig remains in certain class (Table 1). The parameter beta is the transmission rate of infection and was adopted from van der Gaag and Huirne (2002). The size of population was 37 pigs which were in the Exposed class (E) at day 0. This model was run for 108 days, the follow-up period reported in Nielsen at al. (1995).

The results of the model are shown in Figure 2. Classes E, I and R were added to E1, I1, and R1, respectively. Although the parameterisation seems to be arbitrary, the model appears to explain in a great degree and predict closely the real situation. The values from the deterministic model we developed are in agreement with the critical values extracted from the article of Nielsen et al. (1995).

Table 1: Rates of the model

Rates	Explanation	Value
beta	Transmission rate of infection	0.07
sigma	Rate of moving from Exposed to Infectious class (1G and 2G)	1
gamma	Recovery rate	1/18
gamma1	Recovery rate (2G)	gamma*2
kapa	Rate of moving from Recovered to Susceptible Class (1G and 2G)	1/197

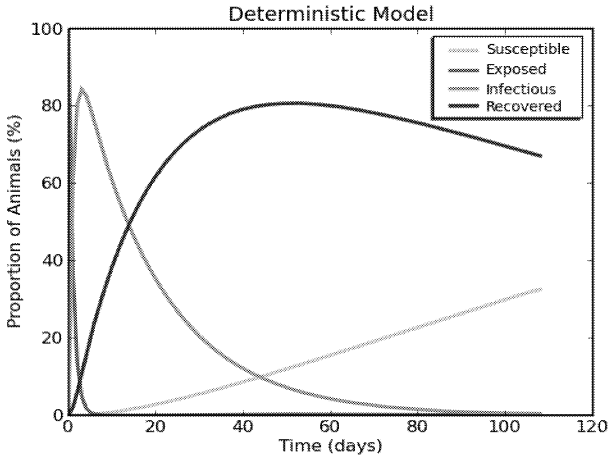

Figure 2: Results of the deterministic model

According to Nielsen et al. (1995), during the first week approximately 80% of the pigs were excreting S. Typhimurium, but subsequently the excretion decreased rapidly. This pattern is predicted by our model as shown in Table 2. Moreover, on day 62 post-infection only 1 pig was infectious at the experiment, while the model predicted 1.44 infectious pigs.

Table 2: Proportion of infectious animals as derived from the deterministic model for the first ten days

day	% Infectious
0	0
1	61.21
2	80.42
3	84.36
4	82.85
5	79.5
6	75.62
7	71.7
8	67.9
9	64.27
10	60.83

Unfortunately pigs in recovered classes cannot be compared readily with the seropositive pigs of the experiment at least for the first days. This is because there is an overlapping between seropositive and shedding stages, while in our model the pigs in infectious classes cannot belong also in the recovered classes. However, there are two critical dates, the 30th and 37th, when the seropositives showed a peak at 92% (Nielsen et al. 1995). Making a reasonable assumption that after 30 days all the pigs in the infectious class are already seropositive, we can estimate the total number of seropositive pigs by adding the infectious classes to the recovered ones. The values that the model predicted for the 30th and 37th are 94.33% and 92.18% respectively, which are in accordance with the experiment. Finally, another critical number given at this article is the value of seropositive pigs at the last day (67%), in agreement with the model prediction (67.05%).

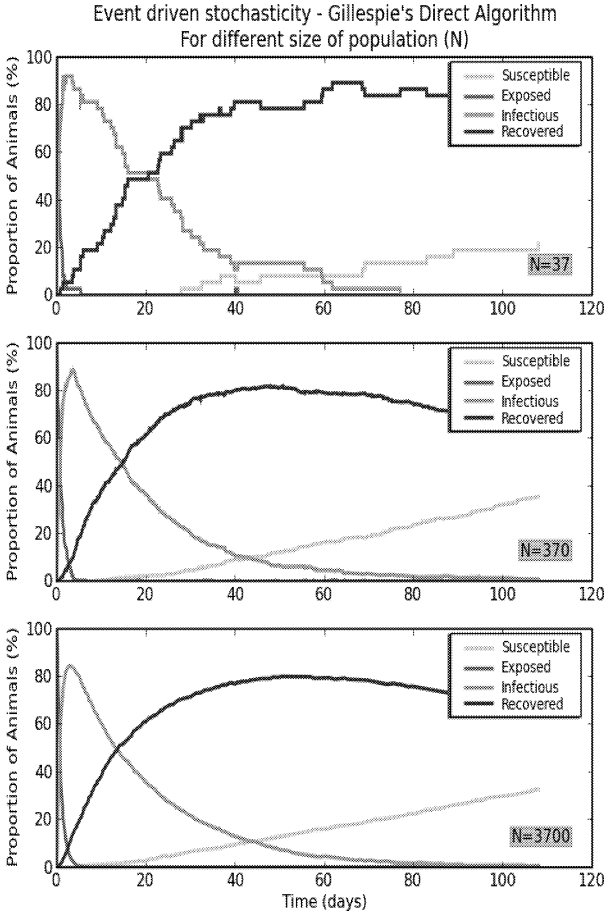

Figure 3: Results of the stochastic model for three different runs with different size of population (N)

Thus, we can conclude that the model we presented despite the arbitrary parameterisation has a good fit and can predict nearly all critical values of the real experiment. However, unlike reality where the number of the pigs should be whole numbers, the results of this model are non-integer. Also, as we will point out with our next (stochastic) model that when the sample is as small as 37 pigs variations may occur. These variations cannot be predicted by the deterministic model, which gives the same results independently of the number of pigs modelled.

THE STOCHASTIC EPIDEMIC MODEL – DEMOGRAPHIC STOCHASTICITY

Demographic stochasticity is defined as fluctuations in population processes that arise from the random nature at the level of the individual (Keeling and Rohani, 2007). In this case, we have to deal with whole number of animals (integers) and individuals experience different fates due to chance. We will use an event-driven approach to incorporate demographic stochasticity in our model and more precisely the Gillespie's Direct Algorithm, as described by Gillespie (1977) and explained for modelling infectious diseases by Keeling and Rohani (2007).

We first have to define all possible events and determine the rate at which each event occurs. In our case, there are seven events which are listed in Table 3, with their respective rates derived from the set of differential equations (1).

Table 3: Events and rates for the event-driven stochastic model.

m	Event	Rate
1	E -> E-1; I -> I+1	sigma * E
2	I -> I-1; R -> R+1	gamma * I
3	R -> R-1; S -> S+1	kappa * R
4	S -> S-1; E1 -> E1+1	beta * S * (I + I1) / N
5	E1 -> E1-1; I1 -> I1-1	sigma * E1
6	I1 -> I1-1; R1 -> R1+1	gamma2 * I1
7	R1 -> R1-1; S -> S+1	kapa * R1

If we define the rate of equations as *R*, and the number of the event as *m*, the total Rate (*Rtotal*) is given by:

$$Rtotal = \sum_{m=1}^{n} Rm \quad (2)$$

The time until the next event occurs is given by:

$$dt = \frac{-1 * \log(RUNIF1)}{Rtotal} \quad (3)$$

where *RUNIF1* is random number from a uniform distribution. We generate a new random number *RUNIF2* and we set as $P = RUNIF2 * Rtotal$. Event *p* occurs if

$$\sum_{m=1}^{p-1} Rm < P < \sum_{m=1}^{p} Rm$$

The time *t* is updated by *dt* and event *p* occurs. This loop happens while *t* is equal or smaller than the total number of days (108).

The results of this model are shown in Figures 3 and 4. In Figure 3 presents three different runs for the different population sizes: 37 (the size used by Nielsen et al. (1995)), 370 and 3700. It should be noticed that the third graph of Figure 3 is very similar to the graph presented in Figure 2. This can be explained by equations 2 and 3: when the population size is too big the *dt* (time until the next event occurs) is very small and many events will happen in the

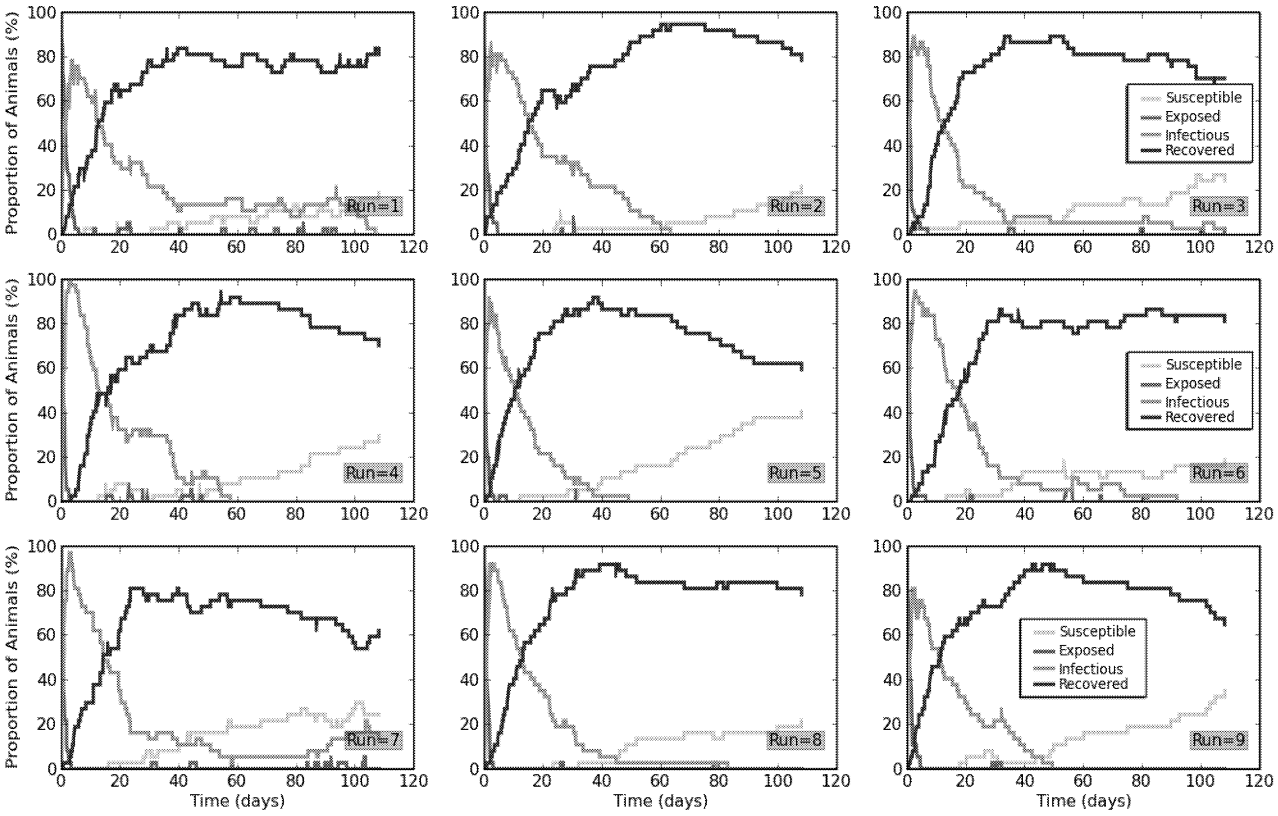

Figure 4: Nine different runs of stochastic model with population size N=37

same time step (in our case one day). In this way, as the population size increases the stochastic model will approximate the deterministic one. In Table 4 there is a comparison of the key values referred previously contrasting the experiment's results, the deterministic model results and the results of the stochastic model with size population N=3700.

Table 4: Comparison of results of Nielsen et al. (1995), deterministic model and event-driven stochastic model

Values	Nielsen et al. (1995)	Determi-nistic	Stochastic*
Max Infectious (3rd day)	~80%	84.36%	85.05%
62nd day (Infectious)	2.70%	3.89%	3.63%
30th day (Recovered)	~92%	94.33%	94.21%
37th day (Recovered)	~92%	92.18%	91.95%

(*) For population size N=3700. These are results from one simulation although there are not big differences among different runs.

For small populations a great variability among runs is observed as illustrated in Figure 4, where graphs of nine runs of simulation with the same parameters and population size N=37 are shown. Notice that, from the graphs, different maximum number of infectious pigs in the first days and different time until the extinction of the disease are produced in different runs. The mean and the standard deviation of the time to extinction of the disease (number of infectious pigs is zero) after 10000 simulations was 57.16 days and the standard deviation 22.18 days. The mean and standard deviation of the values for the four major classes for the last day are shown in Table 5 while histograms with the absolute numbers of the classes for the last day are presented in Figure 5.

Table 5: Mean and standard deviation of classes for day 108 after 10000 simulations

Class	Mean	Standard deviation
Susceptible (S)	35.140%	8.196%
Exposed (E + E1)	0.031%	0.286%
Infectious (I + I1)	0.268%	0.989%
Recovered (R+R1)	64.561%	8.090%

Figure 6 shows the histograms for the four critical values mentioned above and Table 6 lists the mean and standard deviation for these values.

Table 6: Mean and Standard deviation of critical values after 10000 simulations

Values	Mean	Standard deviation
Max Infectious (3rd day)	88.09%	5.07%
62nd day (Infectious)	3.17%	3.21%
30th day (Recovered)	93.59%	4.13%
37th day (Recovered)	91.18%	4.86%

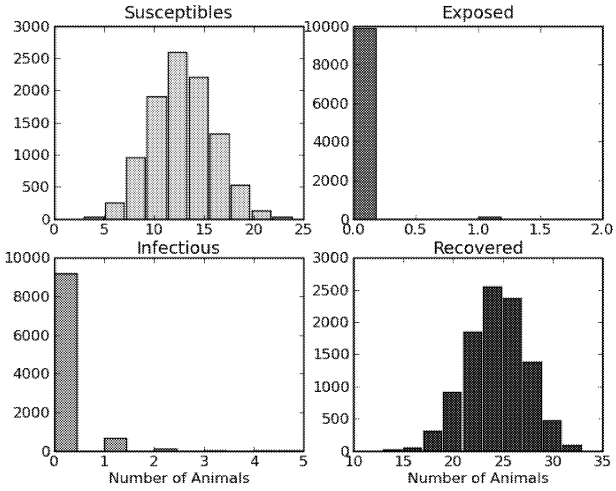

Figure 5: Histograms with absolute values of the main four classes for day 108 after 10000 simulations

CONCLUSIONS – DISCUSSION

Although the deterministic models are too popular they do not seem to adjust well to situations where populations are small and variability seems to have a great role in the final result. Especially, in the case of Salmonella, which seems to propagate mostly through faeces, the pig divisions have a great role in the transmission and modelling at the pen level appears to be more appropriate. A pen usually consists of a batch of 10 to 20 pigs; therefore, stochastic modelling and event-driven approach would be the most appropriate to predict the fluctuations observed at Salmonella prevalence of batches of the same farms arriving to slaughterhouse.

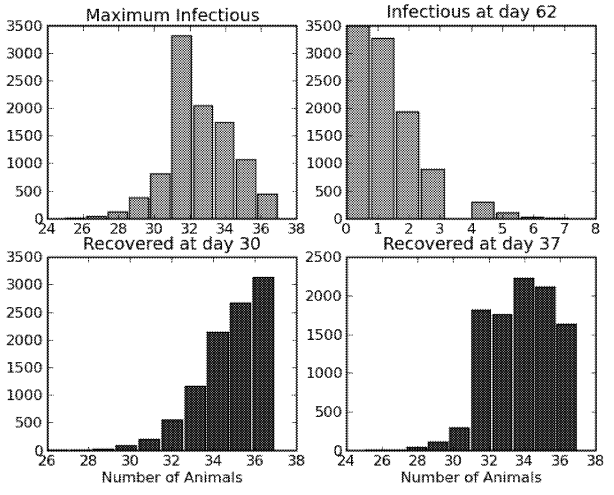

Figure 6: Histograms with absolute values of the critical values after 10000 simulations

One more conclusion drawn from this work is that the way pigs are being sampled at the slaughterhouses (e.g. 24 samples * 3 times a year for serology monitoring in Ireland) might not be sufficient to give an accurate estimate of the infection status of the farm. This effect of small sample size affect also experimental infections such as the ones published by Nielsen et al. (1995), Fedorka-Cray et al. (1994), and Wood et al. (1989). Moreover, accuracy is even more affected because since samples are not taken in a daily basis but every some days or weeks. That makes these experiments generally helpful but prone to produce wrong estimates about the rates used in the models. Thus, modellers should be careful using this kind of data and try more sophisticated parameterisation using data from field's trials.

FUTURE WORK

In real life situations, models are more complicated. In the Nielsen et al. (1995) experiment, that we tried to approach, pigs do not seem to be reinfected, probably because of the experimental environment and the cleanness of the farm. Therefore, the assumption that pigs are infected directly from other pigs seems to work. However, the cleanness of the stable and the practices of the farmer vary a lot and may have big implications as Salmonella tends to survive in faeces at infectious numbers for many days (Straw et al. 2006). Thus, the inclusion of one more class representing survival of S. Typhimurium in the environment seems to be necessary.

Another aspect that we have to keep in mind when we are modelling Salmonella in pig farms is the probability that an infectious transient visitor (commuter) can transmit the pathogen into the farm (like birds, rats, or veterinarians), or from pen to pen (like the farmer). The models developed in this work assumed a closed population with no births and deaths. However, this does not happen in real life. For example, when modelling for example a grower-finisher farm, pigs in batches (one or more pens) are getting out of the farm, pens are cleaned and usually the same number of pigs comes into the farm to replace the ones left and fill the empty pens. Some of the new coming pigs maybe already be infected and introduce the pathogen to the farm. Both of the above ways of importing S. Typhimurium into the farm can be modelled stochastically, but they need to be carefully parameterised.

ACKNOWLEDGEMENTS

The Authors wish to acknowledge the financial support of QPORKCHAINS, an EU 6th Framework project.

REFERENCES

Alban L. and Stark K.D.C., 2005. "Where should the effort be put to reduce the Salmonella prevalence in the slaughtered swine carcass effectively?" *Preventive Veterinary Medicine*, 68, no. 1, 63-79.

Fedorka-Cray P.J.; Whipp S.C.; Isaacson R.E.; Nord N.; and Lager K., 1994. "Transmission of Salmonella-typhimurium to swine." *Veterinary Microbiology*, 41, no. 4, 333-344.

Gillespie D.T., 1977. "Exact stochastic simulation of coupled chemical reactions." *Journal of Physical Chemistry*, 81, no. 25, 2340.

Hill A.A.; Snary E.L.; Arnold M.E.; Alban L.; and Cook A.J.C., 2007. "Dynamics of Salmonella transmission on a British pig grower-finisher farm: a stochastic model." *Epidemiology and Infection*, 1-14. doi:10.1017/S0950268807008485. URL http://dx.doi.org/10.1017/S0950268807008485.

Hindmarsh A., 1983. ODEPACK, "A Systematized Collection of ODE Solvers." In R.e.a. Stepleman (Ed.), Scientific Computing: Applications of Mathematics and Computing to the Physical Sciences. North-Holland, Amsterdam, Netherlands;

New York, U.S.A., IMACS Transactions on Scientific Computing, vol. 1, 55-64.

Hunter J.D., 2007. "Matplotlib: A 2D Graphics Environment". *Computing in Science and Engineering*, 9, no. 3, 90-95. ISSN 1521-9615.

Ivanek R.; Snary E.L.; Cook A.J.C.; and Grhn Y.T., 2004. "A mathematical model for the transmission of Salmonella Typhimurium within a grower-finisher pig herd in Great Britain." *Journal of Food Protection*, 67, no. 11, 2403-2409

Keeling M.J. and Rohani P., 2007. "Modeling Infectious Diseases." Princeton University Press. ISBN 978-0-691-11617-4.

Kermack W.O. and McKendrick A.G., 1927. "A contribution to the mathematical theory of epidemics." Proceedings of the Royal Society, London A, 115, 700721.

Nielsen B.; Baggesen D.; Bager F.; Haugegaard J.; and Lind P., 1995. "The serological response to Salmonella serovars typhimurium and infantis in experimentally infected pigs. The time course followed with an indirect anti-LPS ELISA and bacteriological examinations." *Veterinary Microbiology*, 47, no. 3-4, 205-218.

Petzold L., 1983. "Automatic Selection of Methods for Solving Stiff and Nonstiff Systems of Ordinary Differential Equations." *SIAM Journal on Scientific and Statistical Computing*, 4, no. 1, 136-148.

Straw B.E.; Zimmerman J.J.; D'Allaire S.; and Taylor D.J. (Eds.), 2006. "Diseases of swine." Blackwell, 9th ed.

van der Gaag M.A. and Huirne R.B., 2002. "Elicitation of expert knowledge on controlling Salmonella in the pork chain." *Journal on Chain and Network Science*, 2, no. 2, 135-147.

van der Gaag M.A.; Saatkamp H.W.; Backus G.B.C.; van Beek P.; and Huirne R.B.M., 2004a. "Cost-effectiveness of controlling Salmonella in the pork chain." *Food Control*, 15, no. 3, 173-180.

van der Gaag M.A.; Vos F.; Saatkamp H.W.; van oven M.; van Beek P.; and Huirne R.B.M., 2004b. "A state-transition simulation model for the spread of Salmonella in the pork supply chain." *European Journal of Operational Research*, 156, no. 3, 782-798

van Rossum G., 2007. "Python Programming Language". Python Software Foundation, 2.5.1 ed. URL http: //www.python.org/.

Wood R.L.; Pospischil A.; and Rose R., 1989. "Distribution of persistent Salmonella typhimurium infection in internal organs of swine." *American Journal Veterinary Research*, 50, no. 7, 1015-1021.

AUTHOR BIOGRAPHY

ILIAS SOUMPASIS was born in Thessaloniki, Greece and went to the Aristotle's University of Thessaloniki, where he studied veterinary and obtained his degree in 2002. From 2002 for 2003 he did his military service, where he worked for 14 months as veterinarian in a veterinary food laboratory with main activities microbiological food safety. From 2003 to 2007 he worked as a practitioner in private veterinary hospitals, and for 2 years in veterinary public administration with main activities animal health and public health. In parallel, from 2004 to 2006, he studied Master in Business Administration at the University of Macedonia, Economic and Social Sciences, in Thessaloniki, and his thesis was on the use of Free/Open Source Software in Businesses and Organisations. In 2007, he enrolled the School of Agriculture, Food Science and Veterinary Medicine in University College Dublin as a PhD scholar and joined the risk assessment team in the department of Biosystems Engineering.

A COMPARISON OF A SIMPLE SPREADSHEET TOOL FOR RISK ASSESSMENT AND A FUZZY RISK ASSESSMENT TOOL FOR RANKING OF FOODBORNE PATHOGENS IN POULTRY MEAT

Beatriz Aybar-Barboza and Francis Butler
University College Dublin,
Belfield, Dublin 2, Dublin, Ireland
Email addresses: beatriz.aybarbarboza@ucd.ie; f.butler@ucd.ie

Abstract:

A comparison using a Fuzzy Risk Assessment tool (FRAT) and a simple spreadsheet tool (Risk Ranger) for microbial risk ranking is described. The trials take *Campylobacter, Salmonella* and Enterohemorrhagic *Escherichia coli* as foodborne pathogens in poultry meat. These tools have similar structure and embody established principles of food safety risk assessment, i.e., the combination of probability of exposure to a food-borne hazard, the magnitude of hazard in a food, and the probability and severity of outcomes that might arise from that level and frequency of exposure. Fuzzy Risk Assessment tool works in Matlab, mathematic software; while Risk Ranger tool works in Excel. The outcomes are calculated by the tools when qualitative inputs are converted into numerical values and combined with the quantitative inputs. The outcomes are expressed in terms of public health risk such as total predicted illnesses per annum in the population of interest and a risk ranking score. The results using the FRAT and the Risk Ranger are similar for *Campylobacter, Salmonella* and Enterohemorrhagic *Escherichia coli.* Quantitative microbial risk assessments from Europe and the U.S. were used to partially validate the results of the simple risk assessment tools.

Introduction:

This work explains a comparison using FRAT and Risk Ranger tool to rank foodborne pathogens for poultry. These tools have similar structure to estimate the outcomes and they are expressed in: terms of a total predicted illnesses per annum in the population of interest and a risk ranking score. Risk Ranger is a tool that works in spreadsheet software format. It embodies established principles of food safety risk assessment, i.e., the combination of probability of exposure to a food-borne hazard, the magnitude of hazard in a food when present, and the probability and severity of outcomes that might arise from a specific level and frequency of exposure (Ross and Sumner, 2002). FRAT is a tool that uses fuzzy values for system parameters and interval arithmetic to characterize hazards and to compute risk. The tool is useful for early stage microbial risk assessment in food systems, in particular, for ranking risks based on total illness and severity of illness (Davidson et al., 2006). This work was undertaken as part of an EU funded 6th Framework project (Sigma Chain) to evaluate food chain traceability systems, including methodologies for the identification of priority contaminants. This study was carried out as part of the work to identify priority microbial contaminants that might arise throughout the food chain for a poultry meat product.

Procedure

The Risk Ranger tool requires the user to select from qualitative statements and to provide quantitative data concerning factors that will affect the food safety risk arising from a specific food product and specific hazard to a specific population, during the steps from harvest to consumption. The spreadsheet has been developed as 11 questions grouped within three parts (Ross and Sumner, 2002):

- Susceptibility and Severity.
- Probability of exposure to food.
- Probability of food containing an infectious dose.

FRAT includes some elements that are similar to the Risk Ranger spreadsheet tool but there are some key differences. FRAT represents most inputs as fuzzy values unless the user chooses to specify a crisp number as an input. A simple model is defined to estimate changes in hazard level from point of introduction to consumption and there is an explicit dose–response analysis based on the estimated hazard level at the point of consumption. All calculations are based on interval arithmetic and the results are presented as fuzzy membership functions

as well as point estimates using "center-of-gravity" defuzzification. This risk assessment tool is based on an input set of nine values that describe (Davidson et al., 2006):

- The initial hazard level in contaminated servings,
- likelihood that a serving is contaminated,
- Possible changes in hazard level at subsequent stages (distribution and consumer preparation) and exposure factors.

Using the Risk Ranger or the FRAT, it is needed to work with the appropriate information about:

- Food-borne hazard in the food chain.
- Information about observation studies,
- Empirical data,
- Demographic information, etc.

As this work was a ranking of the risk of different pathogens within a particular product, a number of the questions relating to frequency of consumption, proportion of the population consuming the product and the size of the population of interest could be set to nominal values that then did not change for the three pathogens being considered (*Campylobacter, Salmonella* and Enterohemorrhagic *Escherichia coli).* A population of 100000 was assumed to make the output of the total predicted illnesses per annum in the population of interest to be consistent with other published estimates of illness. The Risk Ranger and the FRAT models were populated with appropriate answers for the three pathogens being considered. Table 1 gives an example of the answers entered into the Risk Ranger model for *Salmonella.*

Table 1. Chosen responses to the questions asked by the Risk Ranger model for *Salmonella*

No.	Question	Answer
	A. SUSCEPTIBILITY AND SEVERITY	
1	Hazard Severity	Moderate Hazard
2	How susceptible is the population of interest	General
	B. PROBABILITY OF EXPOSURE TO FOOD	
3	The Frequency of Consumption	Weekly
4	Proportion of Population consuming the product.	All (100%)
5	Size of consuming Population.	100 000
6	Probability of contamination of raw product per serving.	Infrequent (1 per cent)
7	Effect of processing.	No effect
8	Is there potential for recontamination after processing?	Yes-minor frequency (1%).
9	How effective is the post-processing control system?	Well controlled
	C. PROBABILITY OF FOOD CONTAINING AN INFECTIOUS DOSE	
10	What increase in the post-processing contamination level would cause infection or intoxication to the average consumer?	Moderate
11	Effect of preparation before eating	Meal preparation usually eliminates (99%) hazards.

Results and Discussions:

The following table shows the results expressed in Risk Ranking and Total predicted illnesses per annum in population of interest using the Risk Ranger and the FRAT (Table 2). Both Risk Ranger and FRAT gave approximately the same risk ranking score (49 – 52) out of a possible score of 0 – 100 where 0 represents no risk and 100 represents a risk where every member of the population eats a meal that contains a lethal dose of the hazard every day (Ross & Sumner, 2002). It was only in the total predicted illnesses that the risk models distinguished between the pathogens, predicting that *Campylobacter spp* would cause a higher number of illness / annum (55 – 73 per 100000) than the other two pathogens (5 – 10 per 100000).

As a partial validation of the Risk Ranger and the FRAT models, data is available from two published risk assessments of *Salmonella* in whole chicken carried out in the US (Oscar, 2003) and in Denmark (Hald et al., 2004). The US study predicted 0.44 cases of Salmonellosis per 100000, whereas the Danish study predicted 1.61 cases per 100 000. These predictions agree well with the predictions from Risk Ranger and FRAT which predict values of 5.2 and 10 cases per 100000 respectively.

Table 2. Results of the trials in poultry using the Risk Ranger and the FRAT

Pathogens	Risk Ranking		Total predicted illnesses/annum in population of interest (*)	
	Risk Ranger	FRAT	Risk Ranger	FRAT
Campylobacter spp.	52	51	55	73
Salmonella spp.	50	49	5.2	10
Enterohemorrhagic *E. coli*	50	49	5.2	10

* assumed to be 100000

Conclusions:

The results obtained using the Risk Ranger and the Fuzzy Risk Assessment Tool were comparable for the three pathogens being considered, *Campylobacter, Salmonella* and Enterohemorrhagic *Escherichia coli.* The results confirm that the three pathogens are all of significant concern for poultry processors. The two ranking tools were relatively easy to use and give a rapid indication of risk which is sufficient for initial risk ranking exercises. For more detailed consideration of the risk, a more thorough quantitative risk assessment would be required

Acknowledgements

This work was funded by SigmaChain, an EU 6th Framework Project, funded by the European Union.

References:

Brown M. H. 2002. "Quantitative microbiological risk assessment: principles applied to determining the comparative risk of Salmonellosis from chicken products". *International Biodeterioration & Biodegradation 50 (2002) 155 – 160.*

Davidson V. J., Rysks J. and Fazil A. January 2006. "Fuzzy risk assessment tool for microbial hazards in food systems". *Fuzzy Sets and Systems 157 (2006) 1201 -1210.*

Hald T., Vose D., Wegener H. C. and Koupeev T. 2004. "A Bayesian Approach to quantify the contribution of Animal food sources to Human Salmonellosis". *Risk Analysis, Vol. 24, No. 1.*

Oscar T. P. December 2003. "A quantitative risk assessment model for Salmonella and whole chickens". *International Journal of Food Microbiology 93 (2004) 231 – 247.*

Ross T. and Sumner J. January 2002. "A simple, spreadsheet-based, food safety risk assessment tool". *International Journal of Food Microbiology 77 (2002) 39– 53.*

Biography:

Beatriz Aybar-Barboza was born in Lima, Peru and went to the National Agricultural University La Molina, where she studied food engineering and obtained her degree in 2002. After working 4 years in the food industry (Nestle Peru and Gloria Group S.A.) in food quality and safety department, she started a Master of Engineering Science by Research in 2006 in University College Dublin, where she has been working ever since in Quantitative risk ranking of food hazards, a research funded by Sigma Chain, an EU 6th Framework Project, funded by the European Union.

PREDICTIVE MICROBIOLOGY APPLIED TO FOOD AND BIO-INDUSTRIES

INDIVIDUAL-BASED MODELLING AND FLOW CYTOMETRY: TWO SUITABLE TOOLS FOR PREDICTIVE MICROBIOLOGY

Clara Prats Soler
Jordi Ferrer Savall
Daniel López Codina
Universitat Politècnica de Catalunya
Av. Canal Olímpic 15
08860-Castelldefels, Spain
E-mail: clara.prats@upc.edu

Josep Vives Rego
Universitat de Barcelona
Av. Diagonal 465
08028-Barcelona, Spain
E-mail: jvives@ub.edu

KEYWORDS

Individual-based Modelling, simulation, flow cytometry, bacterial growth cycle.

ABSTRACT

Predictive microbiology has usually been tackled by means of continuous modelling. In recent years, Individual-based Modelling (IbM) has been introduced in this area. We present several examples of the IbM potential in studying the bacterial growth cycle in axenic cultures, and its combination with flow cytometry measurements: (i) the use of IbM simulations as virtual experiments to test theoretical models; (ii) the IbM potential in showing the biomass distribution dynamics during the growth cycle, as well as in tackling the single cell scope; and (iii) the suitability of cytometry measurements to check these dynamics. Then, we gather the general perspectives of IbM in this area regarding the axenic cultures, mixed cultures and the spatial heterogeneity. Thus, the suitability of IbM and flow cytometry in the framework of predictive microbiology is shown, without forgetting the potential of classic continuous models.

INTRODUCTION

Predictive Modelling in Foods

Food microbiology deals with food quality assurance, predictive modelling and risk analysis (Fleet 1999). Predictive microbiology has usually been tackled by means of continuous modelling. In recent years another methodology has been introduced in this area: Individual-based Modelling.

Continuous models have a long tradition behind them. Once the appropriate equations have been proposed and solved, they are ready to be used. Thus, they are truly useful in the framework of predictive microbiology.

Generally, continuous modelling does not aim to decipher the processes that control growth at the cellular and population levels. That is, continuous models require a certain knowledge of these processes to build better models, but it is not indispensable if there are enough experimental data to extract general rules.

Grimm (1999) defines Individual-based Modelling (IbM) as 'simulation models that treat individuals as unique and discrete entities which have at least one property in addition to age that changes during the life cycle'. IbM has been used in ecology since the 1970s, and during the last decade it has also come to be used in microbiology (Ginovart et al 2002a and Kreft et al 1998).

IbMs are bottom-up approaches. Several rules are applied to individuals (microorganisms) and their environment, and the resulting behaviour of statistical systems is studied.

IbM is conceptually easy to understand, but practically difficult to use. Although IbM simulations can be accurately parameterized in order to obtain quantitative information about specific cases, the required work to carry out the parameter estimation, calibration and sensitivity analysis is time-consuming. So, why is Individual-based Modelling a tool with great potential in food microbiology? The hard part of IbM is the understanding element. The need for modelling the individual microorganism's behaviour when building an IbM requires an understanding of the processes that take place at an individual level. The simulations allow control of the phenomena and resulting processes that emerge from these individual rules, both at the mesoscopic and the population levels.

Furthermore, from the microbiological point of view one of the biggest difficulties is that microbial populations in foods consist of diverse combinations of species and cell densities, and each of the single microorganisms exhibits substantial spontaneous genetic variability. Also, the environmental variability to which the food is exposed is not only important but frequently unpredictable. IbM simulations are specifically suitable for dealing with microbial diversity, as well as any environmental change that is in need of study.

Thus, the main value of IbM is its capacity to test the proposed models for individual behaviour and to compare the simulation outputs with the available experimental information in order to accept or to reject the model, or even to re-interpret the experimental data. This capacity can be extended to the testing of existing mathematical models at a population level: IbM can be used in virtual experiments to carry out first trials (Hilker et al. 2006).

IbM, when applied to microbial systems, has already produced many interesting results in the past decade that are to be found in the specialized literature. For instance, BacSim is a simulator for individual-based modelling of bacterial colony growth (Kreft et al. 1998). This simulator was used to study the intermediate lag phase due to changes in temperature (Dens et al. 2005a and 2005b). The I+C+D theory of cell division (Képès 1986) was explored to study

cellular adaptation to medium and temperature shifts. Several simulations were performed with BacSim, assuming different models for the adaptation at an individual level. They found an unexpected result: theory predicted no intermediate lag due to temperature shifts, while experiments showed that this lag existed.

Two explanations were proposed: (i) the product m·(C+D) is not constant, because it decreases at lower temperatures; and (ii) a lag in biomass growth appears for shifts from low temperatures. BacSim simulations assuming each model produced consistent results with the experimental data, but they could not elucidate which was the correct model. Thus, the conclusion was drawn that further research was needed in order to distinguish between the two proposed mechanisms.

Another example of IbM simulations to study microbial systems is INDISIM, which stands for INDividual DIScrete SIMulation (Ginovart et al. 2002a). INDISIM simulations have succeeded in topics as diverse as bacterial growth in agar plates (Ginovart et al. 2002c), where the spatial effects of concentration gradients were tackled, and the study of the influence of the bacteria size and shape in yoghurt processing (Ginovart et al. 2002b), in which the interaction between two bacterial species (*S. thermophilus* and *L. bulgaricus*) was tackled by means of the study of axenic and mixed cultures.

IbMs and Flow Cytometry

As we noted above, IbM models and simulations are specific approaches lying between microscopic and macroscopic models. They use the available microscopic information to build the models, and the simulation output can be compared with the macroscopic (population level) experimental data (e.g. the growth curve, the lag parameter, the doubling time and the growth rate, among others). Therefore, experimental techniques assessing non-viable counts such as microscopy counts, and viable counting techniques such as plate counts or Most Probable Number, have been the major source of information for IbM.

However, none of these techniques possesses the full simulation capacity of IbM; they do not allow experimental assessments of the distribution of individual properties among the population. The dynamics of these distributions along the growth cycle are an important source of information about the processes that take place at the individual, population and mesoscopic levels.

Through cytometry techniques like flow cytometry, size distributions at different moments of the growth cycle may be obtained and their distribution dynamics may be observed, measured and analyzed with precision.

In this paper we present several examples of the IbM potential for the study of bacterial growth cycle in axenic cultures, and its combination with flow cytometry measurements. We focus on INDISIM results, since this is the IbM methodology used by our research group. Finally, we gather the general perspectives of IbM in this survey.

IbM RESULTS FOR AXENIC CULTURES

The initial bacterial lag phase in axenic cultures has been tackled with INDISIM in two publications (Prats et al 2006, Prats et al 2008). The results presented in these publications are proof of the potential of IbM in the study of transient processes of bacterial growth.

A Theoretical Approach to the Lag Phase

Prats et al. (2008) presented a theoretical approach to the bacterial lag phase, in which INDISIM was used as a virtual experimental method to test a mathematical model. This is one of the possible applications of IbM simulations.

In the paper, the lag phase was defined as the time that it takes for the growth rate to reach its maximum value. Within the lag phase, two sub-phases were identified (Fig.1): the initial phase, which is the time until the first division takes place (t_1), and the transition phase, which is the period between the first division and the time at which the growth rate reaches its maximum value (t_2).

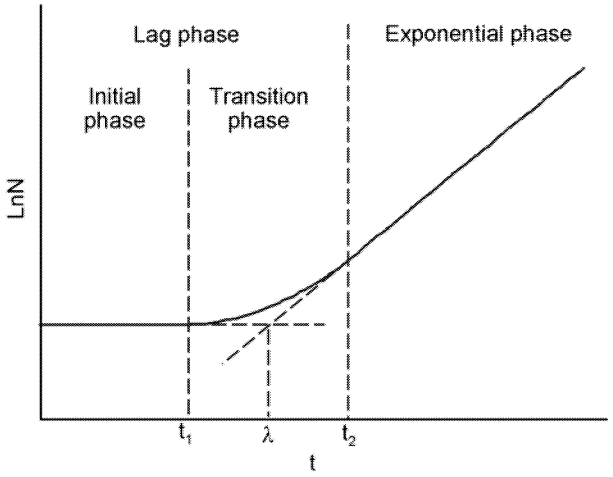

Figure 1: Graphical representation of the sub-phases defined in the lag phase (Prats et al. 2008). The lag parameter λ is also shown.

A mathematical model was proposed to shape the growth rate evolution during the initial and transition phases (Eq. 1, 2 and 3):

$$\mu_N = 0 \qquad t \le t_1 \qquad (1)$$

$$\mu_N = a \cdot (t - t_1) \qquad t_1 \le t \le t_2 \qquad (2)$$

$$\mu_N = \mu_{EXP} \qquad t \ge t_2 \qquad (3)$$

where $\mu_N = 1/N \; dN/dt$ and $a = \mu_{EXP}/(t_2 - t_1)$.

This mathematical model was fit to the INDISIM simulation results, showing a good correlation between them. Figure 2 shows an example of an INDISIM simulation output where the mathematical model was fitted, with the correlation coefficient $r=0.999$.

IbM Simulations and Flow Cytometry Experiments

Prats et al. (2006) studied the biomass distribution dynamics during the bacterial growth cycle. The growth of an inoculum with an initial low mean mass (that is, an inoculum taken from a pre-inoculation culture in stationary phase) was simulated, and the biomass distribution showed a forwards shift during the lag phase, remained stable during

the exponential balanced growth, and showed a backwards shift during the stationary phase (Fig.3).

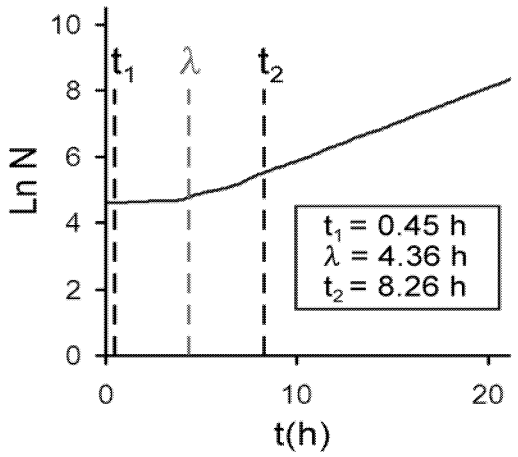

Figure 2: INDISIM simulation output for an axenic batch culture. The mathematical model parameters are shown (t_1 and t_2), as well as the lag parameter (λ) (Prats et al. 2008).

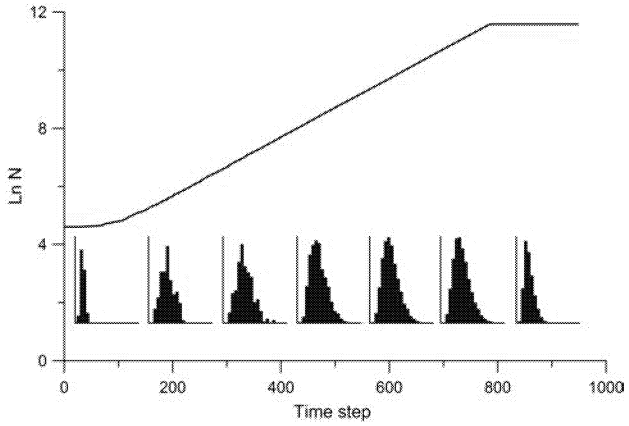

Figure 3: INDISIM simulation output showing the evolution of the biomass distribution during the growth cycle. The solid line shows the growth curve, and the graphs below the curve show the culture biomass distribution at different points of the growth (Prats et al. 2006).

A mathematical tool for assessing the evolution of the biomass distribution was built and called *product distance* (Eq. 4):

$$D(t) = \frac{\overline{m}(t) - \overline{m}_{EXP}}{\overline{m}_{EXP}} \cdot \sum_{k_m=1}^{25} \left| p_{km}(t) - \overline{p}_{km,EXP} \right| \qquad (4)$$

where $\overline{m}$ is the instantaneous mean mass of the culture (t) or its mean value during the exponential phase (*EXP*), and p_{km} is the instantaneous normalized biomass distribution (t) or its mean value during the exponential phase (*EXP*). The *product distance* accounts for the distance between the instantaneous biomass distribution and the mean distribution. The simulations show that it decreases roughly linearly during the lag phase, remains in oscillation around 0 during the exponential phase, and increases when the culture enters the stationary phase.

Specific experiments were designed to check this predicted behaviour. As noted above, the chosen experimental technique was flow cytometry, since this allows for size distribution assessment along the culture growth. Prats et al. (2007) showed the following experimental results. *Escherichia coli* bacteria in a pre-inoculation stationary phase were inoculated into fresh M9 medium at 35ºC (for further details on the experimental details see the above-mentioned paper). During the growth, several samples of the culture were analysed with the flow cytometer.

Figures 4 and 5 show the growth predicted by INDISIM simulation and the experimentally measured evolutions for the *product distance* along the growth of an axenic batch culture. As can be seen, the qualitative evolution of this variable is the same: an initial decrease during lag, almost zero during the exponential phase, and a final increase when entering the stationary phase.

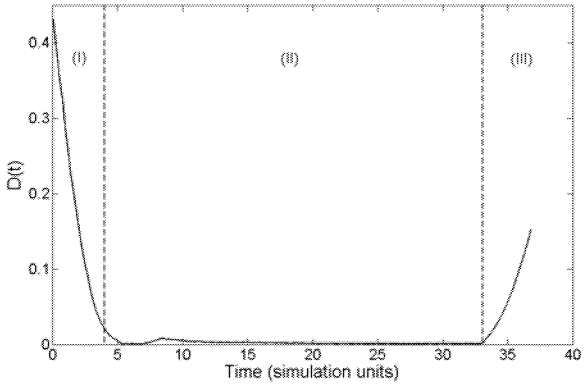

Figure 4: *Product distance* (*D(t)*) evolution during an INDISIM simulated growth of an axenic batch culture. The lag (I), exponential (II) and stationary (III) phases are shown (Prats et al. 2007).

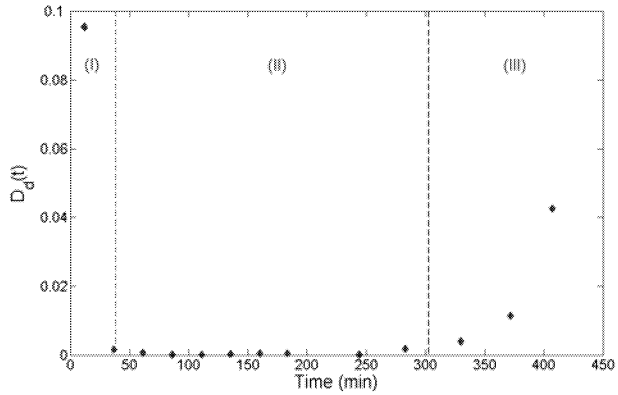

Figure 5: Measured *product distance* ($D_d(t)$) evolution of an *E coli* axenic batch culture growth (35ºC), using flow cytometer. The lag (I), exponential (II) and stationary (III) phases are shown (Prats et al. 2007).

These results show the great potential when combining IbM simulations and cytometry measurements: they provide information on the culture's evolution at a mesoscopic level, which gives descriptive information of the phenomena that take place at an individual level.

Mesoscopic Approach and Balanced Growth

We have seen that IbMs are bridges between individuals and populations. This is especially useful when dealing with the distribution of individual properties among a population. If a culture is under balanced growth conditions, all cellular

constituents have the same growth rate. Therefore, the distribution of the individual properties among the culture (for instance the biomass distribution or the DNA content distribution) is also constant.

If we keep working with the biomass distribution, we can express the balanced growth in terms of this variable. The *product distance* is a good tool to evaluate whether a biomass distribution is really stable: the *product distance* fluctuation indicates that the biomass distribution is not stable, and the culture is not growing in a balanced manner in terms of the biomass distribution. When the *product distance* remains approximately constant around 0, we can be certain that the balanced growth conditions in terms of biomass distribution have been achieved.

Figure 6 shows an example of a *product distance* application that distinguishes between non-balanced and balanced growth conditions. It corresponds to an INDISIM simulation with a single cell inoculum in a batch culture. Due to the initial low cell concentration, the balanced growth conditions take longer to reach. Actually, the difference between the lag parameter (λ) and the time at which the culture is in balanced growth conditions (t_B) is significant. It means that the culture starts growing exponentially when the lag ends, but the steady state is not reached until several hours later.

These results should be experimentally evaluated by flow cytometry.

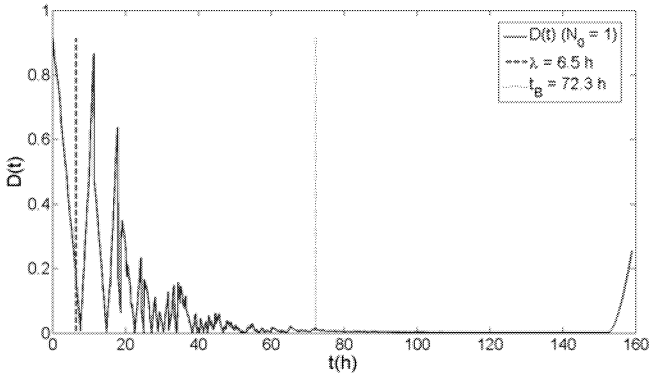

Figure 6: Evolution of the *product distance* (*D(t)*) for an INDISIM simulation with $N_0 = 1$ cell. The corresponding lag parameter, λ, calculated by means of the geometrical definition and the time of initiation of balanced growth, t_B.

IbM and Single Cells

The above-described case presents INDISIM-simulated growth of a single cell. Due to the IbM characteristics, this methodology may be very powerful when tackling the scope of the individual cell. IbM simulations control each cell of the culture at every moment. Thus, we can easily study parameters related with single cells such as the first division time or the cell cycle duration. Using the existing experimental methods these are difficult if not impossible to significantly assess.

Figure 7 shows the relationship between the time to the first division and the inoculum size. These results correspond to a series of simulations with different initial cell concentrations, taking the inoculum individuals from the same pre-inoculation culture. Several repetitions are performed for each inoculum size.

Here, a statistical effect emerges: the mean of the first division times (t_{FD}) of the simulations with $N_0 = 1$ cell is much greater than the mean of the t_{FD} of the greater inocula simulations. In the inocula with many cells, we are likely to find a big cell that adapts rapidly to the new medium and, therefore, divides in the first stages of the culture growth, resulting in a small t_{FD} for the culture. In contrast, in the small inocula that contain fewer cells, it is possible that in one repetition one of the inoculated cells is big, but the average also includes the small cells' growth. Therefore, the mean t_{FD} is much greater and, at the same time, the standard deviation increases.

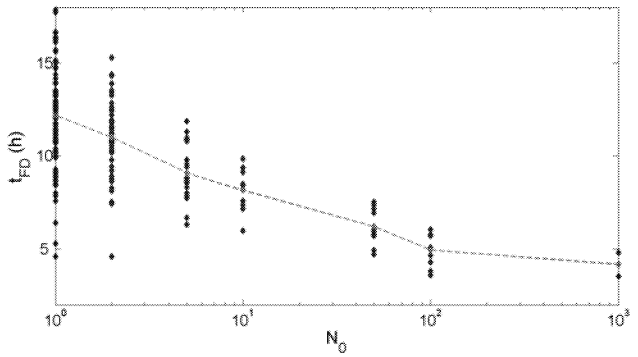

Figure 7: Simulation results assessing the relationship between the first division time and inoculum size. The dotted line indicates the mean values for each N_0.

PERSPECTIVES FOR IbM AND CYTOMETRY

The present examples illustrate the potential of IbMs in tackling the bacterial growth cycle, as well as the suitability of flow cytometry in assessing the necessary experimental data. Although the IbM results found in the literature have already answered many questions, new ones have been suggested and new paths to explore have been opened. These are a few of the multiple possibilities for further developments in this field, either with INDISIM or with other IbM simluations.

Axenic Cultures

In order to progress in the comprehension of the processes involved in the bacterial growth cycle, the model that describes the bacteria's individual behaviour should be improved by distinguishing different compartments in each cell: DNA, RNA, proteins and other components. Such compartmentalization should improve our analysis of the cell cycle, and the likelihood of substantial progress in studying the causes of the bacterial lag and the processes that take place during the stationary phase will be increased.

Another interesting component to be taken into account when tackling the stationary phase is spores. The study of spores with these approaches will be especially stimulating and challenging in food microbiology, since the presence of spores drastically conditions the technological treatment and the safety risk. As the final quality and organoleptic properties of the food depend on the type, duration and

hardness of the applied safety treatments, our modeling system might be extremely useful.

A complete understanding of balanced growth is especially interesting when studying, for instance, the transition between different metabolisms. The division of the cells into the above-mentioned compartments should allow a more-in-depth study of the balanced growth conditions since it should allow one, for instance, to distinguish between the balanced growth in terms of DNA and the balanced growth in terms of RNA, proteins or other fundamental macromolecules.

The improvements in the bacterial modelling area should provide the opportunity to tackle more complex lag phases - for instance, those caused by a change in the principal nutrient source. An initial approach was made by Prats et al. (2006); however, the model used to simulate the bacterial adaptation to the new nutrient source was quite simple, and it requires further development.

Flow cytometry should provide the perfect experimental frame for testing this type of metabolic adaptation, when it is combined with IbM simulations. The dynamics of the size distribution during the lag phase may be a key point in identifying the processes that take place at an individual level. These experiments could be complemented with microcalorimetric measurements, in order to identify the changes in cellular metabolism. In fact, microcalorimetry experiments would be the suitable technique to check the INDISIM results described in Prats et al. (2008).

Mixed Cultures and Spatial Effects

The interaction of different species during the lag or the stationary phases and the spatial effects in the different phases of growth are two key factors in the bacterial evolution in foods and they constitute very promising areas for study with combined IbM simulations and cytometric methods.

When two or more bacterial species coexist and interact in the same environment, the crossed effects between them are essential; the competition for nutrients and the inhibitory effects generated by their secondary metabolites may be crucial for the growth or survival of each species. Consequently, an advanced model for a complex space is essential in food microbiology. The batch culture conditions that often yield a homogeneous space are absolutely unreal in these systems. The coexistence and interaction of different phases (solid, liquid, gas), as well as the interfaces between them, influence the environmental conditions and, therefore, the bacterial growth.

Moreover, a complete space model that describes the temperature effects, heat transfer, water activity and pH is necessary to deal with the effect of these parameters in bacterial growth and dynamics.

CONCLUSIONS

Mathematical or continuous modelling is essential in the progress toward deeper understanding of basic and applied microbiology, particularly in the food industry.

Individual-based Modelling may be considered a part of the basic research in this field. It is necessary to improve our understanding of bacterial systems, what is essential to improve the mathematical models. Furthermore, IbM simulations are truly useful to test continuous models and to design specific experiments. Cytometry experiments are a suitable experimental technique for carrying out the measurements needed to verify IbM predictions in the framework of predictive microbiology.

REFERENCES

Dens, E.J; K. Bernaerts; A.R. Standaert; J.U. Kreft; and J.F. Van Impe. 2005a. "Cell division theory and individual-based modeling of microbial lag. Part II. Modeling lag phenomena induced by temperature shifts." *Int. J. Food Microbiol.*, 101, 319-332.

Dens, E.J; K. Bernaerts; A.R. Standaert; and J.F. Van Impe. 2005b. "Cell division theory and individual-based modeling of microbial lag. Part I. The theory of cell division." *Int. J. Food Microbiol.,* 101, 303-318.

Fleet, G.H. 1999. "Microorganisms in food ecosystems." *Int. J. Food Microbiol.,* 50, 101-117.

Ginovart, M.; D. López; and J. Valls. 2002a. "INDISIM, an individual-based discrete simulation model to study bacterial cultures." *J. Theor. Biol.,* 214, 305-319.

Ginovart, M.; D. López; J. Valls; and M. Silbert. 2002b. "Simulation modelling of bacterial growth in yoghurt." *Int. J. Food Microbiol.,* 73, 415-425.

Ginovart, M.; D. López; J. Valls; and M. Silbert. 2002c. "Individual-based simulations of bacterial growth on agar plates." *Physica A,* 305, 604-618.

Grimm, V. 1999. "Ten years of Individual-based Modelling in ecology: what have we learned and what could we learn in the future?" *Ecol. Model.,* 115, 129-148.

Hilker, F.M.; M. Hinschb; and H.J. Poethkec. 2006. "Parameterizing, evaluating and comparing metapopulation models with data from individual-based simulations." *Ecol. Model.* 199, 476-485.

Képès, F. 1986. "The cell cycle of Escherichia coli and some of its regulatory systems." *FEMS Microbiol. Reviews,* 32, 225-246.

Kreft, J.U.; G. Booth; and J.W.T. Wimpenny. 1998. "BacSim, a simulator for individual-based modelling of bacterial colony growth." *Microbiology,* 144, 3275-3287.

Prats, C.; D. López; A. Giró; J. Ferrer; and J. Valls. 2006. "Individual-based modelling of bacterial cultures to study the microscopic causes of the lag phase." *J. Theor. Biol.,* 241, 939-953.

Prats, C.; J. Ferrer; B. Flix; A. Giró; D. López; and J. Vives-Rego. 2007. "Evolution of biomass distribution during bacterial lag phase through flow cytometry, particle analysis and Individual-based Modelling." In: G. Nychas et al. (Ed.), *5th International Conference on Predictive Modelling in Foods. Proceedings*, p. 301-304, Agricultural University of Athens, Greece (ISBN: 978-960-89313-7-4).

Prats, C.; J. Ferrer; A. Giró; D. López; and J. Vives-Rego. 2008. "Analysis and Individual-based Modelling simulation of the stages in bacterial lag phase: basis for an updated definition." *J. Theor. Biol.*, 252, 56-68

BIOGRAPHY

CLARA PRATS was born in Barcelona, Spain, and attended the *Universitat de Barcelona*, where she studied physics and obtained her degree in 2002. She is now an assistant professor at the *Universitat Politècnica de Catalunya*, and a member of the research group "Discrete Modelling and Simulation of Biological Systems-MOSIMBIO" (web site: http://mie.esab.upc.es/mosimbio).

Predictive modelling of *Listeria monocytogenes* in Irish smoked salmon

S.D. Chitlapilly[1], N. Abu-Ghannam[1], E.J. Cummins[2]

[1] Department of Food Science and Environmental Health,
Dublin Institute of Technology, Cathal Brugha Street - Dublin 1, Ireland
[2] School of Agriculture, Food science and Veterinary Medicine, College of Life School,
University College Dublin, Belfield -Dublin 2, Ireland
Email: s.chitlapilly@dit.ie

Abstract:

The effect of four storage temperatures on the simultaneous growth of *Listeria monocytogenes* and food flora in vacuum packed cold-smoked salmon was investigated. The growth data (log_{10} CFU g^{-1}) of all the bacteria at 4, 10, 17 and 24 ºC were modelled as a function of time using DM-Fit (Baranyi and Roberts, 1994) and the kinetic parameters such as maximum specific growth rate (μ_{max}), lag phase (λ) and maximum population density (MPD) were obtained. This investigation shows that *Listeria monocytogenes* grows in vacuum packed smoked salmon held at 24 to 4ºC with colony forming units ranging from a minimum of 1.2cfu/g at 4ºC and a maximum of 8.21cfu/g at 24 ºC showing a six-fold increase from the minimum value after a period of 18 days. The growth data of the food flora showed that Lactic acid bacteria grew well in all temperatures studied and showed an 8-fold increase after 18 days at 24ºC, while the mesophils grew well at 24ºC and reached up to 10^9 log_{10} CFU g^{-1} and the psycrophils grew well at 4 and 10ºC reaching up to $10^4 log_{10}$ CFU g^{-1} after 18 days. The Arrhenius and square root models were used to describe the effect of different storage temperature on $\mu_{max.}$ The effect of the temperature was better interpreted by the Arrhenius type model. When kinetic parameters were compared with the predictive models – Com Base Predictor and Pathogen modelling programme (PMP) – the experimental data were in line with the predictive models at 4 and 10ºC.

Keyword: *Listeria monocytogenes*; predictive microbiology; smoked salmon; Arrhenius equation and square root model

Introduction:

Listeria monocytogenes is a major concern to producers of ready-to-eat foods because of the high mortality rate associated with listeriosis and the widespread nature of the organism (WHO, 2006). *L. monocytogenes* contamination is one of the leading causes of recalls in industrially processed foods. The *Listeria* species are psychrotolerant and have the ability to grow from 1 to 45ºC, but their optimal growth rate ranges from 30 to 37ºC. The ability to proliferate at low environmental temperature obviously presents a major challenge to food safety.

In the field of predictive microbiology, mathematical models are developed to describe microbial growth, inactivation and survival in food products at certain environmental condition. These models can be used by the food industry and the government to minimize and estimate food poisoning. Large amount of work has been done in relation to growth models of *Listeria monocytogenes*. However, when assessing their performance in food, it is often found that they overestimate the growth of *Listeria monocytogenes*, as the majority of them have been built from the data obtained from broth experiments in the laboratory rather than real food products.

The objectives of this work were: (a) to study the growth parameters of *L. monocytogenes* and food flora on cold smoked salmon under vacuum packed conditions at different storage conditions (b) to test the applicability of Arrhenius equation and square – root model to describe the effect of temperature on μ_{max} (c) to compare the experimental data with the predictive models — Com Base and PMP.

Materials and Method:

Samples and Experimental design

Smoked salmon was brought from retail outlet. On the day of purchase smoked salmon was divided into 25g per bag aseptically and vacuum packed. The vacuum packed bags were kept at 4, 10, 17 and 24ºC. The packs were stored until expiry date which ranged approximately from 18 to 20 days. The samples were withdrawn at regular intervals and analysed.

Selective Isolation of *Listeria monocytogenes* and other food flora on smoked salmon

Each stored sample pack was opened aseptically and blended with 225ml of *Listeria* enrichment broth base (OXOID Ltd., Basingstoke, Hampshire, England) in a stomacher. 0.1ml- aliquot was plated on PALCAM (OXOID Ltd., Basingstoke, Hampshire, England) and OXFORD (OXOID Ltd., Basingstoke, Hampshire, England) and incubated at 37 and 30ºC respectively for 48 hrs. MRS (Oxoid Ltd., Basingstoke, Hampshire, England) was used for the growth of Lactic acid bacteria and PCA (Oxoid Ltd., Basingstoke, Hampshire, England) was used to grow mesophils and psychrotropic bacteria.

Data Analysis

The growth data (log_{10} CFU g^{-1}) of all the bacteria at 4, 10, 17 and 24 ºC were modelled as a function of time using DM-Fit (Baranyi and Roberts, 1994) and the kinetic parameters such as maximum specific growth rate (μ_{max}), lag phase (λ) and maximum population density (MPD) were obtained (J. Baranyi, Institute of Food Research, Norwich, UK). Growth model Com Base Predictor (http://www.combase.cc),pathogen modelling programme-

PMP (http://www.arserrc.gov/mfs/pmp7_start.htm) were used to give predictions for the growth of *L. monocytogenes* and food flora on cold-smoked salmon. The effect of the storage temperature on the (μ_{max}) derived parameter were interpreted by means of the Arrhenius equation and square root model.

Arrhenius equation:

$\mu_{max} = A^* \exp(-E_a / RT)$

Where T is the temperature (K), E_a is the activation energy (KJ/mol). A is a preexponential factor (log (CFU $g^{-1)}$ $days^{-1}$) and R is the gas constant 8.31 (KJ $(Kmol)^{-1)}$. The activation energy E_a is considered as the sensitivity of the microorganism to temperature change. The equation is linearised by taking natural log on both sides of the equation.

$\ln \mu = \ln A - E_a/RT$

The value of Ea is calculated by plotting ln μ vs. 1/T.

Square root model:

$\sqrt{\mu_{max}} = a_\mu \times (T - T_{min})$

a_μ is the slope of the regression line for μ_{max}. T_{min} is the theoretical minimum temperature value for cell growth (ºC).

Results and Discussion

A total of 120 cold-smoked salmon were analysed. 13 cold-smoked samples were positive for the presence of *L. monocytogenes* (confirmed by using 16srRNA universal primer).

Fig. (1) represents the growth rate of *L. monocytogenes* and food flora at 4, 10, 17, 24ºC. Table 2 shows the kinetic parameters estimated by DM- Fit.

At 17 and 24ºC, *L .monocytogenes* presents a rapid growth with smaller lag phase. After four days of storage rapid growth was observed at 24 and 17ºC with an average increment of three log from the initial numbers. Growth rate of 0.576 at 24ºC and 0.301 at 17ºC was observed which was in contrast to the predictive models — fig. (2) and (table 2). The variability could be due to the presence of indigenous food flora with initial concentrations of mesophilic bacteria, lactic acid bacteria and psychrotropics at 6.8, 4.7 and 1.6 cfu/g respectively. Slower growth of *Listeria* in food matrix could be accounted to the presence of indigenous food flora which could compete with each other for deriving nutrition from the smoked salmon. At 4 and 10ºC, the growth of *Listeria* is much more retarded than at 17 and 24ºC, and presenting a lag time of 5.4 to 4.8 days respectively (Table 2). A total increment of 1.2 and 2.31 cfu/g was observed after 18 days. At 4 and 10ºC maximum population density of 6.01 log cfu/g and 7.31 log cfu/g was reached after 18days (Table 2).

In general, results showed that the growth of *L. monocytogenes* was relatively low at 4 and 10ºC when compared to other abuse temperatures. The performance of the predictive models at 4 and 10ºC showed similar behaviour of *Listeria monocytogenes* in broth to that in food (experimental data) could possibly be due to limiting condition in this case low temperature.

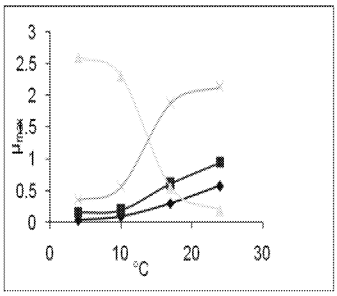

Fig .(1): Growth rate of *L. monocytogenes* (■), Lactic acid bacteria(●) Psycrotrops(▲), Mesophils(x)

Fig (2): Growth rate of *L. monocytogenes* on smoked salmon, fitting of DM-fit (-■-) with predictive models combase (-●-) and PMP (-▲-)

Initial concentrations of Mesophilic, Lactic acid and Psychrotropic bacteria at 4 and 10ºC were 3.7 - 1.3 - 5.2 log cfu/g and 5.4 - 3.2 – 5.7log cfu/g respectively (Fig. 1).

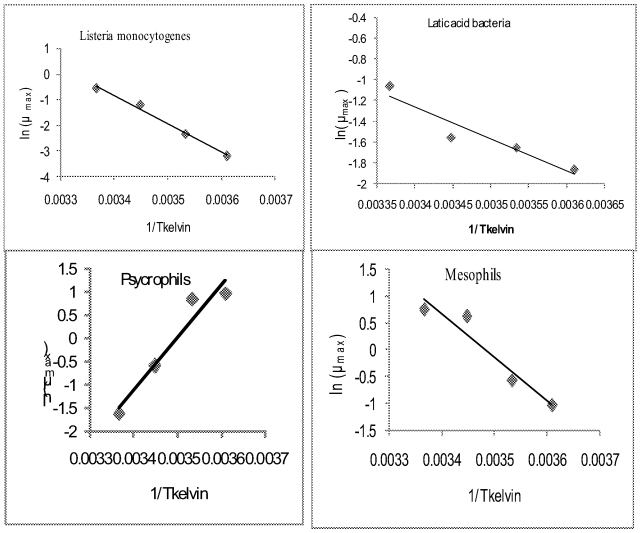

Fig. (3) Arrhenious plot of ln (μ_{max}) vs 1/T (Kelvin) for *Listeria monocytogenes, lactic acid bacteria, Psycrophils and Mesophils.*

The Arrhenius equation and the square root model which describe the effect of temperature on μ_{max} were applied for both *L. monocytogenes* and food flora. Fig. (3) describes the effect of temperature on the growth rate for *L. monocytogenes* and food flora. *Listeria monocytogenes* showed a higher activation energy 94 kJ/mol when compared to the other food flora, which indicates that the growth of *Listeria* is affected both by temperature shift and growth rate of other microorganism such as Lactic acid bacteria, Psycrophils and Mesophils (activation energy for each bacteria presented in Table 1).

Fig.(4) the square root model is presented. The Arrhenius model was slightly more accurate than the square root model with respect to higher R^2 value.

Table 1: Summary of activation energies and minimum temperature value based on maximum growth rate

Microorganism	Arrhenius - Equation		Square – root model	
	E_a (KJ/mol)	R^2	T_{min}	R^2
Listeria monocytogenes	94	0.991	2.25	0.98
Lactic acid bacteria	47	0.90	3.78	0.89
Psycrotrops	86	0.97	-3.64	0.93
Mesophils	32	0.88	11.64	0.91

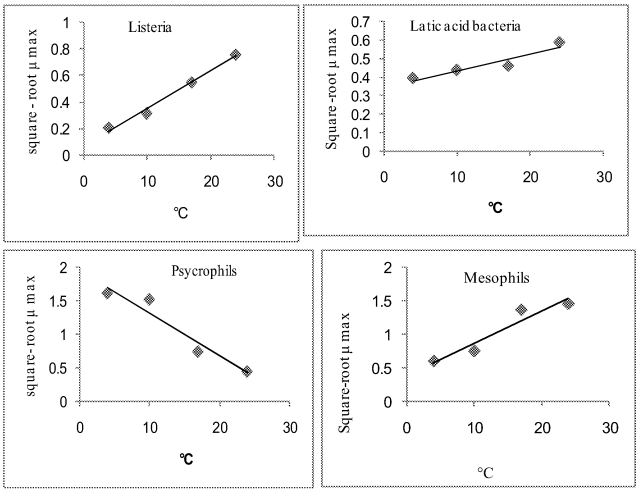

Fig 4: Square- root model of $\sqrt{\mu_{max}}$ vs Temperature (ºC) for *Listeria monocytogenes, lactic acid bacteria, Psycrophils and Mesophils*

Table2: Kinetic parameters of *Listeria monocytogenes* estimated by DM-Fit at 4,10,17,24ºC and kinetic parameters predicted by PMP and ComBase

DMFIT				PMP				ComBase			
Temp ºC	**λ**	**Growth rate**	**MPD**	**Temp ºC**	**λ**	**Growth rate**	**MPD**	**Temp ºC**	**λ**	**Growth rate**	**MPD**
4	5.4	0.042	6.82	4	4.6	0.026	6.01	4	5.1	0.031	6.01
10	4.8	0.096	7.31	10	4.3	0.077	6.37	10	4.5	0.092	6.37
17	0.9	0.301	8.01	17	1.1	0.534	8.92	17	0.6	0.753	8.92
24	0.6	0.576	8.42	24	0.7	0.768	9.01	24	0.1	0.895	9.01

Temp ºC – Temperature
λ - Lag time (days)

MPD – Maximum population density
Growth rate – (logcfu/h)

References:

1)**Carrasco, E.,Perez-Rodrigues,F,A (**2007). Growth of *Listeria monocytogenes* on shredded, ready –to-eat iceberg lettuce. Food Control **19**:487-494

2) **Baranyi, J., and T. A. Roberts. (**1994). A dynamic approach to predicting bacterial growth in food. Int. J. Food Microbiol. **23:**277–294.

3) **Gandhi.M,** and **Chikindas**. **M. L.** (2007) Listeria: A foodborne pathogen that knows how to survive**.** *International Journal of Food Microbiology***.** 113(**1**):1-15

4) **WHO** (2006) Risk assessment of *Listeria monocytogenes* in ready-to-eat foods, MRA Series 4 & 5. Microbiological Risk Assessment Series, No. 4, Interpretive Summary ISBN 92 4 156261

5) **Francisco, D-G., Daniel. B, Pal. A** (2007) Modeling the growth of Listeria monocytogenes based on a time to detect model in culture media and frankfurters. *International Journal of Food Microbiology. 113 : 277-287*

6) **Mataragas,E.H, Drosinos, H, Vaidanis, G and Metaxopoulos, I** (2006). Development of a predictive model for spoilage of cooked cured meat product and its validation under constant and dynamic temperature storage condition. Journal of Food Science,71 (**6**) 157-167

Assessment of the Sensorial Shelf Life of Cultivated Mushrooms

Debabandya Mohapatra
Fernanda A. Rodrigues

Process & Chemical Engineering Department
University College Cork, College Road
Cork City, Ireland

Jesus M. Frias
School of Food Science and Environmental Health
Dublin Institute of Technology

Cathal Burgha Street

Dublin 1, Ireland

ABSTRACT

Cultivated mushrooms are highly perishable on account of their high water content and lack of cell wall protection. Refrigerated storage is commonly employed to maintain the sensory attributes of mushrooms and therefore to extend their shelf life. Two main parameters are perceived to hinder the shelf life management of mushrooms i) the variability between mushroom batches ii) the variability in the consumer perception of high quality mushrooms.

The objectives of this work were i) to estimate the effect of temperature on the shelf life of mushrooms based on consumer acceptance/rejection of sensory attributes and ii) to assess the relative importance of product and consumers variability.

Fresh mushrooms were stored at 5, 10, 15°C and 3.5°C (control). Each day samples were removed from the chamber and sensory trials were conducted. The panelists judged the mushroom based on their overall appearance, texture of cap and stem, gill colour and opening, stipe elongation, flavour and overall acceptability. Logistic linear mixed effect models (LLMM) were built using this data to estimate: i) the effect of time and temperature on the acceptance/rejection of a particular sensory attribute from mushrooms in the form of two linear main effects and ii) the uncertainty in this acceptance/rejection associated with product variability and consumer variability.

All sensory properties degraded substantially with time, till those were no longer acceptable by the consumer. Temperature of storage was found to be playing a significant role in the rejection as well. The overall acceptability and the cap hardness were found to be the critical parameters. The overall acceptability, cap hardness and maturity were the most affected by temperature. The uncertainty related to consumer variability was the most sensitive one. Stochastic simulations allowed in predicting the probable time of product rejection. Given the product and consumer variability, the model predicted a shelf life shorter than 2 days to ensure less than 5% of rejection rate in mushroom batches stored at 5°C.

This study presents a methodology to define conservative shelf life estimations on risk analysis principles, without resourcing to “rule-of-thumb” conservative estimations in a highly perishable product like mushrooms.

INTRODUCTION

Cultivated mushrooms are highly perishable on account of their high water content and lack of cell wall protection. Refrigerated storage is commonly employed to maintain the sensory attributes of mushrooms and therefore to extend their shelf life. Two main parameters are perceived to hinder the shelf life management of mushrooms i) the variability between mushroom batches ii) the variability in the consumer perception of high quality mushrooms.
The objectives of this work were i) to estimate the effect of temperature on the shelf life of mushrooms based on consumer acceptance/rejection of sensory attributes and ii) to assess the relative importance of product and consumers variability.

MATERIALS AND METHODS

Fresh white button mushrooms were stored at 5, 10, 15°C and 3.5°C (control). Each day samples were removed from the chamber and sensory trials were conducted. The panelists judged the mushroom based on their overall appearance, texture of cap and stem, gill colour and opening, stipe elongation, flavour and overall acceptability.

Modelling of sensory attribute kinetics

Logistic linear mixed effect models (LLMM) were built using this data to estimate: i) the effect of time and temperature on the acceptance/rejection of a particular sensory attribute from mushrooms in the form of two linear main effects and ii) the uncertainty in this acceptance/rejection associated with product variability and consumer variability.
The linear mixed effect model (Pinheiro and Bates, 2000) is represented as:

$$SQ \sim \beta X + b_{ij} + \varepsilon_{ij} \qquad (1)$$

where SQ is the logistic transformed sensory panel response, β is the fixed effect (storage time and temperature) term for the jth mushroom and b_{ij} is random effect term of the ith batch and εij is the associated error term, which were assumed to be normally distributed.

RESULTS AND DISCUSSION

The time and temperature effect on the different sensory attributes translates in a decrease in a following decrease in

average overall acceptability. at lower temperature the consumer variance is much more as compared to higher Table 1temperature. this translates into the idea that at higher temperature the changes in the sensory properties was much more predominant, thus resulting in less variation in sensory characteristics analysis.

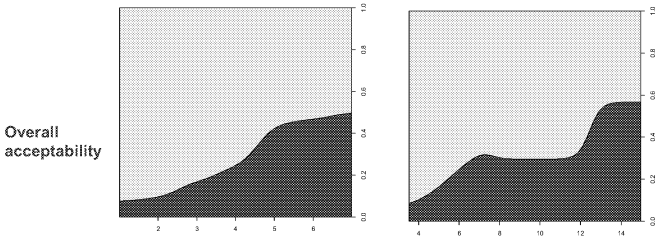

Figure 1 Cumulative Distribution Plot Showing The Dependence Of The Acceptance /Rejection Odds Ratio Of The Overall Visual Acceptability On The Storage Conditions

A final model was developed integrating both time and temperature which showed negative impact on sensory qualities studied in a linear fashion. The results can be seen in the **Figure 2**.

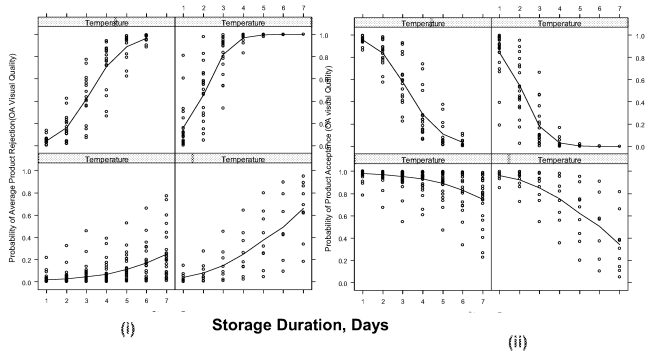

Figure 2 Average Population Of Overall Acceptability Best Linear Unbiased Predictions at Storage Temperatures of 3.5 (a), 5(b), 10(c) and 15°C (d) Showing The Probability Of Consumer Acceptance (i) And (ii) Rejection

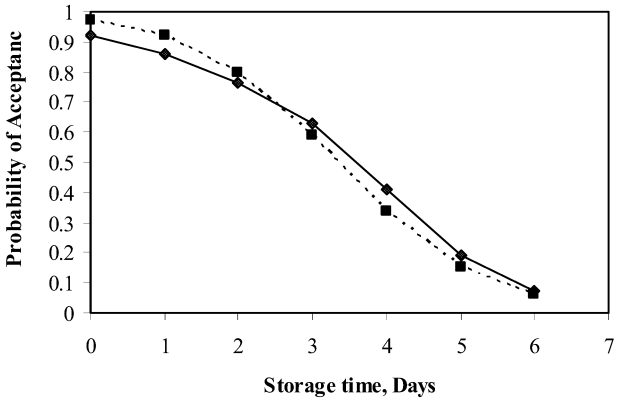

Figure 3 Change In The Probability of Overall Quality Acceptance With Time Compared To The Minimum Of The Probability Of Acceptance Of All Sensory Evaluation Factors During Storage At 10°C.

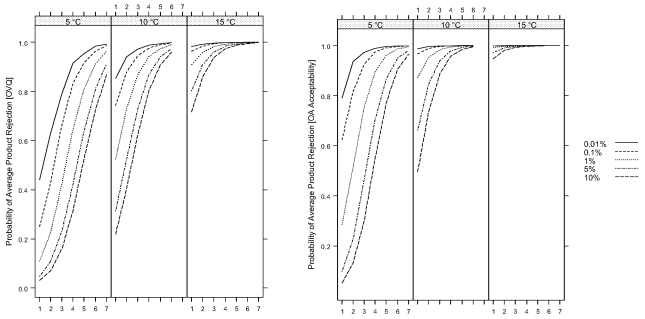

Figure 4 Probability Of Average Product Rejection Kinetics Of (i) Overall Visual Quality, (ii) Overall Acceptability Of The Product at 90, 95, 99, 99.9 & 99.99 % Confidence For Different Storage Temperatures.

At 99.99% confidence interval, product rejection becomes very high at even lower temperature of 5°C, causing the mushrooms to have a shelf life even lower than 6 days.

The overall visual quality (OVQ) of mushroom at 5°C stored for 1 day will still be accepted by 95% of the consumer but increasing the storage temperature by 2°C would result in the increase of the rejection odds, pushing the product below marketability level. Similarly the gill colour of the mushrooms stored over 2 days at 4°C will have chances of being accepted by 95% of the consumer, while storing the same product at 10°C during the same storage time, it is mostly likely to be rejected by 95 % of the consumer. Overall acceptability of the mushrooms would decrease by 1 ¾ day if the temperature increase by 1°C.

The presented models can be employed to declare a shelf life time that will consider a tolerance of rejection taking into account the consumer (sensory panel) and batch variability.

Table 2 Fixed Efect Trms Of The Generalised Linear Mixed Effect Model Fitted To Different Sensory Characteristics. The Standard Error Of The Estimated Parameters Appears Between Brackets ().

Sensory Parameters	Fixed effects Estimate$_{(std.\ error)}$		
	Intercept	Day	T
Overall visual quality	$8.2_{(0.9)}$	$-0.90_{0.10)}$	$-0.43_{(0.05)}$
Cap hardness	$10._{(1.1)}$	$-1.07_{(0.13)}$	$-0.61_{(0.06)}$
Stem hardness	$7.8_{(0.8)}$	$-0.76_{(0.10)}$	$-0.47_{(0.05)}$
Maturity	$10.09_{(1.16)}$	$-0.99_{(0.13)}$	$-0.61_{(0.06)}$
Gill colour	$9_{(1)}$	$-0.92_{(0.12)}$	$-0.56_{(0.06)}$
Aroma	$6.7_{0.7)}$	$-0.65_{(0.09)}$	$-0.42_{0.04)}$
Overall acceptability	$9.2_{1.0)}$	$-1.03_{(0.12)}$	$-0.58_{(0.06)}$

*** all estimates are significant at p< 0.0001

Table 3 Random Efect Trms Of The Generalised Linear Mixed Effect Model Fitted To Different Sensory Characteristics. The Standard Error Of The Estimated Parameters Appears Between Brackets ().

Sensory Parameters	Consumer	Batch	Scaled Error
Overall visual quality	1.197	0.521	1.646
Cap hardness	0.636	0.957	1.093
Stem hardness	1.092	0.117	1.223
Maturity	2.958	0.446	1.115
Gill colour	0.526	0.173	1.452
Aroma	1.018	0.207	1.003
Overall acceptability	2.827	0.689	1.569

The temperature dependence of these qualities further gives an insight to choose proper time-temperature management during storage. Storage under low temperature would delay the biological decay process and would extend the shelf life of the product. All the sensory characteristics were more influenced by individual consumer preference than the variation arise due to inherent biological variation.

The sensory data analysis gave an insight to quantise the sensory characteristics in stead of following a qualitative approach. These mathematical models can be useful in predicting the shelf life of fresh mushrooms under a temperature range of 3.5-15°C, which is mostly used during distribution chain and storage of mushrooms.

This study presents a methodology to define conservative shelf life estimations on risk analysis principles, without resorting to “rule-of-thumb” conservative estimations in a highly perishable product like mushrooms.

REFERENCES

Pinheiro, J. C. & Bates, D. M. Mixed-Effects Models in S and S-PLUS'. ISBN 0-387-98957-9, 2000.

BIOGRAPHY

DEBABANDYA MOHAPATRA received her Bachelor of Technology in Agricultural Engineering in 1996 from Orissa University of Agriculture and Technology , India . She completed her Master of Technology in Post Harvest Engineering from the Department of Agricultural and Food Engineering at the Indian Institute of Technology, Kharagpur in 1998. After completion of her PhD from the Department of Agricultural and Food Engineering at the IIT, Kharagpur in 2004, she worked as a lecturer in Bidhan Chandra Krishi Vishwavidyala, India and a post doctoral researcher at the IIT, Kharagpur. She was appointed as a post doctoral researcher in this Department in 2005.

JESUS M. FRIAS Dr Frías’s BSc is in Food Science and Technology from the Pharmacy Faculty of Basque Country University and his PhD is in Biotechnology from the ESBUCP (Portugal). He was a Marie Curie funded postdoctoral research fellow at the Food Engineering Department of the ENSIA (1998-2000, Massy, France) and a postdoctoral research fellow at the Process Engineering Department of NUI Cork (2000-2002) before joining the School of Food Science and Environmental Health of the Dublin Institute of Technology as a lecturer in Food Chemical Analysis and presently works as the (Acting) Head of the Food Science Department of the School. His research interests are in the areas of Mathematical modelling of food kinetic phenomena, Fruit and vegetable technology; product natural variability and shelf life modeling, Vitamin stability, Drying technologies and mechanical stress during dehydration.

FERNANDA A. RODRIGUES has been extensively involved with the development of undergraduate and postgraduate programmes, encompassing international training. She has co-edited two books, co-authored more than 50 publications in international peer-reviewed journals, and presented over 100 communications in international congresses. She has also an extensive track record in European programmes, both as a partner and co-ordinator of research projects and scientific networks. Her experience in industrial interaction focus on the food distribution chain management. Her research interest are in the areas of Postharvest Technology Modified Atmosphere Packaging Perforated-mediated atmosphere packaging for fresh fruits and vegetables Shelf Life Estimation Predictive Modelling Improved estimation of kinetic parameters in food research Thermal processing Mass Transfer

OPTIMAL DYNAMIC EXPERIMENT DESIGN AS A TOOL FOR ACCURATE ESTIMATION OF MICROBIAL GROWTH CARDINAL TEMPERATURES

Eva Van Derlinden, Lyn Venken, Kristel Bernaerts and Jan F. Van Impe
Chemical and Biochemical Process Technology and Control Section (BioTeC)
Katholieke Universiteit Leuven
W. de Croylaan 46, B-3001 Leuven, Belgium
Tel. +32-16-32.14.66 Fax. +32-16-32.29.91
E-mail: jan.vanimpe@cit.kuleuven.be

KEYWORDS

cardinal temperatures, parameter estimation, optimal experiment design, temperature, dynamic experiments

ABSTRACT

Accurate model predictions of the microbial evolution ask for correct model structures and reliable parameter values with good statistical quality. Given the widely accepted validity of the Cardinal Temperature Model with Inflection (CTMI) (Rosso *et al.*, 1995), this paper focuses on the accurate estimation of its four parameters (T_{min}, T_{opt}, T_{max} and μ_{opt}). This secondary model describes the influence of temperature on the microbial specific growth rate from the minimum to the maximum temperature for growth. The technique of optimal experiment design for parameter estimation is applied to maximize the parameter estimation accuracy and reliability. Dynamic temperature profiles are optimized within two temperature regions ([15°C, 43°C] and [15°C, 45°C]), focussing on the minimization of the parameters joint confidence region (D-optimal design). The optimal temperature profiles are implemented and CTMI parameters are identified from the resulting experimental data. Approximately the same parameter values were derived irrespective of the temperature region, except for T_{max}. The latter could only be estimated accurately from the optimal experiments within [15°C, 45°C]. This observation underlines the importance of selecting the upper temperature constraint for OED/PE as close as possible to the true T_{max}. A robustness study is performed to evaluate the effect of the nominal values on this nonlinear design problem. The study shows a rapid convergence of the iterative OED/PE process, except when the nominal value for T_{max} is significantly lower than its true value.

INTRODUCTION

By combining microbial knowledge, experimental data and mathematical techniques, predictive microbiology designs models in order to describe, understand and predict microbial behavior in food products. Implementation of predictive models for food safety and food spoilage management ask for model predictions which closely represent reality. The prediction error of a model system is mainly determined by the error in the model structure and the uncertainty in model input(s) and model parameters. So, once a correct model structure is defined and validated, the remaining objective is the accurate identification of model parameters. Unique and accurate estimation of model parameters based on a given experimental data set is often not straightforward due to (one or a combination of) the following reasons: (*i*) a too small amplitude of system output sensitivities with respect to the model parameters, (*ii*) a high model sensitivity to experimental noise, (*iii*) model parameter correlation, (*iv*) measurements with limited accuracy and/or small measurement frequency, (*v*) a lack of measurements for certain (biologically important) state variables and (*vi*) model and reality are not perfectly corresponding since the model omits variables in order to control the complexity of the model (e.g., Pinto (1998); Bernaerts and Van Impe (2004)). Moreover, the uncertainty on the model prediction is mainly influenced by the uncertainty on the parameter(s) to which the model is most sensitive. Analysis of the sensitivity functions, in which the effect of small changes in parameter values on the model output is quantified, can reveal to what extent certain model parameters can be accurately estimated from a given set of experimental measurements. The information enclosed in the model output sensitivities can be exploited via the technique of optimal experiment design for parameter estimation (OED/PE) (e.g., Walter and Pronzato (1997)).

Table 1: *Cardinal Temperature Model with Inflection* (Rosso *et al.*, 1995), with T_{min}, T_{opt} and T_{max} respectively the minimum, optimum and maximum temperature for growth [°C], and μ_{opt} the maximum specific growth rate at the optimum temperature [1/h].

	μ_{max}	=	$\mu_{opt} \cdot \gamma(\mathrm{T})$
$\mathrm{T} < T_{min}$	$\gamma(\mathrm{T})$	=	0
$T_{min} \leq \mathrm{T} \leq T_{max}$	$\gamma(\mathrm{T})$	=	$\frac{(T-T_{min})^2(T-T_{max})}{(T_{opt}-T_{min})((T_{opt}-T_{min})(T-T_{opt})-(T_{opt}-T_{max})(T_{opt}+T_{min}-2T))}$
$\mathrm{T} > T_{max}$	$\gamma(\mathrm{T})$	=	0

The objective of this paper is to derive accurate CTMI parameter estimates of *Escherichia coli* K12 MG1655 by means of a one-step identification based on dynamic experiments with optimally designed temperature profiles. The kinetic model under investigation describes the influence of temperature on the microbial specific growth rate from the minimum to the maximum temperature for growth. *E. coli* K12 MG1655 was selected because the effect of temperature on its behavior was already extensively investigated and reported (Bernaerts *et al.*, 2002; Swinnen *et al.*, 2005, 2006), and good reference data are available (Bernaerts *et al.*, 2006). Via the methodology of OED/PE, a series of dynamic temperature profiles is optimized with respect to the D-criterion, which emphasizes on the minimization of the parameters joint confidence region. The optimized dynamic temperature profiles are implemented in a computer controlled bioreactor and the CTMI parameters are identified from the resulting cell density measurements. The validity of the CTMI model and the reliability of the cardinal temperatures is evaluated.

MATERIALS AND METHODS

Mathematical models

Cell density as function of time is described by the growth model of Baranyi and Roberts (1994):

$$\begin{aligned} \frac{dn(t)}{dt} &= \frac{Q(t)}{Q(t)+1} \cdot \mu_{max}(T(t)) \cdot [1-\exp(n(t)-n_{max})] \\ \frac{dQ(t)}{dt} &= \mu_{max}(T(t)) \cdot Q(t) \end{aligned} \tag{1}$$

with $n(t)$ [ln(CFU/mL)] the natural logarithm of the cell density at time t, n_0 the initial and n_{max} the maximum value for $n(t)$ and μ_{max} [1/h] the maximum specific growth rate. $Q(t)$ [-] is a measure for the physiological state of the cells. The dependence of the maximum specific growth rate as function of temperature is incorporated in Equation 1 by the Cardinal Temperature Model with Inflection (CTMI) (Rosso *et al.*, 1995) enclosing four parameters (see Table 1).

Optimal experiment design for parameter estimation

Given a certain experimental input, the information content with regard to parameter estimation of an experiment with continuous (Equation 2) or discontinuous (Equation 3) outputs, can be quantified by the Fisher information matrix (see e.g., Walter and Pronzato (1997)):

$$\mathbf{F} \triangleq \int_0^{t_f} \left(\frac{\partial \mathbf{y}}{\partial \mathbf{p}}(t,\mathbf{p})|_{\mathbf{p}=\mathbf{p}^\circ}\right)^T \mathbf{Q} \left(\frac{\partial \mathbf{y}}{\partial \mathbf{p}}(t,\mathbf{p})|_{\mathbf{p}=\mathbf{p}^\circ}\right) dt \tag{2}$$

$$\mathbf{F} \triangleq \sum_{i=1}^{n_t} \left(\frac{\partial \mathbf{y}}{\partial \mathbf{p}}(t_i,\mathbf{p})|_{\mathbf{p}=\mathbf{p}^\circ}\right)^T \mathbf{Q} \left(\frac{\partial \mathbf{y}}{\partial \mathbf{p}}(t_i,\mathbf{p})|_{\mathbf{p}=\mathbf{p}^\circ}\right) \tag{3}$$

$\mathbf{F}$ combines information on (*i*) the error on the output measurements (typically $\mathbf{Q}$ is defined as the inverse of the measurement error variance matrix) and (*ii*) the sensitivities of the model output $\mathbf{y}(t,\mathbf{p})$ to small variations in the model parameters $\mathbf{p}$ (expressed in the sensitivity matrix $\partial\mathbf{y}/\partial\mathbf{p}$). The former is determined by the experimental measurement errors while the latter depends on the choice of the experimental conditions. OED is the result of the minimization or maximization of a scalar function of the Fisher information matrix by optimal choice of the experimental input. The selected scalar function determines the focus of the design. D-optimal design aims at the minimization of the joint confidence region on $\mathbf{p}$ via the maximization of the determinant of $\mathbf{F}$. For nonlinear models, the model output sensitivities (and thus $\mathbf{F}$) depend on the unknown parameters $\mathbf{p}$. During experimental design, $\mathbf{F}$ is therefore computed for $\mathbf{p} = \mathbf{p}^\circ$, with $\mathbf{p}^\circ$ an initial guess for the unknown model parameters, i.e., the so-called nominal parameters.

Application to the case study

In this case, the measured output equals $n(t)$ while the temperature $T(t)$ is the experimental input to be optimized. The unknown parameters are the four parameters of the CTMI: $\mathbf{p} \triangleq [T_{min}\ T_{opt}\ T_{max}\ \mu_{opt}]^T$. The duration of the lag phase, determined by environmental factors and the physiological state of the cells, is not accurately predictable. Therefore, a reduced form of the

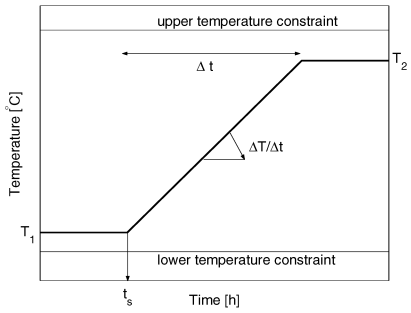

Figure 1: Parameterized temperature profile characterized by four degrees of freedom: T_1 [°C] the initial temperature, t_s [h] the time at which the increase or decrease in temperature starts, $\Delta T/\Delta t$ [°C/h] the rate of temperature change and Δt [h] the duration of the temperature change. T_2 indicates the final temperature and is calculated from the other profile characteristics. Temperature is bounded between a lower and an upper temperature boundary.

model of Baranyi and Roberts (1994) (Equation 1), in which the state variable $Q(t)$ is omitted, was used to design the optimal experiments.
The optimization problem is formulated as a series of two-parameter estimation problems. Given the four CTMI parameters, six different parameter combinations can be taken and for each parameter couple, the temperature profile is optimized, while the two remaining CTMI parameters are assumed perfectly known. The weighting matrix reduces to a single value, namely the inverse of the measurement error variance (s_n^2), which is taken equal to 3.27×10^{-2} (experimentally determined in the laboratory). The Fisher information matrix is calculated as displayed in Equation 2. Following a continuous OED/PE approach guarantees an overall optimal experiment, independent of an imposed number of samples. An advantage of the two-by-two estimation approach is that, when parameter estimates are obtained from a series of experiments, erroneous cell density measurements can be compensated by other experiments incorporating the same temperatures. Due to biological variability and errors on the cell density measurements, microbial growth data are noisy. Significant measurement errors in highly informational temperature zones can influence the parameter estimation.

Optimal experiments are designed for *E. coli* K12 MG1655, for which realistic CTMI parameters are: $T_{min} = 11.33$°C, $T_{opt} = 40.85$°C, $T_{max} = 46.54$°C, and $\mu_{opt} = 2.397$ 1/h (Bernaerts *et al.*, 2006). These values are adopted as nominal values during experiment design. The initial and maximum cell density are set at 7.000 ln(CFU/mL) and 22.55 ln(CFU/mL) respectively, which are both realistic values.

The time-varying temperature input $T(t)$ is parameterized to obtain a finite dimensional dynamic optimization problem (Figure 1). The optimization problem is solved based on a hybrid optimization method whereby the stochastic Integrated Control Random Search algorithm (ICRS) (Banga *et al.*, 1997) is combined with a deterministic algorithm (E04UCF) (The Numerical Algorithms Group Ltd.). Random values from the normal distribution in ICRS are generated with the pseudo-random generator G05FAF, combined with G05CCF to set the seed to a non-repeatable initial value (The Numerical Algorithms Group Ltd.). Values for the three heuristic parameters k_1, k_2 and n_e are set at the default values declared in Banga *et al.* (1997). In all algorithms, differential equations are numerically integrated with the NAG routine D02EJF.

Experimental setup

Bacterial strain and inoculum preparation

E. coli K12 MG1655 (CGSC♯6300) is stored at -80°C in Brain Heart Infusion broth (BHI) (Oxoid), supplemented with 25% glycerol (Acros Organics). The inoculum is prepared by subculturing the stock culture in 20mL BHI sequentially for 9h and 15h at 37°C (shaken).

From the appropriate pre-culture, the bioreactor (see below) was inoculated at approximately 7 ln(CFU/mL). After inoculation, cells were allowed to adapt to the new temperature for 2h to 4h prior to implementation of $T(t)$ and sampling, in order to minimize the initial lag. When the initial temperature (T_1) was equal to 45°C, a prolonged adaptation phase (≥6h) was implemented in order to avoid a possible phase of growth disturbance at 45°C (Van Derlinden *et al.*, 2008).

Bioreactor experiments

Dynamic experiments were performed in a bench top bioreactor (BioFlo 3000, New Brunswick Scientific Inc.). The reactor vessel, filled with 4.5L BHI was aerated at 2L/min and the stirrer speed was set at 400rpm. To avoid accumulation of foam, 1mL of anti-foam agent (Sigma) was added at the start of the experiment. Time-temperature profiles were implemented via the AFS-Biocommand Software (New Brunswick Scientific Inc.), with an accuracy of 0.2°C (RTD). The bioreactor unit was connected to a circulation cooler (CFT-33, Neslab Instruments Inc.) enabling temperature control below room temperature. pH was kept constant at 7.55 by the addition of base (1N KOH) (Acros Organics) or acid (1N H_2SO_4) (Acros Organics). At regular time intervals, a sample was taken aseptically to determine the cell density via plate counting on BHI agar (i.e., BHI supplemented with 6g/L technical agar nr 3., (Oxoid)).

Table 2: Optimized temperature profiles for all two-parameter combinations of the CTMI parameters (D-optimal design). (Letter codes refer to the graphs of the performed experiments.)

[15°C, 43°C]	T_1 [°C]	t_s [h]	$\Delta T/\Delta t$ [°C/h]	Δt [h]	T_2 [°C]	$\lvert\mathbf{F}\rvert$	real $\lvert\mathbf{F}\rvert$	
(T_{max}, μ_{opt})	40.85	1.385	-5.000	4.519	18.26	1.077×10^5	8.067×10^4	(A)
(T_{max}, T_{min})	29.45	5.037	-1.699	7.473	16.76	9.720×10^3	3.189×10^4	(B)
(T_{max}, T_{opt})	43.00	2.290	-5.000	5.270	16.65	1.880×10^3	1.699×10^3	(C)
(T_{min}, μ_{opt})	40.85	1.780	-5.000	4.788	16.91	1.800×10^6	2.991×10^6	(D)
(T_{min}, T_{opt})	31.15	4.382	-2.388	5.978	16.87	7.674×10^4	2.051×10^5	(E)
(T_{opt}, μ_{opt})	43.00	1.658	-5.000	5.089	17.55	7.911×10^5	7.911×10^5	(F)
[15°C, 45°C]	T_1 [°C]	t_s [h]	$\Delta T/\Delta t$ [°C/h]	Δt [h]	T_2 [°C]	$\lvert\mathbf{F}\rvert$	real $\lvert\mathbf{F}\rvert$	
(T_{max}, μ_{opt})	45.00	3.835	-5.000	6.000	15.00	8.482×10^5	6.950×10^5	(G)
(T_{max}, T_{min})	45.00	2.854	-5.000	5.812	15.94	1.117×10^5	1.140×10^5	(H)
(T_{max}, T_{opt})	45.00	2.938	-5.000	5.676	16.62	8.198×10^4	9.943×10^4	(I)
(T_{min}, μ_{opt})	40.85	1.780	-5.000	4.788	16.91	1.800×10^6	2.991×10^6	(D)
(T_{min}, T_{opt})	31.15	4.382	-2.388	5.978	16.87	7.674×10^4	2.051×10^5	(E)
(T_{opt}, μ_{opt})	45.00	2.801	-5.000	5.666	16.67	1.547×10^6	1.724×10^6	(J)

Data processing

Parameter estimation and confidence

Parameters were estimated via the minimization of the global sum of squared errors (SSE_{global}), using the *lsqnonlin* routine of the Optimization Toolbox of Matlab version 6.5 (The Mathworks Inc.). Differential equations are integrated by the *ode23s* routine (with an accuracy of 0.1%). The CTMI parameters and the maximum cell density (n_{max}) were jointly determined, while the initial cell density $n_{0,j}$ and the initial physiological state of the cells $Q_{0,j}$ are specific for each experiment.

The asymptotic 95% confidence interval on the parameter estimates $\hat{\mathbf{p}}$ was calculated using the parameter variance (s_i^2).

$$\left[\hat{p}_i \pm t_{(1-\frac{\alpha}{2}, n_t - n_p)} \cdot \sqrt{s_i^2} \right] \tag{4}$$

with $\hat{p}_i$ the i^{th} parameter estimate, t the *Student t* distribution value, α the significance level, n_t the total number of experimental data, n_p the total number of parameters, and $n_t - n_p$ the degrees of freedom. The parameter variances (s_i^2) were obtained from the main diagonal of the parameter covariance matrix $\mathbf{P}$ which was calculated from the Jacobian matrix determined simultaneously with the global identification.

Given the parameter variances, confidence and prediction limits on the model output can be calculated as explained in Van Impe *et al.* (2001).

RESULTS AND DISCUSSION

Defining the framework of OED/PE

In order to obtain a finite dimensional optimization problem, the dynamic temperature input $T(t)$ is parametrized as shown in Figure 1. After an initial period at constant temperature, temperature linearly decreases/increases to reach a final phase at constant temperature.

When designing optimal temperature profiles, two prerequisites should be fulfilled, namely practical feasibility of the optimal experiments and validity of the considered models.

(i) Practical feasibility. Practical feasibility and acceptable measurement errors need to be assured. When temperatures approach the lower boundary for growth, specific growth rates become very small. The lower temperature boundary (T_{low}) is therefore set at 15°C, a temperature at which an accurate measurement of the growth rate is guaranteed. Analogous, $T(t)$ is constrained by an upper temperature boundary T_{high} (see further). The duration of the designed experiments is fixed *a priori* at 38h from a practical point of view.

(ii) Model validity. The validity of both the primary growth model and the secondary, kinetic model has to be guaranteed throughout each experiment. Combining both models inherently assumes immediate adaptation of the specific growth rate to changing temperature, according to the CTMI model. It is, however, revealed by Swinnen *et al.* (2005) and Bernaerts *et al.* (2002), that abrupt temperature changes induce a transient disturbance of the exponential growth phase and thus violate the model validity. Immediate adaptation of the growth rate to changing temperatures is only guaranteed when moderate temperature changes are implemented, i.e., between -5°C/h and 5°C/h.

A second problem of model validity arises due to the disturbed growth kinetics at temperatures close to T_{max} (see Van Derlinden *et al.* (2008) for full details). The exponential growth phase of *E. coli* K12 MG1655 is disturbed when grown at temperatures close to the maximum temperature for growth. Up to 43°C, smooth growth curves can be observed, while at higher temperatures, growth curves are disturbed due to the different response of cells to the stressing temperature. At 45°C, the exponential growth phase is interrupted by an apparent phase of growth delay and at 46°C, a short period of growth is followed by inactivation. When designing

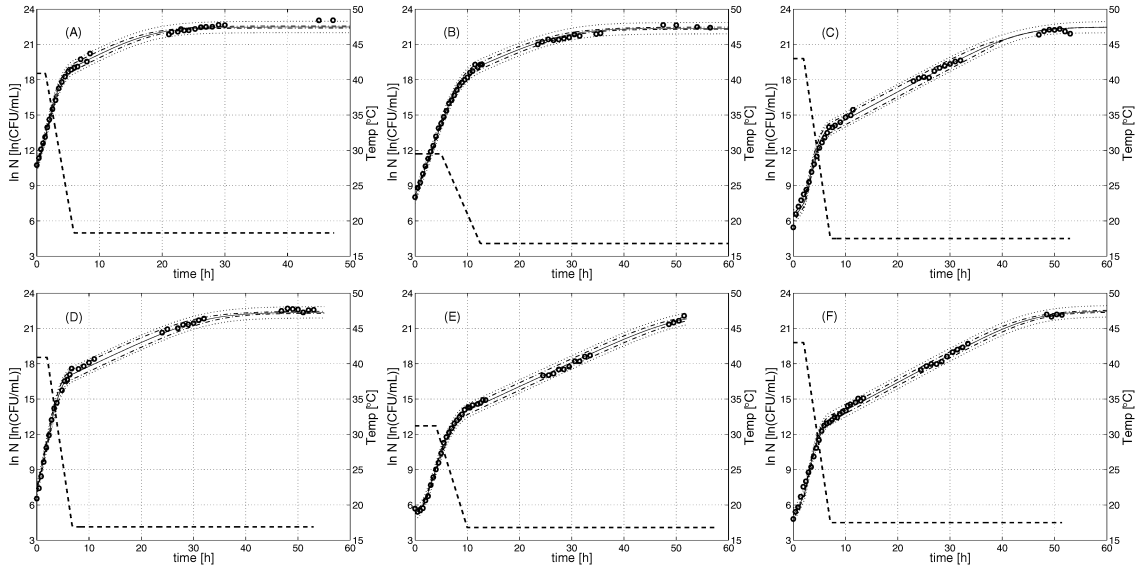

Figure 2: Global identification of the six optimal experiments designed within [15°C, 43°C]: experimental data (o), global identification curve (-) and temperature profile (- -). The confidence and prediction intervals are represented by (- ·) and (· ·), respectively. Parameter estimates are given in Table 3.

optimal dynamic experiments, this problem of disturbed exponential growth can be tackled in two ways.

1. The dynamic temperature profiles are confined to [15°C, 43°C], ensuring smooth growth curves (T_{high} = 43°C).
2. The inoculated cells are pre-adapted to cultivation at temperatures close to T_{max} such that smooth growth can be assumed up to 45°C. Hence, $T(t)$ can vary between 15°C and 45°C (T_{high} = 45°C).

Design of optimal temperature profiles

Optimal temperature profiles, i.e., yielding the largest determinant of **F** given the selected nominal values (Table 3), are summarized in Table 2. Experiments with a linearly decreasing temperature embed the most information, irrespective of the parameter couple. All optimal $T(t)$ profiles have similar characteristics: a temperature decline starts after a relatively short period (1.5h - 5h) at T_1 (43°C - 29.5°C), and is followed by a long period at a lower temperature T_2 (15°C - 18.3°C). The optimal rate of temperature decrease coincides in most cases with the lower boundary on $\Delta T/\Delta t$ (i.e., -5°C/h).

Similar to previous research (in which temperature profiles were optimized for solving a two-parameter estimation problem of a simpler kinetic model as function of temperature), rapid and large temperature changes are preferred to slow and small changes (Bernaerts *et al.*, 2000). The initial temperature T_1 strongly differs between parameter couples and ranges between 29.5°C and the upper temperature boundary (T_{high}). However, the lower boundary of the admissible temperature region, i.e., 15°C, is rarely attained.

Irrespective of the temperature boundaries, identical experiments are obtained for two parameter combinations, namely (T_{min}, μ_{opt}) and (T_{min}, T_{opt}) (profiles (D) and (E) in Table 2). For the parameter combinations (T_{max}, μ_{opt}), (T_{max}, T_{min}), (T_{max}, T_{opt}) and (T_{opt}, μ_{opt}), T_1 shifts to the higher temperature boundary (45°C) when optimized within [15°C, 45°C] (profiles (A)-(G), (B)-(H), (C)-(I) and (F)-(J) in Table 2).

Experimental implementation and parameter estimation

Before implementation, temperature profiles are simplified. The values of T_1, T_2 and $\Delta T/\Delta t$ are rounded as temperature is only measured and controlled up to one decimal digit (± 0.2°C). Likewise, t_s is expressed up to one decimal digit. The effect of input profile simplification and the discontinuous sampling on the determinant of **F** was very small, i.e., the *real* D criterion values approximate the theoretical values from the continuous optimization (see Table 2).

Subsequently, the optimized temperature profiles in Table 2 are implemented in a computer controlled bioreactor. The experimental protocol was chosen such that microorganisms were expected to grow exponentially when sampling started. However, four experimental curves ((E), (G), (I) and (J)) show a short but not negligible growth delay. While this corresponds with initial lag for experiment (E), the growth delay in Figures (G), (I) and (J) is most likely due to the disturbed growth at 45°C (see Van Derlinden *et al.* (2008)). To cope with this growth retardation, the state variable $Q(t)$ was retained in the model of Baranyi and Roberts (Equation

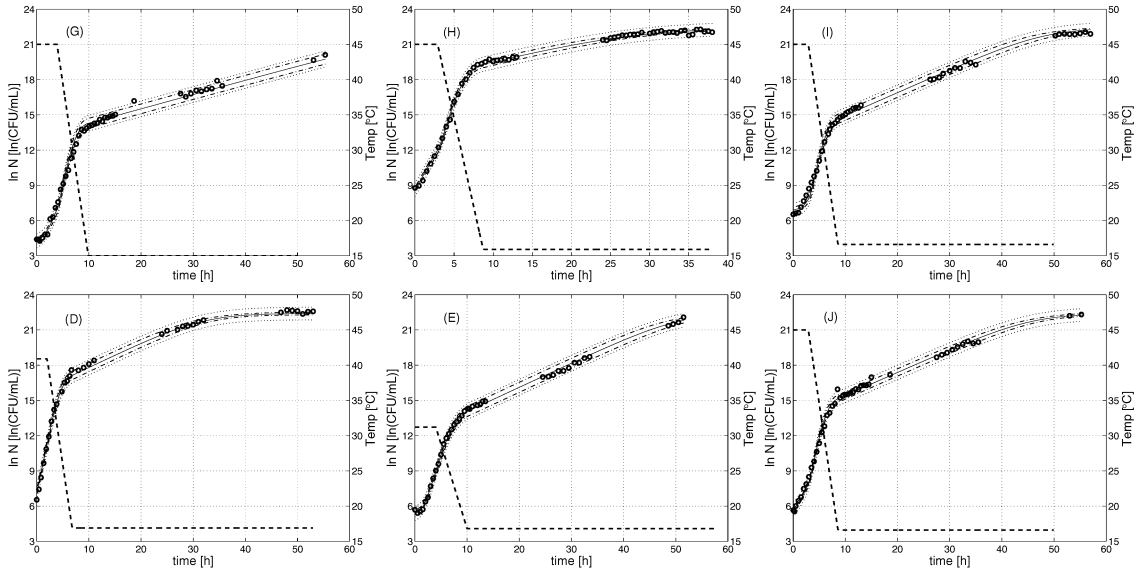

Figure 3: Global identification of the six optimal experiments designed within [15°C, 45°C]: experimental data (o), global identification curve (-) and temperature profile (- -). The confidence and prediction intervals are represented by (- ·) and (· ·), respectively. Parameter estimates are given in Table 3.

(1)) and Q_0 was also estimated during global parameter estimation. Global identification yields a good description of the experimental data as shown in Figure 2 and Figure 3. CTMI parameter estimates and corresponding 95% confidence limits are listed in Table 3.

All parameter estimates from the optimal, dynamic experiments ([15°C, 43°C] and [15°C, 45°C]) are characterized by a (very) good statistical quality (i.e., less than 5% uncertainty error). For T_{min}, T_{opt} and μ_{opt} both estimates and their corresponding 95% confidence limits are comparable. The maximum temperature for growth, however, is estimated significantly lower from experiments with the temperature boundary fixed at 43°C than from experiments within [15°C, 45°C]. The latter T_{max} estimate is assumed accurate as it closely agrees with the nominal, and thus the reference T_{max} value. The reason why T_{max} can not be estimated correctly from designs within [15°C, 43°C] can be found in the sensitivity of T_{max}. No experimental data are available between 43°C and 46.54°C (T_{max}°). However, it is in this region that μ_{max} is most sensitive for changes in T_{max}. Hence, the curvature of the CTMI between T_{opt} and T_{max}, and the value of T_{max} are uncertain. Designs with the upper temperature boundary close to the real T_{max} result in an accurate and reliable T_{max} estimate.

(i) Comparison with nominal values. Parameter estimates are compared with values from Bernaerts *et al.* (2006) (used as nominal values during optimal experiment design). In this research, cardinal parameters were estimated from a large set of static experiments. These values are considered as reference parameters. The new estimates for T_{opt} and T_{max} are in good agreement with the reference parameters and literature (Nauta and Dufrenne, 1999; Membré *et al.*, 2005). A large and significant discrepancy can be observed between T_{min} estimates from the optimal dynamic experiments (8.616°C and 9.139°C) and the reference value (11.33°C). In literature, the minimum growth temperature for different *E. coli* strains is situated between 4.9°C and $\geq$ 7°C (Nauta and Dufrenne, 1999; Jones *et al.*, 2004; Membré *et al.*, 2005), such that the new T_{min} estimates seem most reliable.

(ii) Comparison with estimates from non-optimized dynamic experiments. To conclude, the parameter estimates and corresponding 95% confidence limits are compared to results published in Bernaerts *et al.* (2006). In the latter work, CTMI parameters were also derived from four dynamic, non-optimal experiments. CTMI parameters derived from these four experiments are included in Table 3. Values for the optimum and maximum temperature for growth, and the optimum specific growth rate μ_{opt} are in agreement and again a significant difference can be observed for T_{min}. The latter parameter was overestimated when identified from the four non-optimized experiments. These four dynamic experiments do not contain sufficient information for the estimation of T_{min}. This is in contrast with the optimal experiments. Next to information build up when crossing the suboptimal temperature region during temperature decrease, information on the maximum specific growth rate at lower temperatures can be gathered during the prolonged period at the final temperature T_2, which is for all profiles situated between 15.0°C and 18.3°C.

Robustness of the design approach

Due to the nonlinearity of the model, the optimized dynamic temperature profiles will depend on the nominal parameters ($\mathbf{p}^\circ$). This problem is typically dealt with by iterative OED/PE, systematically improving the (nominal) parameters. The above sections showed convergence after a single design round as nominal values were close to the true parameters and temperature boundaries were chosen properly. Via a robustness study at simulation level, the effect of inaccurate nominal values on the efficiency and convergence of the presented optimal design approach is evaluated.

The robustness study is based on simulated optimal experiments designed with *erroneous* nominal values. The nominal values listed in Table 3 are taken as true parameters ($\mathbf{p}^*$). Optimal experiments are designed based on nominal parameters ($\mathbf{p}^\circ$) deliberately differing from the true values ($\mathbf{p}^*$). During experiment design, conditions and constraints applied in the above sections are retained, except for T_{low} and T_{high} which are set at ($T_{min}{}^\circ$+2°C) and ($T_{max}{}^\circ$-2°C), respectively. Simulated experimental data are generated using the true parameter values and adding normally distributed experimental noise (with zero mean and a variance equal to 3.27×10^{-2}). From these fictive data, CTMI parameters are identified through global identification.

(i) One deviating nominal value. Initially, the design approach is evaluated with only one nominal parameter different from its true value. For all possibilities ($p_i^\circ = p_i^* \pm 10\%$), parameter values derived are close to the true values after a first round of OED/PE, except when $T_{max}{}^\circ$ is much lower than $T_{max}{}^*$. The latter results in a significant underestimation of T_{max}, which is due to the lack of information in the region sensitive for its estimation (namely, very close to the $T_{max}{}^*$).

(ii) Several deviating nominal values. CTMI parameters are identified from experiments designed with several nominal parameters different from their true values. Even optimal experiments designed from these sometimes unrealistic initial CTMI parameters nearly always lead in a first round of OED/PE to parameter estimates close to the real parameters. Analogous to the first case, estimated parameter values only significantly deviate from the real values when the initial T_{max} was underestimated.

This proves that, in general, the applied design approach is robust and parameter estimates will easily converge to the true values. However, when the maximum temperature is initially chosen lower than its true value, T_{max} is significantly underestimated. Due to the initial underestimation of the maximum temperature for growth, little information on the effect of temperature is available in the temperature range between the true T_{opt} and T_{max}. Hence, the curvature of the CTMI is uncertain in the neighborhood of the true T_{max}. As seen in the robustness study, this results in an inaccurate estimate of the maximum temperature for growth. This observation emphasizes on the importance of a good T_{max} estimate or the selection of an appropriate upper temperature boundary for the design of the optimal experiments.

CONCLUSIONS

Within the presented research, the focus is on the accurate estimation of the cardinal temperatures of *E. coli* K12 MG1655 by means of optimal dynamic experimental design for parameter estimation.

Due to the nonlinearity of the model, optimal temperature profiles are determined by the nominal values. The robustness and convergence of the design procedure was proven. However, when the maximum temperature is initially chosen lower than its true value, T_{max} is significantly underestimated. This implies that the maximum temperature for growth can only be identified accurately when the temperature profile encloses temperatures very close to the true T_{max}.

The optimal dynamic temperature profiles were designed within two temperature regions with a different upper temperature constraint, namely [15°C, 43°C] and [15°C, 45°C]. The focus of the D-optimal design was on parameter accuracy. Only when the upper temperature constraint was close to the *true* maximum temperature for growth, T_{max} can be estimated accurately, an observation which corresponds with the conclusion from the robustness study. The parameter values resulting from six optimally designed experiments within [15°C, 45°C] are accurate and believed to be reliable. Next to underlining the importance of selecting an appropriate upper temperature constraint, this observation also uncovers a major drawback of the OED/PE procedure. Only when the maximum temperature for growth is known relatively well, the approach will result in a reliable and accurate T_{max} estimate.

T_{opt} and T_{max} estimates are in good agreement with their nominal values. The discrepancy with the nominal T_{min} value (based on static experiments) seems to be due to a lack of data at and below 15°C. By selecting the informational temperature regions, the application of OED/PE significantly improves the outcome of a one-step identification approach for secondary model parameters. Currently, the design includes six dynamic experiments. Further research will reveal if less experiments are as informative. The number of samples and the time of sampling is not yet taken into account but could further improve the results.

REFERENCES

Banga, J. R., A. A. Alonso and R. P. Singh (1997). Stochastic dynamic optimization of batch and semicontinuous bioprocesses. *Biotechnology Progress* **13**, 326–335.

Baranyi, J. and T. A. Roberts (1994). A dynamic approach

Table 3: Parameter estimates and corresponding 95% confidence limits for the CTMI parameters.

	Optimal designs		Bernaerts *et al.* (2006)	
	[15°C, 43°C]	[15°C, 45°C]	Nominal values	Non-optimal experiments
T_{min}	$8.616 \pm 3.581 \times 10^{-1}$	$\mathbf{9.139 \pm 4.449 \times 10^{-1}}$	$11.33 \pm 5.867 \times 10^{-1}$	$11.31 \pm 4.865 \times 10^{-1}$
T_{opt}	$39.49 \pm 4.563 \times 10^{-1}$	$\mathbf{39.59 \pm 5.550 \times 10^{-1}}$	$40.85 \pm 1.923 \times 10^{-1}$	$40.54 \pm 2.758 \times 10^{-1}$
T_{max}	$43.56 \pm 1.709 \times 10^{-1}$	$\mathbf{46.71 \pm 5.362 \times 10^{-1}}$	$46.54 \pm 1.270 \times 10^{-1}$	$46.68 \pm 8.843 \times 10^{-1}$
μ_{opt}	$2.233 \pm 8.808 \times 10^{-2}$	$\mathbf{2.095 \pm 8.122 \times 10^{-2}}$	$2.397 \pm 3.265 \times 10^{-2}$	$2.347 \pm 5.837 \times 10^{-2}$
MSE_{global}	5.775×10^{-2}	7.082×10^{-2}	5.931×10^{-2}	1.867×10^{-2}
(n_t, n_p)	(228, 17)	(262, 17)	(127, 4)	(112, 16)

to predicting bacterial growth in food. *International Journal of Food Microbiology* **23**, 277–294.

Bernaerts, K. and J. F. Van Impe (2004). Data driven approaches to the modelling of bioprocesses. *Transactions of the Institute of Measurement and Control* **26**, 349–372.

Bernaerts, K., E. Van Derlinden and J. F. Van Impe (2006). Estimation of cardinal temperature parameters from dynamic microbial growth experiments: a comparison of different approaches. In: *Proceeding of the 9th European conference Food Industry and Statistics* (M. Vivien and C. Reyns, Eds.). pp. 201–208. Faculté de Pharmacie, Montpellier (France), January 25 - 27, 2006.

Bernaerts, K., K. J. Versyck and J. F. Van Impe (2000). On the design of optimal dynamic experiments for parameter estimation of a Ratkowsky-type growth kinetics at suboptimal temperatures. *International Journal of Food Microbiology* **54**, 27–38.

Bernaerts, K., R. D. Servaes, S. Kooyman, K. J. Versyck and J. F. Van Impe (2002). Optimal temperature input design for estimation of the Square Root model parameters: parameter accuracy and model validity restrictions. *International Journal of Food Microbiology* **73**, 145–157.

Jones, T., C. O. Gill and L. M. McMullen (2004). The behaviour of log phase *Escherichia coli* at temperatures that fluctuate about the minimum for growth. *Letters in Applied Microbiology* **39**, 296–300.

Membré, J. M., B. Leporq, M. Vialette, E. Mettler, L. Perrier, D. Thuault and M. Zwietering (2005). Temperature effect on bacterial growth rate: quantitative microbiology approach including cardinal values and variability estimates to perform growth simulations on/in food. *International Journal of Food Microbiology* **100**, 179–186.

Nauta, M. J. and J. B. Dufrenne (1999). Variability in growth characteristics of different *Escherichia coli* O157 :H7 isolates, and its implications for predictive microbiology. *Quantitative Microbiology 1* **1**, 137–155.

Pinto, J. C. (1998). On the cost of parameter uncertainties. Effects of parameter uncertainties during optimization and design of experiments. *Chemical Engineering Science* **53**, 2029–2040.

Rosso, L., J. R. Lobry, S. Bajard and J. P. Flandrois (1995). Convenient model to describe the combined effects of temperature and pH on microbial growth. *Applied and Environmental Microbiology* **61**(2), 610–616.

Swinnen, I. A. M., K. Bernaerts and J. F. Van Impe (2006). Modelling the work to be done by *Escherichia coli* to adapt to sudden temperature upshifts. *Letters in Applied Microbiology* **42 (5)**, 507–513.

Swinnen, I. A. M., K. Bernaerts, K. Gysemans and J. F. Van Impe (2005). Quantifying microbial lag phenomena due to a sudden rise in temperature: a systematic macroscopic study. *International Journal of Food Microbiology* **100**, 85–96.

Van Derlinden, E., K. Bernaerts and J. F. Van Impe (2008). Dynamics of *Escherichia coli* at elevated temperatures: effect of temperature history and medium. *Journal of Applied Microbiology* **104(2)**, 438–453.

Van Impe, J. F., K. Bernaerts, A. H. Geeraerd, F. Poschet and K. J. Versyck (2001). Modelling and prediction in an uncertain environment. In: *Food process modelling* (L. M. M. Tijskens, M. L. A. T. M. Hertog and B. M. Nicolaï, Eds.). pp. 156–179. Woodhead Publishing Limited. England.

Walter, E. and L. Pronzato (1997). *Identification of Parametric Models from Experimental Data*. Springer. Masson.

ACKNOWLEDGEMENTS This research is supported in part by OT/03/30 and the K.U.Leuven-BOF EF/05/006 Center-of-Excellence Optimization in Engineering of the Research Council of the Katholieke Universiteit Leuven, the Belgian Program on Interuniversity Poles of Attraction, initiated by the Belgian Federal Science Policy Office. K. Bernaerts is a Postdoctoral Fellow with the Fund for Scientific Research Flanders (FWO-Vlaanderen).

EVA VAN DERLINDEN was born on August 10th, 1981 in Turnhout (Belgium). From 1999 till 2004, she attended the Katholieke Universiteit Leuven from which she obtained a masters degree in Bioscience Engineering. She performed her master thesis at the Chemical and Biochemical Process Technology and Control Section supervised by Prof. Jan F. Van Impe. In 2004, she started her PhD in this research group under the supervision and daily guidance of Prof. Jan Van Impe and Dr. Kristel Bernaerts, respectively.

CHEMICAL RISK ASSESSMENT/ EXPOSURE ASSESSMENT

AN EXPOSURE ASSESSMENT OF MYCOTOXINS FROM FEED-TO-FOOD IN DAIRY MILK

*Rory Coffey
Enda Cummins

School of Agriculture, Food Science and Veterinary Medicine
University College Dublin
Belfield, Dublin 4, Ireland
E-mail: rory.coffey@ucd.ie

KEYWORDS

mycotoxins, milk, exposure assessment

ABSTRACT

The objective of this study was to develop a quantitative Monte Carlo exposure assessment model for mycotoxins in dairy milk and to assess the potential human exposure levels. Mean concentrations of mycotoxins in milk were estimated using the simulation model (Aflatoxin M1 = 0.0161 µg/kg , Ochratoxin A = 0.0002 µg/kg , Deoxynivalenol = 1 µg/kg , Fumonisin B1 = 0.36 µg/kg , Zearalenone = 0.39 µg/kg , T-2 = 0.0722 µg/kg) while the simulated Tolerable Daily Intakes (TDI's) from milk for males and females all fell below European Union guidelines. Aflatoxin M1 was a toxin of greatest concern as it had potential to exceed the EU limit of 0.05 µg/kg in milk. The sensitivity analysis identified the concentration of toxins in maize as the area which needs most attention in relation to crop management and agricultural practice. The sensitivity analysis assessed also identified the carry over rate as a factor closely related to risk and as a factor which required further research.

INTRODUCTION

Quantitative Exposure Assessment is a methodology used to analyse scientific information in order to estimate the probability and severity of an adverse event. This methodology was applied to model the human exposure to mycotoxins resulting from mycotoxin contamination of dairy feed and, subsequently carried over to dairy milk for human consumption. Mycotoxins are secondary metabolites produced by fungi when cereals or animal feed are colonised by moulds. Excretion of such toxins in bovine milk has been documented (Yiannikouris and Jouany, 2002; Blüthgen, Hammer, and Teufel, 2004) and their carryover to dairy produce represents a potential threat to human health. Studies have demonstrated that human dietary exposure to mycotoxins may lead to severe illness and can lead to liver cancer (Marquardt, 1996; Notermans, 2003). This assessment specifically focused on six mycotoxins of concern to humans (Aflatoxin B1/M1, Ochratoxin A, Deoxynivalenol, Fumonisin B1, Zearalenone and T-2 toxin) and involved analysing data on the occurrence of these mycotoxins in three dairy feed ingredients (barley, wheat and maize), inclusion rates in dairy feed, carryover rates to milk and on subsequent human exposure. By combining the estimated individual mycotoxin concentrations in milk with available consumption data for the Irish population, the daily intake of mycotoxins from milk by individuals was calculated. The exposure was characterised by the probability that viable mycotoxin concentrations were in milk at the time of consumption. Information and data for the development of the model were obtained from Irish studies and expert opinion and, when not available, from research in other countries. The basic model structure is given in Figure 1.

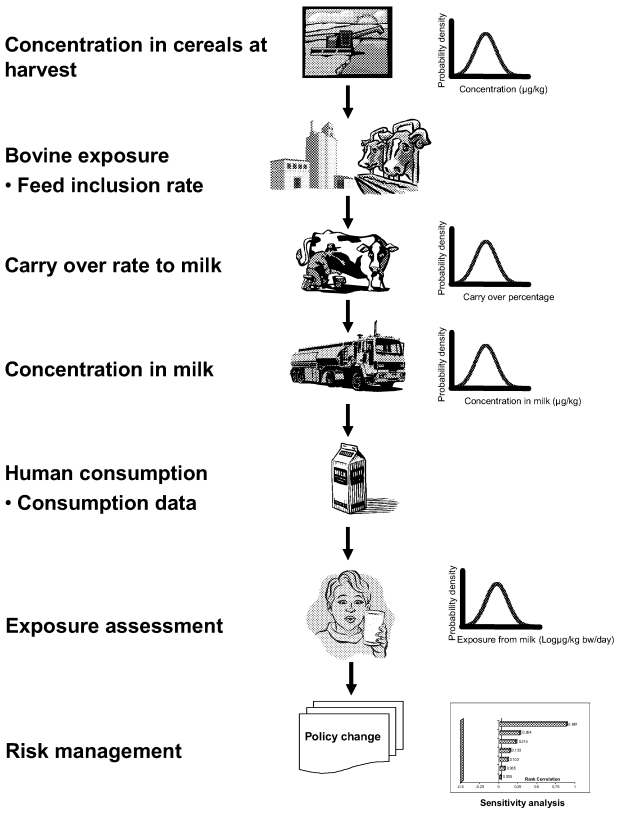

Figure 1: Model structure for simulating feed to food transfer of mycotoxins in bovine milk.

METHODOLOGY

The developed model relies upon the generation of random variables from input probability distributions and these are represented in the model equations by the name of the probability distribution (e.g. Poisson, triangular etc.) followed by the parameters in brackets. The model used Monte Carlo simulation techniques (Vose, 2000) to create the output distributions. Monte Carlo methods repeatedly select values randomly from distributions to create multiple scenarios of a problem. Together, these scenarios give a range of possible solutions, some of which are more probable and some less probable resulting in a probability distribution for the solution parameter.

Model inputs

Cereal inclusion rates in feed

In order to gain a comprehensive insight into the inclusion rates of barley, wheat and maize/maize products in dairy cow concentrate feeds, various feed formulations used within Ireland were examined and assessed. This included feeding studies conducted by Teagasc (2001) on sample dairy cow concentrate rations, maximum inclusion levels of feed components in concentrate mixes and concentrate feeding to balance grass/silage based diets.

Mycotoxin contamination in feed ingredients

From the literature reviewed, it was considered that there was only a remote chance of Aflatoxin B1 (AFM1) contamination in feed ingredients (barley, wheat) produced within Ireland (D'Mello et al. 1999; Placinta et al. 1999; Larsen et al. 2004). This was due to the fact that the Irish climate does not favour the formation of Aflatoxins in cereals. However, because a lot of the components of bovine concentrate feed are imported, maize from other countries was identified as a possible source of Aflatoxin B1 contamination of dairy cow concentrate feeds. To assess the presence of Aflatoxin B1 in maize, data from a survey by The Ministry for Agriculture, Food and Fisheries (MAFF 1999), which analysed maize imported into the UK intended for use in animal feed, was used. 139 samples in total were analysed with the limit of detection (LOD) being 0.1 µg/kg. Out of the 139 samples, 51 proved positive for Aflatoxin B1 with the highest concentration being 16.4 µg/kg.

To estimate the typical concentrations of Ochratoxin (OTA) in barley, a survey of stored grain by Prickett et al. (1999) was examined. Out of 106 barley samples analysed, 20 proved positive for OTA with a minimum concentration of 0.3 µg/kg and a maximum concentration of 117 µg/kg. The probability of OTA being present in barley was modelled using a beta distribution (n = 106, s = 20).

The survey carried out by Prickett et al. (1999) also tested stored barley and wheat for Deoxynivalenol (DON). In relation to barley there were 75 positive samples out of the total of 106. The minimum recorded positive concentration was 20 µg/kg and the maximum was 370 µg/kg. To account for this variability, the level of DON in barley was modelled using a cumulative distribution based on the data collected by Prickett et al. (1999)

Table 1: Model distributions and inputs for mycotoxin contamination level, carry over rate and concentration in dairy milk.

Symbol	Description	Distribution	Units
	Mycotoxin A=Aflatoxin M1/B1 (AFM1)		
P_{Amz}	Probability of AFB1 presence or absence in maize	Beta (n=134, s=51)	fraction
L_{Amz}	Level of AFB1 contamination in maize	Uniform, minimum 0.1, maximum 2	ug/kg
AV_A	Average AFB1 concentration in feed	$I_{mz} \times L_{Amz}$	ug/kg
CO_A	AFM1 carry over rate to milk	Exponential, mean 1.61	percentage
CM_A	Concentration of AFM1 in milk	$AV_A \times CO_A$	ug/kg
	B= Ochratoxin A (OTA)		
P_{Bb}	Probability of OTA presence or absence in barley	Beta (n=106, s=20)	fraction
P_{Bw}	Probability of OTA presence or absence in wheat	Beta (n=201, s=32)	fraction
P_{Bmz}	Probability of OTA presence or absence in maize	Beta (n=139, s=14)	fraction
L_{Bb}	Level of OTA contamination in barley	Cumulative (based on Prickett et al. 1999)	ug/kg
L_{Bw}	Level of OTA contamination in wheat	Cumulative (based on Prickett et al. 1999)	ug/kg
L_{Bmz}	Level of OTA contamination in maize	Uniform	ug/kg
AV_B	Average OTA concentration in feed	$(I_b \times L_{Bb})+(I_w \times L_{Bw})+(I_{mz} \times L_{Bmz})$	ug/kg
CO_B	OTA carry over rate to milk	Fixed value, 0.01%	percentage
CM_B	Concentration of OTA in milk	$AV_B \times CO_B$	ug/kg
	C= Deoxynivalenol (DON)		
P_{Cb}	Probability of DON presence or absence in barley	Beta (n=106, s=75)	fraction
P_{Cw}	Probability of DON presence or absence in wheat	Beta (n=201, s=198)	fraction
P_{Cmz}	Probability of DON presence or absence in maize	Beta (n=41, s=32.52)	fraction
L_{Cb}	Level of DON contamination in barley	Cumulative (based on Prickett et al. 1999)	ug/kg
L_{Cw}	Level of DON contamination in wheat	Cumulative (based on Prickett et al. 1999)	ug/kg
L_{Cmz}	Level of DON contamination in maze	Triangular, minimum 3, maximum 3700	ug/kg
AV_C	Average DON concentration in feed	$(I_b \times L_{Cb})+(I_w \times L_{Cw})+(I_{mz} \times L_{Cmz})$	ug/kg
CO_C	DON carry over rate to milk	Fixed value, 0.22%	percentage
CM_C	Concentration of DON in milk	$AV_C \times CO_C$	ug/kg

From the literature reviewed, it was concluded that the only real risk from Fumonisin (FB1) in bovine feeds would be from maize and maize products. This was due to the fact that the occurrence of FB1 in barley and wheat was rare and represented a negligible risk. Data from the

MAFF survey (1999) was used to assess the risk of FB1 occurring in maize. From the 139 samples examined, all of them contained concentrations of FB1. The ranges of concentrations with the survey on FB1 were 0 - 10 μg/kg (0 samples), 10 - 100 μg/kg (30 samples), 101 - 500 μg/kg (42 samples), 501 - 1000 μg/kg (28 samples) and 1001 - 5000 μg/kg (39 samples). These results were incorporated into a continuous empirical distribution and used to model FB1 levels.

Table 1: Continued.

Symbol	Description	Distribution	Units
	D= Fumonisin B1 (FB1)		
P_{Db}	Probability of FB1 presence or absence in barley	Fixed value, 0	fraction
P_{Dw}	Probability of FB1 presence or absence in wheat	Fixed value, 0	fraction
P_{Dmz}	Probability of FB1 presence or absence in maize	Beta (n=139, s=139)	fraction
L_{Db}	Level of FB1 contamination in barley	Fixed value, 0	ug/kg
L_{Dw}	Level of FB1 contamination in wheat	Fixed value, 0	ug/kg
L_{Dmz}	Level of FB1 contamination in maize	Uniform	ug/kg
AV_D	Average FB1concentration in feed	$(I_b \times L_{Db})+(I_w \times L_{Dw})+(I_{mz} \times L_{Dmz})$	ug/kg
CO_D	FB1 carry over rate to milk	Fixed value, 0.05%,0.11%	percentage
CM_D	Concentration of FB1 in milk	$AV_D \times CO_D$	ug/kg
	E= Zearalenone (ZEA)		
P_{Eb}	Probability of ZEA presence or absence in barley	Beta(n=31, s=31)	fraction
P_{Ew}	Probability of ZEA presence or absence in wheat	Beta (n=317, s=164.4)	fraction
P_{Emz}	Probability of ZEA presence or absence in maize	Beta (n=139, s=135)	fraction
L_{Eb}	Level of ZEA contamination in barley	Triangular, minimum 1, mode 4.3 maximum 21	ug/kg
L_{Ew}	Level of ZEA contamination in wheat	Cumulative, (ased on Vrabcheva et al. 1996)	ug/kg
L_{Emz}	Level of ZEA contamination in maize	Cumulative (based on	ug/kg
AV_E	Average ZEA concentration in feed	$(I_b \times L_{Eb})+(I_w \times L_{Ew})+(I_{mz} \times L_{Emz})$	ug/kg
CO_E	ZEA carry over rate to milk	Cumulative, based on data	percentage
CM_E	Concentration of ZEA in milk	$AV_E \times CO_E$	ug/kg
	F= T-2 toxin (T-2)		
P_{Fb}	Probability of T-2 presence or absence in barley	Beta (n=70, s=21)	fraction
P_{Fw}	Probability of T-2 presence or absence in wheat	Beta (n=921, s=321.2)	fraction
P_{Fmz}	Probability of T-2 presence or absence in maize	Beta (n=57, s=53)	fraction
L_{Fb}	Level of T-2 contamination in barley	Cumulative (based on Galtier, 1998; Yiannikouris and Jouany, 2002)	ug/kg
L_{Fw}	Level of T-2 contamination in wheat	Exponential	ug/kg
L_{Fmz}	Level of T-2 contamination in maize	Uniform, minimum 1.3, maximum 6	ug/kg
AV_F	Average T-2 concentration in feed	$(I_b \times L_{Fb})+(I_w \times L_{Fw})+(I_{mz} \times L_{Fmz})$	ug/kg
CO_F	T-2 carry over rate to milk	Uniform minimum 0.5, maximum 2	percentage
CM_F	Concentration of T-2 in milk	$AV_F \times CO_F$	ug/kg

Zearalenone (ZEN) in barley was surveyed in the UK by Tanaka et al. (1984). 4 (13%) out of 31 samples contained traces of ZEA with the mean concentration being 1 μg/kg. To represent this uncertainty, the probability of the presence of ZEN in barley was modelled using a beta distribution (n = 34, s = 4). Additional surveys on 10 samples in Scotland revealed that 100% of samples were contaminated with ZEN. The mean value recorded was 9 μg/kg. A study by the HGCA (Home Grown Cereals Authority UK) in 2004 revealed a mean concentration of 3 μg/kg, a maximum surveyed value of 21 μg/kg and a 95th percentile of 10 μg/kg. The uncertainty in the mean level of ZEN in barley was modelled using a triangular distribution with the minimum and maximum values corresponding to those given by Tanaka et al. (1984) and the mean equal to that given in the survey work by the HGCA (2004).

70 samples of barley were collected in the UK in 2004 and tested for the presence of T-2 toxin (HGCA, 2004). 70% of the samples (49) were less than the limit of quantification (<10 μg/kg) with 30% (21) proving to have T-2 contamination. This uncertainty in the probability of a positive sample of T-2 in barley was modelled using a beta distribution (n = 70, s = 21). The average concentration of T-toxin in the barley was 12 μg/kg, the 95th percentile was 37 μg/kg and the mean was 12 μg/kg. To account for this variability, the level of T-2 in barley was modelled using a normal distribution with a mean of 12 μg/kg and a standard deviation calculated such that the 95th percentile corresponded to 37 μg/kg as suggested by the HGCA (2004).

Mycotoxin carry over rates

The extent to which AFM1 is carried over to milk has varied greatly. Jones et al. (1994) reported the carry over rate to be circa 1.7 % while studies by the European Food Safety Authority (EFSA) in 2004 suggested a mean carry over rate of 2 % increasing to 6 % for high yielding cows. Henry et al. (2004) suggested ranges from 0.2 – 4 %. More recent studies estimate a wider carry over range from 0.3 - 6.2 % (Henry et al. 2004). An approximate carry over of 0.1% was suggested by Bluthgen et al. (2004). To account for the uncertainty in the percentage carry over of AFM1 to milk, the individual rates described above were fitted to an exponential distribution.

Due to the fact that OTA is degraded by rumen microflora in bovines, it has been suggested that the carry over rate to milk is minimal. Few studies have been carried out in this area. However, a study by Galtier (1998) calculated that if a cow was fed an oral dose of 1g/day, it would result in 100 μg/kg of OTA in milk. This results in a carry over rate of 0.01% and was taken as a fixed value to represent OTA carry over to milk in the model.

Similarly with DON, transfer to bovine milk is estimated to be small; however there is very little research in the area. A carry over of 0.22% was calculated from figures of dose and resulting concentration in milk (Galtier 1998). Again this was taken as a fixed value in the model.

For the carry over of FB1 to milk, two values were identified. The first was a value of 0.11% reported by the EFSA (2005). A transfer rate of 0.05% was reported as the average carry over rate for a single administration of 3 mg of toxin per kg of feed by Yiannikouris and Jouany (2002). A uniform distribution (minimum = 0.05, maximum = 0.11) was used to account for this uncertainty.

Transfer of ZEN to milk has revealed varying carry over rates. Yiannikouris and Jouany (2002) reported transfer rates of 0.06%, 0.016% and 0.008%, depending on the dose of the toxin administered. Rates of 0.00625% and 1.924 % were estimated from other feeding studies (Galtier 1998). A cumulative distribution was used to model the uncertainty surrounding ZEN carry over to milk using the transfer rates reported by Yiannikouris and Jouany (2002) and Galtier (1998).

The presence of T-2 residues in cows milk was reported to have been found in the range of 0.05 - 2% (Yiannikouris and Jouany 2002). Research by Galtier (1998) found a carry over rate in milk of between 0.02 and 0.32% for dairy cows fed 50,000 μg/kg of body weight. The variability in the transfer of T-2 toxin to milk was modelled using a cumulative distribution fitted to the carry over data suggested in the literature.

Consumption Data

Data on the quantities of milk consumed by Irish consumers was obtained from the Irish Universities Nutritional Alliance Survey (IUNA 2001). The mean consumption of wholemilk, low fat skimmed and processed milks for adult males (18-64 years) was 195 g/day, 80 g/day and 5 g/day, respectively. The standard deviations were 220 g/day, 149 g/day and 32 g/day, respectively. To account for the variability in wholemilk, low fat skimmed and processed milk consumption, a normal distribution was used corresponding to the mean and standard deviation for each product. For adult females, average consumption of wholemilk was equal to 110 g/day, low fat skimmed was equal to 95 g/day and processed milk was estimated at 5 g/day. Standard deviations were 141 g/day, 132 g/day and 31 g/day, respectively. Similar to male consumption, a normal distribution corresponding to the given mean and standard deviation for female consumption of each product was used to account for uncertainty.

Product exposure assessment

The product exposure assessment provides an estimate of how likely it is for an individual to be exposed to mycotoxin residues and in what quantities they are likely to be ingested. In order to calculate the human exposure to a mycotoxin from wholemilk, low fat skimmed milk or processed milks, firstly the concentration of the mycotoxin in milk was calculated. This is estimated using the equation:

$$(CMx/1000) \times P/M$$

Where

CMx = concentration of mycotoxin in milk (ug/kg)(subscript x = mycotoxin A, B, C, D, E or F),

P = milk product consumption; male or female (g/day)(wholemilk/low fat skimmed milk/processed milk)

M = mass of individual (kg): male or female, assumed to be 82.9 kg for males and 67.5 kg for females as given in IUNA study (2001)

Model assumptions

Simulation models frequently need to use necessary subjective assumptions. Such assumptions can have an impact on the results obtained in risk and exposure assessments. Consequently, assumptions made must be taken in context when considering model outputs. The following modelling assumptions have been made in the development of this exposure assessment:

- Feed production processes have little or no effect on initial mycotoxin concentrations in grain.
- Feed is not pelleted and is fed in ration form.
- Due to the fact that comprehensive data on mycotoxins in feed grains was unavailable for Ireland, data from other countries is representative of what occurs in Ireland. The authors acknowledge that this may not be the case in all circumstances but believe pessimistic values have been used therefore representing the upper end of risk.
- Dairy cows are fed a fixed feed formulation.

- Milk production processes (such as pasteurisation) have no effect on mycotoxin concentration in milk. This is due to the fact that the majority of mycotoxins are heat stable (Bata and Lásztity, 1999).
- Mycotoxins were assumed to be uniformly distributed throughout the milk.

Model Simulation

The exposure model was developed using Monte Carlo simulation techniques and probability distributions to account for model uncertainty and variability. The @RISK software package, version 4.0 (Palisade, USA), in combination with Microsoft Excel 2000 (Microsoft, USA) was used to run the simulation. The simulation was run for 10,000 iterations and reflects the inherent uncertainty in the production of bovine feed, in milk consumption and in the uncertainty of the mathematical process. The probability of a toxin in milk, the level of the toxin in milk and the probability of human exposure were outputs of the mathematical model. Monte Carlo simulation was also used to perform a sensitivity analysis of the model to assist in the identification of critical points in the process.

RESULTS AND DISCUSSION

For each toxin, the risk assessment model produced a probability density distribution (representing the uncertainty about the true mean value) of the potential level of these toxins in bovine milk consumed by humans. A summary of the simulation results, including uncertainty analysis and comparison with EU regulations for each analysed mycotoxin, is given in Table 2.

A probability-exposure distribution for males and females in relation to milk consumption (EWMf/m,x) was also produced. Table 3 displays a summary of these results together with existing legislation in the EU.

A sensitivity analysis was subsequently conducted to provide a measure of the most important factors affecting the risk to human health from an individual mycotoxin in milk. This information was displayed on a bar chart and can be seen in Figure 2. The sensitivity analysis may be the most important result of the risk assessment. It can be used to identify factors for which risk management strategies can be based in order to reduce the overall exposure to mycotoxins. Rank order correlation determines the correlation between input variables and outputs. The correlation coefficient lies between –1 (direct negative correlation) and +1 (direct positive correlation). Correlation values in the vicinity of zero indicate a weak predictive value of the variable (Cassin, Lammerding, Todd, Ross and McColl, 1998).

On examination of the sensitivity results for all the assessed mycotoxins, it was clear that in most cases risk estimates were very sensitive to the initial concentration of each toxin in maize followed by the level in barley and wheat. This concurs with the literature reviewed. The sensitivity analysis also singles out the concentration of toxins in maize as the area which needs most attention in relation to crop management and agricultural practice. The carry over rate also warrants further investigation.

Table 2: Simulated level of mycotoxins in bovine milk including uncertainty analysis

	AFM1 (ug/kg)	OTA (ug/kg)	DON (ug/kg)	FB1 (ug/kg)	ZEN (ug/kg)	T-2 (ug/kg)
Mean	0.016	0.0002	1	0.36	0.39	0.072
5th percentile	0.0002	8.84E-07	0.0049	0.0093	0.0002	0.0006
95th percentile	0.83	0.0009	4	1.44	2.55	0.29
Limit	0.5[a]	3[b]	500[c]	400[d]	50[c]	[e]

[a]EU limit for AFM in milk (Commission Regulation 2003/2174/EC)
[b]EU limit for cereal based food (Commission Regulation (EC) 472/2002)
[c]EU limits for cereal based foods (no limits exist for milk) (Commission Regulation (EC) No 856/2005)
[d]EU limits for maize based products (no limits exist for milk) (Commission Regulation (EC) No 856/2005)
[e]No limit for the presence of T-2 in milk/food products exists (Commission Regulation (EC) No 856/2005)

Table 3: Simulated exposure to individual mycotoxins from milk for males and females

	AFM (log µg/kg bw/day)		OTA (log µg/kg bw/day)		DON (log µg/kg bw/day)		FB1 (log µg/kg bw/day)		ZEN (log µg/kg bw/day)		T-2 (log µg/kg bw/day)	
	Male	Female	Male	Female	Male	Female	Male	Female	Male	Female	Male	Female
Mean	-5.06	-5.03	-7.34	-7.31	-3.22	-3.19	-3.49	-3.45	-4.36	-4.33	-4.49	-4.46
5th percentile	-6.45	-6.42	-8.80	-8.77	-5.00	-4.99	-4.77	-4.74	-6.32	-6.32	-6.03	-6.01
95th percentile	-3.67	-3.62	-5.63	-5.62	-1.87	-1.86	-2.33	-2.30	-2.18	-2.16	-3.01	-2.93
Tolerable daily intake (ug/kg bw/day)	a	a	0.005[b]	0.005[b]	1[b]	1[b]	2[b]	2[b]	0.2[b]	0.2[b]	0.06[b]	0.06[b]
Tolerable daily intake (log ug/kg bw/day)	a	a	-2.30	-2.30	0.00	0.00	0.30	0.30	-0.70	-0.70	-1.22	-1.22

a = No tolerable daily intake has been estimated (UK food standard agency,2004)
b = Tolerable daily intake estimated by the EU (Commission Regulation (EC) No 856/2005)

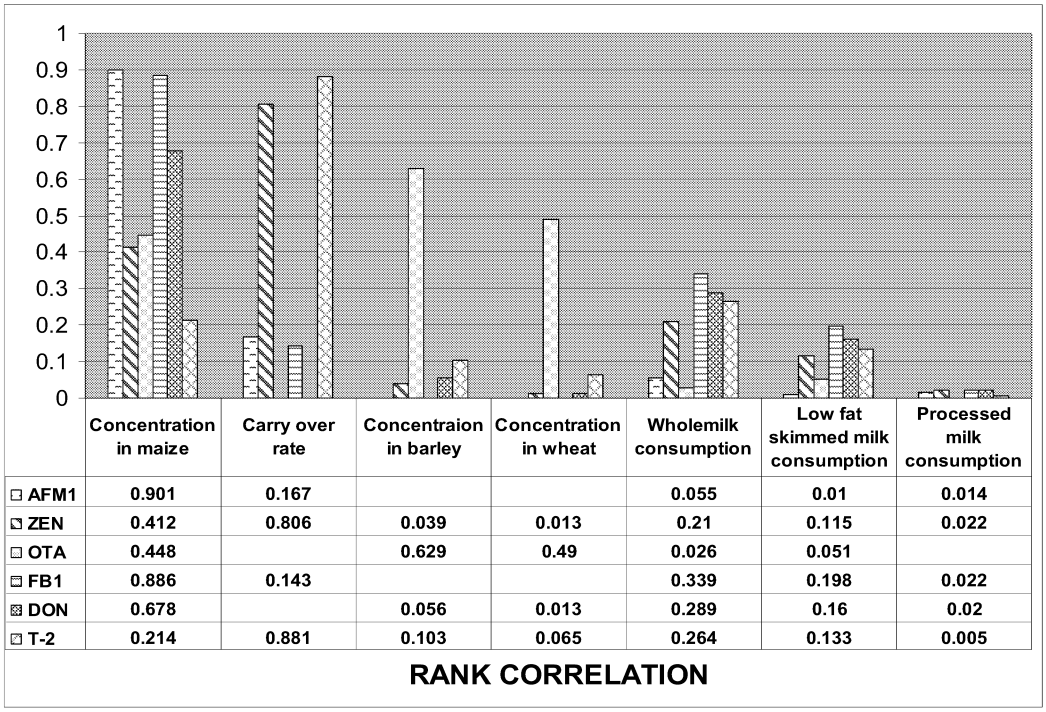

	Concentration in maize	Carry over rate	Concentraion in barley	Concentration in wheat	Wholemilk consumption	Low fat skimmed milk consumption	Processed milk consumption
AFM1	0.901	0.167			0.055	0.01	0.014
ZEN	0.412	0.806	0.039	0.013	0.21	0.115	0.022
OTA	0.448		0.629	0.49	0.026	0.051	
FB1	0.886	0.143			0.339	0.198	0.022
DON	0.678		0.056	0.013	0.289	0.16	0.02
T-2	0.214	0.881	0.103	0.065	0.264	0.133	0.005

Figure 2: Sensitivity analysis for human exposure to mycotoxins in bovine milk.

CONCLUSIONS

As natural and unavoidable contaminants of important agricultural commodities, mycotoxins have continued to severely impact animal health and consequently human health, which may have implications for livestock production, crops production and the economy. The risk is well recognised, but at present it has not been quantified accurately. Exposure modelling and risk assessment can be valuable tools in assessing risks to humans and animal from mycotoxins in the feed/food chain. The quantitative exposure assessment developed in this study tries to address deficiency in scientific literature and serves as an initial attempt to link the animal feed chain and the human food chain. The model assesses the potential human exposure to six mycotoxins in dairy milk. Results fit well with observed data, suggesting that the mathematical approximations of all real life variables are justified. The simulated exposure levels suggest that the mycotoxins in milk are all below limits set by the EU. Of all the mycotoxins assessed, only Aflatoxin M1 exceeded EU limits under certain conditions. A sensitivity analysis also suggests that the key to reducing mycotoxin contamination is at the field level prior to the harvesting of grain for feed production. Results from the exposure assessment model suggested that the presence of mycotoxins in bovine feed at normal contamination levels should not give rise to significant mycotoxin concentrations in milk. Evidence suggests that mycotoxins may never be completely removed from the feed-to-food chain but that current exposure levels are likely to be small in dairy milk and well below EU guidelines. It can be concluded that, from a risk perspective, the presence of mycotoxins in bovine milk poses little risk to man. If more accurate data becomes available on the biological fate and carry over of mycotoxins to bovine food products, the developed model should be updated and developed further. The model identified data gaps in these areas while directing future research efforts to fill these gaps.

REFERENCES

Blüthgen, A., Hammer, P. and Teufel P. 2004. "Mycotoxins in milk production. Occurrence, relevance and possible minimization in the production chain feeds-milk". *Kieler Milchwirtschaftliche Forschungsberichte*. 56(4): 219-263.

Yiannikouris, A. and Jouany, J.P. 2002. "Mycotoxins in feeds and their fate in animals: a review". *Animal research*. 51: 81-99.

Blüthgen, A., Hammer, P. and Teufel, P. 2004. "Mycotoxins in milk production. Occurrence, relevance and possible minimization in the production chain feeds-milk". *Kieler Milchwirtschaftliche Forschungsberichte*. 56(4): 219-263.

Teagasc 2001. "Fodder and feed events". Available from:

http://www.teagasc.ie/publications/2001/fodderandfeed/fodderandfeed2001.pdf. Accessed 05/12/05.

D'Mello, J.P.F, Placinta, C.M. and Macdonald, A.M.C. 1999. "A review of worldwide contamination of cereal grains and animal feed with Fusarium mycotoxins". *Journal of Animal Feed Science and Technology*. 78(1-2): 21-37.

Placinta, C.M., D'Mello, J.P.F. and Macdonald, A.M.C. 1999. "A review of worldwide contamination of cereal grains and animal feed with Fusarium mycotoxins". *Animal Feed Science and Technology*. 78(1-2): 21-37.

Larsen, J.C., Hunt, J., Perrin, I. and Ruckenbauer, P. 2004. "Workshop on trichothecenes with a focus on DON: summary report". *Toxicology Letters*. 153(1): 1-22.

MAFF 1999. Ministry for Agriculture Food and Fisheries UK- "Survey for aflatoxins, ochratoxin A, fumonisins and zearalenone in raw maize". Available from: http://archive.food.gov.uk/maff/archive/food/infsheet/1999/no192/192afla.htm . Accessed 21/01/05)/

Marquardt, R.R. 1996. "Effects of molds and their toxins on livestock performance: a western Canadian perspective". *Animal Feed Science and Technology*. 58(1-2): 77-89.

Notermans S. 2003. "Food authenticity and traceability, ensuring the safety of animal feed". Available from: www.foodmicro.nl/ensuringsafety.pdf Accessed 23/11/05.

Prickett, A.J., Macdonald, S. and Wildley, K.B. 1999. "Survey of mycotoxins in stored grain from the 1999 harvest in the U.K". Home-Grown Cereals Authority. Available from: http://www.hgca.com/publications/documents/cropresearch/230_complete_final_report.pdf. Accessed 04/10/05.

Tanaka, T., Hasegawa, A., Matsuki, Y., Lee, U.S. and Ueno, Y. 1986. "A limited survey of Fusarium mycotoxins nivalenol, deoxynivalenol and zearalenone in 1984 UK harvested wheat and barley". *Food Additive Contamination*. 3(3): 247-52.

Home Grown Cereals Authority (HGCA) 2004. "Investigation of fusarium mycotoxins in UK barley and oat production". Available from:http://www.hgca.com/content.template/4/0/About%20HGCA/About%20HGCA/About%20HGCA%20Home%20Page.mspx Accessed 15/02/06.

Jones, F.T., Genter, M.B., Hagler, W.M., Hansen, J.A., Mowrey, B.A., Poore, M.H. and Whitlow, L.W. 1994. "Understanding and coping with the effects of mycotoxins in livestock feed and forage" Available from: http://www.ces.ncsu.edu/disaster/drought/dro-29.html. Accessed 12/12/05.

Henry, S.H., Whitaker, T., Rabbani, I., Bowers, J., Park, D., Price, W., Bosch, F.X., Pennington, J., Verger, P., Yoshizawa, T., van Egmond, H., Jonker, M.A. and Coker, R. 2004. "Aflatoxin M1", Available From:http://www.inchem.org/documents/jecfa/jecmono/v47je02.htm Accessed 16/02/06.

Galtier P. 1998. "Biological fate of mycotoxins in animals". *Revue du Médicine Véterenaire*. 149: 549-554.

EFSA 2004. "Opinion of the Scientific Panel on Contaminants in Food Chain on a request from the Commission related to Aflatoxin B1 as undesirable substance in animal feed". *The European Food Safety Authority Journal*. 39: 1-27.

IUNA 2001. "Irish Universities Nutritional Alliance North/South Ireland Food Consumption Survey". Report Available from Food Safety Authority, Dublin, Ireland.

Vose D. (2001). 'Risk Analysis' second edition, Wiley and Sons Ltd.

Preliminary quantitative risk ranking and prioritisation of chemical contaminants in skim milk powder chain

A.Adekunte
F. Butler
C.O'Donnell

School of Agriculture, Food Science and Veterinary Medicine
Belfield, Dublin 4, Ireland.

E-mail: adefunke.adekunte@ucd.ie

KEYWORDS: Skim milk powder, risk ranking, chemical contaminants, food safety.

ABSTRACT

Consumers' awareness of food contaminants and their risks to human health has increased greatly in recent times. Food safety is high on the agenda of both the food industry and those involved in food regulatory matters as a result of chemical contamination in food products. Contamination occurring along the production chain may have a significant subsequent effect on skim milk powder (SMP) which is a multifunctional ingredient for food industries throughout the world and therefore has the potential to act as an important source of chemical hazard to consumers, particularly infants and young children. However, developing a chemical risk ranking methodology will provide information on relative risks posed by the presence of chemicals in the entire skim milk powder chain. In order to develop an accurate and reliable ranking, the following parameters were considered; genotoxicity (threshold/non-threshold), occurrence (concentration of chemicals in SMP), human exposure and risk based advisory values (e.g. Allowable Daily Intake, ADI) of the chemical contaminants. In this present study, the occurrence and consumption data were from the National Food Residue Database of Ireland (NFRD) and National Dairy Council, Ireland respectively while the genotoxicity data and the risk based advisory values were from regulatory agencies (WHO, JECFA, CODEX & EU). Using the available data and parameters, a quantitative risk ranking methodology was developed for ranking and prioritising chemical contaminants in the SMP chain. From the result, Aflatoxin, Polyaromatic Hydrocarbons and PCBs were high ranked due to their genotoxicity/carcinogenicity actions; zinc, selenium, copper, nitrate and lead were ranked quantitatively (arranged in order of ranking) while tin, arsenic, cadmium and mercury were ranked low as occurrence data showed that they were below the detection limit.

INTRODUCTION

In recent years, skim milk powder is one of the most implicated milk products contaminated with microbial toxins and chemical residues, which are leading to continuing health and regulatory concern. At the farm level, cattles are potentially exposed to contaminants which are naturally present (cadmium, arsenic, lead) or deposited on grass from industrial emissions (dioxin, polycyclic aromatic hydrocarbon) or present in soil as a result of use agrochemicals (pesticides, fertilizers) or through feedingstuffs (mycotoxins, metals, veterinary drugs) (IDF, 1997) thereby making milk and milk products susceptible to contamination (see Figure 1 for the entire skim milk powder chain). From a food safety point of view, there is a need to increase consumers' confidence in skim milk powder by identifying and prioritising contaminants of natural and possibly malicious origin that may occur along the chain. Risk ranking is a useful and valuable methodology that can be used for identifying the most significant risks in a food product. Chemical risk ranking fits within the larger field of risk assessment and involves the following steps; hazard identification, risk estimation, development of a ranking list, comparing the risks and placing them in order. This technique allows the relative comparison of several contaminants of foods, which can either drive risk management decisions directly in terms of resource prioritisation or alternatively, it can identify priority contaminants that require further risk assessment. A risk ranking model can be utilised in the first step of a HACCP programme (FAO, 1997) whereby once potential contaminants are identified for a particular foodstuff, ranking approach can then prioritise contaminants to be controlled by the implementation of appropriate critical control points (HACCP Principal Two). Quantitative risk ranking using risk estimation puts two parameters into consideration; exposure (dose) and allowable daily intake. A considerable amount of work has been done in risk ranking of chemicals for

environmental applications (Swanson et al., 1995; Kocher et al., 2002; Giannopoulou and Katsiri, 2005). There are fewer applications of risk ranking of foods, though a number of papers have been published on ranking pesticide risks in foods (Low et al., 2004; Calliera et al., 2006; Juraske et al., 2007). Low *et al.* (2004) assessed the relative risk of pesticide residues in consumers by defining risk as a measure of exposure (residue intake) and ADI, where risk is proportional to hazard and exposure. ADI values are based on a lifetime's exposure, which means the amount of chemical that can be consumed everyday for the entire lifetime of a consumer without an appreciable health risk (Low et al., 2004). ADI or TDI (Tolerable Daily Intake) values can be sourced from recommendations by International organisations such as World Health Organisation (WHO), Codex Alimentarius (Codex), Joint Expert Committee Food Additives and Contaminants (JECFA) and European Union (EU).

METHODOLOGY

A risk ranking methodology was developed and used for prioritising and ranking chemical contaminants in skim milk powder chain using the following parameters;

Risk based advisory score – generally the Allowable Daily Intake (when available) – Measure of toxicity/hazard.

Exposure – Residue intake (depends on availability of occurrence and contamination data).

Genotoxicity/Carcinogenity – Threshold/ Non-threshold. Figure 2 shows the methodology and steps involved in ranking of chemical contaminants. Prior to quantitative risk ranking, a preliminary ranking (qualitative) has been carried for all identified chemical contaminants along the chain by using the following decision tools:

A. Probability of contamination on farm (animal feed, raw milk).

B. Probability of contamination (from other sources, such as water, environment, contact surfaces) at subsequent stages in the farm-to-fork chain.

C. Probability of decrease/reduction in the level of hazard (chemical contaminant) during the journey from farm to fork, including removal of fat from skim milk powder.

These decision tools assisted in describing the chemical pathways from 'farm to fork' (see Figure 1, step 2) as well as sifting out some contaminants that were deemed to be of very low probability of occurrence. Consequently, contaminants that find their way to the final product will be ranked using step 4 or 5 of Figure 2. The risk ranking criteria is essentially an indication of chronic or prolonged exposure as it is based on a risk based advisory score (generally the ADI) which is an estimate of the amount of a chemical substance that may be ingested over a lifetime without appreciable risk to health. Quantitative risk ranking using risk estimation puts two parameters into consideration; exposure (dose) and allowable daily intake. The risk ranking criteria takes the same basic form as Low et al. (2004).

$$\text{Risk estimation} = \frac{\text{Exposure (i.e. residue intake)}}{\text{Allowable Daily Intake (ADI)}}$$

where Exposure (mg/kgbw.d) = Residue concentration (mg/kg) **X** consumption (kg/day)

Worst-case exposure was calculated as follows:

Exposure = Highest concentration detected in food **X** Food consumption.

However, step 8 (Figure 2) represents the situation where by the contaminant does not have ADI or TDI and step 7 (Figure 2) is not applicable. Some genotoxic contaminants such as Aflatoxin and PAH does not have any ADI or TDI. This is because very low levels of exposure to genotoxic carcinogens may increase the risk for adverse outcomes and no exposure threshold is assumed. As a result, genotoxic carcinogens are high ranked than other contaminants with ADI or TDI.

RESULT AND DISCUSSION

Hazard identification involves thorough literature studies and information gathering from various sources such as the official websites of JECFA, FAO/WHO, NFRD, IDF and peer-review publications. Qualitative risk ranking was carried out using decision tools A-C and the most relevant contaminants are presented in Table 1. Using the developed risk ranking methodology, potential chemical contaminants in the skim milk powder chain have been prioritised. Table 2 indicates how the risk ranking index is calculated for several contaminants in SMP (assuming an average consumption of 0.0156kg/day). Average consumption of skim milk powder was calculated based on % of SMP (5%) in 125g of yogurt (since most people consume yogurt everyday rather than SMP). Survey shows that men consume 2.5servings/day while women consume 1.5servings/day (NDC report, 2001) where 1 serving is equivalent to 125g. Thus, average consumption of SMP/day/kg was calculated using % SMP in yogurt and servings/day. Table 1 represents the descriptive statistics of all the relevant data from the Irish National Residue Database while Table 2 shows the overall risk estimation and ranking. Apart from the high ranked carcinogenic chemicals and zinc, all other contaminants (selenium, copper, lead, nitrate, mercury, cadmium, tin and arsenic were ranked low. Calliera et al., (2006) formulated a similar chronic

indicator, HAPERITIF$_{chr}$, based on the ratio between the estimated daily intake and the admissible daily intake (ADI). The present study takes a similar approach to this study. The risk ranking criteria is essentially an indication of chronic or prolonged exposure as it is based on the ADI which is an estimate of the amount of a chemical substance that may be ingested over a lifetime without appreciable risk to health. The risk ranking criteria does not at present consider the possibility of acute short term exposure arising from a catastrophically high level of a contaminant being present in a food that causes immediate illness. It can be argued that the frequency of such events is so low and the fact that no realistic testing programme can give any reliable protection against such an event that it is justifiable to concentrate on chronic or prolonged exposure in the first case.

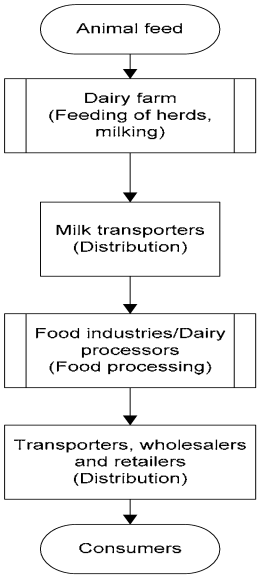

Figure 1: An outline of the entire skim milk powder chain from 'farm-to-fork'

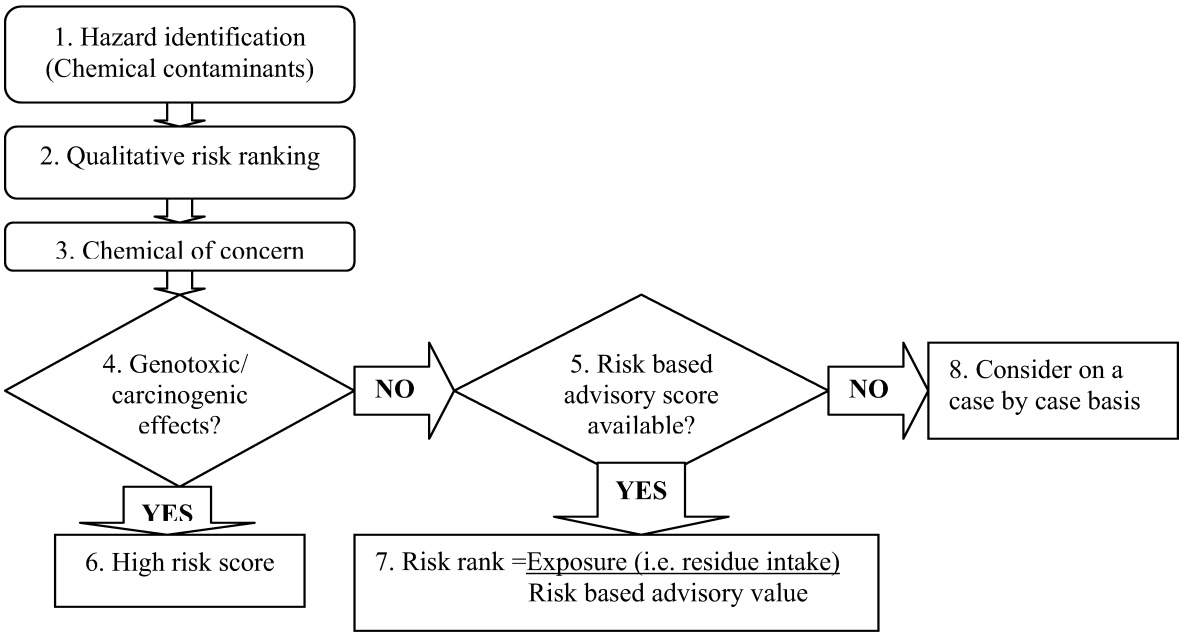

Figure 2: Schematic diagram of a risk ranking methodology

Table 1: Descriptive statistics of potential contaminants in skim milk powder

Contaminant	n	Mean ± S.D	Median	Mode	Minimum	Maximum
Aflatoxin M1	19	0.0001 ± 3.4E-05	0.00009	0.00009	0.00004	0.00015
Benzo(a)pyrene	9	0.0002 ± 0.0002	0.0001	0.00001	0.00001	0.0005
Acenaphthene	19	0.00027 ± 0.00016	0.0002	0.0002	0.0001	0.0007
Fluorene	15	0.00084 ± 0.0004	0.0007	0.0006	0.0003	0.0016
Naphthalene	1	0.0011	0.0011	N/A	N/A	N/A
Phenanthrene	14	0.0038 ± 0.004	0.00195	0.0014	0.0011	0.017
Pyrene	1	0.0009	0.0009	N/A	0.0009	0.0009
PCDD/PCDF	*	*	*	*	*	*
PBDE	*	*	*	*	*	*
PCB	*	*	*	*	*	*
Zinc	71	45.2 ± 2.78	44.95	42.6	39.6	54.7
Selenium	71	0.17 ± 0.041	0.16	0.16	0.1	0.34
Copper	71	0.5 ± 0.17	0.51	0.3	0.26	0.88
Nitrate	75	26.2 ± 23.09	20	16	0.5	121
Lead	2	0.029 ± 0.007	0.029	N/A	0.024	0.034
Tin	71	0	0	0	0	0
Arsenic	71	0	0	0	0	0
Mercury	71	0	0	0	0	0
Cadmium	71	0	0	0	0	0

Note:
Values in mg/kg
**- No data is available for PCDD/PCDF, PBDE and PCB*

Table 2: Overall risks of specific chemical/food combination in a skim milk powder

Chemical contaminant	ADI (mg/kg)	Highest concentration detected (mg/kg)	Residue intake (mg/person/day) Exposure	Overall risk score
Aflatoxin M1	-	0.00015	-	High risk
Benzo(a)pyrene	-	0.0005	-	High risk
Acenaphthene	-	0.0001	-	High risk
Anthracene	-	0.0001	-	High risk
Fluorene	-	0.0016	-	High risk
Naphthalene	-	0.0011	-	High risk
Phenanthrene	-	0.017	-	High risk
PCDD/PCDF	-	*	*	*
PBDE	-	*	*	*
PCB (dioxin-like)	-	*	*	*
Zinc	0.1451	54.7	0.85	5.89
Selenium	0.0063	0.34	0.005	0.84
Copper	0.0212	0.88	0.014	0.65
Nitrate	3.65	121	1.89	0.51
Lead	0.025	0.034	0.000531	0.021
Tin	14	0	0	0
Arsenic	0.015	0	0	0
Mercury	0.005	0	0	0
Cadmium	0.007	0	0	0

Note:
***** *No ADI*
- Data from National Food Residue Database showed that tin, arsenic, mercury and cadmium are below detection limits in skim milk powder. No data is available for PCDD/PCDF, PBDE, and PCB.

CONCLUSION

A quantitative risk ranking criteria was developed for ranking and prioritising chemical contaminants in SMP chain. This technique represents a relationship between risk, toxicity and quantity of chemical consumed in a food. Results may vary when using this methodology as the availability of data and parameters to be considered are crucial. Conclusively, this chemical ranking methodology has provided information on the risk posed by some chemical contaminants in the skim milk powder chain based on the data from Irish National Food Residue Database (NFRD) and the approach is applicable for use in other food products.

Acknowledgements

This research (ΣChain) is supported by the European Union through the Sixth Framework programme (Food Quality and Safety)

REFERENCES

Calliera M., Finizio A., Azimonti G., Benfenati E., Trevisan M. (2006). Harmonised pesticide risk trend indicator for food (HAPERITIF): the methodological approach. Pest Management Science 62(12): 1168 -76.

FAO (1997). Codex Alimentarius – Basic texts on food hygiene, Second Edition, Rome.

Low F., Lin H.M, Gerrard J.A., Cressey P.J., Shaw I.C. (2004). Ranking the risk of pesticide dietary intake. Pest Management Science 60(9): 842-8.

National Dairy Council (2001). The role of dairy foods in Health. http://www.ndc.ie/.

National Food Residue Database (NFRD). http://www.nfrd.teagasc.ie/.

Swanson M.B., Socha A.C. (1997). Chemical ranking and scoring: Guidelines for relative assessments of chemicals Florida: Setac Press.

Giannopoulou L., Katsiri A. (2005). A methodological approach to estimate risks to

human health from the use of pesticides in Agriculture. Proceedings of the 9th International conference on Environmental Science and Technology, Rhodes island, Greece.

International Dairy Federation (1997). Monograph on residues and contaminants in milk and milk products. IDF special issue 9701, Brussels, Belgium.

International Dairy Federation (1996). Bacteriological quality of raw milk. IDF, Brussels, Belgium.

Joint WHO/FAO Expert Committee on Food Additives (2007). Sixty-eight report on evaluation of certain food additives, flavouring agents and contaminants.

Joint WHO/FAO Expert Committee on Food Additives (2001). Fifty-Sixth report on meetings of expert committees and study groups, Geneva. Evaluation of certain mycotoxins.

Juraske R., Anton A., Castells F., Huijbregts A.J. (2007). PestScreen: A screening approach for scoring and ranking pesticides by their environmental and toxicological concern. Environmental International 33(7): 886-893

Kocher D.C., Greim H. (2002). An approach to comparative assessments of potential health risks from exposure to radionuclides and hazardous chemicals. Environmental International 27(8): 663-671.

A METHODOLOGY FOR PREDICTING BARLEY β-GLUCAN LEVELS DURING PRE-HARVEST STAGES

Uma Tiwari and Enda Cummins
UCD School of Agriculture, Food Science and Veterinary Medicine,
University College Dublin,
Belfield, Dublin 4,
Ireland
E-mail: uma.tiwari@ucd.ie

KEYWORDS
Model design, β-glucan, Simulation, Sensitivity analysis.

ABSTRACT

This study looks at the development of a farm-level baseline model to simulate the impact of various genotypic, environmental and agronomic factors influencing the level of β-glucan content in both hulled (H_B) and hull-less barley (H_{LB}) varieties. Monte Carlo simulation techniques were employed to model various stages in pre-harvest processes and to simulate the factors impacting the β-glucan content of barley cultivars. Probability density functions were fitted to relevant data sets collated from the scientific literature to capture the inherent uncertainty and variability in the factors. The model was developed in Microsoft Excel using the @Risk add-on package and the model run for 10,000 iterations. The mean simulated level of β-glucan was estimated to be 4.53 g/100g and 6.27 g/100g for hulled (H_B) and hull-less barley (H_{LB}) varieties, respectively. A sensitivity analysis illustrated that barley cultivar, harvest delay, germination time, storage days and precipitation are factors significantly influencing the β-glucan content (correlation coefficients of 0.62, 0.45, -0.33, -0.24 and -0.17 for hulled and 0.74, 0.38, -0.29, -0.22 and -0.14 for hull-less barley) This study highlights the influence of pre-harvest operations on β-glucan content and thus allows strategies to be identified to influence its content.

INTRODUCTION

β-glucan is a major soluble dietary fibre component of barley grain. Recent interest in health promoting foods and industrial applications has resulted in the development of new barley genotypes with improved phytochemical content. Varieties are typically classified according to the presences or absence of a hull on the grain. Hull-less barley varieties are nutritionally superior to the hulled varieties, which results in greater potential in industrial applications for hulled varieties including in chemically leavened products such as muffins, pancakes, bread, biscuits and cookies (Bhatty 1995). The β-glucan content in barley is reported to vary between 4.0 and 12.0 g/100g dry matter (Jeraci and Lewis 1989), however, the new genotypes may contain between 11 g/100g and 17.4 g/100g β-glucan (Miller and Fulcher 1994). β-glucan has been shown to have an important influence on human glycaemic control (lowering postprandial blood glucose) (Yokoyama et al. 1997). β-glucans have been used as food ingredients, as fat replacers and in formulations of beverages, meats, non-dairy creamers and canned soups (Morin et al. 2001). Studies from Pérez-Vendrel et al. (1996) reported that cultivar, environmental factors and agronomic factors (such as nitrogen fertilisation) affect the level of β-glucan in barley. This paper details the development of a baseline simulation model used to simulate the impact of various agronomical factors on β-glucan content. Monte Carlo simulation techniques were used to assess the influence of pre-harvest stages on β-glucan content using this farm-level simulation model.

MATERIALS AND METHODS

Model development

A flow diagram of the baseline model describing the various factors impacting β-glucan content is shown in Figure 1. The novelty of the approach used in this study lies in quantifying both the uncertainty and variability in factors influencing β-glucan content of barley grains, while modelling Irish agricultural practices. The uncertainty and variability in the input data were represented by probability density functions (PDF) and are summarised in Appendix A.

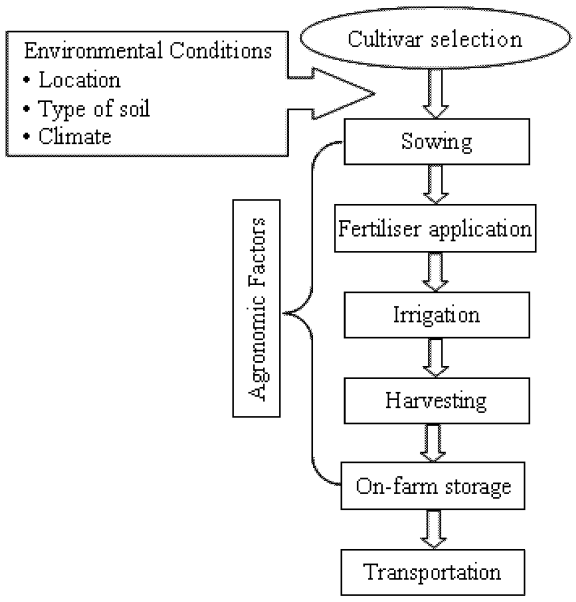

Figure1: Schematic representation for pre-harvest processing of barley.

Input data description

Genotypic factors

In assessing the genotypic factors, the initial level of β-glucan in seed grain was modelled using data collated from existing scientific literature (Prentice and Faber 1981; Pérez–Vendrell et al. 1996; Oscarsson et al.1996; Güler 2003) relating to sixty popular hulled and hull-less barley cultivars primarily used for food purposes. To capture the variability in β-glucan content in both barley cultivars, a lognormal distribution was used with a mean of 4.25 ± 1.28 g/100g for hulled (H_B) and 5.88 ± 2.54 g/100g for hull-less (H_{LB}) varieties. Figure 2a-b shows the resulting probability distribution for β-glucan content in hulled (H_B) and hull-less barley (H_{LB}).

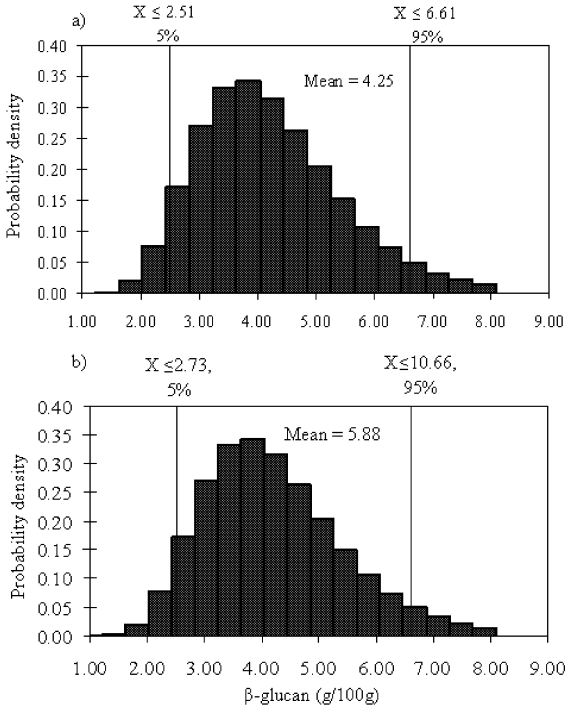

Figure 2: Probability distribution for β-glucan level in a) Hulled (H_B) and b) Hull-less barley (H_{LB})

Environmental Conditions

The barley β-glucan content is affected by many environmental factors, including soil nitrogen level and precipitation (Pérez–Vendrell et al. 1996). Location (L_{OC}) and growing area may have an influence on β-glucan content (Zhang et al. 2001); however effects appear to be small within regions. As a result a factor of 1 was assumed for the effect of location (L_{OC}) in Ireland as climatic conditions such as rainfall, solar radiation, and topography of land are reasonably consistent in barley growing regions. The recommended soil pH for optimum growth of barley is between 5.0 and 8.3. Current research does not indicate any effect from soil pH at these levels. As a result, a factor of 1 for soil pH (S_{PH}) was assumed in the model. Barley can be grown on many soil types (well drained, fertile loams and lighter clay soils). Research from Conry 1997 indicated the impact of different soil types (S_T) (light sandy loam, medium loam and heavy loam soil) on β-glucan content, ranged from 0.9 to 1 (factor basis). Thus, a uniform distribution was used to model the influence of soil type on β-glucan content with a minimum of 0.9 and a maximum of 1, thus remaining within the bounds given by Conry (1997).

Precipitation is shown to be negatively correlated with β-glucan content in barley (Güler 2003). The availability of water during grain maturation has been shown to significantly influence the level of β-glucan, for example. dry conditions before harvest have been related to high β-glucan levels (Anderson et al. 1978). Pérez-Vendrell et al. (1996) reported that mild temperatures (<11.7°C) lead to lower β-glucan content. Data from Pérez-Vendrell et al. (1996) was used in the software programme BESTFIT and an uncertainty distribution created for precipitation (P) and temperature (T) using a logistic distribution with mean value of α (Appendix A). Based on existing scientific evidences, it is difficult to separate the individual effects of precipitation and temperature on β-glucan content. Therefore, a response surface analysis was carried out to quantify the reliance of β-glucan on these two independent factors (rainfall and temperature). In order to find a suitable approximation for the true functional relationship between independent variables (rainfall and temperature) and their interaction on the response (β-glucan content) a second order polynomial was fitted to the data given by Pérez-Vendrell et al. (1996) using Minitab® (v15.0). Equation 1 shows the second order polynomial model used for predicting individual and interactive effects of rainfall and temperature on β-glucan. The predicted model was significant ($p<0.05$) with R^2 (coefficient of determination) equal to 0.57.

$$\beta\text{-glucan} = 1.0456 + 2.7 \times 10^{-4}R + 2.4 \times 10^{-2}T - 1.77 \times 10^{-3} \times T^2 - 6.0 \times 10^{-7}RT \quad (1)$$

Where R is rainfall (mm), T is temperature (°C)

Agronomic factors

During barley growing, several authors have reported a minimal or non significant influence on β-glucan content in the harvested grain from the seeding rate and sowing date, but highlighting it may significantly effect yield (Blackett and Taylor 1982). Hence, a factor of 1 (i.e. no effect) was assumed for the sowing date (S_{DF}) in the baseline model (Appendix A).

The nitrogen content of soil is a major factor influencing agronomic yield and biomass of the barley crop while also having an influence on the level of β-glucan in barley. High nitrogen levels in soil and increasing nitrogen (N) fertiliser rates significantly increased β-glucan content in barley. An increase of total β-glucan content with increasing Nitrogen (N) application has been reported by several researchers (Güler 2003). In Ireland, the recommended nitrogen (N) application for barley is 160 kg/ha. However variations around this may occur (depending on soil type etc) ranging from 60 to 170 N kg/ha (Coulter et al. 2005). To capture the uncertainty in this parameter a triangular distribution was used with a minimum dose of 60 kg/ha (i.e essential for the growth and development of the plant), most likely of 160 kg/ha and a maximum of 170 kg/ha. In a study, Humphreys et al. (1994) reported that higher doses of nitrogenous fertiliser may lead to plant lodging (due to excessive vegetative growth), and can reduce the grain yield, albeit adequate nitrogen is necessary for crop growth. To maximise

both grain protein and β-glucans, growers should optimise the nitrogen nutrition of the crop such that there is no excess of fertiliser applied early during crop development.

Since Ireland receives sufficient rainfall throughout the year, very little irrigation is required for barley crops and is not a common practice in Ireland. Hence, in the baseline model a factor of 1 (i.e. no effect) was assumed for irrigation (I_F). Anthesis (flowering) in barley generally occurs while the spike is in the boot (i.e. Growth stage 69 according to Zadok stage) and is ready for harvesting after 19 days (i.e Growth stage 88). Prentice and Faber (1981) reported that the β-glucan content starts to increases following 12 days after anthesis and increases thereafter up to 36 days. To capture the uncertainty in the delay in harvest days (H_D), a triangular distribution was used, with minimum of 0 days (i.e 19 days after Zadok growth stage 69), most likely of 10 days (i.e 29th day after Zadok growth stage 69) and a maximum of 17 days (i.e 36 days after Zadok growth stage 69). Data from Prentice and Faber (1981) highlights the increase in β-glucan content in the days following anthesis. This data was used to model the Harvest delay factor (H_{DF}).

If moist and humid conditions prevail in the field and they persist for long periods, it may induce germination of the grains. It may affect the embryo and thereby its bio-active components (β-glucan). Prentice and Faber (1981) found that there is an exponential decrease in β-glucan content during germination over a four day germination period. To capture the uncertainty in the germination time (G_{Time}), an exponentially decreasing distribution was used with minimum of 1 day and beta value equal to 1 such that 95th percentile of the distribution was equal to 4 days, thus remaining within the bounds suggested by Prentice and Faber (1981). The germination temperature (G_{Temp}) temperature was assumed to be fixed at 16 ^{o}C. The decrease in β-glucan due to the germination time was modelled by fitting an empirical distribution to the data from Prentice and Faber (1981).

Storage

Harvested grains are sometimes stored on-farm (temporary storage), which can last for up to one month before drying or commercial usage of the harvested grain. Storage conditions in terms of storage temperature and moisture can play a crucial role in determining the level of β-glucan in barley grain. The recommended moisture content for storage is 12 – 13.5% for barley. Research has indicated that the β-glucan content decreases with increasing storage time (Gajdošová et al. 2007). Thus highlighting the decrease in β-glucan content during prolonged storage. These changes may be due to the activity of enzymes (β-glucanase) naturally present in the grain which hydrolyses the β-glucan. A data set presented by Gajdošová et al. (2007) indicated a storage time of up to 49 days on the farm and this data was used to model the underlying uncertainty in the warehousing process (storage time (S_{Time}) and temperature (S_{Temp})), a uniform distribution was used for storage time (days) with the minimum of 0 and maximum 49 days assuming temporary storage of barley prior to off farm transportation to the merchant's premises. The uncertainty about the storage temperature was modelled in accordance with typical Irish temperatures as derived from Irish Meteorological Department (Met Éireann 2007); a triangular distribution with minimum storage temperature of 5^{o}C, most likely value of 8^{o}C and maximum of 15 ^{o}C was used (Appendix A). Current scientific data suggests that a lower storage temperature (<8^{o}C) results in greater β-glucan stability when compared to storage at higher temperatures (Gajdošová et al. 2007). A storage factor (S_F,) describing the reduction in β-glucan during storage was created by fitting a third order polynomial model to the dataset from Gajdošová et al. (2007). Equation 2 and 3 shows the polynomial model for β-glucan during storage at temperature <8^{o}C (R^2 = 0.96) and >8^{o}C (R^2 = 0.98) respectively.

$$Y = 6 \times 10^{-05}X^3 - 4.0 \times 10^{-03}X^2 + 0.021X + 4.02 \quad (2)$$

$$Y = 4 \times 10^{-05}X^3 - 4.1 \times 10^{-04}X^2 - 0.129X + 3.85 \quad (3)$$

Model Run

The input parameters were combined onto a spreadsheet (Microsoft Excel, 2003) running the @Risk add-on package (Palisade Software, Newfield, NY, USA) and the simulation was performed using Latin Hypercube sampling. Generally, Latin Hypercube sampling requires fewer samples than Monte Carlo sampling for similar accuracy. The simulation was performed using the parameters and calculations presented and the model run for 10,000 iterations. A table summarising all the model inputs for the baseline model is provided in Appendix A.

RESULTS AND DISCUSSION

The model resulted in a number of output distributions which were used to predict the likely β-glucan content of harvested grain and the impact of various pre-harvest stages on β-glucan content. The model allows for a comparison of β-glucan content between hulled (H_B) and hull-less barley (H_{LB}) varieties. The predicted mean value for β-glucan was 4.53 and 6.27 g/100g for hulled (H_B) and hull-less barley (H_{LB}), respectively (95th percentile 6.61 and 10.66 g/100g for hulled and hull-less cultivars, respectively) which is within the range of previously published values for β-glucan (Wu et al. 1994; Fastnaught et al. 1996; Kawka et al. 1998). Bhatty 1995 reported higher β-glucan content in hull-less barley in contrast to hulled barley. These values suggest that model predictions are within the expected range while validating the models estimates.

A sensitivity analysis is a systematic evaluation of model inputs; it can be used to identify model parameters which significantly influence the level of β-glucan in barley grain and allow us to gain insight into the behaviour of the model. A sensitivity analysis can be used to simplify the model complexity, by highlighting the critical inputs and thus may help in communicating the model structure and results. A sensitivity analysis of model inputs to β-glucan content in barley grain is given in Figure 3. The analysis showed that the parameter having the highest impact on model predictions was the initial level of β-glucan content of the seed barley (H_B, H_{LB}). A positive correlation coefficient of 0.62 and 0.74 was found for hulled (H_B) and hull-less barley (H_{LB}) cultivars, respectively. This highlights that the initial selection of cultivar is more important in determining the β-glucan content of the gain than any of the agronomical

factors analysed. This finding is consistent with other reported studies where the genotype (cultivar) is considered more important than environmental conditions as a determinant of the final β-glucan content of the grain (Ozkara et al. 1998). Another critical factor greatly influencing the level of β-glucan was the harvesting date after maturity (H_D) as highlighted in the sensitivity analysis (correlation coefficient 0.45 and 0.38 for hulled (H_B) and hull-less (H_{LB}) cultivars, respectively). This highlights the importance of harvesting a crop after Zadok growth stage 87 (i.e. 19 days following anthesis). Nitrogen dose and the soil conditions also show a positive correlation. Germination time (G_{Time}) was an influential factor having a negative effect on β-glucan (-0.33 and -0.29 for hulled and hull-less cultivars, respectively) which might be critical for the Irish climate. This highlights the importance of harvesting the crop at the point (or as near to the point) of maturity as possible, thus reducing the potential for germination. Due to greater probability of rain all year round in Ireland there is a greater probability of germination if harvesting is delayed, this can negatively affect β-glucan levels. On-farm storage time (S_{Temp}) was another factor predicted to be a critical factor affecting levels of β-glucan (correlation coefficient -0.24 and -0.22 for hulled (H_B) and hull-less barley (H_{LB}), respectively). This indicates that storage time should be kept as short as possible with reduced storage temperature (<8°C). Other input parameters were having a smaller impact on the model results. The analysis indicates that data collection initiatives should be directed towards gathering information on β-glucan levels in seed grain and the influence of harvest date on bio-active components.

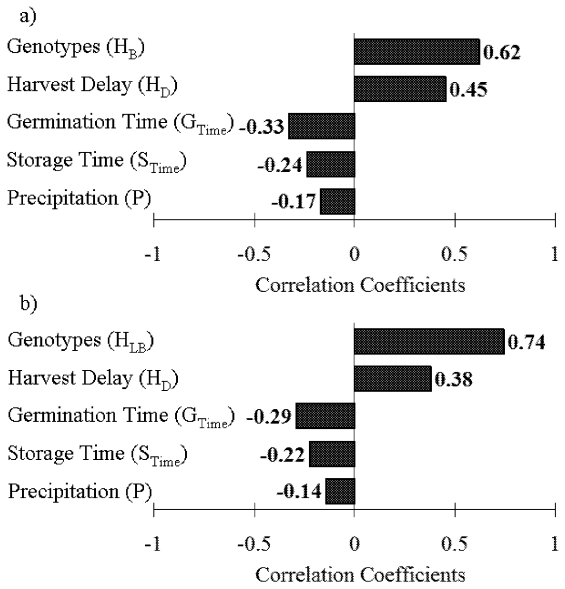

Figure 3: Sensitivity Analysis for β-glucan level in a) Hulled (H_B) and b) Hull-less barley (H_{LB})

CONCLUSIONS

This study represents an initial attempt to model the pre-harvest and storage aspects of barley and their probable effect on β-glucan content in harvested grains. This approach of using predictive modelling techniques to assess the level of nutrients in cereals has not been reported in scientific literature and represents a novel aspect to this study. The predicted simulated mean level of β-glucan in hulled (H_B) and hull-less barley (H_{LB}) was 4.53 g/100g and 6.27 g/100g, respectively, which is within the range of reported values found in the literature. This model indicates that initial level (i.e. genotype of barley) plays a significant role in determining the final β-glucan level in harvested grain and is more important than any agronomical factor. This study highlights the applicability of Monte Carlo simulations technique to assess the influence of pre-harvest operations on β-glucan content in barley and to facilitate the identification of optimisation techniques.

ACKNOWLEDGEMENTS

The authors wish to acknowledge the Irish Department of Agriculture and Food for their funding of this project under the Food Institutional Research Measure.

Appendix A: Table of model distributions and inputs for the predicting β-glucan in barley

Symbol	Input data description	Mean	Distribution	Units
Cultivar Data				
H_B	Hulled Barley	4.25	lognormal (4.25,1.28)	g /100g
H_{LB}	Hull-less Barley	5.88	lognormal (5.88,2.54)	g /100g
Environmental Conditions				
Loc	Location	1	fixed factor	
S_T	Soil types		given in text	
S_F	Soil factor	0.95	factor	
S_{pH}	Soil pH	1	fixed factor	
Climatic Condition				
P	Precipitation	346	logistic (346.36, 106.82)	mm
T	Temperature	10.67	logistic(10.6673, 1.1577)	°C
C_F	Climatic factor	0.86	factor	
Agronomic Practices				
S_{DF}	Sowing date factor	1	fixed factor	days
Fertiliser Application				
N	Nitrogen dose	130	triangle(min-60, max-170)	kg/ha
N_F	Nitrogen factor	1.06	factor	
Irrigation				
I_F	Irrigation factor	1	fixed factor	
Harvesting Delay				
H_D	Harvesting delay	9	triangle(min-0,max-17)	days
H_{DF}	Harvest delay factor	2.02	factor	
Germination				
G_{Time}	Germination Time	1	exponential	days
G_{Temp}	Germination Temperature	16	fixed value	°C
G_F	Germination factor	0.99	factor	
On-farm Storage				
S_{Time}	Storage time	25	uniform(min-0, max-49)	days
Stemp	Storage temperature	9	triangle(min-5, max-15)	°C
S_F	Storage factor	0.66	factor	

REFERENCE

Anderson, M. A., Cook, J.A. and Stone, B. A. "Enzymatic determination of 1-3,1-4-β-glucans in barley, grain and other cereals". *Journal of the Institute of Brewing*, 84.

Bengtsson, S, Åman P, Graham, H, Newman, C .W, Newman, R .K., 1990. "Chemical studies on mixed-linked β-glucans in hull-less barley cultivars giving different hypocholesterolaemic responses in chickens". *Journal of the Science of Food Agriculture*, 52, pages 435-445.

Bhatty, R. S., 1995. "Hull-less barley bran: a potential new product from an old grain". *Cereal Foods World*, 40, pages 819-824.

Blackett, G.A. and Taylor, B.R.., 1982. "An evaluation of inputs to maximise the yields of Midas spring barley in the north of Scotland". *Journal of the National Institute of Agricultural Botany*, 16, pages 7–14.

Conry, M.J., 1997. "Effect of fertiliser on the grain yield and quality of spring malting barley grown on five contrasting soils in Ireland". *Biology and. Environment*, 97,pages 185–196.

Coulter, B. S., Murphy, W.E., Culleton, N., Quinlan G. and Connolly, L., 2005. "A survey of fertilizer use from 2001-2003 for grassland and Arable crops". In Project report no. ARMIS 4568, TEAGASC, ISBN No. 1 84170 389 3.

Gajdošová,A, Petruláková ,Z, Havrlentová, M, Cervená, V, Hozová, B, Šturdík, E and Kogan, G., 2007. "The content of water-soluble and water-insouble β-D-glucans in selected oats and barley varieties". *Carbohydrate polymer*, 70, pages 46-52.

Güler,M., 2003. "Barley grain β-glucan content as affected by nitrogen and irrigation". *Field Crops Research*, 84, pages 335–340.

Humphreys, D. G., Smith, D. L., & Mather, D.E., 1994. "Nitrogen fertiliser and seedling date induced changes in protein, oil and β-glucan contents of four oat cultivars". *Journal of Cereal Science*, 20, pages 283-290.

Jadhav, S.J., Lutz, S.E., Ghorpade, V.M., & Salunkhe, D.K., 1998. "Barley: chemistry and value-added processing". *Critical Reviews in Food Science and Nutrition*, 38, pages 123-171.

Jeraci, J.L., Lewis, B.A., 1989. "Determination of soluble fibre components: (1→3; 1→4)-β-d-glucans and pectins". *Animimal. Feed Science Technology*, 23, pages 15–25.

Kawka, A., Anioła, J., Chalcarz , A and Kołodziejczyk, P, 1998. "Proc. XXIX Conference Committee of Technology and Food Chemistry Polish Academy of Science on Technological Processes and Food Quality", pages. 369–370.

MacGregor, A. M., Dushnicky, L. G., Schroeder, S. W., & Balance, G. M, 1994. Chances in barley endosperms during early stages of germination. *Journal of the Institute of Brewing*, 100, pages 85–90.

Met Éireann, 2007. Irish meteorological data available online at http://www.met.ie/.

Miller, S.S., Fulcher, R.G., 1994. "Distribution of (1-3) (1-4)-β -D-glucan in kernels of oats and barley using micro spectrofluorometry". *Cereal Chemistry*, 71, pages 64–68.

Morin, L. A., Temelli, F., & McMullen. L, 2001. "Physical and sensory characteristics of low-fat breakfast sausages utilizing barley β-glucan as a fat replacers" Technical Program Listing 2001 IFT Annual Meeting, June 23-June 27; New Orleans, LA.

Oscarsson,M., Andersson,R., Salomonsson, P.S, and Åman 1996. "Chemical Composition of Barley samples focusing on dietary fibre components". *Journal of cereal science*, 24, pages 161-170.

Ozkara, R., Basman, A., Köksel, H., & Elik, S, 1998. "Effects of cultivar and environment on β-glucan content and malting quality of Turkish barleys". *Journal of the Institute of Brewing*, 104, pages 217-220.

Pérez –Vendrell, A. M, Brufau, J, Molina-Cano, J. L, Francesh M, Guash, J. 1996. "Effects of cultivar and environment on β-(1→3)(1→4)-D-glucan". *Journal Cereal Science*, 23, pages 285-292.

Peterson, D.M., Wesenberg, D.M. and Burrup. D.E, 1995. "β-glucan content and its relationship to agronomic characteristics in elite oat germplasm". *Crop Science*, 35, pages 965–970.

Prentice, N.and Faber S, 1981. "β-D-glucan in developing and germinating barley kernels". *Cereal Chemistry*, 58,pages 77-79.

Wu, Y. V., Stringfellow, A. C., & Inglett, G. E, 1994. "Protein and β-glucan-enriched fractions from high-protein, high β-glucan barleys by sieving and air classification". *Cereal Chemistry*, 71, page 220.

Yokoyama, W. H., Hudson, C. A., Knuckles, B. E., Chiu, M. M., Sayre, R. N., & Turnlund, J. R.,1997. "Effect of barley β-glucan in durum wheat pasta on human response". *Cereal Chemistry*, 74, pages 293–296.

Zhang, G., Chen,J., Wang and Ding,S.,2001. "Cultivar and Environmental effect on (1-3,1-4)β-glucan and protein content in Malting Barley". *Journal of Cereal Science*, 34, pages 295–301.

EXPOSURE ASSESSMENT TO PHYCOTOXINS BY RECREATIVE SHELLFISH HARVESTERS : A SAMPLING PLAN

Cyndie Picot, François-Gilles Carpentier, Alain-Claude Roudot and Dominique Parent Massin
Laboratoire de Toxicologie Alimentaire et Cellulaire
Université Européenne de Bretagne - Université de Bretagne Occidentale (UEB-UBO)
6 avenue Victor le Gorgeu – CS 93837
29238 BREST Cedex 3
FRANCE
E-mail: alain-claude.roudot@univ-brest.fr

KEYWORDS
Sampling, MCMC simulation, Variability, Exposure.

ABSTRACT

Nowadays, phycotoxins produced by harmful microalgae are widespread all over the world. Shellfish accumulate these toxins and can provoke dangerous diseases in humans. Available data concern only acute intoxications. There is very little information on the exposure to phycotoxins by recreative harvesters who are the most exposed people. In order to evaluate this public health problem, one needs to know the actual contamination level and hence one needs to define a good sampling plan taking into account the different variabilities encountered : spatial, temporal, inter and intra species, and so on. This paper proposes a review of all the sampling parameters and will describe a sampling procedure which can be applied in such a work.

INTRODUCTION

Phycotoxins are a diverse group of poisonous substances produced by harmful marine microalgae (phytoplankton). Bivalve shellfish filter-feed these toxic phytoplankton and accumulate phycotoxins until become unfit for human consumption. Eating contaminated shellfish can lead to various acute intoxications and cause death in cases of potent toxins, extreme exposure or sensitivity. We focus on three toxin groups distributed all over the world and mainly accumulated in shellfish, i.e Okadaic Acid (OA), Domoic Acid (DA) and Saxitoxin (STX). OA, DA and STX are the major toxins involved in Diarrheic Shellfish Poisoning (DSP), Amnesic Shellfish Poisoning (ASP) and Paralytic Shellfish Poisoning (PSP), respectively. Phycotoxins are increasingly controlled and considered as an important food safety issue because of their expansion as far as their frequency, intensity and geographic distribution are concerned. But accurate data on exposure to phycotoxins via shellfish consumption are very limited. That's why an exposure assessment is primordial.
Exposure assessment needs two types of information: data on consumption and data on contamination. Then these data are incorporated in a probabilistic MCMC (Markov-Chain, Monte-Carlo) simulation method in order to evaluate the exposure level of the special-interest group.
Consumption data specify the quantity of contaminated foods ingested and what is the consumption of potentially relevant risk groups, including high consumers. As recreational shellfish harvesters are generally coasters, harvest everywhere, at any time and eat their harvests, they appear to be high shellfish consumers and a potential high risk group concerning phycotoxins.
Contamination data provide information on the nature and the amount of contaminants existing in a given food and/or the diet in general. Nowadays many countries have introduced a reglementation and routinely monitor the shellfish contamination by phycotoxins. But it prevents only acute intoxications. However, OA is known to be a tumour promoter and toxicological sub(chronic) studies on DA and STX are lacking. Therefore chronic consumption of shellfish containing low doses of toxins could lead to human health problems. Investigation of chronic exposure levels of shellfish harvesters appears to be primordial in a public health context. But no information exists on this issue. In order to conduct this study, one of the key points is the production of accurate contamination data, which implies a reflective and appropriate sampling plan.

SAMPLING PLAN

A sampling plan defines the methodologies and procedures to be followed in order to obtain a representative laboratory sample from a given product lot (Blanc, 2006). It is a multistage process: sampling, sample preparation and analysis. There are uncertainties associated with each step. Normally, sampling contributes the largest relative error while analysis comprises the least. That is why we focus on the sampling. It specifies how the sample will be physically selected or taken from the lot and the size of this sample (Park and Pohland 1989; Whitaker, 2006). The difficulty of sampling is to obtain a representative sample (a sample in which the characteristics of the lot from which it is drawn are maintained (Codex Alimentarius, 2004)). This representative sample has to provide results as accurate (close to the true value) and precise (variability limited) as possible. For that, the European Union put in force a package of directives concerning sampling procedures for the most predominant mycotoxins (another type of natural toxins produced by fungus) (Miraglia *et al.* 2005) but no legislation exists for phycotoxins. Thus each one must define its own sampling method.
The main types of sampling used in production of food composition data are (Greenfield and Southgate 2007) :
- random sampling (sample collected in a way that ensures that any unit has an equal chance of being included)

- stratified sampling (it consists of dividing the lot into different strata or zones, each stratum being more homogeneous than the original lot. Within each stratum the samples are taken randomly)
- selective sampling (sample chosen in a way that excludes or selects material with defined characteristics)
- convenience sampling (samples are taken on the basis of reasons not directly concerned with sampling parameters : accessibility, expediency…).

In order to avoid any dispute over the representativeness of the sample, the Codex Alimentarius (2004), advises to choose a random sampling procedure, whenever possible, alone, or in combination with other sampling techniques. But it's known that when the lot is heterogeneous, a random sample may not be representative of the lot. Shellfish contamination by phycotoxins presents a great heterogeneity of contamination within the lot. This heterogeneity is spatial, temporal, inter and intra species. In this case, stratified sampling may be a solution because within these strata contamination will be more homogeneous than the entire lot. Then a random sample can be drawn from each of these strata.

Spatial variability

The spatial variability is largely unknown. In fact phycotoxin occurrence depends on phytoplankton presence. But local variations can be very important (Bogan *et al.* 2007). This spatial variability can also depend on the chosen phycotoxin, and/or on the shellfish species.

According to the phycotoxins monitoring conducted in the western Brittany (our area of interest), we had been able to notice that each toxin is globally more present in particular zones. DSP, ASP and PSP are predominantly found in South, in Center and in North of our region of interest, respectively. Therefore, the first stratification can concern the type of phycotoxins and the area can be divided in 3 main zones.

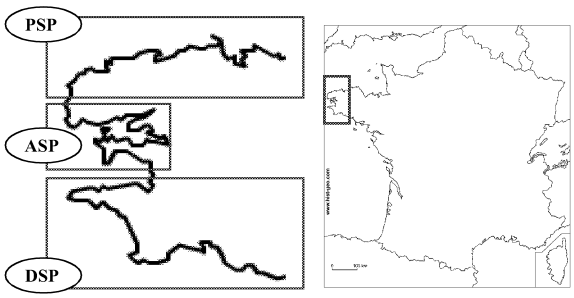

Figure 1 : First geographical stratification of the area of interest

Within each zone, all beaches can't be sampled, thus a second geographical stratification can be defined according to the potential human health risk. In order to choose beaches within each zone, two pieces of information are necessary: beaches suspected of having the highest levels of contamination and where regular harvesters are present. Data on beach frequentation can be got by prospecting. Data on contamination can be obtained by the national monitoring and might be complemented with a preliminary study in order to compare the main beaches of interest (with regular contamination and attractive for shellfish harvesters). Assembling all these data, a choice of beaches within each zone could be made (USEPA 2000).

Temporal variability

Classically the toxic period generally happens during the warm season (i.e. between April and September on French coasts). This is due to proliferation of phytoplankton at these periods. However, it has been shown that the toxic period can happen even with a low presence of phytoplankton, and even in cold water. No clear explanation is given to these facts. Toxic compounds could accumulate in the sediments during summertime, and could be consumed by shellfish during cold periods. Some researchers (Frémy and Lassus 2001) also think that algal contaminant concentration could be higher during cold periods. Unfortunately no proof of these theories has ever been demonstrated. In order to take into account this variability, samples must be taken regularly and for a long period to cover all seasons. In our study, we have chosen a monthly sampling for 2 years.

Inter species variability

Each phycotoxin seems to have dominant contamination vectors. For instance, Hess *et al.* (2001) showed (in Scotland) that for domoic acid, 73% of scallops, 50% of razor clams and only 26% of mussels were affected. James *et al.* (2005), in Ireland, obtained greater differences with 89% of scallops, and only 2% of mussels for the same toxin. In these two studies, the level of contamination was also the highest in scallops (up to 240 µg/g) and the lowest for mussels (0.09 µg/g). The same differences exist with other toxins: for okadaic acid, mussels are the more often contaminated and with the highest concentration (Frémy and Lassus 2001, Reizopolou *et al.* 2008). These differences between species can be also associated with the shellfish ability to accumulate phycotoxins and their rapidity to depurate toxins. Retention time of these phycotoxins after contamination appears to be very variable, some considering a retention period of a few days, while others consider a period of a few years! The only issue being largely accepted is that detoxification has a biphasic pattern: a rapid release, and then a gradual loss (Pavela-Vrancic *et al.* 2006). The problem is the duration of each phase.

As far as consumer exposure assessment is concerned, the choice of target species must be based on two main criteria: species the most commonly consumed locally and species which have the greatest ability to accumulate phycotoxins (USEPA 2000). Therefore we propose a third stratification according to species: the most consumed species in each zone and the most contaminated species for each phycotoxin (OA, DA and STX). The most consumed species will be provided by a consumer survey. The most contaminated species will be defined according to a preliminary study on 7 bivalves (which are known to accumulate phycotoxins and to be present in our area of interest) : mussel, oyster, cockle, razor clam, queen scallop, surf clam and venus clam. Moreover the sampling must be made on shellfish of harvestable size.

Intra species variability

Several studies were made on several different shellfish and a great variability of contamination in the same gathering area is to be noted. For instance, Reizopolou *et al.* (2008) found a minimum concentration of okadaic acid of 11 ng/g in clams with a maximum of 351 ng/g on the same place in Greece. Frémy and Lassus (2001) reported a minimum value of 1.2 µg/g and a maximum of 38 µg/g of domoic acid in mussels in the same bay. This variability could have been considered as a spatial variability if differences of the same order had been measured on other shellfish. But it is not the case. Hence, one can consider that each species can show a great variability in contamination.

This variability cannot be reduced by stratification (otherwise a stratification should be made for each shellfish, that is inconceivable) but in order to minimize it, EFSA (2008) recommends to average the sample by using composite samples of about 150g shellfish (without shell) as it is done for mycotoxins (Whitaker, 2006). Concretely, sample should be an accumulation of many small portions taken from many different locations throughout the lot (Whitaker *et al.* 2006). The different portions must be equal. Thus we suggest that a random sampling should be made on each selected beach and for the two species chosen, based on a regular spatial partitioning. Moreover, as we want assess consumer exposure, the size of the final sample (addition of many small portions) could be roughly equal to the mean portion size of shellfish consumed by meal.

This variability affects also the number of samples required. The greater the variability is, the more important the number of samples needed is. Therefore in order to calculate the necessary number of samples, information is first required on the variability of the contamination of the food. In practice needed information is often incomplete, so one has to proceed intuitively or conduct an other preliminary study to estimate the local variability. The optimum sample size is based formally on calculation from the following equation:

$$t = \frac{x-\mu}{SD/\sqrt{n}}$$

Where x = sample mean ; µ = population mean ; SD = standard deviation of the sample mean and n = sample size. The equation can be arranged as follows:

$$n \geq \frac{(t_{\alpha,n-1})^2 * SD^2}{(accuracy * mean)^2}$$

The values for α define the confidence limits required. The value for *t* is taken from standard statistical tables (Student's *t* table), using the required value of α and a guesstimate of sample size. Accuracy is the required closeness of the estimated value to the true value (unknown) (Greenfield and Southgate 2007).

CONCLUSION

Two spatial stratifications will be defined with an aim of taking into account the spatial variability. The first is based on the type of toxins and partitions the area of interest into three zones. The second enables to choose beaches within each zone. Selected beaches are those with a high potential risk (incidence of toxins and presence of regular harvesters). The third stratification tries to take into account the inter species variability. Only two species are selected (the most contaminated and the most consumed). Lastly, on each beach, for each toxin and for each shellfish species, a random sample is taken. For that, selected beaches are partitioned regularly and many portions are collected and assembled in order to obtain a random and representative sample.

REFERENCES

Blanc M. 2006. Sampling : the weak link in the sanitary quality control system of agricultural products. Molecular Nutrition & Food Research **50,** 473-479.

Bogan YM, Bender K, Hervas A, Kennedy DJ, Slater JW, Hess P. 2007. Spatial vatiability of domoic acid concentration in king scallops *Pecten maximus* off the southeast coast of Ireland. Harmful Algae **6,** 1-14.

Codex Alimentarius Manual of Procedures**.** 2004. General guidelines on sampling CAC/GL 50-2004.

European Food Safety Agency. 2008. Marine biotoxins in shellfish – okadaic acid and analogues. Scientific opinion of the panel on contaminants in the food chain. The EFSA Journal **589**, 1-62.

Frémy JM, Lassus P. 2001. Toxines d'algues dans l'alimentation. Editions Quae.

Greenfield H, Southgate DAT. 2007. Données sur la composition des aliments, production gestion et utilisation. FAO. Rome

Hess P, Gallacher S, Bates LA, Brown N, Quilliam MA. 2001. Determination and confirmation of the amnesic shellfish poisoning toxin, domoic acid , in shellfish from Scotland by liquid chromatography and mass spectrometry. Journal of AOAC International **84**(5), 1657-1667

James KJ, Gillman M, Amandi MF, Lopez-Rivera A, Puente PF, Lehane M, Mitrovic S, Furey A. 2005. Amnesic shellfish poisoning in bivalve molluscs in Ireland. Toxicon **46**, 852-858

Miraglia M, De Santis B, Minardi V, Debegnach F, Brera C. 2005. The role of sampling in mycotoxin contamination : An holistic view. Food Additives and Contaminants, Supplement 1, 31-36.

Park DG, Pohland AE. 1989. Sampling and sample preparation for detection and quantitation of natural toxicants in food and feed. Journal of AOAC **72**(3), 399-404.

Pavela-Vrancic M, Ujevic I, Nincevic Gladan Z, Furey A. 2006. Accumulation of phycotoxin in the mussel Mytilus Galloprovincialis from the central adriatic sea. Croatia Chemica Acta **79**(2), 291-297

Reizopolou S, Strogyloudi E, Giannakourou A., Pagou K, Hatzianestis I, Pyrgaki C, Graneli E. 2008. Okadaic acid accumulation in macrofilter feeders subjected to natural blooms of *Dinophysis acuminata*. Harmful Algae **7**, 228-234

Wekell JC, Trainer VL, Ayres D, Simons D. 2002. A study of spatial variability of domoic acid in razor clams: recommendations for ressource management on the Washington coast. Harmful Algae **1**, 35-43

Whitaker TB. 2006. Sampling food for Mycotoxins. Food Additives and Contaminants **23**(1), 50-61

U.S EPA (U.S. Environmental Protection Agency). 2000. Guidance for Assessing Chemical Contaminant Data for Use In Fish Advisories - Fish Sampling and Analysis. Volume 1. Third Edition. EPA 823-B-00-007. Office of Water, Washington, DC.

BIOGRAPHY

CARPENTIER F.G, PARENT MASSIN D., PICOT C AND ROUDOT A.C work in the laboratory of Food Toxicology at the Western Brittany University which is a founder member of the European University of Brittany. The laboratory fields of interest concern both food toxicology and risk assessment, including effects of xenobiotics on hematopoiesis and risk assessment of natural toxins.

MODELLING AND SIMULATION IN FOOD SCIENCE AND BIOTECHNOLOGY

A tendency model for dynamic simulation of an industrial crystallisation process

Michel Benne*, Brigitte Grondin-Perez, Jean-Pierre Chabriat
Université de La Réunion, LE2P, EA 4079, 97715, St-Denis, La Réunion, France
{benne|bgrondin|chabriat}@univ-reunion.fr

1. Introduction

Crystallisation involves complex reactions: nucleation, growth and dissolution. Many authors have proposed models to describe these mechanisms. During the last 10 years, these investigations have greatly helped to enhance the development of both dynamic and steady state first principles' models of crystallisation in pure solution. Given the difficulties encountered when trying to adapt nucleation, growth and dissolution models to describe crystallisation inside impure solutions, we assume that a simplified kinetics model of the growth phase could only include a crystal growth term. The present work is based on this assumption and presents a technical answer, easy to implement in an industrial context.

Section **2** outlines the process modelling and control, and the experimental environment at Bois Rouge sugar mill (BR[1]). The **3**rd paragraph, dealing with the mechanistic model, presents the mass and energy balances. In section **4** a close comparison between simulation results and industrial data is presented to illustrate the reliability of this simplified approach.

2. Process modelling and control: the industrial problem

Previous works showed the limitations of traditional control strategies for maximising exhaustion during the growth phase of low grade crystallisation processes (Bonnecaze, 2003). To overcome these limitations, we plan the development of an advanced control strategy, which requires the development of a process simulator. Basing our work on several previous works (Feyo de Azevedo *et al.*, 1997; Georgieva *et al.*, 2003; Hassani *et al.*, 2001), this study is centred around the development of a model of the growth phase of a low grade crystallisation process.

2.1. Low grade crystallisation: the experimental environment

Traditionally, raw sugar is produced efficiently by crystallisation from syrup in three steps. Marketable sugar meeting standards is produced by A-grade and B-grade plants from high purity syrups. B-molasses are returned to C-grade plants to product C-sugar and C-molasses. Since it is important to maximize the yield at each stage of the process, the fact remains that a key step in sugar recovery is the exhaustion of C-molasses. At BR, this final step is performed through a series of semi-batch vacuum evaporation pans, fed with low purity products from different B-grade pans showing variable specifications and irregular operating conditions. In order to perform an efficient supervision of one of them, the C540 tank has been equipped with a set of sensors.

2.2. Problems and development

An efficient process control scheme has to take into account disturbances like the reduction of available heating steam, the variation of the quality of feeding juices and molasses, *etc.* In addition, on a season scale, the properties of the sucrose solutions vary according to the composition of the raw material, of vegetable origin. Therefore the crystal growth can be considered as a time varying chemical process. If PID controllers have proved to be suitable in constant operating conditions, advanced control strategies may be required to meet steadiness and quality demands, in spite of strong irregularities of operating conditions and physical-chemical properties variations (Cadet *et al.*, 1999; Benne *et al.*, 2000). In the present context, since we plan to implant an model based control (MBC) strategy, an off-line validation stage is required on two accounts to evaluate the performance of the control algorithm:

- to evaluate its precision (*ie* the difference between the process output and the set point);
- and to evaluate its capacity to correct the drift of the process due to disturbances.

The validation stage requires the development of a model of the growth phase: the process simulator. The most widely accepted approaches suggested to describe the mechanisms of sucrose crystallisation take into account the main physical-chemical

[1] Bois Rouge sugar mill, La Reunion, France

phenomena involved during this reaction (Georgieva *et al.*, 2003): dissolution, growth and nucleation. Yet, although much research has been devoted to model these phenomena inside pure solutions (A-grade, Randolph & Larson, 1988; Brown & Alexander, 1992; Berglund & deJong, 1992; Koiranen et al., 1999), little information is available about low grade crystallisation (C-grade) in the industrial context. There, low grade sucrose solutions contain a high proportion of impurities, which considerably changes their properties, and makes it difficult to adapt A-grade models to C-grade modelling.

2.3. Towards a simplified approach

Mass and energy balances can be written using five ordinary differential equations (ODE). Four ODEs represent the variation in mass for water (m_w), impurities (m_i), sucrose in solution (m_s) and crystals (m_c). The fifth describes the enthalpy balance.

Usually the mass balance should take into account growth, nucleation and agglomeration. To model the growth phase of a low grade crystallisation, we ought to put forward the theory that nucleation doesn't happen (supersaturated state), and that agglomeration and abrasion are negligible phenomena. In other words, we assume that crystal growth is preponderant (Pautrat et *al.*, 1997). Based on this assumption, the variation in m_c can be deduced from the variation in crystal content cc. In practice, cc is obtained using two technologies for dry substance content measurement. Indeed, apart from impurities, the massecuite (mc) is a mixture of a solid part, the crystals, and a water retaining part of dissolved sucrose, called the mother liquor (ml).

Different technologies have been developed to measure the sucrose percentage in massecuite and mother liquor (Saska & Rein, 2001; Theisen & Diringer, 2003):

- gamma density meters and microwave sensors supply the dry substance content in the massecuite Bx_{mc};
- refractometers provide the dry substance content in the mother liquor Bx_{ml}.

Using Bx_{mc} and Bx_{ml} the crystal content is given by: $cc = (Bx_{mc} - Bx_{ml})/(1 - Bx_{ml})$. As the mass balance represents the variation in m_w, m_i, m_s and m_c, these variables are considered to be state variables. In that case, cc ought to be expressed using the states, not the Brix measurements, which leads to the formula:

$$cc = \frac{m_c}{m_s + m_i + m_w + m_c}$$

Easy to implement within the framework of a first principles' model, this technique features several advantages, particularly as regards impure solutions:

- it simplifies the resolution of the mass balance;
- it avoids the difficulties related to the interpretation of electrical conductivity;
- and it avoids the estimation of ss and other kinetic parameters, classically based on empirical relationships (power-law type) for growth rates computation.

3. Description of the growth phase: a tendency model

3.1. Simplifying assumptions

The mixed magma is considered as a homogeneous system. Consequently, the measured thermo-dynamical properties are supposed to be uniform in the whole pan. In practice, $Bx^{\%}_{ml}$ and $Bx^{\%}_{mc}$ are taken to be uniform in the total volume, and T_{mc} is calculated using three measurements (foot, middle and top of the pan) to take the temperature gradient into account.

Two experimental assumptions lead to an estimation of non measurable variables: the potential heating power and the evaporation capacity assessment.

H1 Considering that the time delay between the heating steam supply (F_{hs}) and the condensed water outlet ($F_{cw\leftarrow hs}$) could be ignored with regard to the process inertia, the heating power brought by steam condensation in the tube network can be calculated using the measured $F_{cw\leftarrow hs}$: $F_{hs} = \alpha_Q \; F_{cw\leftarrow hs}$;

H2 Assuming that the evaporation of $1\,kg$ of water from the magma consumes about $1\,kg$ of heating steam, the evaporation capacity is calculated using $F_{vap} = \alpha_{vap} \; F_{cw\leftarrow hs}$.

In practice, these assumptions govern the model parameterization.

3.2. Mass and energy balances

The mass balance depends on four transfer terms. Two inputs: feed (f) and dilution water (d). One output, emitted vapour (vap). And one phase change: the crystallisation flow (cris). (1) describes the mass balance for water (w), (2) for impurities (i), (3) for dissolved sucrose (s) and (4) for sugar crystals (c):

$$\frac{dm_w}{dt} = \dot{m}_f \left(1 - Bx_f\right) + \dot{m}_d - \dot{m}_{vap} \quad (1)$$

$$\frac{dm_i}{dt} = \dot{m}_f \, Bx_f \left(1 - Pur_f\right) \quad (2)$$

$$\frac{dm_s}{dt} = \dot{m}_f \, Bx_f Pur_f - \dot{m}_{cris} \quad (3)$$

$$\frac{dm_c}{dt} = \dot{m}_{cris} \quad (4)$$

In these equations the purity (Pur_f) of feed is supposed to be constant during a growth phase. The mass flow rate for feed and dilution water are calculated using the flow measurements F_f and F_d: $\dot{m}_f = \rho_f F_f$ and $\dot{m}_d = \rho_d F_d$. The part of emitted vapour from massecuite evaporation is quantified by the mass flow rate $\dot{m}_{vap} = \rho_{vap} F_{vap}$ (*Cf.* § 3.1). The term $\dot{m}_{cris}$ (3, 4) represents the crystallisation flow rate, given by the variation of m_c at each instant t during a period Δt: $\dot{m}_{cris} = \Delta m_c(t) / \Delta t$, with $m_c(t) = cc\ m_{mc}(t)$. $m_{mc} = m_w + m_s + m_i + m_c$ and cc is taken as a constant during integration.

Secondly, the energy balance is calculated with the derivative of the enthalpy $H_{mc} = m_{mc} Cp_{mc} T_{mc}$ with respect to t:

$$\frac{dT_{mc}}{dt} = \frac{1}{m_{mc} Cp_{mc}} \left(\dot{W} + \dot{Q} + \dot{m}_f h_f + \dot{m}_w h_w \ldots - \dot{m}_{vap} \lambda_{vap} + \dot{m}_{cris} \lambda_c - \frac{dm_{mc}}{dt} h_{mc} \right) \quad (5)$$

$Cp_{mc} = cc\ Cp_c + (1 - cc) Cp_{ml}$ (Cp_{mc} is taken to be constant inside the temperature interval.

The mechanical mixing power is modelled using the measurement of intensity with $380\,V$ supply: $\dot{W} = 380\, I_{stir}$. And assuming hypothesis 3.1, the heating power is written using the latent heat ℓ^w_{vl} of condensation: $\dot{Q} = \alpha_Q\ \rho_{hs} F_{hs} \ell^w_{vl}$.

When considering heating steam (*hs*) and emitted vapour (*vap*), temperature is calculated using the corresponding pressure and the saturation law. The whole system call for a number of thermodynamic properties as density (ρ), specific heat capacity (C_P), enthalpy (h) and latent heat (λ) given by empirical correlations, widely used in the relevant bibliography.

3.3. Model structure and parameter-fitting

The model structure depends on the available measurements. On the C540 tank, on-line sensors supply the experimental data listed in Table 1. Let $u(t)$ be the observation vector and $x(t)$ the state vector. The estimated output vector is expressed from the combination of state variables:

$$u(t) = \left(Bx_f^{\%}, Pur_f^{\%}, F_f, F_d, F_{cw}, P_{hs}, P_{vac}, I_{stir} \right)$$

$$x(t) = \left(m_w, m_s, m_i, m_c, T_{mc} \right)$$

$$\hat{y}(t) = \left(\hat{Bx}_{ml}^{\%}, \hat{Bx}_{mc}^{\%}, \hat{T}_{mc} \right)$$

with $\hat{Bx}_{ml}^{\%} = (m_s) / (m_w + m_i + m_s)$

$\hat{Bx}_{mc}^{\%} = (m_s + m_c) / (m_w + m_i + m_s + m_c)$

Table 1
Experimental measurements (C540 tank)

Feeding solution (syrup, liquor, molasses)		
$Bx_f^{\%}$	Brix (refractometer)	%
F_f	flow rate	$m^3.s^{-1}$
T_f	temperature	$°C$
Massecuite (or magma)		
$Bx_{mc}^{\%}$	Brix (μwave sensor)	%
T_{mc}	temperature ($T_{ml} = T_{mc}$)	$°C$
Mother liquor		
$Bx_{ml}^{\%}$	Brix (refractometer)	%
Heating steam – condensed water (from *hs*)		
P_{hs}	heating steam pressure	bar
$F_{cw \leftarrow hs}$	flow rate	$m^3.s^{-1}$
Dilution water		
F_w	flow rate	$m^3.s^{-1}$
T_w	temperature (dilution)	$°C$
Thermo-mechanical conditions		
P_{vac}	vacuum pressure	bar
I_{stir}	intensity (stirrer current)	A
L	level in the pan	%

Model identification can be pursued by determining a set of parametric equations that accurately describe the operating conditions. In the present approach, the fitting procedure only requires the estimation of two adjustable constants involved in equations (1), (3), (4) and (5): α_{vap} and α_Q. This task has been realized following a classical non-linear least-squares regression using industrial databases. $\hat{Bx}_{ml}^{\%}$, $\hat{Bx}_{mc}^{\%}$ and $\hat{T}_{mc}$ could be compared with the corresponding measurements: α_{vap} and α_Q have been adjusted to make these outputs fit the relevant measurements.

4. Simulation of an industrial low grade crystallisation process

The set of differential equations (1), (2), (3), (4) and (5) is solved using MATLAB ODE procedures. For each simulation run, the initial conditions (x_0 and y_0) are chosen using average measurements taken over a two minutes 'window'. $x(t)$ is initialised with the values

of m_w, m_i, m_s, and m_s calculated using averages of Bx_{ml}, Bx_{mc} and T_{mc}, the initial properties of the solution (Pur_{ml} and Pur_{mc}) and the initial volume (V_0). $\hat{y}(t)$ is initialised directly from average measurements (y_0).

4.1. *Comparison between simulation results and industrial data*

The model validation is based on the comparison between online measurements of $Bx_{ml}^{\%}$, $Bx_{mc}^{\%}$ and T_{mc} and the relevant estimation outputs. Fitting and simulation were carried out for experimental data collected during several growth phases (about 120 minutes long) at BR. Each one corresponds to normal conditions observed at the end of a campaign (batch 1: Nov. 23, and batch 2: Nov. 19).

The simulation results presented below were obtained using the following parameters (see Table 2).

Table 2
Adjusted parameters

α_{vap}	1.3893
α_Q	1.5275

In the following Figures, the horizontal axis shows the time in minutes, the upper vertical axis indicates the physical variables. For $Bx_{mc}^{\%}$ and for $Bx_{ml}^{\%}$, the same trends are observed for simulations and measurements, with absolute mean errors of the order of 1 point over the normal range. Admittedly, the comparison of T_{mc} simulation results with the measurements may appear rather inconclusive. Nevertheless both show the same trends, even when estimation error reaches $3\ °C$ during a batch.

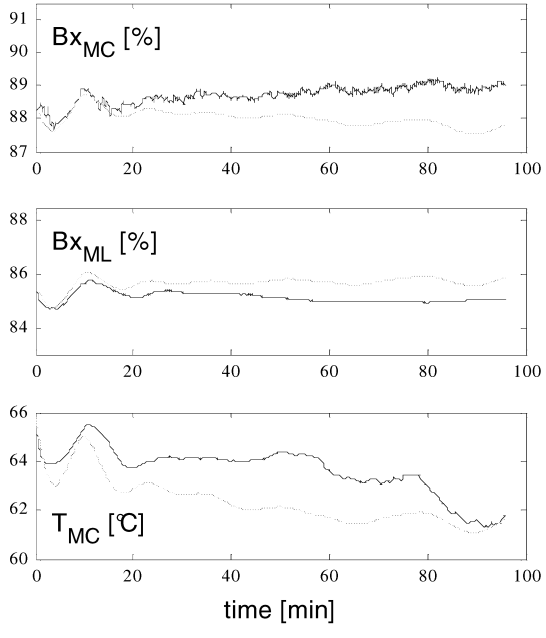

Figure 1: batch 1 – November 23th
bold lines for measurements and thin lines for simulations

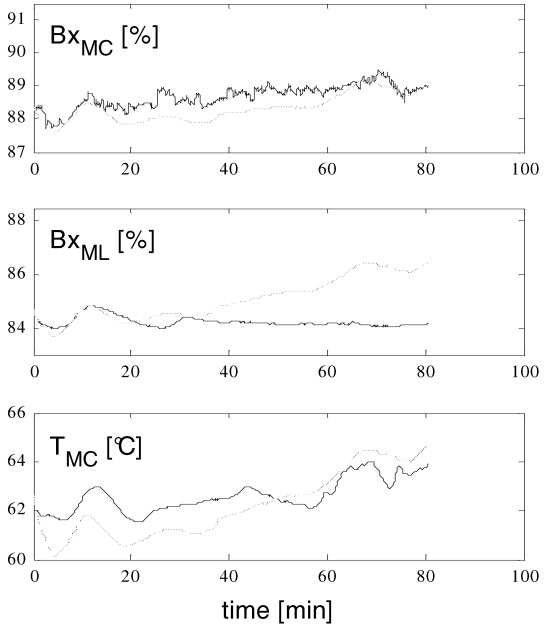

Figure 2: batch 2 – November 19th
bold lines for measurements and thin lines for simulations

One may point out simulation results are sometimes less and sometimes greater than the relevant measurements. This phenomenon reveals the limitations of the present structure. For example, differences in $Bx_{ml}^{\%}$ are the results of difficulties in assessing the fraction of emitted vapour, obviously over-estimated. In addition, differences in T_{mc} result from the heating power under-estimation, the term $Q = \alpha_Q\ \rho_{hs} F_{hs} \ell_{lv}^{w}$ being over-estimated at the end.

4.2. *Discussion*

As a whole, these results illustrate the good performance of the tendency model when it is subjected to experimental data. They prove the reliability of this approach for industrial applications.

For engineering practice, the simulator closely matches the process, closely enough to plan its use in an MBC strategy, which comes up to our expectations.

To improve the accuracy of the model, it is necessary to accurately describe both mass and energy balances. To this end, we referred to several studies highlighting the difficulties of describing nucleation, growth and dissolution. With regard to low grade crystallisation, pilot plant experiments and laboratory tests should enable significant progress towards the development of models of these mechanisms, mainly thanks to growth kinetic identification and crystal size distribution estimation.

5. Conclusion and perspectives

At BR, the process control is carried out using linear PID type controllers. This study is part of a programme of technology transfer and applied research, intended to evaluate the impact of advanced control strategies on the global performance of the crystalline growth phase. This programme covers two stages: development of the tendency model (§ 5.1) and proposition of a predictive control strategy (§ 5.2), using the model as process simulator.

5.1. Model developments

It should be noted that the results are only given for one set of parameters matching normal operating conditions, which pre-supposes poor predictive capability outside similar conditions. To overcome these limitations, hybrid modelling should be investigated in order to obtain a more adaptive representation (§ 5.2). In addition, precision being highly dependent on operating conditions, the online estimation of fitting parameters should be considered to minimize deviation from normal experimental conditions (Simoglou *et al.*, 2005).

5.2. Advanced control simulation

In the industrial context, production constraints make it difficult to run closed loop control schemes in real time. This led us to develop an off-line test protocol, using the tendency model as process simulator, and a predictor of the controlled variables, taking the form of a neural network model, identified using industrial data (Grondin-Perez *et al.*, 2005).

Acknowledgments

The authors gratefully acknowledge the help of Mr. Jean-Claude Pony, Dir. of the BR sugar mill, and its technical staff, and Mr. Jean-Paul Dijoux, networks engineer (CERF).

References

Bonnecaze C., 2003, *Cristallisation C en sucrerie de canne : modélisation de la pureté de la liqueur mère et étude de l'ensemencement*, PhD thesis, Univ. of La Réunion, 187 p.

Feyo de Azevedo S., B. Dahm and F. R. Oliveira, 1997, *Hybrid modelling of biochemical processes: a comparison with the conventional approach*, Computers & Chem. Eng., 21, S751–S756

Georgieva P., M. J. Meireles and S. Feyo de Azevedo, 2003, *Knowledge-based hybrid modelling of a batch crystallisation when accounting for nucleation, growth and agglomeration phenomena*, Chem. Eng. Science, Vol. 58, Issue 16, pp. 3699-3713

Semlali Aouragh Hassani N., K. Saidi and T. Bounahmidi, 2001, *Steady state modeling and simulation of an industrial sugar continuous crystallizer*, Computers & Chem. Eng., Vol. 25, Issues 9-10, pp. 1351-1370

Randolph, A. D., Larson, M. A., *Theory of Particulate Processes*, Academic Press, Inc., San Diego, 1988

Brown D. J. and K. Alexander, 1992, *Rates of nucleation in the crystallization of sucrose*, J. of Crystal Growth, Vol. 118, Issues 3-4, 1 pp. 464-466

Berglund K. A., E. J. deJong, 1990, *The calculation of growth and nucleation kinetics from MSMPR crystallizer data including growth rate dispersion*, Separations Tech., Vol. 1, Issue 1 , 1990, pp. 38-45

Koiranen T., T. Kilpiö, J. Nurmi, H.-V. Nordén, 1999, *The modelling and simulation of dissolution of sucrose crystals*, J. of Crystal Growth, 198/199, pp. 749-753

Pautrat C., J. Génotelle and M. Mathlouthi, 1997, *Sucrose crystal growth: effect of supersaturation, size and macromolecular impurities*, in *Sucrose crystallization, sc. & tech.*, VanHook *et al.*, Bartens, pp. 57-70

Cadet C., Y. Touré, G. Gilles and J.-P. Chabriat, 1999, *Knowledge modeling and nonlinear predictive control of evaporators in cane sugar production plants*, J. of Food Eng., Vol. 40, Issues 1-2, pp. 59-70

Benne M., B. Grondin-Perez, J.-P. Chabriat and P. Hervé, 2000, *Artificial neural networks for modelling and predictive control of an industrial evaporation process*, J. of Food Eng., Vol. 46, Issue 4, pp. 227-234

Simoglou A., P. Georgieva, E. B. Martin, A. J. Morris and S. Feyo de Azevedo, 2005, *On-line monitoring of a sugar crystallization process*, Computers & Chem. Eng., Vol. 29, Issue 6, pp. 1411-1422

Saska M., and P. Rein, 2001, *Supersaturation and crystal content control in vacuum pans,* Proc. of the 10th Sugar Ind. Technologists Meeting, Taiwan, May 2001, pp. 251-261

Theisen K. H., and T. Diringer, 2003, *Recent optimization and developments of concentration measurement by microwaves*, 10th Symposium of AVH Association, Reims, France, March 2003, pp. 39-41

Grondin-Perez B., M. Benne, C. Bonnecaze, J.-P. Chabriat, 2005, *Industrial multi-step forward predictor of mother liquor purity of the final stage of a cane sugar crystallisation plant*, J. of Food Eng., Vol. 66, Issue 3, February 2005, pp. 361-367

Prediction of partition coefficients of plastic additives between food simulants and polyethylene films

Guillaume Gillet[a,b], Olivier Vitrac[c], Stéphane Desobry[b]

[a]*Laboratoire National d'Essais, Centre Energie, Matériaux et Emballage, 29 avenue Roger Hennequin, 78197 Trappes CEDEX, France.*

[b]*Nancy Université, LSGA-ENSAIA-INPL, 2 avenue de la forêt de Haye, BP 172, 54505 Vandœuvre lès Nancy, France.*

[c]*Institut National de la Recherche Agronomique, UMR 1145 Food Chemical Engineering, 1 avenue des Olympiades, 91300 Massy, France*

Abstract

Partition coefficients of n-alkanes, n-alcohols and commercial antioxidants between polyethylene and food simulants (ethanol, methanol), $K_{F/P}$, have been estimated using an off lattice Flory approximation and satisfactory compared to previously published values. The approach demonstrated the preponderant effect of the configurational entropic contribution on the estimate of $K_{F/P}$.

Keywords: thermodynamics, polymer, desorption, chemical potential, Flory-Huggins theory

1. Introduction

In Europe, all materials intended to be in contact with food must comply with the new framework regulation 2004/1935/EC, which enforces a safety assessment and risk management decision for all starting substances and possible degradation products coming from the material. For plastic materials, article 14 of the directive 2002/72/EC introduces diffusion modeling as an alternative to time-consuming and costly experiments for both compliance testing and risk assessment. The fundamentals of probabilistic modeling of the desorption of packaging substances into food has been analyzed by us [1] and applied to different situations [2] including the assessment of consumer exposure to styrene originating from yogurt pots [3]. The main limitation in the use of predictive approaches for both compliance testing and risk assessment is the availability of physico-chemical properties of a wide range of substances, polymers and thermodynamical conditions (temperature, swelling). Robust approaches have been developed for the prediction of diffusion coefficients in polymers [4-5], but no appropriate method exists to predict partition coefficients between a polymer and a food or a food simulant [6]. A first attempt was made by Baner *et al.* [7] using the regular solution theory, but it required an empirical factor, which was dependent on the size and shape of the considered substance. This work examines an off-lattice generalized Flory-Huggins approach to predict activity coefficients in polyethylene (PE) and in different food simulants (ethanol, methanol). The excess in mixing enthalpy is assessed by sampling the nearest-neighbor interactions energies for all possible host-substance pairs [8-9]. This method is an alternative to particle insertion or deletion methods [10], which cannot be applied reliably to penetrants much larger than fluctuation volumes in polymers.

The paper is organized as follows. Section 2 summarizes the theoretical principles used to calculate both the excess in enthalpy and entropy in both phases. Section 3 presents the results obtained for homologous series of alkanes and alcohols as well as for typical hindered antioxidants. When they are available, predictions are compared with values measured between a low density polyethylene and two food simulants with increasing polarity: ethanol and methanol [6-7].

2. Theory and methods of estimation of activation coefficients

2.1. Equilibrium between the packaging material and the food in contact

By noting the thermoplastic packaging, P, and the food product in contact, F, the thermodynamical equilibrium between P and F corresponds to a situation, where the cumulated free energy between P and F, noted G_{P+F}, is minimal. For a $P+F$ system at constant temperature and pressure, the evolution towards equilibrium is accompanied by an exchange of matter between P and F. In this work, only a single species initially present in the polymer, noted i, is assumed to migrate. This model situation corresponds in particular to the contamination of an aqueous food or polar simulant by a plastic additive. For an isolated system $P+F$, G_{P+F} is:

$$\begin{aligned} G_{P+F} &= G_{i+P} + G_{i+F} \\ &= \underbrace{n_P \cdot \overbrace{\mu_P^{id}+\mu_P^{excess}}^{\mu_P} + n_{i,P} \cdot \overbrace{\mu_i^0+\mu_i^{id}+\mu_{i,P}^{excess}}^{\mu_{i,P}}}_{G_{i+P}=G_{i+P}^{id}+G_{i+P}^{excess}} \\ &+ \underbrace{n_F \cdot \overbrace{\mu_F^{id}+\mu_F^{excess}}^{\mu_F} + n_{i,F} \cdot \overbrace{\mu_i^0+\mu_i^{id}+\mu_{i,F}^{excess}}^{\mu_{i,F}}}_{G_{i+F}=G_{i+F}^{id}+G_{i+F}^{excess}} \end{aligned} \quad (1)$$

where $\{n_k\}_{k=P,F}$ and $\{n_{i,k}\}_{k=P,F}$ are the number of molecules k and the number of molecules i in k respectively. Their corresponding chemical potentials are $\{\mu_k\}_{k=P,F}$ and $\{\mu_{i,k}\}_{k=P,F}$ respectively. All energetic terms are further decomposed into an ideal, ^{id}, and an excess part, ^{excess}. From a microscopic point of view, the detailed mass balance at the interface enforces that the partition coefficient at the interface between P and F, noted $K_{F/P}$, is equal to the ratio of frequencies of crossing the interface: $k_{i,P\to F}$ and : $k_{i,F\to P}$. By introducing the free energy of the barrier to cross the interface, $G_i^{\dagger}$, the transition state theory defines $K_{F/P}$ in the canonical ensemble as:

$$K_{F/P} = \frac{p_{i,F}^{eq}}{p_{i,P}^{eq}} = \frac{k_{i,P\to F}}{k_{i,F\to P}} = \frac{\frac{k_B\cdot T}{h}\exp\left(-\frac{G_i^{\dagger}-G_{i+P}}{k_B\cdot T}\right)}{\frac{k_B\cdot T}{h}\exp\left(-\frac{G_i^{\dagger}-G_{i+F}}{k_B\cdot T}\right)} = \exp\left(\frac{G_{i+P}-G_{i+F}}{k_B\cdot T}\right) \quad (2)$$

Where h is the Planck's contact, k_B is the Boltzmann's constant and T the absolute temperature. Eq. (2) can be used to estimate $K_{F/P}$ in the Gibbs Ensemble [11] but it requires calculating the energy of each subsystem after equilibration. An alternative relies on a macroscopic description of equilibrium (dG_{P+F}=0) for a closed system ($dn_{i,F}$=-$dn_{i,P}$), which leads to: $\mu_{i,F}$=$\mu_{i,P}$. By choosing the state of pure i as reference and by expressing the activities of both non ideal mixtures from their volume fractions in i, $\{\phi_{i,j}\}_{j=P,F}$, $K_{F/P}$ is approximated as:

$$K_{F/P} \approx \frac{V_i\cdot\phi_{i,F}}{V_i\cdot\phi_{i,P}} = \exp\left(\frac{\mu_{i,P}^{excess}-\mu_{i,F}^{excess}}{k_B\cdot T}\right) = \frac{\gamma_{i,P}^{v}}{\gamma_{i,F}^{v}} \quad (3)$$

According to the Flory-Huggins theory [12-15], the activity coefficients $\{\gamma_{i,k}^{v}\}_{k=P,F}$ can be derived on a rigid lattice, whose mesh size is commensurable to the volume of the penetrant V_i or to its surface. In this work, V_i is chosen as the volume enclosed within the Connolly surface for a probe similar to a hydrogen atom (i.e. excluding surface as defined in [16]). The basic point of this approach is to consider that the shape of the cavity, where i is inserted, is mainly controlled by the interactions with H host atoms rather than by bare heavy host atoms (C, O, P, N or S in this work). For molecules of k with a volume fraction ϕ_k and consisting in r_k blobs of volume V_i, one gets at infinite dilution of i [17]:

$$\frac{\left\{\mu_{i,k}^{excess}\right\}_{k=P,F}}{k_B\cdot T} = \ln\gamma_{i,k}^{v} = \left(1-\frac{1}{r_k}\right)\cdot\phi_k + \chi_{i,k}\cdot\phi_k^2 \approx \left(1-\frac{1}{r_k}\right)+\chi_{i,k} \quad (4)$$

where $\chi_{i,k}\cdot n_i\cdot\phi_k = H_{i+k}^{excess}/k_B\cdot T$ is the heat of mixing. The first term represents the effect of the configurational entropy associated to the increase of microstates due to the distribution of k around i without changing the effective contact energy between i and k. The absolute value of the first term is expected to be small in polymers (r_k>>1) while it is expected to be significant in simulants consisting in molecules much smaller than i. The term r_k^{-1} is equivalent to the dimensionless size (relative to the size of k) of the cavity required to insert one molecule i.

2.2. Estimation of $\chi_{i,k}$ from pair contact energies

The lattice method has been mainly used to predict the heat of mixing of polymer-solvent systems, which present a significant similarity. Since the blob size and the coordination number of the lattice cannot be modified, the lattice approximation is less accurate to sample the interactions between dissimilar structures including flexible penetrants. A continuous representation of interactions was used instead [8-9]:

$$2\cdot k_B\cdot T\cdot\left\{\chi_{i,k}(T)\right\}_{k=P,F} = g_{i+k}+g_{k+i}-g_{k+k}-g_{i+i} \approx \left\langle z_{i+k}\right\rangle\cdot\left\langle\varepsilon_{i+k}\right\rangle_T+\left\langle z_{k+i}\right\rangle\cdot\left\langle\varepsilon_{k+i}\right\rangle_T-\left\langle z_{k+k}\right\rangle\cdot\left\langle\varepsilon_{k+k}\right\rangle_T-\left\langle z_{i+i}\right\rangle\cdot\left\langle\varepsilon_{i+i}\right\rangle_T \quad (5)$$

where $\langle\ \rangle$ and $\langle\ \rangle_T$ are respectively the average operator and a temperature ensemble average operator. The temperature, T, was set to 313 K as prescribed in the EU regulation by weighting the distribution of energies $p_{A+B}(\varepsilon)$ with the Boltzmann factor $\exp(-\varepsilon/k_B\cdot T)$:

$$\left\langle\varepsilon_{A+B}\right\rangle_T = \frac{\int_{-\infty}^{+\infty} p_{A+B}(\varepsilon)\cdot e^{-\frac{\varepsilon}{k_B\cdot T}}\cdot\varepsilon\cdot d\varepsilon}{\int_{-\infty}^{+\infty} p_{A+B}(\varepsilon)\cdot e^{-\frac{\varepsilon}{k_B\cdot T}}\cdot d\varepsilon} \quad (6)$$

The sampling of $p_{A+B}(\varepsilon)$ was based on a large set of conformers of A (seed molecule) and B (contact molecule) representative of their condensed state (up to 10^4 configurations) and based on all possible contacts of their van der Waals envelopes with spherical symmetric probability (up to 10^9 configurations). Since only the surface farthest away from the center of mass was considered, internal cavities of the seed molecule could only be sampled by a contact molecule smaller than the cavity (e.g. B). The coordination number was determined similarly on a large number of packed configurations (up to 10^4), where van der Waals envelopes are in contact but not overlapping. Polymers based on few monomers were idealized by preventing head and tail atoms to be in contact with any surface. All conformers and sampling energies were performed using the Materials Studio environment version 4.1 (Accelrys, San Diego, USA), its scripting features and the atom-based COMPASS forcefield, which was applied without any cutoff.

2.3. Biases associated to configuration space sampling

In Eq. (5), approximating all enthalpic terms $g_{A+B} = \left\langle z_{A+B}\cdot\varepsilon_{A+B}\right\rangle_T$ as the product of their averages reduces drastically the overall cost computational of the method but it introduces a bias, which is equal to the covariance between z_{A+B} and ε_{A+B}:

$$\beta_{A+B} = \left\langle z_{A+B}\cdot\varepsilon_{A+B}\right\rangle_T - \left\langle z_{A+B}\right\rangle\left\langle\varepsilon_{A+B}\right\rangle_T = \mathrm{cov}\left(z_{A+B},\varepsilon_{A+B}\right) \quad (7)$$

All biases were estimated by calculating the neighborhood-based local covariance for a set of homologous series of molecules:

$$\beta_{A+B} \approx 2\cdot s_{\varepsilon_{A+B}}^2\cdot s_{z_{A+B}}^2\cdot\frac{\Delta_{A+B}}{s_{\varepsilon_{A+B}}^2\cdot\Delta_{A+B}^2+s_{z_{A+B}}^2} \le s_{\varepsilon_{A+B}}\cdot s_{z_{A+B}} \quad (8)$$

where Δ_{A+B} is the expected gradient of z_{A+B} with ε_{A+B}. It is approximated by the gradient assessed when either A or B is replaced by a similar molecule:

$$\Delta_{A+B} = \left.\frac{\partial z_{A+B}}{\partial\varepsilon_{A+B}}\right|_{A,B} \approx \frac{1}{2}\cdot\left(\left.\frac{\partial z_{A+B}}{\partial\varepsilon_{A+B}}\right|_{\mathrm{A,homologous}\ B}+\left.\frac{\partial z_{A+B}}{\partial\varepsilon_{A+B}}\right|_{\mathrm{B,homologous}\ A}\right) \quad (9)$$

s^2_X is the variance estimate of X within the considered sample of homologous molecules and including all repetitions.

According to Eqs (3-5, 6-7), the estimate of the partition coefficient between P and F becomes:

$$\begin{aligned}2\cdot k_B\cdot T\cdot\ln K_{F/P} &\approx 2\cdot k_B\cdot T\cdot r_F^{-1}\\ &+\left(\left\langle z_{i+P}\right\rangle+\left\langle z_{P+i}\right\rangle\right)\left\langle\cdot\varepsilon_{i+P}\right\rangle_T-\left(\left\langle z_{i+F}\right\rangle+\left\langle z_{F+i}\right\rangle\right)\left\langle\cdot\varepsilon_{i+F}\right\rangle_T\\ &-\left\langle z_{P+P}\right\rangle\left\langle\cdot\varepsilon_{P+P}\right\rangle_T+\left\langle z_{F+F}\right\rangle\left\langle\cdot\varepsilon_{F+F}\right\rangle_T\\ &+\beta_{i+P}+\beta_{P+i}-\beta_{i+F}-\beta_{F+i}-\beta_{P+P}+\beta_{F+F}\end{aligned} \quad (10)$$

It is worth to notice that the final result does not depend on the reference chemical potential g_{i+i}. Besides, some non-

symmetric biases (i+P and P+i, i+F and F+i) are expected to balance each other out due to a possible exchange between the roles of seed and contact molecules.

3. Results and discussion

3.1 *Estimation of the enthalpic contribution*

Typical configurations related to minimums of ε_{A+B} and to typical compaction values z_{A+B} are illustrated in Fig. 1.

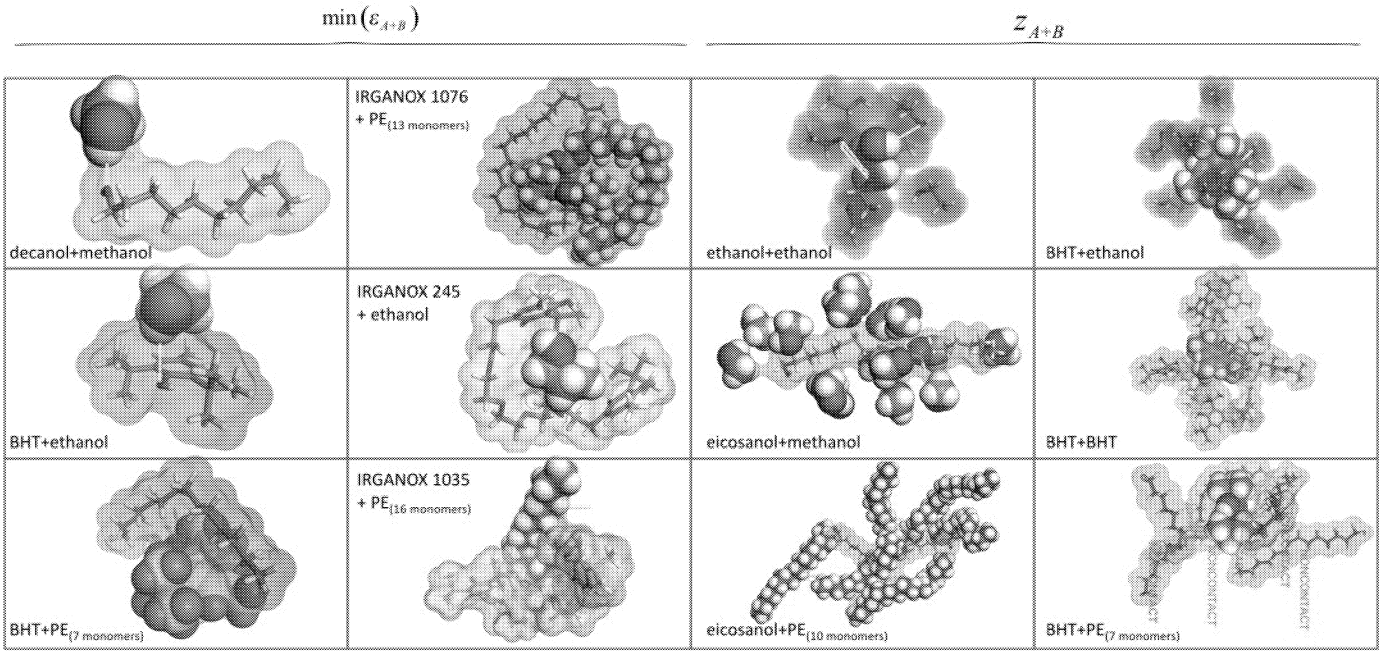

Fig. 1. Typical A+B pair interactions and packing. Tested plastic additives are: BHT (2,6-di-tert-butyl-4-methyl-phenol, CAS 128-37-0), Irganox 1076 (octadecyl 3,5-di-(tert)-butyl-4-hydroxyhydrocinnamate, CAS 2082-79-3), Irganox 245 (Ethylenebis (oxyethylene)bis-(3-(5-tert-butyl-4-hydroxy-m-tolyl)-propionate), CAS 36443-68-2), Irganox 1035 (thiodiethylene bis[3-(3,5-di-tert-butyl-4-hydroxyphenyl)propionate], CAS 41484-35-9).

The volume of each molecule is represented either by calotte models or by their Connolly surface. Hydrogen bonding is depicted in dashed lines.

Corresponding distributions of ε_{A+B} are depicted in Fig. 2. ε_{A+B} are symmetric respectively to A and B: $\varepsilon_{A+B} = \varepsilon_{B+A}$. Each distribution relies on 10^7 pair trials. Raw distributions are characterized by a significant kurtosis (Fig. 2a). Introducing a temperature ensemble increases the probability of states of lower energies (Fig. 2b). As result, the negative skew shifts both the average and the mode towards the negative values. When H-bonding is significant between A and B (e.g. methanol+methanol), the distribution becomes bimodal. The first mode is associated to attractive electrostatic-interactions (H-bonding) and the second is associated to the long-range attractive part of van-der-Walls interactions (induced dipole-dipole forces).

Since the used off-lattice approach samples both the conformation and the reorientation phase space, the non-combinatory entropic contribution is accounted in the estimate of $\chi_{i,k}$. Besides, to be physically consistent, the whole approach requires $\chi_{i,P}$ estimates to not depend on the number of monomers, m, used to represent the polymer. For a same molecule i and according to Eq. (5), this condition implies that the variation in the pair interaction energy $g_{i+P}+g_{P+i}$ is exactly balanced by a similar variation g_{P+P} when m is increasing. The best suitable number of monomers, m, must thus minimize the criterion $C_{P+i}(m)$:

$$C_{P+i}^{(m)} = \left| 1 - \frac{\partial g_{i+P}^{(m)}}{\partial g_{P+P}^{(m)}}\bigg|_i - \frac{\partial g_{P+i}^{(m)}}{\partial g_{P+P}^{(m)}}\bigg|_i \right| \qquad (11)$$

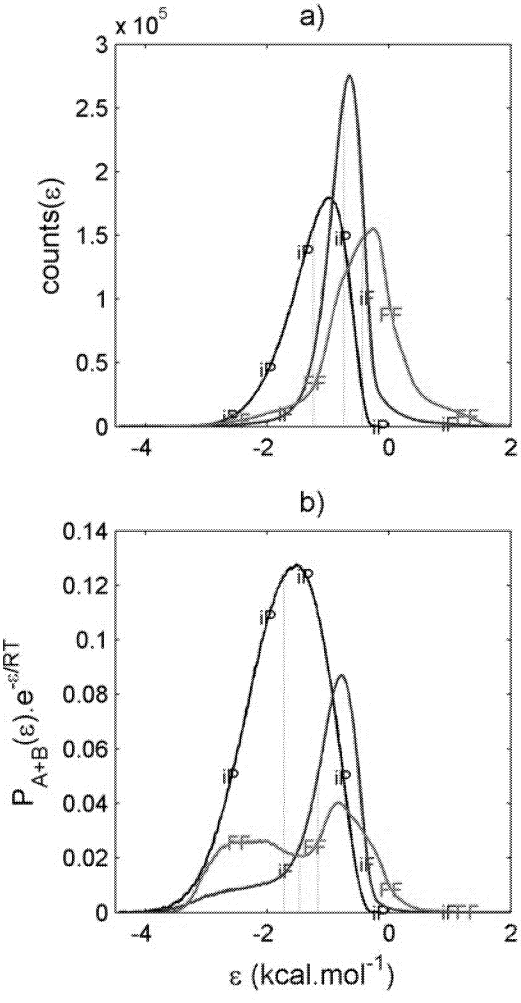

Fig 2. Distribution of pair energy contacts where *i*=decanol, *P*=polyethylene including 5 monomers and *F* = methanol. a) raw distributions, b) reweighted distributions at 313 K.

Since the configuration sampling of large polymer systems is computationally more expensive, the optimal m value is expected to lie for an intermediate number of monomers as a best compromise between convergence cost and possible biases induced by sampling.

Fig. 3 plots the criterion defined in Eq. (11) and the cumulated bias $\beta_{i+P}\big|_i + \beta_{P+i}\big|_i - \beta_{P+P}\big|_i$ for flexible chains, which resemble the polymer. As it could be intuitively expected, both the bias and the criterion tend to be minimal when the size of the seed and the size of the contact molecule coincide approximately. This condition corresponds to the situation where g_{i+P} and g_{P+i} are close to be symmetric. For small m values, the overall bias is minimum but $C_{P+i}(m)$ is high and decreases linearly with m. This trend is associated to almost constant ε_{i+P} values, which are followed by an overall increasing coordination number $z_{i+P}+z_{P+i}$. Indeed, the rigidity of small oligomers combined with non contact heads and tails prevents the number of contacts (and consequently the contact energy) from increasing (from decreasing). When polymer segments become larger, end effects vanish but all biases increase in particular due to a significant $\beta_{P+P}\big|_i$ contribution. It is worth to notice that the asymptotic bias estimated in our simulations (between $0.14 \cdot k_B \cdot T$ and $0.31\ k_B \cdot T$) are close to the theoretical correction of $0.35\ k_B \cdot T$ conventionally applied to fit the Flory-Huggins theory to the solubility of linear alkanes in polyethylene (see p 81 of reference [18]).

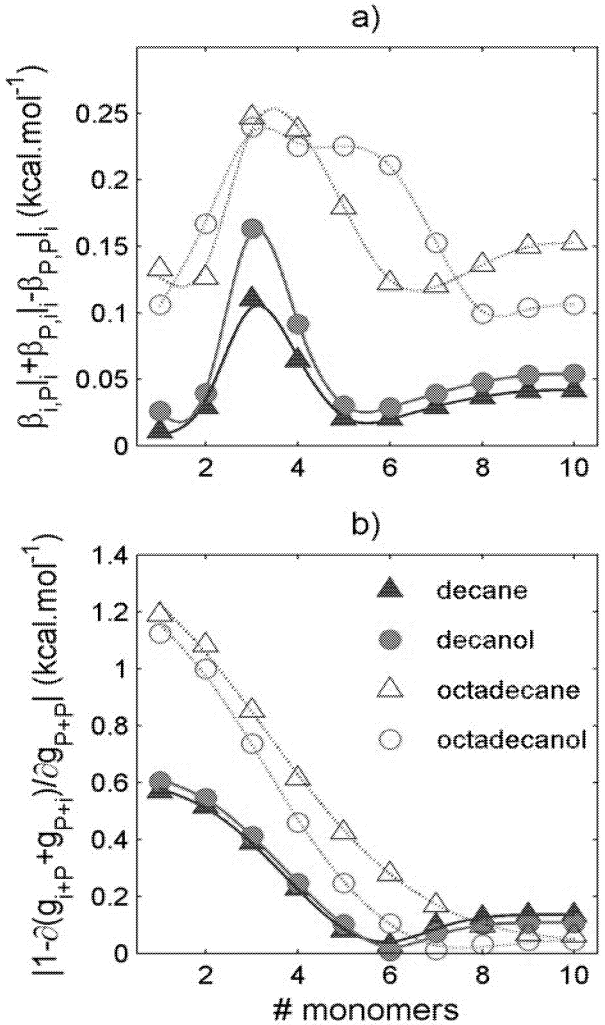

Fig. 3. a) Cumulated bias and b) convergence criterion C_{P+i} according to the number of monomers used to idealize the interactions between flexible molecules and the polymer.

The effect of m on $\chi_{i,P}$ is plotted in Fig. 4 for both a linear molecule (decanol) and four typical phenolic antioxidants. As previously discussed, $\chi_{i,P}$ decreases with m when C_{P+i} is also decreasing. For small additives, an optimal polymer length exists to predict polymer interactions, whereas several minima can occur for large ones. Minima values were considered in the remainder of this work.

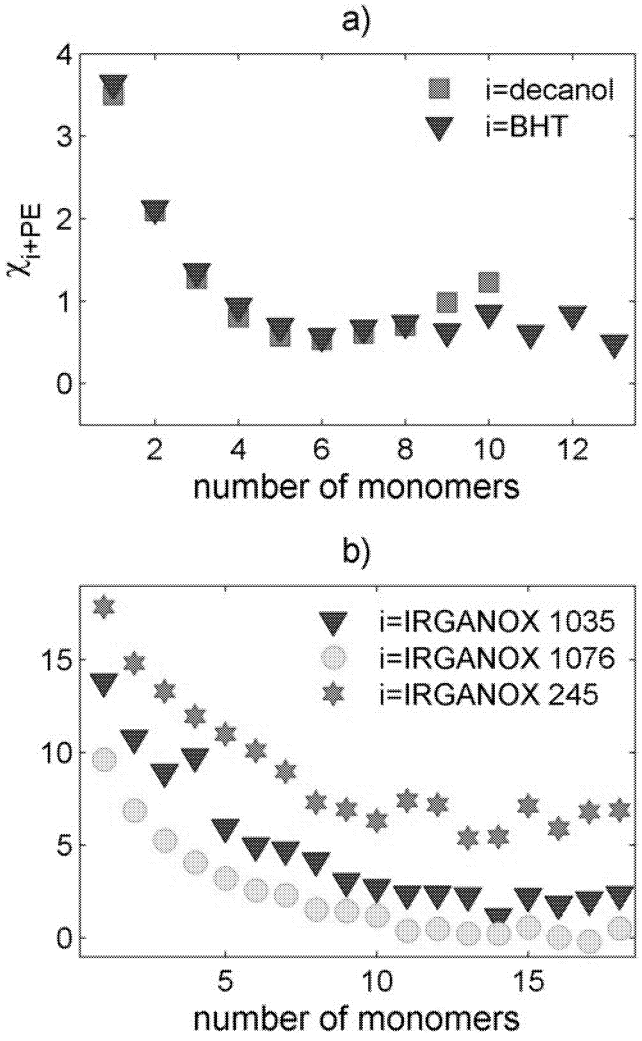

Fig. 4. Effect of the number of monomers on the estimation of $\chi_{i,k}$.

Values of $\chi_{i,P}$ and $\chi_{i,F}$ for a series of n-alkanes and n-alcohols and four antioxidants are plotted in Fig. 5. The interactions were maximal in F and low in P except for Irganox 245. Since all antioxidants included one or two BHT patterns, the different behaviors observed in P were mainly related to the stiffness of the side or bridging chain, which is stiffer in Irganox 245 than in Irganox 1035 (see Fig. 1). The high values in simulants were related to the presence of large molecules, which reduced the possibility of hydrogen bonding. This effect was higher when the surface of the substance i exposed to F was higher (e.g. for linear molecules rather than hindered antioxidants).

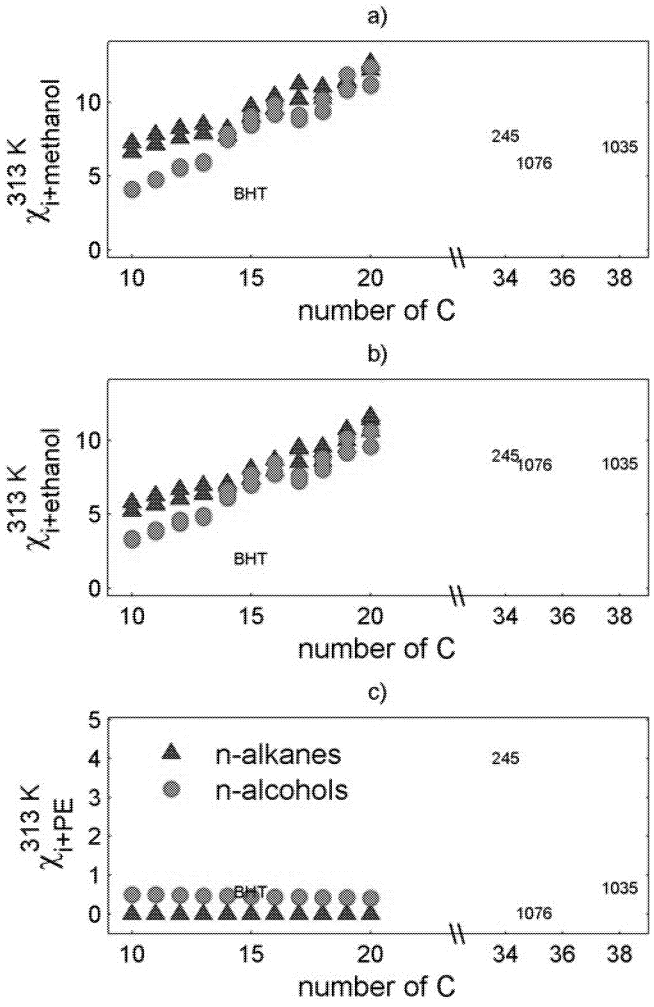

Fig. 5. $\chi_{i,k}$ estimated at 313 K in methanol, ethanol and PE. For PE, the values were derived for the number of monomers, which led to the lowest $\chi_{i,P}$ value (see Fig. 2). Irganox molecules are depicted by their numerical codes: 245, 1035, and 1076.

3.2. Partition coefficient estimates

Eq. (10) can only estimate partitioning between the amorphous regions of PE and *F*. Since the dense crystalline regions are assumed to be free of any substance, calculated values were compared with values obtained on a low density PE [6-7] subsequently to a correction according to the amount of amorphous phase. As first approximation, the entropic contribution r_F^{-1} was estimated by considering that the substance *i* would displace a volume of *F* commensurable to the volume enclosed into its averaged Connolly surface. This approximation is particularly realistic at high dilution rate (non-interacting substances *i*), where *F* molecules smaller than *i* would act as a continuous phase with a specific volume close to its molar volume at the same temperature. The corresponding results are plotted in Fig 4.

Without any fitting, the magnitude orders were similar. The deviation was higher in ethanol, where the proposed approach tended to underestimate $K_{F/P}$ of linear molecules while it overestimated the value of hindered additives (BHT and Irganox 1076).

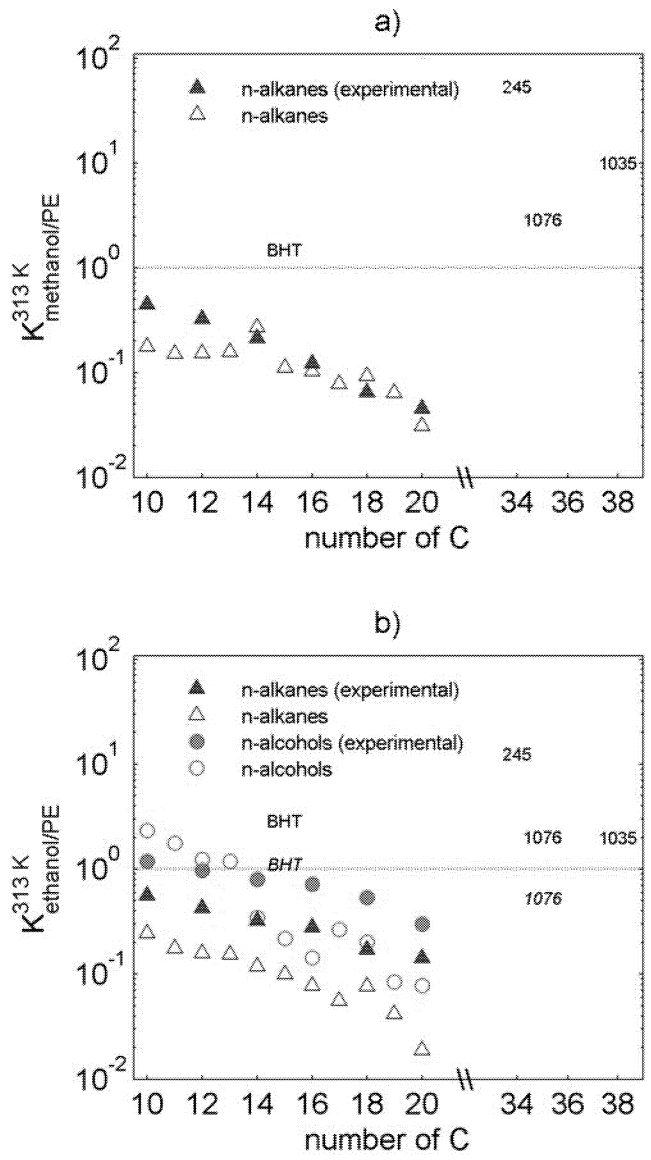

Fig. 6. Predicted and experimental (filled symbols or in italic) partition coefficients between amorphous regions of polyethylene and two polar simulants.

Bias analysis and a sensitivity analysis demonstrated that the uncertainty was mainly related to the entropic contribution. The number of ethanol molecules associated to the blob of a linear molecule should be higher for alkyl segments and lower for hindered groups (e.g. BHT pattern), which can contribute to hydrogen bonding.

3.3 Uncertainty on the entropic contribution

The definition of the cavity volume required to insert a molecule *i* in the medium *F* has a significant impact on the prediction of partitioning (see Eq. 10). In particular, increasing the volume of the cavity in *F* increases the predicted affinity for *F* due to a higher entropic contribution. For polar *F* substances, it is expected that the introduction of a hydrophobic substance *i* may modify the network of hydrogen bonding so that the orientation of *F* molecules may not be random around *i* and may increase the size of the effective cavity. On the opposite, the possibility of hydrogen bonding between *i* and *F* may lead to a contraction of the cavity. Both effects are illustrated in Fig. 7 on a mixture methanol+BHT at 313 K in the NPT ensemble.

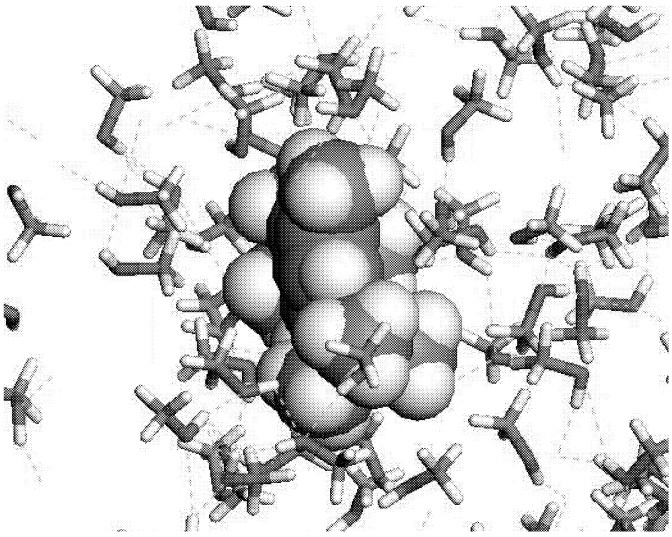

Fig. 7. Volume occupied by a molecule of BHT in methanol. Hydrogen bonding is depicted in dashed lines.

Different dimensionless cavity sizes $1/r_F$ were compared with their theoretical value, which matched the experimental partition coefficients, as the ratio:

$$R = \frac{r_F^{-1}}{\left(\ln K_{F/P}^{313K}\right) - \left(\chi_{i,P} - \chi_{i,F}\right)} \quad (11)$$

Two typical volumes were considered for the cavity: a lower value enclosed within the Connolly surface of *i*, an upper value defined by the molar volume of pure *i*. Although these bounds are not absolute, the likely value is expected to lie between them. Indeed, a volume even lower would imply attractive interactions stronger than those found within *F*. A higher value would require by contrast long-range modifications of *F* structure at a length scale similar to *i*.

R values corresponding to both bounds are presented in Fig. 8. Since volumes of *i* derived from their Connolly volumes and molar volumes are highly correlated for all tested molecules (i.e. the Connolly volume is about 67% of the molar volume), only the accuracy of *K* estimates is modified while the ratio of *K* between homologous molecules is unchanged.

When the shape of *i* relies of a pattern close to *F* (aliphatic alkanes and alcohols in ethanol), the molar volume was the best estimate of the size of the cavity. In other cases, the lowest volume was more appropriated. The direct calculation of partial molar volumes from molecular dynamics simulations of F+*i* mixtures in the NPT ensemble (our current work) confirms these conclusions. When the considered bounds did not enclose the unity, the deviations were either attributed to biased estimations of the entropic error or to experimental errors on *K*. The overall sampling error on $\chi_{i,P}$-$\chi_{i,F}$ was estimated lower than 1.2 (corresponding relative error on *K* lower than exp(1.2)=3.3). Plastics additives with high melting temperature may lead to underestimated *K* measurements due to difficulties in their incorporation and mixing during the processing (see as an example p 155 of reference [19]). As a result, residual crystallites of additives may remain out of equilibrium during experimental *K* determinations.

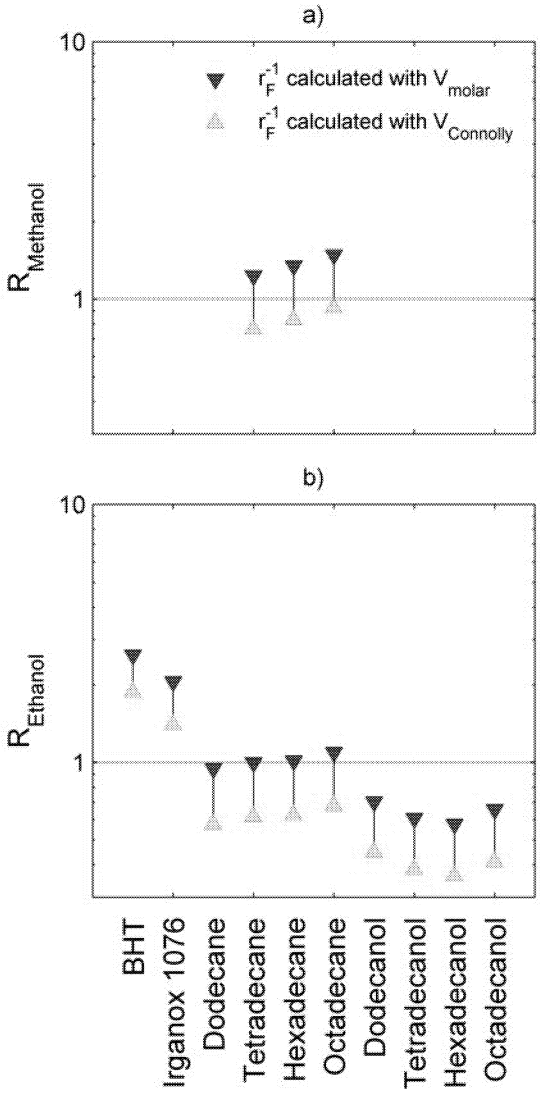

Fig. 8. Dimensionless dimension of the cavity required to insert a molecule *i* in *F* on a log-scale.

A detailed comparison of experimental and predicted values is presented in Fig. 9. *K* values were calculated for both r_F estimates. Uncertainties related to experimental errors (concentrations measurements, crystallinity) were also considered to point out the lack of reference data.

Splitting the data between values with a intermediate affinity for *F* and a high affinity for F shows that acceptable correlations can be attained for *K* values lower than 1, in spite of a tendency of the model to underestimate the overall migration. The non-correlation for K values close or higher than 1 was associated to the difficulties in measuring such values at high F/P ratios (as it occurs in packaging applications). A better definition of the cavity volume required to insert a molecule *i* in the medium *F*, using in particular partial molar volumes, could also be suggested.

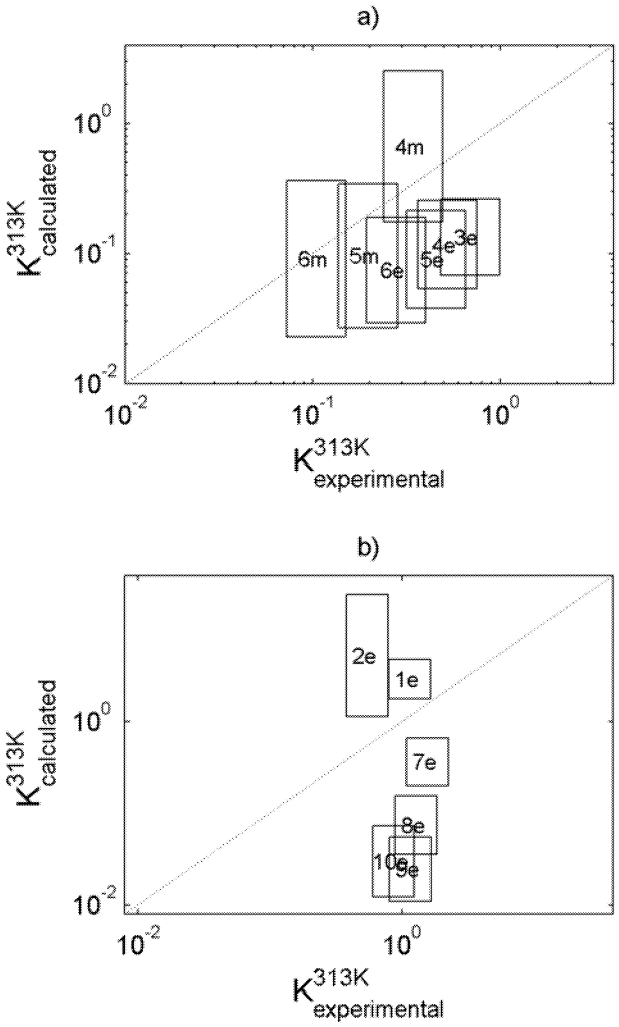

Fig. 9. Experimental partition coefficients in methanol (m) and ethanol (e) and the corresponding calculated values. Plots include error on experimental values and variation of entropic contribution if calculated with molar volume or the volume enclosed within the Connolly surface. a) Molecules with partition coefficient significantly lower than 1. b) Molecules with partition coefficients close or higher than 1. Molecules are: 1. BHT, 2. Irganox 1076, 3. dodecane, 4. Tetradecane, 5. hexadecane, 6. octadecane, 7. dodecanol, 8. tetradecanol, 9. hexadecanol, 10. Octadecanol.

3. Conclusions

The proposed off-lattice generalized Flory-Huggins approach seems a promising approach to predict partitioning between food packaging materials and food simulants. It does not require an explicit representation of the entangled polymer and provides further insight on molecular phenomena, which lead to the contamination of food. In particular, the simulations demonstrated that even if plastic additives have by design a good solubility in polymers, they have a significant chemical affinity for liquids consisting in small molecules. This entropic effect was underestimated in previous studies and would lead to a high migration of antioxidants in food at high temperature when their diffusion and solubility in F are not limiting. Similar observations were made during migration in water, although equilibrium properties are difficult to establish due to a rapid hydrolysis of additives after their migration [20]. Extending Eq. (4) to higher concentrations in i is highly desirable to predict the risk of migration up to the solubility limit in F.

References

[1] O. Vitrac and M. Hayert, 2005. Risk assessment of migration from packaging materials into foodstuffs. AIChE Journal, 51, 4, 1080-1095.

[2] O. Vitrac, B. Challe, J.-C. Leblanc and A. Feigenbaum., 2007. Contamination of packaged food by substances migrating from a direct-contact plastic layer: Assessment using a generic quantitative household scale methodology. Food Additives and Contaminants. 24, 1, 75-94.

[3] O. Vitrac and J.-C. Leblanc, 2007, Exposure of consumers to plastic packaging materials: assessment of the contribution of styrene from yoghurt pots. Food Additives & Contaminants. 24, 2, 194–215.

[4] O. Vitrac, J. Lézervant and A. Feigenbaum, 2006, Application of decision trees to the robust estimation of diffusion coefficients in polyolefines. Journal of Applied Polymer Science, 101, 2167–2186.

[5] O. Vitrac and M. Hayert, 2007, Effect of the distribution of sorption sites on transport diffusivities: a contribution to the transport of medium-weight-molecules in polymeric materials. Chemical Engineering Science, 62, 9, 2503-2521.

[6] O. Vitrac, A. Mougharbel and A. Feigenbaum, 2007, Interfacial mass transport properties which control the migration of packaging constituents into foodstuffs. Journal of Food Engineering. 79, 3,1048-1064.

[7] A. L. Baner and O. G. Piringer, 1991, Prediction of solute partition coefficients between polyolefins and alcohols using the regular solution theory and group contribution methods. Industrial and Engineering Chemistry Research, 30, 1506-1515.

[8] M. G. Bawendi and K. F. Freed, 1988, Systematic correction to Flory-Huggins theory: Polymer-solvent-void systems and binary blend-void systems, Journal of Chemical Physics, 88, 4, 2741-2756.

[9] M. G. Bawendi, K. F. Freed and U. Mohanty, 1987, A lattice field theory for polymer systems with nearest-neighbor interaction energies. Journal of Chemical Physics, 87, 9, 5534-5540.

[10] B. Widom, 1963, Some Topics in the Theory of Fluids, Journal of Chemical Physics, 39, 2808.

[11] A. Z. Panagiotopoulos, 1992, Direct Simulation of Fluid Phase Equilibria by Simulation in the Gibbs Ensemble: A Review, Molecular Simulation, 9, 1.

[12] P. J. Flory, 1941. Thermodynamics of high polymer solutions. Journal Chemical Physics. 9, 660-661.

[13] P. J. Flory, 1942, Thermodynamics of high polymer solutions. Journal of Chemical Physics. 10, 51-61.

[14] M. L. Huggins, 1942a. Derivation of Molecular Relaxation Parameters of an Isomeric Relaxation. Journal of Chemical Physics, 46, 151-153.

[15] M. L. Huggins, 1942b. Theory of Sulutions of high polymers. Journal of the American Chemical Society, 64, 1712-1719.

[16] E. Silla, A. Arnau and Iñaki Tuñón (2001). Fundamental principles governing solvents use. In. "*Handbook of Solvents.*" Ed. I. Wypych, ChemTec Publishing, Toronto, 7-63.

[17] V. J. Klenin, 1999, Thermodynamics of systems containing flexible-chain polymers. Elsevier Science, Amsterdam. 826p.

[18] G. M. Kontogeorgis (2007). The Hansen solubility parameters (HSP) in thermodynamic models for polymer solutions. In. "*Hansen Solubility Handbook – 2nd Edition*", *Ed.* C. M. Hansen, CRC Press, Boca Raton. 75-94.

[19] J. C. J. Bart, 2006, Physical chemistry of additives in polymers, Firenze University Press, Firenze, 378p.

[20] T. P. Gandek, T. Alan Hatton, and R. C. Reid, 1989. Batch extraction with reaction: phenolic antioxidant migration from polyolefins to water. 2. Experimental results and discussion. Industrial & Engineering Chemistry Research. 28, 1036-1045.

REACTION ENGINEERING FOR SPONGE CAKE BAKING: DEVELOPMENT OF A METHODOLOGY TO EXTRACT AN APPARENT IDENTIFIABLE REACTION SCHEME

Souad FEHAILI
Barbara REGA
Pierre GIAMPAOLI
AgroParisTech , UMR 1211 Sciences de l'Aliment et de l'Emballage
INRA, UMR 1211 Sciences de l'Aliment et de l'Emballage
1, av. des Olympiades, F-91300 Massy

Souad FEHAILI
Mathilde COUREL
Catherine BONAZZI
INRA, UMR 1145 Génie Industriel Alimentaire
AgroParisTech, UMR 1145 Génie Industriel Alimentaire
1 av. des Olympiades, F-91300 Massy

Cedric BRANDAM
Xuan MEYER

UMR 5503 Laboratoire de Génie Chimique
CNRS/UPS/INPT, 5 rue Paulin Talabot

F-31106 Toulouse, France

E-mail: souad.fehaili@agroparistech.fr

ABSTRACT

The food properties often results from a set of complex chemical reactions initiated by technological treatments. The ultimate objective of this work is to develop rational operating strategies for foods in order to preserve the integrity of the nutritional compounds or to enhance the production of positive newly formed compounds. A "reaction engineering" approach will allow building robust and reliable knowledge on the mechanisms and on the reaction kinetics and then formalizing them into models to optimize the product/process system. The present paper describes the first stage of this approach. It consists in extracting an apparent identifiable reaction scheme on the basis of theoretical knowledge of the system and observable experimental data and on the use of statistical methods.

1. INTRODUCTION

The role of the Maillard reaction in building food quality has been a matter of interest for years. Despite abundant literature, few studies are dealing with the simultaneous effect of physical and chemical variables on the development of Maillard reaction products; in papers dealing with thermal treatment, the latter is merely considered as a mass and energy transfer operation and the link with the chemical variables is not approached (Broyart and Trystram, 2002]. One of the main objectives of this project is to understand how the processes act on reactions and can favour the appearance, disappearance or preservation of newly formed compounds during the baking of sponge cake. The reaction system can be described as a complex network of many chemical reactions. But only a small part of all the molecules synthesized by these reactions are observable. A major stake of this work will be to extract a simplified reaction pathway which can give a reliable representation of the complex reaction system based on observable compounds. It will be necessary to determine the reactions which really take place and to specify the occurrence of these reactions during the process. The theoretical knowledge of the system and the use of statistical methods should make it possible to extract an apparent reaction pathway from available experimental information. The methodological approach is as follows:

i) Selection of the key-reaction pathways related to previously defined organoleptic and nutritional qualities of the sponge cake and the links occurring between the different reaction pathways (Rega *et al.* 2006)]. Three types of reactions will be focussed on: Maillard, lipid oxidation and caramelization reactions.
ii) Definition and selection of relevant chemical markers to follow the reactions pathways.
iii) Extraction of an apparent but identifiable reaction scheme regarding the observable components from the complete set of theoretical reactions by making as little assumptions as possible.
iv) Acquisition of experimental data taking into account the key-variables likely to influence the reaction.
v) Validation of the reaction scheme from experimental data.
vi) Development of a knowledge based model and selection of the right assumptions to be made: which physical phenomena have to be integrated in the unit operation model and which reactions are to be taken into account and with which kinetic model?

Only the first three points will be developed in this paper.

2. STATE OF THE ART ON THE KINETICS OF MAILLARD REACTION

The majority of the published work dealing with the kinetics of the Maillard reaction rely on simple kinetic models to describe either loss of reactants (sugars, amino acids, amino acid residues in proteins) or formation of products (Hydroxymethylfurfural, Amadori compounds...). On the use of this approach, van Boekel concluded that the results are very much dependent on experimental conditions and on the extent of the reaction (Boekel, 2001). To better understand reaction mechanisms, an advanced approach is

necessary, considering reaction pathways in more detail. Kinetic modelling using multiresponse models has proven to be a useful tool to enable further unravelling of reaction mechanisms in the Maillard reaction (Mundt and Wedzicha, 2003; Martins and Boekel,2005). A first proposed reaction mechanism is tested by the multiresponse analysis where the degradation of the reactants is analysed simultaneously with the formation of the intermediates (Martins and Boekel, 2005). It is a very interesting approach which makes it possible to identify the mechanisms of formation/disappearance of the compounds. The multiresponse approach has already been validated for acrylamide formation in model solutions of glucose and asparagines (Knol, 2005) and on Maillard reaction in milk (Boekel, 1998). However, this method is not easily applicable in a real food system like sponge cake: first, it is a complex formulated solid where reaction compounds do not react in the same way as in a simple model solution; second, only a small part of all the molecules that can be synthesized by thermal reactions are observable and it would be almost impossible to identify the whole reaction scheme.

3. SELECTION OF KEY REACTION PATHWAYS

The early Maillard reaction consists of the non-enzymatic formation of a covalent bond between the carbonyl group (sugar) and the free amine group (R-NH_2). The occurring chemical reactions can be broadly divided into three main stages: (i) the early stage, consisting of the formation of the Amadori product; (ii) the advanced stage, comprising degradation of the Amadori product, and (iii) the final stage, typified by the production of brown polymers and co-polymers, the melanoidins. The degradation of the Amadori product depends on the pH of the system. At pH 7 or below, it mainly undergoes 1,2-enolisation with the formation of 3-deoxyosones. At pH above 7 the degradation of the Amadori compound is thought to involve mainly 2,3 enolisation, where 1-deoxyosones are formed. The key intermediate compounds of this reaction are the α-dicarbonyl (3-deoxyosones and 1-deoxyosones) which are also formed by the caramelization reaction [9]. Thus, the compounds derived from the degradation of the 1- and 3-deoxyosones are indistinctly generated either by the caramelization or by the Maillard reaction (Figures 1).

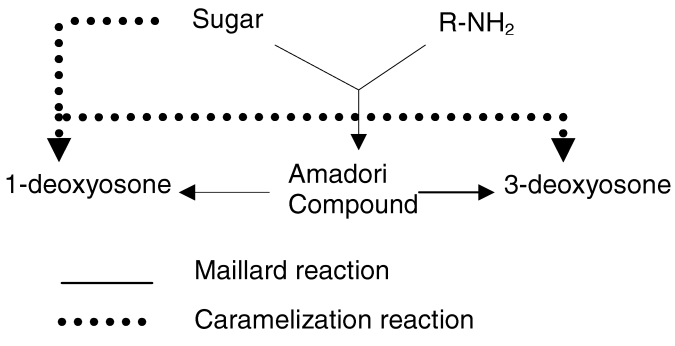

Figures 1: Interaction between Maillard and caramelization reactions

3.1 Compounds Derived From The Degradation Of The Deoxyosones

The 3-deoxyosone will undergo successive dehydrations and a displacement of the double bond to form hydroxymethylfurfural (HMF) (Kroh, 1994), while the 1-deoxyosone generates the 2,3-dihydro-3,5-dihydroxy-6-methyl-4H-pyran-4-one (pyranone) as a typical marker of this reactive pathway (Davidek, *et al*, 2005). Pure 2,3-dihydro-3,5-dihydroxy-6-methyl-4H-pyran-4-one was found to be converted into maltol, hydroxymaltol, and isomaltol (Yaylayan and Mandeville, 1994). Maltol can also be formed directly from the Amadori compound and from disaccharides (Yaylayan and Mandeville, 1994). The deoxyosones are also degraded by the Strecker reaction. This reaction puts in presence the deoxyosones on the one hand and the amino acids on the other hand. This is an autocatalytic reaction, which occurs in food with high concentrations in amino acids and strong temperatures or under pressure (Cremer *et al*, 2000]. The formed α-aminoketone can induce the genesis of pyrazines.

3.2 Compounds Derived From The Interaction Between Maillard Reaction And Lipid Oxidation

Lipid autoxidation reactions generate a multitude of new compounds, in particular, a great number of aliphatic aldehydes. Nevertheless these aldehydes can further react with heterocyclic compounds formed by Maillard reaction. For instance aliphatic aldehydes may react with pyrazines and result in the formation of compounds with long alkyl chains, the alkylpyrazines (Shi and HO, 1994)

3.3 Schematic Overall Reaction

A first scheme of the main reaction pathways involved in the three studied reactions and their interactions is proposed in Fig 2. The concentration of the products as well as various processing variables are likely to influence the advancement of the Maillard, lipid oxidation and caramelization reactions. Manipulating these variables can affect the balance of the various chemical pathways making up the three reactions of interest.

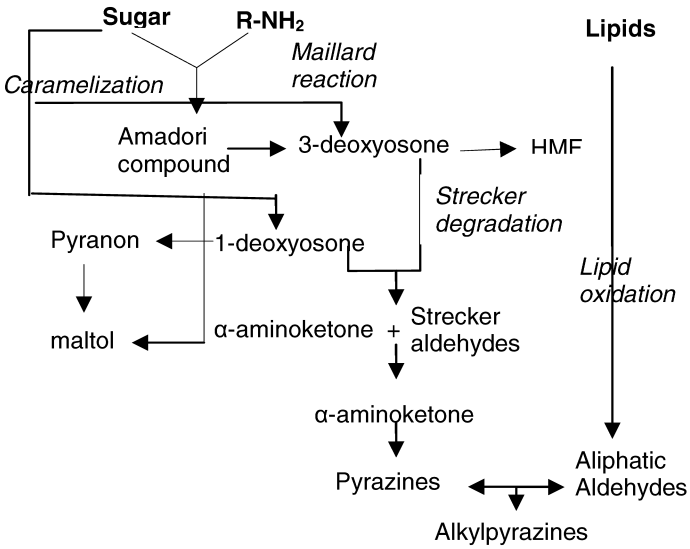

Figures 2: Proposal of a first scheme of the main pathways involved in the three studied reactions and their interactions, *i.e.* Maillard, lipid oxidation and caramelization reactions

4. SELECTION OF RELEVANT MARKERS TO FOLLOW THE REACTION PARTHWAYS

The reaction markers are selected according to their ability to point out different advancement steps of the chemical reactions, taking into account the availability of reliable methods of analysis. A reaction marker can be either a substrate or a product of a reaction pathway, possibly with an organoleptic interest. The Amadori compound and aliphatic aldehydes were chosen as Maillard reaction and lipid oxidation markers respectively. No marker has been selected for the caramelization reaction since the deoxyosone formation intermediates are unstable and therefore difficult to analyse. HMF et 2,3-dihydro-3,5-dihydroxy-6-methyl-4H-pyran-4-one were selected as typical markers of 3-deoxyosone and 1-deoxyosone degradation (Davidek, *et al*, 2005) and maltol, because of its organoleptic interest. To track the Strecker degradation and alkylpyrazine formation, two Strecker aldehydes and pyrazines were chosen.

5. EXTRACTION OF OBSERVABLE REACTION PATHWAYS

The available reaction markers do not permit observing all the reaction pathways presented in the initial scheme (Figures 2). The reaction scheme at the current state is not identifiable. To reach observable reaction pathways, a stoichiometric matrix is built. The matrix rank indicates the number of independent reactions. An identifiable reaction system is a system which matrix rank equals the number of total reactions [Fillon *et al* ,1995; Moreau *et al*, 1999].

5.1 Construction Of The Stoichiomatric Matrix

The construction of the stoichiometric matrix requires that both the reaction scheme and the values of the stoichiometric coefficients are known. For example, if we assume that A, B, C, D and E components obey to the following reaction scheme:

$A + B \rightarrow C + D$ (I)
$D \rightarrow B + E$ (II)
$A \rightarrow E$ (III)

Then the matrix of stoichiometric coefficients is:

A	B	C	D	E
-1	-1	1	1	0
0	1	0	-1	1
-1	0	0	0	1

The matrix constructed from the initial reaction scheme consists of 21 lines corresponding to the chemical reactions pathways and 13 columns corresponding to selected reaction markers.

5.2 Extraction Of An Observable Reaction Pathways

The obtained stoichiometric matrix has a rank of 8, which means that only 8 out of the 21 reactions are linearly independent, and therefore observable. Consequently, the building of an *observable* reaction scheme requires reducing the initial one by: i) eliminating the unlikely reactions based on literature and ii) searching linear dependencies. For instance, in the previous example, reaction III is the sum of reactions I and II; as these reactions are linearly dependent and cannot be distinguished, they must be condensed into reaction III.
This implies that some assumptions must be drawn *a priori* and validated *a posteriori*.
The observable system obtained (Table 1) is less exhaustive than the overall reaction scheme but it should give a reliable representation of the real and complex reaction system.

Table 1: Observable reactions issued from the stoichiometric matrix of rank 8

1	Sugar + RNH_2 ↔ Amadori compound + H_2O
2	2 Amadori compounds → 4 H_2O + Maltol + HMF
3	Sugar → 2 H_2O + pyranone
4	Sugar → 3 H_2O + HMF
5	Disacharide → 2 H_2O + Maltol + monosacharide
6	RNH_2 + deoxyosone → Strecker aldehyde + α-aminoketone + CO_2
7	2 α-aminoketone → Pyrazines + 2 H_2O
8	Pyrazines + Aliphatic aldehyde → alkylpyrazine + H_2O

6. CONCLUSION

The successful implementation of such an approach is highly dependent on the quality of the experimental data that will be obtained. Appropriate experimental tools have been designed to guaranty the reliability of the kinetic models that will be derived from experiments: i) reliable analytical methods giving access to reaction products ii) A discontinuous lab-scale baking oven was specially designed to achieve a good reproducibility of the baking conditions. Hence, the model of heat and mass transfer has to be associated to the kinetic model in order to relate the control variables of the process to the building of the quality through chemical reactions.

7. ACKNOWLEDGMENT

This work is carried out in the framework of the project ANR-06-PNRA-023 with the financial support of the French National Research Agency within the « Programme National de Recherche en Alimentation et nutrition humaine ».

8. REFERENCES

Boekel, M.A.J.S.v., Acta Horticulturae, 1998. **476**: p. 149-155.

Boekel, M.A.J.S.v, *Kinetic aspects of the Maillard reaction; a critical review.* Nahrung 2001. **45**: p. 150-159.

Broyart, B. and G. Trystram, *Modelling heat and mass transfer during the continuous baking of biscuits.* J. Food Eng., 2002. **51**(1): p. 47-57.

Cremer, D.R., M. Vollenbroeker, and K. Eichner, *Investigation of the formation of Strecker aldehydes from the reaction of amadori rearrangement products with alpha-amino acids in low moisture model systems.* Eur food Res Technol, 2000. **211**: p. 400-403.

Davidek, T., e N. Clety, S. Devaud, F. Robert, I. Blank, *Simultaneous quantitative analysis of Maillard reaction precursors and products by high-performance anion exchange chromatography.* J. Agric Food Chem., 2003. **51**: p. 7259-7265.

Fillon M., M. Meyer, H. Pingaud, X. Joulia (1995) Data reconciliation based on elemental balances applied to batch experiments. 5th European Symposium on Computer Aided Process Engineering, ESCAPE 5, Bled, Slovenia, 11 - 14 June 1995, Supplement to Computers & Chemical Engineering, 19, pp S293-S298, (1995)

Knol, J.J., et al., W.A.M. Van Loon, J.P.H. Linssen, A. Ruck, M.A.J.S. Van Boekel, A.G.J. Voragen
Toward a kinetic model for acrylamide formation in a glucose-asparagine reaction system. J. Agric Food Chem., 2005. **53**: p. 6133-6139.

Kroh, L.W., *Caramelisation in food and beverages.* Food chemistry, 1994. **51**: p. 373-379.

Martins, S.I.F.S. and M.A.J.S. van Boekel, *A kinetic model for the glucose/glycine Maillard reaction pathways.* Food Chemistry, 2005. **90**: p. 257-269.

Martins, S.I.F.S., A.T.M. Marcelis, and M.A.J.S. van Boekel, *Kinetic modelling of Amadori N-(1-deoxy-D-frucyos-1-yl)-glycine degradation pathways. Part I-Reaction mechanism.* Carbohydr. Res., 2003. **338**: p. 1651-1663.

Moreau A., Truong-Meyer X.M., Pingaud H., Strehaiano P. (1999) Metabolic engineering of *Brevibacterium linens* at a macroscopic level. 9th European Congress of Biotechnology 9 (ECB9), 12-15 juillet 1999, Bruxelles, Belgique.

Mundt, S. and B.L. Wedzicha, *A kinetic model for the glucose-fructose-glycine browning reaction.* J. Agric Food Chem., 2003. **51**: p. 3651-3655.

Rega, B.; Guerard, A.; Maire, M. and Giampaoli P. (2006) Searching the missed flavour: chemical and sensorial characterisation of flavour compounds released during baking. In : W.P.L. Bredie, & P.M.A., Flavour Science, Recent advances and trends (pp.605-608). Copenhagen : Elsevier.

Shi, H. and C.-T. HO, *The flavour of poultry meat.* ,In *Flavour of meat and meat Products*, F. Shahidi, Editor. 1994, Chapman & Hall: New York. p. 52-70.

Yaylayan, V.A. and S. Mandeville, *Stereochemical control of maltol formation in Maillard reaction.* J. Agric. Food Chem., 1994. **42**: p. 771-775.

ENERGY EFFICIENCY IMPROVEMENT

AN APPLICATION FOR ENERGY DIAGNOSIS IN SUGAR PLANTS

Merino A., Alves R.,
Center of Sugar Technology.
University of Valladolid. Edificio Alfonso VIII. 47011
Valladolid, Spain.
e-mail: {alejandro,raul}@cta.uva.es

Acebes L. F., Mazaeda R., de Prada C
Department of System Engineering and Automatic Control.
University of Valladolid. Spain.
e-mail: {felipe,rogelio, prada}@autom.uva.es

KEYWORDS

Data reconciliation, steady state simulation, energy efficiency, optimization, sugar factories.

ABSTRACT

An application for the energetic state determination of a sugar plant has been developed. The tool acquire real data from the plant and using a steady state model of the process and an optimization algorithm, is capable to provide information about non measured variables, detect deviation of measured variables and calculate indexes related with the energetic efficiency.

One of the pretended objectives is to allow an easy reconfiguration of the application. For that purpose a library of steady state models and a configurable SCADA have been developed.

The application has been configured for a sugar plant and tried during the last sugar beet campaign with good results.

INTRODUCTION

In the last years, the sugar industry is crossing an important crisis, caused in part by the sugar market reform carried out in the European Union, and in other hand, by the fuel increasing price. So, the reduction of production costs related with fuel consumption is imperative.

In this paper, a tool to diagnose the energetic state in a sugar plant is presented. This tool pretends to be useful in order to know the process energetic situation, to help to decision support and to make progress to the optimum process operation in an economic way. To obtain this information, a mathematical model of the plant is adjusted using optimization techniques, from measured process variables. With this model, steam consumptions and efficiency of process units can be calculated being also possible to detect operation failures.

On the other hand, the amount of produced sugar and its cost can be calculated from raw materials and fuel prices and at the same time, using the adjusted mathematical model and optimization techniques it is possible to determine the amount of raw materials and fuel necessary to minimize the production costs and maximize the sugar production.

The paper is organized as follows. Next section presents a short description of the sugar production process. Next the data reconciliation problem, and the approach to solve the proposed problem are introduced. Following the features and architecture of the developed are presented. Finally the paper shows some conclusions and the future work.

SUGAR PRODUCTION PROCESS DESCRIPTION

In Spain, sugar is produced from sugar beet. Sugar production process starts with the washing and cutting of the sugar beets. Then, sugar beet strips are introduced in an equipment, called diffuser, where the sugar is removed from the beet by being dissolved it in hot water. Finally, a juice containing sucrose is obtained. Juice needs to be purified to remove non sugar substances. This process takes place at the depuration process, where non sugars are precipitated and filtrated by a chemical treatment. Then, depurated juice is concentrated in the evaporation section. After that, concentrated juice is carried to the called, sugar house, where crystal sugars are obtained in batch evaporative crystallizers. Finally, obtained sugar is dried and stored.

In sugar production steam streams are highly linked, high pressure steam is produced in boilers, these steam is used in the evaporation section and at the same time, the steam produced in the evaporation section is used as heating media in sugar house, heat exchangers, etc. being complex to determine the optimum operation conditions. As it has been explained, different steam pressures are available from the evaporation section to be used in other plant equipment, being critical to determine the producers and consumers coupling. Other important decisions are; the amount of extracted water to be used in the diffusion section, the evaporative crystallisers sequentiation, pressure set points, etc.

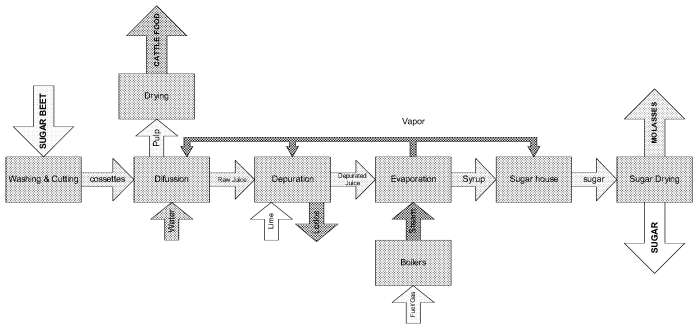

Figure 1. Sugar production process diagram

DATA RECONCILIATION

In process plants exists a set of measured variables, and there are also non measured variables. For any applications is important to obtain reliable estimations of the non

measured variables, also, plant measures are frequently corrupted by noise, so it is important to minimize these disturbances.

Data reconciliation is an application that, taking advantage of the existence of a stationary plant model, faces the problem of correcting plant measures and calculating non measured variables.

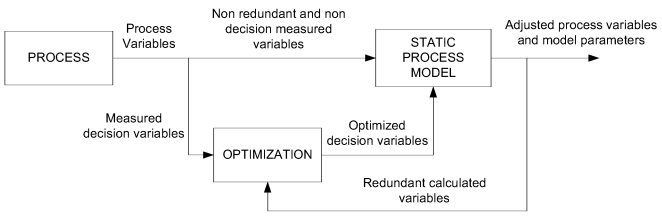

Figure 2: Block diagram for the data reconciliation used.

Data reconciliation is possible when processs extra measures, called redundant measures, are available. That will allow to adjust same or whole process variables, in a way that the process model is fulfilled and the error in the measured variables is minimized. The reliability of the calculated variables depends on the number of redundant measures. Then a function of the difference between the measured process variable ($x_{p,i}$) and the process variable that fulfils the process model ($x_{c,i}$) is minimized. Decision variables, used by the optimizer to adjust redundant variables (y), are also subjected to errors, so these variables can also be included in the objective function to minimize:

$$J = min \sum_{i=1}^{N} \alpha \left(x_{p,i} - x_{c,i} \right)^2 + min \sum_{j=1}^{N} \beta \left(y_{p,j} - y_{c,j} \right)^2 \quad (2)$$

In this function, α and β are weights that can be adjusted, representing the confidence on the measured variables or in the instrument.

APLICATION FEATURES

The developed software application captures process data and applies to them a mathematical treatment, based on the steady state model of the sugar plant, in order to adjust material and energy balances, returning corrected measured variables, non measured variables, and interesting data.

The main features of the developed application are:

- Periodic characterization of the plant status, using a steady model of the sugar plant.
- On line connection with the plan Distributed Control System (DCS) to obtain regularly, the measured variables necessary for the balances and plant model identification.
- Data reconciliation, correcting measured variables in a way that the model is adjusted and calculating at the same time that unknown variables and model parameters. As a by-product of the data reconciliation behaviour indexes are estimated from calculated values in the reconciliation.

Mathematical models

To adapt the application to different plants, a library containing the main components existing in a sugar plant has been developed; heat exchangers, evaporators, steam bolilers, turbines, etc. The models are based on stationary material and energy balances. An Object Oriented Modelling and Simulation tool, named EcosimPro, have been used to implement them (EcosimPro, 2007))

Connecting basic models components, the whole model is built, then the simulation tool determines its computational causality, the boundary conditions of the model, selected by the modeller, are the non redundant process variables. Finally EcosimPro acts as a C++ simulation code generator compiler.

SCADA

On the other hand, it is necessary to have a system to acquire data form the plant, send them to the model and optimizer, visualize the results and handle the main features of the application. For that purpose a configurable SCADA has been developed, EDUSCA with their configuration tool SetupEdusca.

- EDUSCA: Is SCADA (Supervisor Control And Data Acquisition) system software. EDUSCA has been developed using Visual C++ (Alves et al, 2006) It is configurable and allows OPC data access.
- SetupEDUSCA: Configuration tools for EDUSCA that allows making different configurations for different process plants in an easy way.

Other tools

- DLLAdapter: Allows the use of the simulation created by EcosimPro in others computers.
- DLLOptimizer: Is a DLL (Dynamic Link Library) containing the optimization created by EcosimPro.
- COMOptimizer: Is a DCOM component that is able to access to the DLL that content the optimization. This component is used by the supervisory software. It has an interface that allows reads and writes data to the model variables.

ARCHITECTURE

Two architectures can be distinguished: Development mode and execution mode.

Development mode:

- This architecture allows creating different configurations for the optimization tool developed, using the described tools (model optimization and supervisory system). (Figure 4):

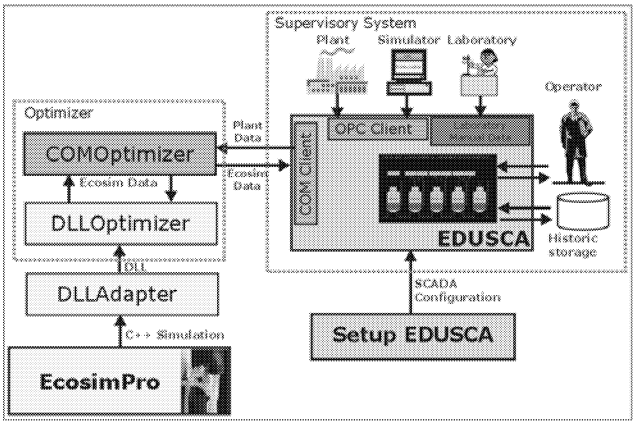

Figure 3: Development mode.

- Execution mode: In execution mode EDUSCA take data from the plant via OPC and send it to the optimizer via COM interface. Then, it sends the order to the optimizer to make the optimization and waits, then takes the calculated data from the optimizer and store it.

RESULTS

The explained methodology has been applied to the Toro sugar plant, owned by Azucarera Ebro S.L. Up to now developed tool allows four different possibilities:

- Detection of inconsistent measures (Figure 6).
- Evaluation of energetic behaviour indexes, efficiency, comparison between process heat transfer coefficients versus theoretical coefficients. (Figure 7).
- Determination of unmeasured variables, some of them relevant for the energy evaluation such as steam consumptions.
- Evolution of variables during the sugar beet campaign, helping managers to locate malfunctions in the process or equipment fouling.

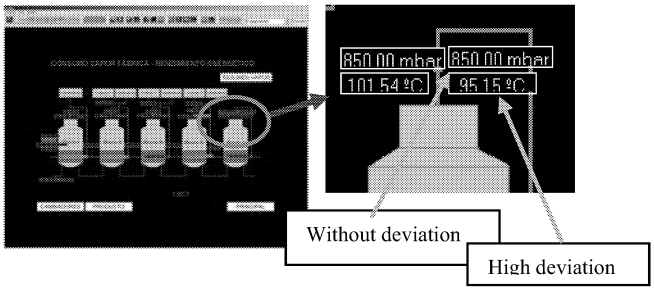

Figure 4. Inconsistency in measured variables.

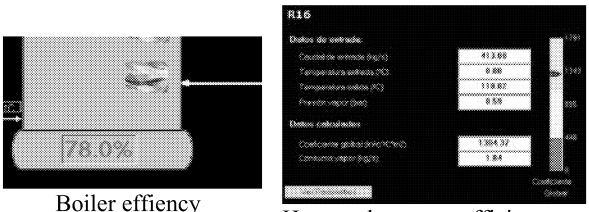

Boiler effiency

Heat exchanger coefficients

Figure 5. Behaviour indexes.

CONCLUSIONS AND FUTURE WORK

A tool for diagnosis of energetic state of sugar plant has been developed. This tool uses a steady state model of the plant, and an optimization algorithm to determine unmeasured variables, detect deviations in measured variables and provide information about the efficiency of the energy use in the plant, being very useful to have a shot of the energy state of the plant. Although obtained results are aparently consistent, they must be treated carefully because the number of measured variables in the analized plants is very low, and consecuently the redundance is poor. The study on plant redundancy is useful to make recommendations about the additional instrumentation needed to obtain more confident results.

In a second stage, this project will face the decision support module, based on the information provided by the diagnosis tool that will help the plant managers to decide the best actions in order to drive the process to the minimum energy consumption.

REFERENCES

Alves R., Normey-Rico J.E., Merino A., Acebes L.F. and de Prada C.. EDUSCA (EDUCATIONAL SCADA): Features and Applications..7th IFAC Symposium in Advances in Control Education. ACE 2006. 21-23 June 2006, Madrid, Spain.

Bagajewicz M. J. “Process Plant Instrumentation: Design and upgrade” Thechnomic Publications. 2001.

EcosimPro by EA Internacional, Dynamic Modeling & Simulation Tool, [Online], http://www.ecosimpro.com, accedido en Abril de 2007.

Gordon A.. Programación COM y COM+. Anaya Multimedia. ISBN 84-415-1146-2, 2000.

Iwainitz Frant and Lance Jurguen. 2002. “OPC-Fundamentals, Implementation and Application”, ISBN 3-7785-2883-1, 2002.

Mc Ginnis R. A. “Beet sugar technology”. 3d Edition. Beet Sugar Development Foundation. Colorado, USA, 1982.

Merino A., Santos R., Acebes L. F.. “A training simulator for the evaporation section of a beet sugar production process” The 2005 European Simulation and Modelling Conference. 24-26 October. Porto, Purtugal.

van der Poel P. W., Schiweck H., Schwartz T. “Sugar Techonology: Beet and Cane Sugar Manufacture” Ed. Bartens. Berlín 1998. ISBN: 3-87040-065-X

Computer-Aided Energy Efficiency Evaluation of Microwave Thawing

L. Boillereaux[1], C. Josset[2], B. Auvity[2], E. Akkari[1], C. Castelain[2]

[1] GEPEA, UMR CNRS 6144, ENITIAA, rue de la Géraudière, BP 82225, 44322 Nantes
[2]LTN, UMR CNRS 6607, Polytech'Nantes, rue Christian Pauc, 44306 Nantes

NOMENCLATURE

T	temperature (°C)
z	coordinate
m	mass (kg)
L	thickness of sample (m)
n	dimension of the state space
t	time (s)
ρ	density (kg.m^{-3})
C	apparent specific heat (J.kg^{-1}.K^{-1})
h	convective coefficient (W.m^{-2}.K^{-1})
U	internal energy of the product (J)
κ	thermal conductivity (W.m^{-1}.K^{-1})
Φ	electromagnetic flux density (W.m^{-2})
S	exchange surface (m^2)
$\eta_{Process}$	process efficiency
$\eta_{Microwave}$	microwave efficiency
t_d	time of defrosting

Subscripts

inc	incident
a	air
w	water
0	initial
in	inlet
out	outlet
v	at constant volume
p	at constant pressure

INTRODUCTION

With a turnover close to 140 billion euros in 2005, Agri-food is the first industrial sector in France, and is in the second place behind USA. The energy consumption of French food industry is about 5 millions of ton oil equivalent, which represents 13% of the energy consumption of the whole French industry. The main part of this consumption comes from the numerous thermal operations, whatsoever for the purpose of transformation or conservation. However, because energy represents today less than 10% of the total cost of a manufactured food, this component is rarely taking into account in the criteria of choice of a thermal process. It is obvious that, in a relatively close future, the energy will occupy a more and more important place in food industry.

For thermal food processes, many different energy sources can be used: natural or forced convection, infrared, microwave, pulsed electric fields, ohmic heating, high frequency, induction, steam (…). Depending on the products and on the process, these energy sources are more or less appropriate. Combining these energy sources within a same process can be an interesting way to improve the final products, by benefiting of the advantages of an a priori non appropriate source while avoiding its non-expected effects. In [1], the author shows the interest of combining a tangential and cold air blast with microwaves, allowing to reduce considerably the thawing time but with avoiding the well-known thermal runaway effect. Nevertheless, in this study, only the relevance of the approach is underlined, but the control objectives are not defined in terms of energy efficiency.

In this paper, we propose to use computer simulation to verify the effect of different choices of control parameters on the energy efficiency of the thawing process. This study is thus organised as follows:

- the first section is devoted to a brief description of the process,
- the second section deals with the design of the process simulator, with the implemented control law and its experimental validation,
- in the third section are presented the tools for the energy evaluation of the process, and their application in different strategies of control.
- Finally, a conclusion is proposed.

DESCRIPTION OF THE PROCESS

Microwaves constitute an interesting solution to defrost food, due to their flexibility and rapidity, compared to convective approaches. Nevertheless, they are few developed in the food industry due to a major phenomenon particularly embarrassing for food defrosting, called *thermal runaway*. Figure 1, from [2], illustrates the thermal runaway, obtained with a block of methylcellulose (Methocel® A 4MFG, DOWChemicals) filling a microwave guide (section 86 mm x 43 mm). The microwave energy is supplied by a MES® generator with variable power at 1 kW, 2.45 GHz, TE_{01} mode. The sample is 50 mm thick and two optical fibres (LUXTRON Fluroptic Thermometer, model 790, accurate to ±0.5°C) are inserted close to the top and bottom surfaces.

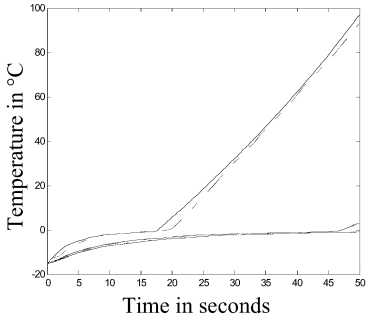

Figure 1. Illustration of thermal runaway – continuous line: experiment – dotted line: model

It can be verified the instability of the process (the variation of top surface temperature increases considerably while bottom surface is always frozen). In [1], Akkari proposes to combine a tangential air blast to the microwave generator to limit this effect. The process is illustrated schematically on figure 2. In order to consider a one-directional heat transfer with a cold air jet circulating at the upper surface, the sample (10 x 43 x 40 mm) is inserted in a polystyrene support (figure 1), located in the center of the guide, where the electric field can be considered as constant. The cold air stream circulates tangentially at a fixed speed (30 $m.s^{-1}$) in a rectangular channel ($S_{channel}$: 42 x 5 mm^2).

To ensure that only a minimal amount of microwave is reflected back to the sample, a water flow is circulated at the end of the microwave guide. The incident power and the power reflected at the upper surface of the food sample are measured. The power transmitted to the water is measured too.

DESIGN OF THE SIMULATOR

Heat transfer

Modeling of heat transfer with phase changes is widely reported in literature, and an exhaustive survey can be consulted in [3]. In the sequels, the following assumptions are considered:

- The incident power microwave is considered homogeneous at the upper surface product,
- The heat transfer by conduction is one directional along the vertical axis.
- The exchange at the top surface ($z = 0$) is essentially convective, whereas the bottom surface ($z = L$) is perfectly insulated.

The heat transfer is governed by the following equation:

$$\rho C_p(T)\frac{\partial T}{\partial t} = \frac{\partial}{\partial z}\left(\kappa(T)\cdot\frac{\partial T}{\partial z}\right) - \frac{\partial \Phi}{\partial z} \qquad (1)$$

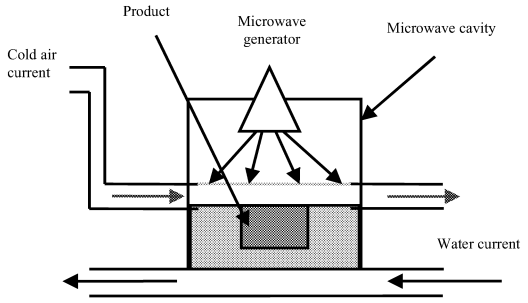

Figure 2. Schematic description of the process

The local variation of the electromagnetic flux density can be written as follows (see [1,2] for more details):

$$\frac{\partial \Phi}{\partial z} = -\gamma(T)\cdot\frac{\Phi(z)}{dz} \qquad (2)$$

The previous heat equation can be reduced into a finite dimensional problem using 1D finite volume scheme. With n the number of volumes and $\delta z = L/n$ the thickness of these volumes, it comes:

$$f_1\cdot\frac{dT_1}{dt} = h\cdot(T_{a\_in} - T_1) + \kappa_1\frac{T_2 - T_1}{\delta z} + \gamma_1\cdot\Phi_{inc} \qquad (3)$$

$$f(T_n)\cdot\frac{dT_n}{dt} = \kappa_n\frac{(T_n - T_{n-1})}{\delta z} + \prod_{j=1}^{n-1}(1-\gamma_j)\cdot\gamma_n\cdot\Phi_{inc} \qquad (4)$$

and for $1 < i < n$:

$$f_i\cdot\frac{dT_i}{dt} = \kappa_i\cdot\frac{(T_{i+1} - 2T_i + T_{i-1})}{\delta z} + \prod_{j=1}^{i-1}(1-\gamma_j)\cdot\gamma_1\cdot\Phi_{inc}$$
$$f_j = \rho(T_j)\cdot C_p(T_j)\cdot\delta z,\quad \kappa_j = \kappa(T_j),\quad \gamma_j = \gamma(T_j). \qquad (5)$$

Control law

One relevant way to control the thermal runaway while ensuring a short thawing time consists in tracking reference trajectories for the coldest point, T_n, and for the most microbiologically sensitive point, T_1. T_1 and T_n constitute thus respectively the outputs to control, denoted respectively in the sequels y_1 *and* y_2.

Given that the system under consideration is multivariable, a Global Linearizing Control [4] approach can be applied provided that the number of manipulated variables, i.e., inputs of the system, is equal to the number of outputs to control. In this study, this hypothesis is verified because we propose to consider as manipulated variables the

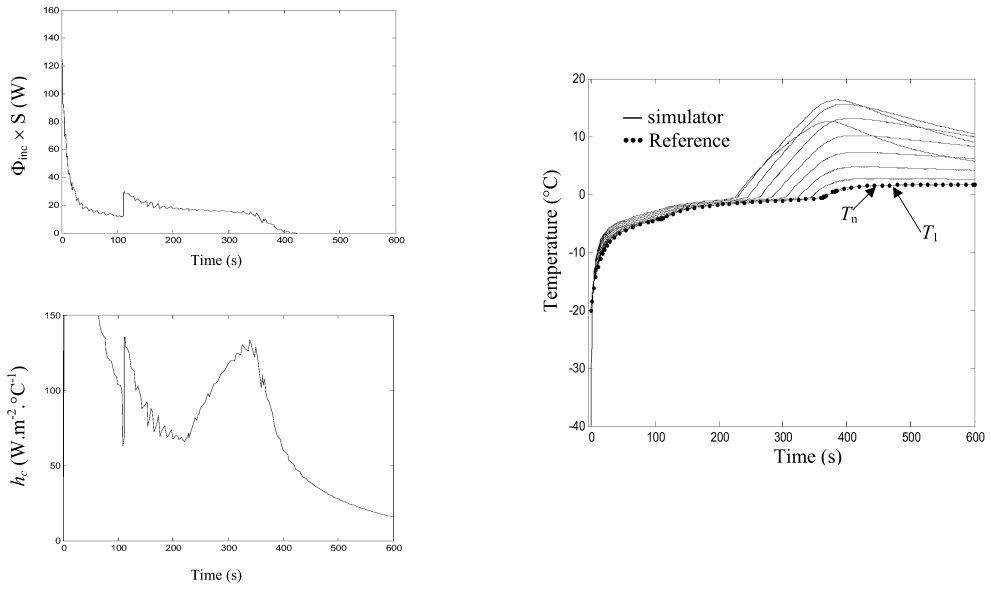

Figure 3. Experimental validation of GLC approach (from [1])

microwave power and the convective heat transfer coefficient, denoted respectively u_1 and u_2.

Linearizing control consists in an input/output linearization of the system [5]. Such a linearization can be obtained by differentiating the outputs until one input appears explicitly in the result. The number of differentiation required for an input is called the relative degree of this input. Using the reduced model presented above, the relative degrees are equal to 1 and the input/output expressions are straightforwardly deduced from equations (3) and (4), by replacing T_1, T_2, h and Φ_{inc} respectively by y_1, y_2, u_1 and u_2.

The next step consists in establishing the expression of the manipulated variables in closed loop, taking into account the reference trajectories to track, denoted respectively y_{1sp} and y_{2sp}:

$$u_2 = \frac{f_n\left(\dot{y}_{2sp} + k_2\Re_2\right) - \kappa_n\left(\frac{T_{n-1} - T_n}{\delta z}\right)}{\prod_{j=1}^{n-1}\left(1-\gamma_j\right)\gamma_n} \qquad (6)$$

$$u_1 = \frac{f_1\left(\dot{y}_{1sp} + k_1\Re_2\right) - \kappa_1\left(\frac{T_2 - T_1}{\delta z}\right) - \gamma_1 u_2(t)}{T_{a\_in} - T_1} \qquad (7)$$

$\Re_1 = y_{1sp} - y_1$ and $\Re_2 = y_{2sp} - y_2$ represents the tracking errors.

More details concerning these analytical results and experimental validations can be consulted in [1].

In figure 3 is proposed an illustration of the simulator combining heat transfer model and GLC. The test is carried out with an air temperature of -20°C, by considering the thermal and dielectric properties of a block of tylose in the geometrical conditions described in section *description of the process*. The initial temperature is -40°C. The figure on the right represents the simulated temperatures and the reference trajectories, whereas figures on the left represent the microwave power and convective coefficient computed by the GLC algorithm. It can be noticed that the reference trajectories y_{1sp} and y_{2sp} are identical in this simulation.

ENERGY EVALUATION

In the following, the energy efficiency will be investigated for an inlet air temperature varying from -30°C to -5°C, and some expected thawing times from 100 to 600s.

Energy balance

Let us consider the whole system as described in figure 2, with the following assumptions:

- The energy loss between the microwave cavity and the external medium is negligible,
- The input temperature of the air and water current is constant during the process.

The energy balance applied to the considered multi-energy thawing process is given by the equation:

$$S \cdot \Phi_{inc}(t) = \frac{dU(t)}{dt} + \dot{m}_a(t) C_{pa}\left(T_{a\_out}(t) - T_{a\_in}\right) + \dot{m}_w(t) C_{pw}\left(T_{w\_out}(t) - T_{w\_in}\right) \quad (8)$$

$$dU = \rho_{product} \cdot S \cdot \int_0^L C_v(T) dT \cdot dz \quad (9)$$

$$\dot{m}_{air} = \rho_a \cdot S_{channel} \cdot v_a \quad (10)$$

The convective coefficient is related to the air velocity via the classical Colburn Nusselt expression.

The integration of equation (8) as a function of time yields to:

$$S \cdot \int_0^t \Phi_{inc}(t) \cdot dt = \Delta U + \int_0^t \dot{m}_a(t) \cdot C_{p\_a}\left(T_{a\_out}(t) - T_{a\_in}\right) \cdot dt + \int_0^t \dot{m}_w(t) \cdot C_{p-\_}(T_{w\_out}(t) - T_{w\_in}) \cdot dt \quad (11)$$

Microwave efficiency

We propose to define the microwave energy efficiency as the ratio between the energy variation within the product and the energy supplied by the microwave generator:

$$\eta_{Microwave} = 100 \cdot \frac{\Delta U}{S \cdot \int_0^t \Phi_{inc}(t) \cdot dt} \quad (12)$$

This parameter has been evaluated for the temperature and thawing time ranges proposed above. This parameter is observed to be almost constant and equal to about 37% (±0.1%), which is consistent to values reported in the literature.

Process efficiency

As the previous ratio does not permit to exhibit an optimum set of parameters, another parameter must be introduced.

Let's consider that the product is totally defrosted when the minimal temperature within the product has reached 0°C. The minimal energy that has to be supplied to the product is:

$$\Delta U_{\min} = \rho_{product} \cdot S \int_0^L \int_{T_0}^{0°C} C_v(T) dT dz \quad (13)$$

Then the process efficiency can be defined as:

$$\eta_{Process} = \frac{100 \cdot \Delta U_{\min}}{S \cdot \int_0^t \Phi_{inc}(t) dt} \quad (14)$$

Table 1 presents the different process efficiencies. No clear dependence on the inlet air temperature can be exhibited. Though, the shorter the thawing time is, the smaller the process efficiency is. Nevertheless, the over-consumption of microwave energy induced by the reduction of the thawing time is not significant regarding to the increase in productivity.

Table 1. process efficiency versus thawing time and inlet air temperature

t_d (s) \ T_a (°C)	-5	-10	-20	-30
100	27.8	27.7	27.8	27.6
200	27.8	27.9	28.0	27.8
300	28.1	28.1	28.2	28.2
400	28.3	28.3	28.2	28.3
500	28.4	28.2	28.5	28.5
600	28.6	28.6	28.6	28.7

However, the maximal incident power required increases drastically for the shortest thawing times, as illustrated on figure 4. This implies a more powerful installation, and then a higher investment cost.

If we focus on the temporal evolution of the convective heat transfer coefficient for the extreme condition (100s, -5°C), we can notice that non realistic values are reached (h >5000 $W.m^{-2}.K^{-1}$), whereas these values are correct for less constraining thawing times, see figure 5.

In the following section, we propose to limit the maximal value of the convective coefficient in the GLC algorithm to 250 $W.m^{-2}.K^{-1}$.

Corrected process efficiency

The previous conclusions lead us to consider the pressure loss across the cooling air channel, in order to take into account the required mechanical energy to obtain the expected convective heat transfer coefficient.

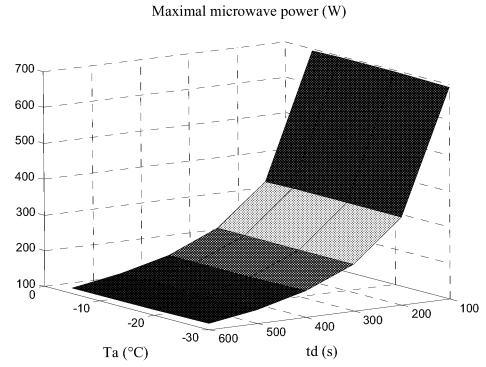

Figure 4. Maximal microwave power vs T_a and t_d

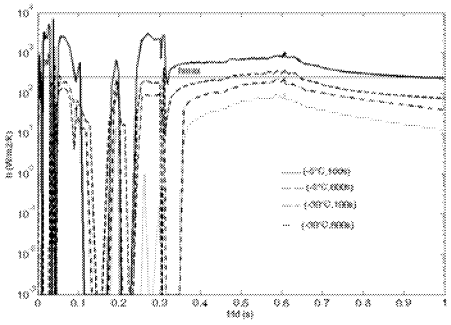

Figure 5. Evolution of the convective coefficient for different couples of parameters

The mechanical energy can be written as follows:

$$\int_{t_0}^{t_{end}} \dot{m}_a \xi \frac{v_a^2(t)}{2} dt$$

where ξ represents the pressure drop coefficient of the air channel. This value has been fixed to a moderate level of 0.5.

Then a corrected process efficiency can be proposed:

$$\eta_{corrected} = \frac{100 \cdot \Delta U_{\min}}{S \cdot \int_0^t \Phi_{inc}(t) dt + \int_{t_0}^{t_{end}} \dot{m}_a \xi \frac{v_a^2(t)}{2} dt}$$

Table 2 presents this corrected efficiency under the same conditions as table 1.
For the couple (-5°C, 100s), the result is indicated in italics because the convective coefficient was saturated at its maximal value, 250 $W.m^{-2}.K^{-1}$. Although this extreme value, the reference trajectories were not correctly tracked. It means that a non realistic convective coefficient would be necessary to respect the imposed thawing time.
Except this point, it can be observed that the lower the air temperature and the longer the thawing time are, the higher is the efficiency of the process.

CONCLUSION

In this paper is presented a simulator allowing first to estimate the temperature evolution of the product during a multi-variable controlled microwave thawing process, and second to evaluate the energy efficiency of the couple Process/Controller. For this, some tools have been proposed to evaluate energy efficiency.
It has been shown that the energy efficiency limited to the microwave is insufficient to exhibit optimal control parameters. The process efficiency, based on the ratio between the minimal energy required to achieve the defrosting and the total energy supplied by the microwave generator, seems to be a more relevant tool.

Table 2. Corrected process efficiency versus thawing time and inlet air temperature

t_d (s) \ T_a (°C)	-5	-10	-20	-30
100	*25.4*	25.5	26.3	26.6
200	23.9	25.5	27.0	27.4
300	24.7	26.3	27.7	27.4
400	25.3	27.2	28.0	28.2
500	26.3	27.2	28.4	28.4
600	26.9	28.1	28.5	28.7

Even if the variations of the efficiency remain small, a general tendency can be observed. Besides, the maximal power of the microwave generator required by the process can be evaluated.
Finally, it appears that the corrected efficiency, taking into account the pressure drop of the air current, is a pertinent indicator, allowing to highlight that the lower the air temperature is, the more efficient the process is. In the same way, it appears that a long thawing time is preferable to a short one.
However, more investigations are necessary to exhibit optimal functioning parameters for this controlled process, as including in the criteria of choice:

- the maximal temperature admissible within the product, because this parameter is highly important to verify that the product is undamaged.
- some economic parameters, as for instance the rate of thawing time,
- the energy cost necessary to lower and to maintain the air at low temperatures

It is important to mention here that this process could be studied with higher air temperatures, as for instance positive ones. In this case, the convective exchange would contribute with the microwaves to the defrosting of the product, but non realistic convective coefficients are needed to prevent from the thermal runaway. A relevant solution would be to replace u_1 in the control law by the term $u_1\left(T_{a\_in} - T_1\right)$, which can be adjusted either with a variable air velocity or a variable air temperature.

More generally speaking, the energy evaluation tools proposed above are to be introduced in a state feedback control.

The present approach is based on energy balance using the first principle of thermodynamics. Further information can be extracted using an exergy evaluation (combination of the first and second law of thermodynamics).

The methodology described here can be extended to a wide range of different multi-energy processes.

REFERENCES

[1] Akkari, E., Chevallier, S. and Boillereaux, L.. Global Linearizing Control of MIMO microwave-assisted thawing, *Control E- ngineering and Practice*, in revision.

[2] Akkari, E., Chevallier, S. and Boillereaux, L.. A 2D non-linear "grey-box" model dedicated to microwave thawing: Theoretical and experimental investigation, *Computers & Chemical Engineering,* Vol 30(2), pp 321-328, 2005

[3] Pham, Q.T.. modelling heat and mass transfer in frozen foods: a review. *International Journal of refrigeration*, Vol. 29(6), pp 876-888, 2006

[4] Madar, J., Abonyi, J. and Szeifert, F.. Feedback linearizing control using hybrid neural networks identified by sensitivity approach. *Engineering Applications of Artificial Intelligence*. Vol. 18, pp. 343-35, 2005

[5] Nijmeier, H., Van der Schaft, A. J.: *Nonlinear dynamical control system*. Springer-Verlag, Berlin, Germany, 1990

SIMULATION OF FOOD PRODUCTION SYSTEMS AND THE SUPPLY CHAIN

DISCRETE EVENT SIMULATION WITH LIFECYCLE ASSESSMENT DATA AT A JUICE MANUFACTURING SYSTEM

Björn Johansson
Johan Stahre
Product and Production Development
Chalmers University of Technology
SE-41296 Gothenburg
Sweden

Johanna Berlin
Karin Östergren
Barbro Sundström
Swedish Institute for
Food and Biotechnology
SE-40129 Gothenburg
Sweden

Ann-Marie Tillman
Energy and Environment
Chalmers University of Technology
SE-41296 Gothenburg
Sweden

E-mail: Bjorn.Johansson@chalmers.se

KEYWORDS
Discrete Event Simulation, Lifecycle Assessment, Sustainable Manufacturing, Food Production.

ABSTRACT

In order to measure and evaluate productivity and environmental parameters simultaneously and in consideration to each other, they need to be presented on the same basis and put up on the same table, at the same time. Otherwise, while considering only parts of the relevant parameters at a time, there is a great risk for sub-optimisation. The study presented in this paper shows one way of putting productivity parameters such as batch size, batch frequency, production planning, and resource management on the same table as environmental parameters such as emissions, waste and energy consumption. This is done through the use of lifecycle assessment in combination with discrete event simulation. The result gives an example of a sound basis for decision-making when changes are to be made in the juice production system at hand. The presented case study gives information on energy consumption, waste and pollutants such as CO_2, NO_X, SO_2, and ethene generated from production of juice. Results show that some changes of the system improves both environment and productivity, others improves one and worsens the other!

INTRODUCTION

Food production processes gives environmental footprints on our planet. Food production industries are one of the largest industries in the world, these two factors makes the environmental impact reduction from food production a major player when it comes to e.g. global warming, eutrophication, and acidification. Tools and measurements for assessing environmental effects are being developed. E.g. by Lind et al. (2008) as well as LLamasoft, who released their "Green Supply Chain Modeling Solution" for carbon footprint simulation in January 2008. Focus on climate changes and other related environmental phenomenon are growing as we become more aware on how utilization of resources from the earth affects the environment.

Discrete event simulation has been available for some decades (Banks et al. 1996). Most analysis made with this technology has been done with monetary units in mind, such as reducing cost, increasing profit, short payback times. Not many studies have been made with environmental effects as one of the measurements. One example of such a study is Solding and Thollander (2006), they did use discrete event simulation and included energy as a parameters as input data and could then also analyse to improve system performance with regards to the energy consumption. We are taking additional steps in this direction and include four additional parameters, which of each parameter enters our system with the use of raw material, machines, facilities or transportation. The input data consist of lifecycle assesment data in combination with production data. The various scenarios simulated with changes on the manufacturing floor were analyzed and evaluated on productivity bases as well as on the consumption, waste and pollutants simultaneously. The results presented in this paper is one out of three case studies conducted to find a common methodology for reaching sustainable food production.

DISCRETE EVENT SIMULATION

One of the largest application areas for simulation is that of manufacturing systems, according to Law and McComas (1999). The first uses of this kind of simulation can be traced back to early 1960's. Since then the development of the field has been ongoing and still is. However, the integration of multidisciplinary parameters and their analyses is not common. Simulation is a powerful problem solving tool for industries today. Detailed information on simulation in general can be found in Banks et al. (1996), and Law and Kelton (1999). The technology has been evolving and still is in a swift phase, academic publications and new software features are released in thousands respectively hundreds each year. Discrete event simulation (DES) software and languages has been used for numerous different purposes, such as patient flows in healthcare, military strategies, logistics, call centers, restaurants etc. The most frequent use of DES is probably for economical purposes, analyzing which of the alternative solutions are the most profitable over time. When it comes to that type of analysis, manufacturing systems are among the most common applications to utilize DES as a tool for decision support.

There are many other things which one could measure with DES, in the long run monetary units are of course a parameter which will not be out of the question, however environmental considerations are getting more and more relevant and requires more and more attention as long as humans utilizes the resources from nature. Discrete event simulation in combination with Lifecycle Assessment is one possible road to take for analyzing cause and effect of various scenarios where time, resources, place, and randomness affect the outcome.

LIFECYCLE ASSESSMENT

As stated before, discrete event simulation is a useful tool to evaluate a manufacturing system from a process perspective but to include the environmental impact caused by the production in the same model is rare. The environmental impact from production activities is more commonly assessed in another study made beside or after the evaluation of production parameters. To be able to consider the environment it is important that the environmental parameters are assessed at the same time in the same model as the process parameters, using the same basis for input-data. Then the environmental considerations can be made at the same time as the cost related evaluations. However, so far no unified method for this approach has been found. Lifecycle assessment (LCA) is a tool for evaluating the environmental impact associated with a product during its life cycle. By identifying and quantitatively describing it's requirements for energy and materials, and the emissions and waste released to the environment the calculation can be accomplished. The product under study is followed from the initial extraction and processing of raw materials through manufacturing, distribution, and use, to final disposal, including the transports involved, i.e. its whole lifecycle. Lifecycle assessment is an ISO standardised tool (ISO, 1997, 1998, 2000).

COMBINING DES WITH LCA

Most papers found focused on industrial modeling with the LCA perspective describes static models in comparison to DES. Examples of papers from different industrial areas are; pharmaceutical intermediates (Jödicke et al., 1999), nitric acid plant (Alexander et al., 2000), boron production (Azapagic and Clift, 1999), phenolic-resin manufacturing (Kheawhom and Hirao, 2004), electronics assembly (Stuart et al., 1997) and cement production (Gäbel and Tillman, 2005). By introducing LCA data for each event in a DES model we are be able to follow the environmental impact of the simulated system. Very much the same way as monetary units can be followed the in this kind of system. Each event step in the model have environmental impact parameters. When the event is triggered, the LCA values will be put in play and update model output parameters. In this particular case we did look at a juice production system. Our purpose is to use LCA data as input parameters for all incoming materials and energy arriving into the production system. The calculations will then be done in order to determine how much of the LCA data will be used and put into the products, wasted and consumed. Our intention is to have the LCA on a detailed level where cause and effect can be measured over time with dynamics from DES influencing each products way through the lifecycle. This enables prediction of the outcome from changes in reality more accurately, and also on a more detailed level if needed. Each product going through the system will have a unique value for equivalents of; CO_2, NO_X, SO_2, energy and ethane, in addition to the normal ones used within DES, such as leadtime, utilization, queue lengths etc.

THE JUICE PRODUCTION SYSTEM

The production manager at the juice production company had a gut feeling: "Decreasing batch size would increase profit". The company does also have a very environmental-friendly spirit. They would like to take heed of the environment and at the same time increase the profitability of their business through utilizing machines and production equipment more wise in the future. Hence this combination serves as a perfect test for introducing LCA together with DES in order to test the feasibility of the combination, and at the same time provide detailed decision support both in terms of productivity and environmental effects for the company.

System description

The aseptic package line for fruit juices, soups and compotes in this case study produces about 25 000 000 liters of product per year. The system roghly consists of, see figure 1, three purèe machines, two mix-tanks, three heat exchangers, six buffer-tanks, five packaging machines, three palletizers, as well as many pipes, conveyors and pumps. As shown in figure 1, a in-process inventory is also present. The in-process inventory is a freezer which is located 20 kilometers from the production facility.
Raw fruit is mushed to purèe, then mixed with other ingredients. The mix is pasteurized and put into buffer tanks in order to get hold of a packaging machine.. The juice is then packaged in different sizes and shapes and palletized on pallets. The palletized juice packages are then delivered directly to customer, or placed on stock for future customer deliveries. The purèe or juice which left over in the pipes after packaing will be disregarded if it is a low value product, or sent to the in-production inventory as frozen ingredients awaiting the next scheduled production with that particular ingredient needed, if it is a high value product.

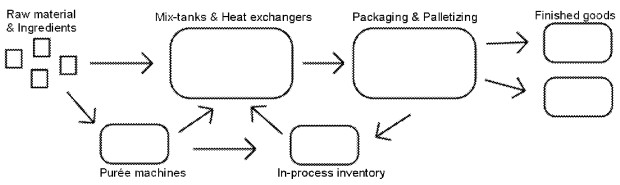

Figure 1: Overall Description of the Production System

Combined DES-LCA model of the system

The simulation model of the juice production system includes normal data such as flowspeed in pipes, setting times of machines, shift schedule, tank volumes, machine speeds, speeds on conveyors, palletizing times etc. This is

normally how DES works. The model is enriched with LCA data in each step as well. Examples of this is data for the incoming ingredients such as:

- Oil
- Paper
- Water
- Apples
- Oranges
- Electricity
- Aluminium
- Polyprophene

The ingredients are then mixed, or added to the product when the event is triggered in the DES model. Accumulation of the total value concerning the product after each event could be extracted from the model if needed. Each event is also measured from the resource perspective. A machine which wastes a part of a product will achieve environmental pollutant in equal quantity to its account. If a test was to be made where two different machines with the same functionality was evaluated. They could be compared against eachother on environmental effets basis. Each of ingredients are implemented with five aspects of environmental impacts:

- SO_2 (g SO_2 equivalents)
- CO_2 (g CO_2 equivalents)
- NOX (g NO_X equivalents)
- Ethene (g ethene equivalents)
- Energy (MJ equivalents)

Figure 2 shows a snapshot from the model made in Automod (Rohrer 2003). The cylinder chaped objects represents tanks, pipes are not shown since they are too many and would only create a more blurry picture of the production system. The large square objects are filling and packaging machines, lines inbetween them are conveyors for filled packages. The larger conveyor in the lower part of the picture represents the exit point of the system where euro-pallets containing juice packages are exiting the system as deliveries are made.

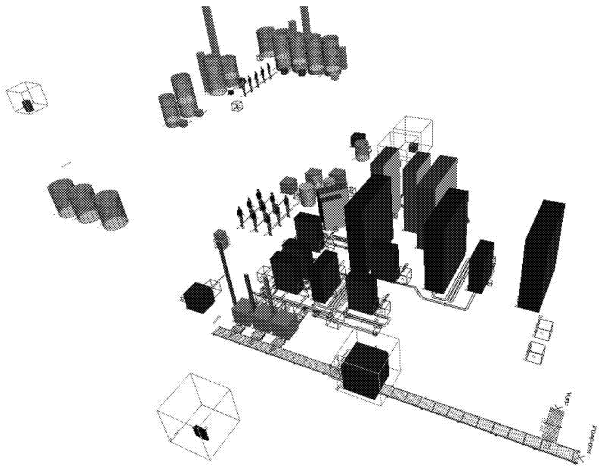

Figure 2: A Snapshot of the Simulation Model

RESULTS AND DISCUSSION

Many analyses were made, and some are actually still not finished while this paper is written. We will briefly describe a few of the most interesting analyses. Initially, a reference scenario was made with the model in order to validate that the model is a well enough representation of the real-world system. For more info on validation see: Sargent (2000). This reference model was then run on a 24/7 basis and used as a comparison to alternative solutions on how to operate the juice production. Tests were made with for example, more tanks, less resetting, smaller batches, larger batches, additional resources, less breakdowns etc… Some of the areas where the results were interesting are presented below, additional test can be found in Persson and Karlsson (2007).

The first test was to validate the model. The reference model with settings according to planned production year 2006 was executed. Comparisons from the model were made with the real-world system. The results arepresented in table 1.

Table 1: Model Validation

	Model data	Real-world data
Raw material (kg)	22 294 365	25 609 711
Finished goods (kg)	21 994 743	25 189 976
Waste (%)	1,34	1,64

The difference is acceptable, due to the fact that the model does not include all products (Wine is excluded from this analysis). The waste % is lower in the model due to critical failures of machines is excluded in the analysis, and that part stands for approximately 0,3% of the waste in the real-world system. Discussions with production personnel at the company also resulted in a conclusion that the model is valid while including consideraions of the differences mentioned. The standard deviation between successive runs, while running the base model in continous mode (24/7),were less than 2%, which also made the requirement for multiple runs less important.

The first comparative analysis, which the company was most interested in was how batch sizes could be altered to achieve shorter throughput times. As stated before, the production manager did have a feeling that smaller batch sizes would decrease throughput times. The results from this analysis is shown in figure 3. From this figure we can find that a lower average batch size, around half the size of today will result in shorter throughput time. However, more experiments is nessesary to find a more precise average batchsize minimum in regards to the hours required for producing one year (2006) worth of products.

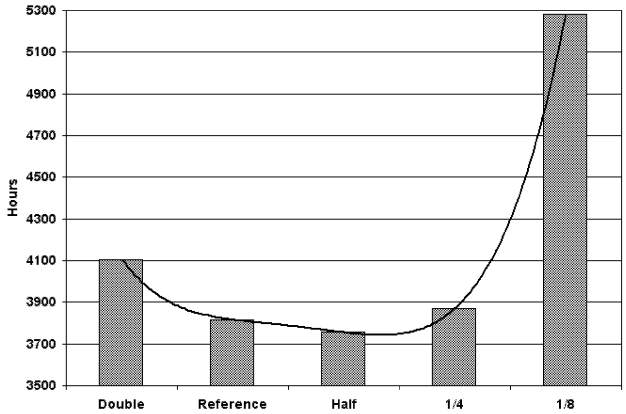

Figure 3: Average Ordersize vs. Hours of Continous Prod.

Figure 4 shows that there is a large change in how much % waste there will be if average ordersizes are too low. Above 20 000 kg there is no significant change. But below 20 000 kg the % waste increases dramatically with lower ordersizes. Each dot in Figure 4 represents one simulation run.

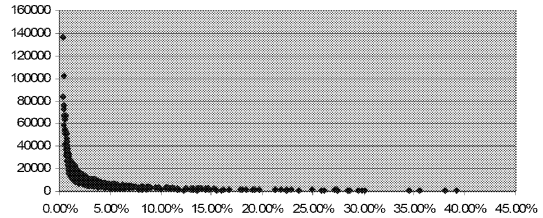

Figure 4: Average Ordersize (kg) vs. Product Waste (%)

Our next analysis was to find out which machine or part of the production is the most critical one, in line with theory of constratins, as described by Goldratt (1990). We added one or more parallel resources to the system where we thought it might be useful, with regards to the resource-utilization from the reference model. Before the runs we thought it to be a good idea to add another mixtank and a operator, however as seen in figure 5, that was not the case. Adding a heat exchanger or even adding a heat exchanger in combination with a new fillmachine was proven to be more valuable.

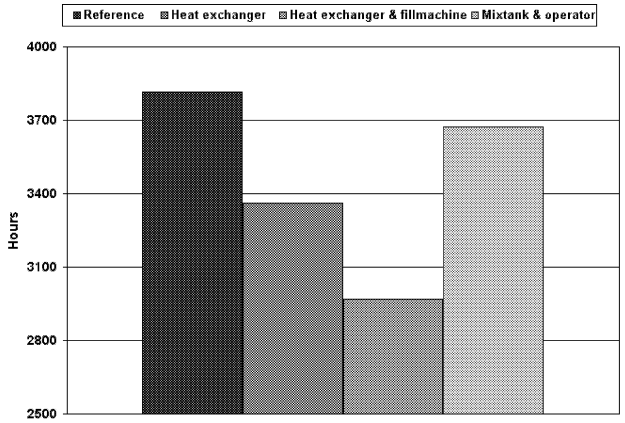

Figure 5: Production Hours Needed for Different Models

While looking at the analysis made so far, we did only make a normal DES study. However, to take a look at the most interesting research-news from this case study. We will now look into the combination of the normal DES analysis, and analysis of environmental effects with LCA.

By looking at the batch sizes and sequencing we did try to find a better solution for both shortening the lead times in production and decrease the environmental impact simultaneously. Figure 6 shows total throughput time for one years worth of product, and the CO_2 emmissions related to production for that specific batchsizes and sequencing. The referens case reflects how the production is batched and sequenced today. Case A reflects the results of double batch sizes with similar sequencing. Case B reflects the results of half batch sizes with similar sequencing. Case C reflects the theoretical minimum of CO_2 emmissins by only optimizing batch sizes and sequencing. Note that Case C will not be feasible for direct use, since it will give too large stocks of finished goods. However, Case C gives a target for low CO_2 emmissions as well as short throughput time.

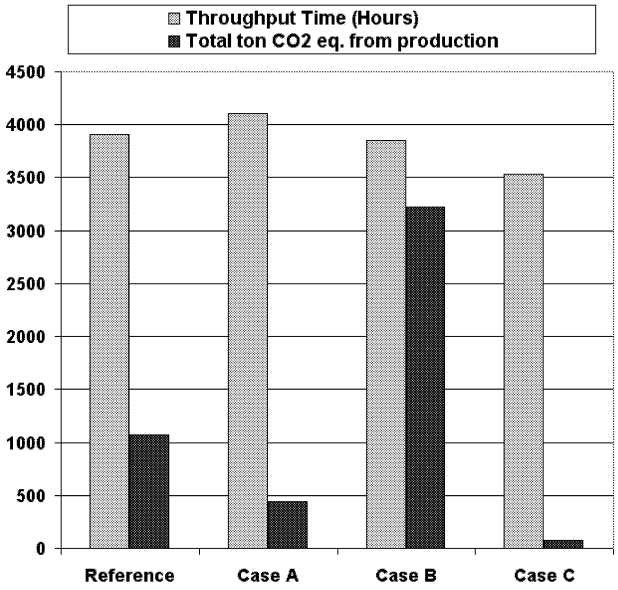

Figure 6: Throughput Time in Relation to CO_2 Emmissions

One of the later analyses made with the model was used to determine if the in-process inventory was unfriendly for the environment. The analysis made to determine the outcome was a comparison between either to:

1 Keep todays system as is, with in-process inventory (for more valuable products) located 20 kilometers from the production facility
2 Waste the additional purée after each time a batch was finished, and quit using the in-process inventory

The results from this analysis show that the environmental effect from wasting purée is much larger (a factor 1 to 400 considering CO_2 eq. emissions only) than the one from freezing and shipping the additional purée back and forth between the in-process inventory freezer to the production facility.

CONCLUSION

A new tool has been developed which can be used for optimizing complex process lines including both processand environmental “efficiency” in order to identify hot spots and suggest improvements in existing process lines. The new tool was found to be time effcient compared with an approach where separate analysis of environmental impact and process efficiency and the fact that all results are based on the very same set of inventory data describing the process conditions assures a true unified analysis.

ACKNOWLEDGEMENTS

The authors would like to express gratitude to industrial project partners within REELIV and to VINNOVA (Swedish Agency for Innovation Systems, integrates research and development in technology, transport and working life.).

FUTURE RESEARCH

A methodology combining discrete event simulation with lifecycle assessment, describing how to conduct a study similar to the one in this paper is under development. Addintional projects are planned to be executed with the whole lifecycle modeled. Including raw material extraction, supply-chain, processing, use, and recycling. Standardisation efforts on interoperability for simulation models such as CMSD (Core Manufaturing Simulation Data) (CMSD 2007) are investigated further in order to see if/how the environmental parameters could be included in the effort.

REFERENCES

Alexander, B.; G. Barton; J. Petrie and J. Romagnoli. 2000. "Process synthesis and optimization tools for environmental design: methodology and structure." *Computers and Chemical Engineering*, 24, 1195-1200.

Azapagic, A and R. Clift. 1999. "Life Cycle Assessment as a Tool for Improving Process Performance: A Case Study on Boron Products." *International Journal of Lifecycle Assessment*, Vol. 4(3), 133-142.

Banks, J.; J.S. Carson and B.L. Nelson. 1996. *Discrete-Event System Simulation*. 2d ed. Upper Saddle River, New Jersey: Prentice-Hall.

CMSD 2007. *Draft core manufacturing simulation data information model part 1:* UML model. CMSD Prod-uct Development Group, Simulation Interoperability Standards Organization. Available via <www.sisostds.org> [accessed March 19, 2008]

Goldratt, E. 1990. *Theory Of Constraints*, North River Press, Inc.

Gäbel, K. and A-M. Tillman. 2005. Simulating operational alternatives for future cement production, *Journal of Cleaner Production* 13(13-14), 1246-1257.

ISO. 1997. *Environmental Management – Life Cycle Assessment – Principles and Framework.* ISO 14040:1997. European Committee for Standardization CEN, Brussels, Belgium.

ISO. 1998. *Environmental Management – Life Cycle Assessment – Goal and Scope Definition and Inventory Analysis.* ISO 14041:1998. European Committee for Standardization CEN, Brussels, Belgium.

ISO. 2000. *Environmental Management – Life Cycle assessment – Life Cycle Interpretation.* ISO 14043:2000. European Committee for Standardization CEN, Brussels, Belgium.

Jödicke, G.; O. Zenklusen; A. Weidenhaupt and K. Hungerbühler. 1999. Developing environmentally sound processes in the chemical industry: a case study on pharmaceutical intermediates, *Journal of Cleaner Production*, 7, 159-166.

Kheawhom, S. and M. Hirao. 2004. Decision support tools for environmentally benign process design under uncertainty, *Computers and Chemical Engineering*, 28, 1715-1723.

Law, A.M. and W.D. Kelton. 1999. *Simulation Modeling and Analysis*. 3d ed. New York:McGraw-Hill.

Law, A.M. and M.G. McComas, 1999. "Simulation of Manufacturing Systems." *In Proceedings of the 1999 Winter Simulation Conference*, ed. P. A.Farrington, H. B. Nembhard, D. T. Sturrock, and G. W. Evans, Pheonix, AZ. pp. 56–59.

Lind, S.; B. Krassi; B. Johansson; J. Viitaniemi; J. Heilala; J. Stahre; S. Vatanen and Å. Fasth. 2008. "SIMTER: A Production Simulation Tool for Joint Assessment of Ergonomics, Level of Automation and Environmental Impacts", in proceedings of FAIM2008, Skövde, Sweden.

Persson, D. and J. Karlsson. 2007. *Flow Simulation of Food Industry Production.* Master's Thesis. Department of Product and Production Development, Chalmers University of Technology, Gothenburg.

Rohrer, M.W. 2003. "Maximizing simulation ROI with Auto-Mod". *in Proceedings of the 2003 Winter Simulation Conference,* Ed. Chick; S., Sanchez; P.J.Ferrin; D., Morrice, D.J., pp.201-209.

Sargent, R. G., 2000. "Verification, Validation, and accreditation of simulation model". in *Proceedings of the 2000 Winter Simulation Conference*, ed. J.A. Joines, R.R. Barton, K. Kang, P.A. Fishwick, Orlando, FL, December 10-13, pp. 50-59.

Solding, P. and P. Thollander. 2006. "Increased energy efficiency in a Swedish iron foundry through use of discrete event simulation". In *Proceedings of the 2006 Winter Simulation Conference*, ed. L. F. Perrone, F. P. Wieland, J. Liu, B. G. Lawson, D. M. Nicol, and R. M. Fujimoto, Monterey, CA, December 3-6 pp. 1971-1976.

AUTHOR BIOGRAPHY

BJÖRN JOHANSSON is an assistant professor at Product and Production Development, Chalmers University of Technology, currently also a guest researcher at National Institute of Standards and Technology in Gaithersburg, Maryland, USA. His research interest is in the area of discrete event simulation for manufacturing industries. Modular modeling methodologies, environmental effects modeling, software development, user interfaces, and input data architectures are examples of interests. His email address is Bjorn.Johansson@chalmers.se.

JOHAN STAHRE is an associate professor and the head of the Division of Production Systems at Chalmers University. His research focus is on human supervisory control in semi-automated manufacturing systems. His email address is Johan.Stahre@chalmers.se.

JOHANNA BERLIN holds a PhD in Environmental Systems Analysis from Chalmers University of Technology and works as a researcher at SIK. Her research interests are environmental system analysis, in particular within the filed of milk products, but also food production in general. Her email address is jbe@sik.se .

KARIN ÖSTERGREN holds a PhD in Food Engineering from Lund University and works as researcher and project leader at SIK. Her research interest is in food engineering and food production engineering. The last ten years she has been project leader of a succeive set of projects focusing on exploring the benefits of combining food process engineering and environmental system analysis for sustainable food production. Her email address is koe@sik.se .

BARBRO SUNDSTRÖM works as researcher and project leader at SIK. Her research interest is in food engineering and food production engineering. She has been working with production of dairy products frequently for many years as well as sustainable food production. Her email address is bs@sik.se .

ANNE-MARIE TILLMAN is a professor and the head of the division Environmental System Analysis at Chalmers University of Technology. Her research interest is in environmental system analysis, lifecycle assessment and sustainability of systems and operations. Her email address is anne-marie.tillman@chalmers.se .

DYNAMIC SIMULATION OF THE CHICKEN MEAT SUPPLY CHAIN FACING AVIAN INFLUENZA CRISIS

Thi Le Hoa Vo and Daniel Thiel
University of Nantes and E.N.I.T.I.A.A. Nantes, LARGECIA-CRGNA
Rue de la Géraudière - BP 82225
44322 Nantes Cedex 3
France
E-mail : {thilehoa.vo, daniel.thiel}@enitiaa-nantes.fr

KEYWORDS
Chicken supply chain management, sanitary crises, avian influenza crisis, dynamic simulation, system dynamics model.

ABSTRACT

In this paper, a system dynamics model is developed to investigate supply chain behaviors influenced by variations of unpredictable downstream consumer behavior resulting from crisis situations as well as by upstream supply capacity shortages. This model is applied to the French case of a chicken meat supply chain suffering an Avian Influenza crisis. Following the model validation based on real data observed in 2005 and 2006, a what-if analysis has been implemented to examine the supply chain stability with different crisis diffusion hypotheses. In addition, the simulation results equally help to provide a deeper insight into the buffer problem of a multi-echelon push-pull supply chain. More generally, this model should be helpful to decision-makers for other fresh food push-pull supply chains when they are facing such crises.

INTRODUCTION

Sanitary crises due to animal diseases are threatening the development of food supply chain and the global economy. During the past two decades, the food supply chains in Europe and France have faced to non-stop food safety crises such as mad cow disease, the dioxin crisis, foot-and-mouth disease or recently, Avian Influenza. This menace seriously influences to human health and the economy of all countries in the world by its huge scope, hazard and soaring haste such as Avian Influenza whose impact on poultry supply chain and the chicken supply chain in particular is extremely significant. The influence of these crises is not only on upstream production capacity shortages resulted from disease infection between animal populations, but also on downstream consumption decrease.

In this high uncertainty context, we are interested in studying the dynamic behaviour of the entire chicken supply chain under uncertain external environment. The upstream production instability caused by livestock diseases crisis and consumer behaviour fluctuation in downstream of the chain lead all of the supply chain deciders to deal with the stock management and pilotage problems. Davis (1993) notes that uncertainty inherent in an environment in which a supply chain operates propagates through the supply chain network, and makes supply chain management (SCM) and control problems more complex. Much of the research in this area focuses on retail systems, with the manufacturing system as an extension of the distribution network (Sterman, 1989; Lee and Billington, 1995). The unifying concept throughout these researches is the emphasis placed on the "bullwhip effect". The literature on the bullwhip effect also recommends actions to minimize its impact on supply chain performance. Takahashi et al. (1987) report on test result of Material Requirements Planning feedback methods that could eliminate bullwhip amplification.

This paper will firstly present the research context regarding system dynamics modelling and simulation of supply chain behaviour. And then, a more detail literature review focusing on system dynamics modelling food supply chain simulation under animal disease crises will substantiate our work of structuring a generic logistic flows model for the entire chicken supply chain. Finally, in order to analyse the stability of this supply chain, we propose an experiment with the real data of Avian Influenza crisis influencing the French chicken supply chain and a sensitivity analysis of the model.
or the remaining pages follow the general guidelines below:

LITERATURE REVIEW

Previous researches on SD modelling and simulation of supply chain behaviour

Created by Jay Forrester, system dynamics modelling has been used as a method of analysis, modelling and simulation for almost 50 years. The first production-distribution system identifies six types of flow in the systems: material, information, order, capital, work force, capital equipment all along the four supply chain echelons (Forrester, 1958). Afterwards, Towill (1996) proposes that the paradigm of delay reduction is effective for reacting quickly to the market changes and his model also allows forecasting the progression of global performance. Thiel (1996) applies Forrester's system dynamics paradigm basing on non-linear feedback systems for improving the understanding of the regulations of industrial firms in the event of dysfunctions in their production systems.

On the other hand, Oliva and Goncalves (2006) use system dynamics and simulation approach for studying the impact

of endogenous customer demand on supply chain instability. Additionally, Sterman (2006) suggests that supply chain network is a complex dynamic system and generates multiple modes of behaviour including business cycles (oscillation in production and inventories), amplification of orders and production from consumption to raw materials (the Bullwhip Effect), and phase lag between the start of intervention and its effect (shifts in the timing of the cycles from consumption to materials). By using system dynamics, Hwarng and Xie (2008) investigate how the variability in orders or inventories and chaos may occur in a multi-level supply chain system and offer insights into how to manage relevant supply chain factors to eliminate or reduce system chaos.

SD modelling and simulation for food supply chain behaviour

Van de Vorst et al. (2000) recognize that the main sources of uncertainty in food supply chain are the length of the order forecast horizon, information availability and data timeliness, decision policies used, inherent supply process, and demand uncertainties in the supply chain. Recent studies on poultry supply chain modelling are focused on understanding the complex behaviour of poultry industry (Minegishi and Thiel, 2000). Basing on a generic model of simulation, the authors show the instability phenomena and controlling methods of logistic systems coped with important fluctuations in sales. The objective of their system dynamics model basing on the Forrester principles is studying the behaviours, identification and modification of disequilibrium symptoms of production systems in the time.

In fact, on one hand, the authors focus on the problems of coordination between the controlling variables of upstream poultry production and the piloting variables of slaughtering and transformation systems. On the other hand, they emphasise on formalizing the regulation cybernetic mechanisms of the global integrated supply chain production – transformation – shipment. In their model, they tried to study the influence of demand fluctuations on production system behaviour. When the demand goes down, the slaughtered chickens inventory increases and the solution to this problem of overstock is by freezing. In addition, Georgiadis et al. (2005) adopt the system dynamics methodology as a modelling and analysis tool to tackle strategic issues for multi-echelon food supply chain. To build their system dynamics model, they first design generic single-echelon inventory systems that incorporate all state variables and policies for both inventory control and capacity planning. Basing on this model, they demonstrate how generic multi-echelon supply chain models can be constructed at a strategic level.

The above researches of system dynamics modelling and simulation application on food SCM show that system dynamics is a relevant tool for solving all short and long terms problems at both decisional and strategic levels for this kind of short life cycle products supply chain.

THE MODEL

Generally, in food supply chain, farm is considered as primary food producers, various types of processing industry, trading companies, the food retail sector and final customer, each different step in the entire production process is viewed as link in the chain. In particular, the stages of the chicken supply chain include the different steps: breeding, hatching, rearing, processing (and/or final manufacturing), distribution, consumption. In addition, there are always storing and transporting activities between the stages. An important characteristic of the chicken supply chain is its flexibility due to its short product life cycle: it could take approximately 70 days from hatching an egg to the stage when a customer consumes a chicken product (rearing stage takes 40 days for standard chickens).

The model includes ten sections: Demand and Master Production Schedule, rearing, slaughtering, processing and final manufacturing, transportation and distribution of both kind of finished products (entire chicken and processed chicken), retail sales, regulation sectors (retail adjustment and order backlog), supply chain performance (unexpected costs and lost products) representing the feedback loops and system process of the entire supply chain. In addition, the model is built following some rules:

- Orders are always filled
- Live chickens are always available on external markets
- Chicken products are always delivered on time

On the other hand the first step in identifying our modelling approach is to define the key system-features and to create a high-level causal loop diagram that captures the key elements of the relevant system including the major short term feedback loops. In this diagram, there exists a whole range of dependent variables and feedback dynamics that capture overall system behaviour and performance over time. On a global level, the SC is seriously disturbed in its downstream and upstream. The causal loop diagrams in our case consist of several segmental loops explaining the dynamics of the entire SC shown in Figure 2.

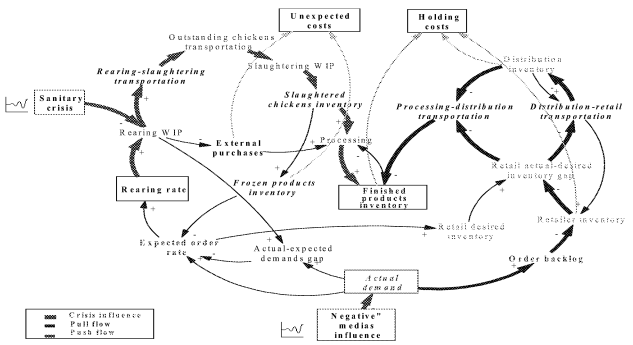

Figure 1. Causal loop diagram for Chicken supply chain model

The principal feedback loops included are described below:
Loop 1: Actual-expected demand gap – Expected order rate – Rearing rate – Rearing WIP.
Loop 2: Expected order rate – Rearing rate – Rearing WIP – Rearing-slaughtering transportation – Outstanding chickens transportation – Slaughtering WIP – Slaughtered chicken inventory – Frozen product inventory.
Loop 3: Processing – Finished products inventory.
Loop 4: Distribution inventory – Distribution-retail transportation.
Loop 5: Retail inventory – Retail actual-desired inventory gap – Distribution-retail transportation.

Our research is interested solely in the SC's short-term actions that only concern the global pilotage of materials flows. Hence, the five homeostatic loops described above are sufficient for representing short term logistic behaviours of the supply chain. However, it must be recognised that other medium and long-term strategic regulation mechanisms equally work on a supply chain undergoing a crisis as regards food health related preventive actions, communication, customer promotion policy, legislation modification, etc., that will not be cited in our case.

Based on this causal diagram, we will define the mathematical formulation of stocks and flow structures by a set of differential level and rate equations needed to study the complexity and stability of such a kind of SC (including non-linearities). The level equations describe the accumulations within the system through the time integrals of the net flow rates, and the rate equations define the rate of change to the levels. Based on the previous literature review, we choose to define the structure of our model of the chicken SCM based on Forrester's fundamental *Industrial Dynamics* model (1958) and on the generic supply chain model of Sterman (2000). Based upon the causal loop diagram and the mathematical formulation of levels and flows diagram, the system dynamics model of the chicken meat supply chain is modelled in *iThink®* software.

SIMULATION RESULTS

First of all, we run the model in equilibrium with constant demand, no sanitary crisis, and the entire SC operates as required. The equilibrium is reached when the available live chicken level for meeting 2,083 tons/days including 1,250 tons/days of EC (60%) and 833 tons/day PC (40%) remains stable at 2,083 tons/day (real data *source:* FIA, 2006 and AGRESTE, 2006). The supply chain fills all of its customers' orders without extended costs due to external purchases or frozen products. Following this, we apply our model for analysing the French chicken supply chain behaviour influenced by the Avian Influenza sanitary crisis during the period from the second week of Oct. 2005 until end of Mar. 2006 (about 161 days). A test for a stationary time series between the simulation result and the real data of standard chicken production trend during the crisis period (Oct. 05 – Mar. 06) is conducted for purposes of validating our model. Comparing these two trends we obtain a ratio between the standard deviation and the average value of the production equal to 0.06 meaning a "relative" error rate of 6 %.

Using this real data for actual demand and rearing capacity, we will focus on analysing certain main supply chain factors representing the entire supply chain behaviour in our simulation model:

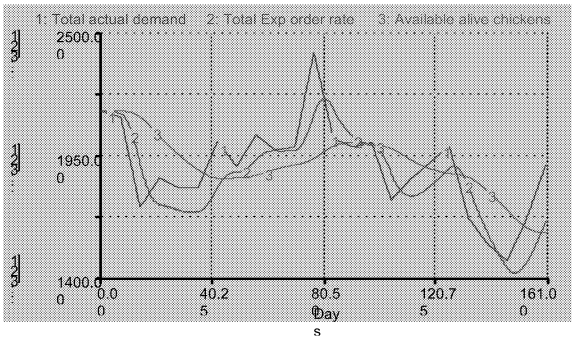

Figure 2. Production fluctuation in accordance with actual demand variation and AI influence.

Figure 2 shows the rearing production response to the fluctuation in the *actual demand* and to the impact of the AI crisis. In fact, the rearing capacity had not been concerned by Avian Influenza until December 2005 while the *actual demand* shrank from October 2005 as a result of the influence of the Media on consumer behaviour. As we can see in the figure, chicken rearing production (*Total Exp order rate* and *available live chickens*) is not bumpy like *total actual demand* (including EC and PC demands) because of the smoothing and adjustment rules in the chain with a time lag of a 40 days rearing cycle.

On the other hand, this is also the reason why there is a rise and fall in the *frozen chicken inventory* and in *external purchases* when the demand seesaws (as shown in the figure 4). For example, the *frozen chicken inventory* reaches the maximum of 138 tons on the 24th day while the *external purchases* are still equal to 0 and inversely, the *external purchases* starts increasing and attains 249.9 tons on the 79th day whereas the *frozen chicken inventory* shrinks to its lowest level of 6 tons.

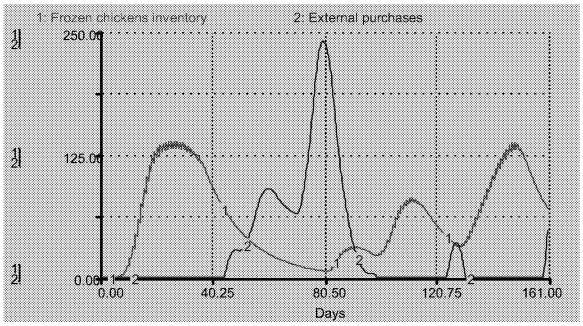

ll

Figure 3. Frozen chicken inventory and external purchases.

These fluctuations in *frozen chicken inventory* and *external purchases* cause the *unexpected costs* for the supply chain to peak at 192,943 Euros on the 79th day when the external purchasing level is maximal. In addition, we recognize that the variation in *retail inventory* level leads to an increase and fluctuation in the *distribution* and *finished products inventory* levels since the retailer orders and purchases to its upstream supplier based on the *actual sale rate* (pull-based scheme). These increases and fluctuations of the stock level at different stages of the supply chain prompt an increase in *holding costs* at each echelon of the chain.

SENSITIVITY ANALYSIS

In our case, in order to analyse the sensitivity of the model, we will now change in this section, the fluctuation degree of the exogenous factors in both upstream (*Avian Influenza influence rate*) and downstream (*actual demand*) of the supply chain (model input) in comparison with their real data. Additionally, we modify some control parameters (operational factors) which can affect the system behaviour and also identify what change of these parameters can reduce the fluctuation level in the supply chain: *demand adjustment time, rearing WIP adjustment time, rearing cycle time, freezing adjustment time, retail inventory coverage time, retail inventory adjustment time*

Table 1. Variations of upstream factors under external influencing fluctuation.

Fluctuation rate of AI influence and actual demand rates	- 50%	+50%
Frozen chicken inventory	- 47%	-11 %
External purchases	+52%	+35%
Unexpected costs	+41%	+ 30%

As we can see in the table, the *frozen chicken inventory* is considerably sensitive to the fluctuation of the *Avian Influenza influence rate* and *actual demand*. When the fluctuation rate decreases 50% (a small fluctuation) the suppliers can reduce nearly 50% of the *frozen chicken inventory*. However, when the fluctuation rate increases they have to keep more chickens in stock but this is still less than the real situation (-11%) because at the same time, the rearing output decreases due to the heightened impact from the AI crisis impact. Additionally, in both cases the external purchasing level always surpasses those in a real situation because the production shortage that fuels the unexpected costs also exceeds the real situation. These results explain that the internal supply chain stability is very sensitive to the changes in the external environment.

We now focus on the fluctuation effect all along of the supply chain, i.e., inventory fluctuations at factory, distribution and retail levels.

Table 2. Variations of downstream factors under demand fluctuation

Fluctuation rates of AI influence and actual demand rates	- 50%	+ 50%
Rearing WIP:	+ 2%	- 2%
EC inventory:		
• at finished products inventory	- 10%	- 8%
• at distribution inventory	- 26%	- 24%
• at retail inventory	- 2%	- 3%
PC inventory:		
• at finished products inventory	- 11%	+ 34%
• at distribution inventory	- 16%	+ 21%
• at retail inventory	+ 2%	- 2%

According to the results shown in this table, we can observe that the level of *rearing work in process* is almost unchanged by daily external influence because of its long *demand adjustment time* (7 days), *rearing WIP adjustment time* (55 days). However, the inventory levels at each echelon of the chain vary considerably, particularly at *finished products inventory* and *distribution inventory* because of their short lead time (1 day).

On the other hand, by modifying the operational factors we find that by increasing the *demand adjustment time* from 1 to 13 days, the amount of *frozen chicken inventory* slightly increases while the quantity of *external purchases*, *unexpected costs* and *total holding costs* of the entire supply chain (finished products inventory, distribution inventory, and retail inventory) shrinks substantially. This means that we can reduce the supply chain costs by increasing the *demand adjustment time*. However, the value of these factors is slightly changed when changing *rearing WIP adjustment time.* In addition, the simulation results show that by increasing the *freezing adjustment time* we can reduce the level of *frozen chicken inventory*, *external purchases*, *unexpected costs* and the *total holding costs.* Though, we cannot actually keep freshly slaughtered chickens for more than 5 days because of their perishability. Then, we also recognise that by increasing the *inventory coverage time* at the retailer's level, all of the supply chain echelons necessarily incur the *holding cost* increase. Yet, if the retailer extends his *inventory adjustment time*, he can reduce his *holding costs* but the manufacturers and the distributors will bear an increase in their *holding costs*.

CONCLUSION AND PERSPECTIVES

In this paper, we have explained why our work focus on simulation modelling for studying the behaviour of the entire chicken meat supply chain threatened by high uncertainties in the supply capacity (the impact of sanitary crises influence on rearing farms) as well as in the customer demand (unpredictable consumer behaviour effecting the sales rate). The simulation results show that fluctuations in customer demand and production are progressively amplified by each supply chain stage and affect the stability of the whole chain. The complexity and particularity of this supply chain behaviour have been

studied and discussed in comparison with the literature review demonstrating that this model allows us to improve our understanding in this field and is useful for SCM decision support purposes. Additionally, the findings in this paper substantiate the previous observations and put forward some important issues that require further research on this kind of supply chain. Future research directions will include a more systematic work of behaviour analysis of such supply chain facing classical "artefacts" on supply and demand for studying its stability.

REFERENCES

Davis T., 1993. Effective supply chain management. *Sloan Management Review*, (34:4), 35-46.

Forrester J.W., 1958. Industrial Dynamics : A major breackthrough fo decision makers. *Harvard Business Review*, (36:4), 37-66.

Georgiadis P., Vlachos D., Iakovou E., 2005. A system dynamics modelling framework for the strategic supply chain management of food chains. *Journal of Food Engineering*, (70:3), 351-364.

Hwarng, H.B., Xie N., 2008. Understanding supply chain dynamics: A chaos perspective. *European Journal of Operational Research*, (184:3), 1163-1178.

Lee, H.L., Billington, C., 1995. The evolution of supply-chain management models and practice at Hewlett-Packard. *Interfaces*, (25:5), 42-63.

Minegishi, S., Thiel, D., 2000. System dynamics modelling and simulation of a particular food supply chain. *Simulation Practice and Theory*, (8:5), 321–339.

Oliva, R., Gonçalves, P., 2006. Evaluating overreaction to backlog as a behavioural cause of the Bullwhip Effect. *Behavioural Research in Operations and Supply Chain Management Conference*, Penn State University, Smeal College of Business.

Sterman, J.D., 1989. Modelling Managerial Behaviour: Misperceptions of Feedback in a Dynamic Decision Making Experiment. *Management Science*, (35:3), 321–39.

Sterman, J.D., 2000. *Business dynamics : systems thinking and modeling for a complex world*. Boston, Mass.: Irwin/McGraw-Hill. 982.

Sterman, J.D., 2006. Operational and Behavioural Causes of Supply Chain Instability, in: O. Carranza, F. Villegas (Eds.), The Bullwhip Effect in Supply Chain, Palgrave McMillan.

Takahashi, K.R., Muramatsu, R., Ishii., K., 1987. Feedback Methods of Production Ordering Systems in Multi-stage Production and Inventory Systems. *International Journal of Production Research*, (25:6), 925-941.

Thiel, D., 1996. Analysis of the behaviour of production systems using continuous simulation". *International Journal of Production Research*, (34), 3227-3251.

Towill, D.R., 1996. Time compression and supply chain management- a guided tour". *Supply Chain Management*, (1:1), 15-27.

Van de Vorst J.G.A.J., Beulens A.J.M, van Beek P. 2000. Modelling and simulating multi-echelon food systems. *European Journal of Operational Research*, (122:2), 354-366.

Websites:

1. AGRESTE (*Agreste-La statistique agricole, Ministère de l'Agriculture et de la Pêche*), 2006 http://agreste.agriculture.gouv.fr/conjoncture_1/aviculture_16/index.html

2. FIA (Fédération des Industries Avicoles): *French Federation of Poultry Industries*, 2006 http://www.fia.fr/

BIOGRAPHY

Daniel Thiel:
D. Thiel, PhD, Eng., is full professor in Industrial Management and Operational Research at ENITIAA. He is a coordinator of the Food Economics and Industrial Management Research Laboratory at ENITIAA composed by six professors, five PhD students and two permanent staff employees. This lab is associated with the Economics and Management Laboratory of the University of Nantes which is composed by 68 professors and 60 PhD students. In the past, he worked more then ten years in different industrial companies.

Thi Le Hoa Vo:
T.L.H Vo is currently completing research for her PhD in management sciences at ENITIAA and the University of Nantes, France. She has obtained Master of Systems Engineering at RMIT University (Australia) in 2002 and Master of Management Sciences at the University of Nantes (France) in 2005. Since 2005, she has been interested in modelling and simulation, especially system dynamics application in order to study the behaviour of food supply chain in crisis situation for her PhD research.

Web-based predictive models for process optimization in small and medium-sized dairy enterprises

M. Schutyser
F. Smit
H. Straatsma
P. de Jong

NIZO food research BV
PO Box 20,
6710 BA Ede, The Netherlands
E-mail: Maarten.Schutyser@nizo.nl

KEYWORDS
Predictive modelling, NIZO Premia, WebSim-MILQ, web application, heat treatment.

Introduction

For more than fifteen years NIZO food research has been involved in applied modelling for the dairy industry. This has led to the development of NIZO Premia, a software environment with predictive models covering practically all processes and products present in dairy industry[1-3]. Premia is the abbreviation for PREdictive Models ready for Industrial Application. The NIZO Premia software consists of multiple model units describing heat treatment, membrane filtration, evaporation, spray drying, cheese production, shelf-life prediction. One of the main advantages of the software is that different model units can be coupled to simulate and optimise a complete production chain.

Predictive modelling of heat treatment

The model unit NIZO Premia QSIM is aimed at optimization of heat treatment processes. NIZO Premia QSIM comprises two different model types:

1. Process models

Models that need input on the process configuration of the equipment and can predict temperature versus time profiles and wall temperatures. E.g. models for tubular, and plate heat exchangers, direct steam injection, steam infusion, regenerative heating sections, bactofuge.

2. Product models

Kinetic models that predict the transformation of food components and inactivation or growth of contaminants. E.g. models to predict the concentration of micro-organisms in final products as a result of growth, adherence, release and inactivation in process equipment, kinetic models that predict the transformation of food components related to the food properties recognised by the consumer (e.g. off-flavour, taste, colour, and shelf-life). The combination of both process and product models allows the user to simultaneously optimize process efficiency and product quality.

MILQ-QC-TOOL

The ability of predictive models to contribute to product quality improvements, process efficiency and cost reduction is recognized by the majority of dairy companies. To facilitate the use of predictive models specifically for small and medium dairy enterprises (SME's), a web-based version of NIZO Premia was developed. Together with 16 SME's, NIZO food research and Wirelessinfo took the initiative to set up the EU project MILQ-QC-TOOL. The 16 SME's from various EU countries (Figure 1) produce a whole range of dairy products, such as several types of cheese, yoghurt, cream, and chocolate milk.

The objective of the project was to make the predictive models from NIZO Premia QSIM available on the Internet to the SME's. The SME's should be able to use and update the models via the Internet. To facilitate the use and implementation of the internet application in the SME's, multilingual tutorials and manuals were prepared. These were used during several training sessions during which the application was introduced to the SME's. In Figure 2 a screenshot of the main screen is shown. In this main screen the user can find information about the process configuration, selected product components and

process conditions. The user can specify the detailed configuration of process equipment and product transformation kinetics in submenus. In figures 3-5 screenshots are shown of the user manual. In addition to the development of the application also an optimization of a selected heating process (e.g. pasteurisation) was carried out together with each SME. The optimization involved product sampling, analyses, model calibration, optimization and validation of the optimization.

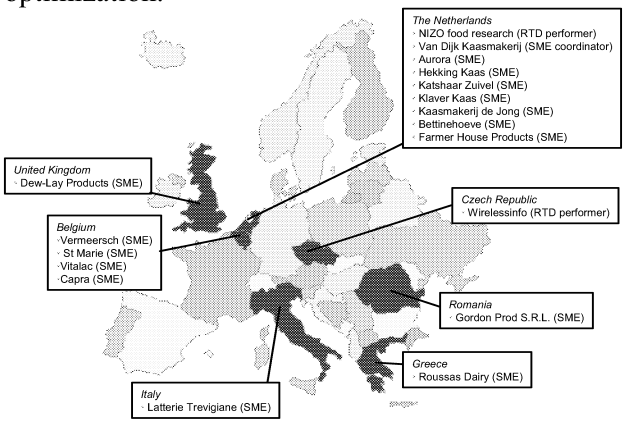

Figure 1. Geographical overview of participants in the EU project MILQ-QC-TOOL.

Project results

In December 2007 the development of the internet application called WebSim-MILQ was finalized together with the project[4]. The internet application is a unique web-based modelling platform and now available at websim.milq.org. The optimization of the selected heat treatment processes resulted in significant benefits for the participating SMEs, e.g.:

- Increase in cheese yield by adapting the cheese milk pasteurization (produce 1 cheese extra for each 100 cheeses from the same volume of milk). For 1 company this resulted in a yearly additional income of 100.000 euros.
- Reduced risk of biofouling with streptococci from serious to negligible by adapting the pasteurization process.
- Improved product safety after microbial analysis of pasteurized milk samples and extensive cleaning cycles.
- Identified opportunity for extension of running time in UHT plant by reduction of protein fouling (with 40%).

Other results of the project involved amongst others the collection of new kinetic data on heat-induced protein denaturation in different milk types. The availability of appropriate kinetic data on transformation of food components or inactivation of microorganisms is of crucial importance for accurate prediction.

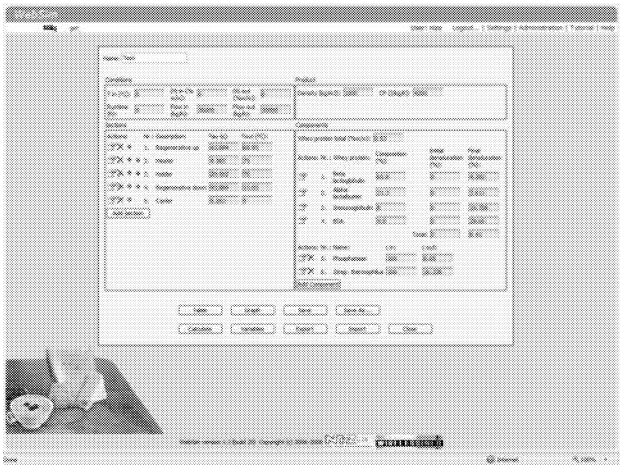

Figure 2. Desktop representing main overview of WebSim-MILQ.

Extensive evaluation of the web application by both developers and end-users assured specifications to be designed to the needs of SME's. The majority of SME's became enthusiastic to join follow up projects to extend the web application to support and optimize their complete processes. The web application is now available also to third parties.

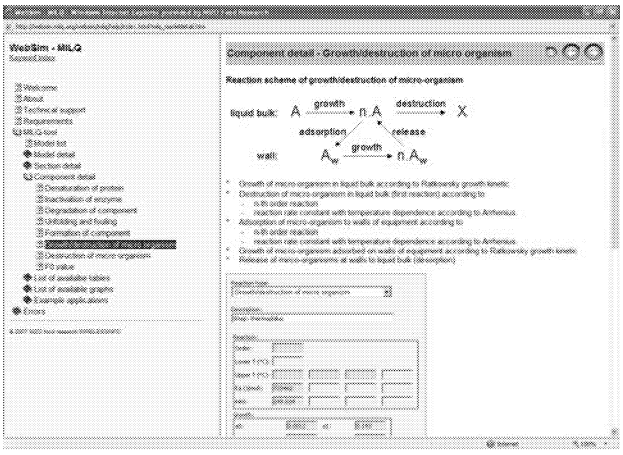

Figure 3. Screenshot of the manual of WebSim-MILQ with detailed explanation of the growth and inactivation modelling of microorganisms.

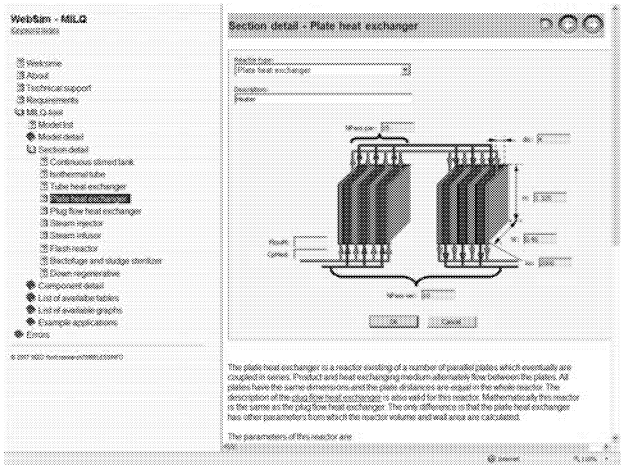

Figure 4. Screenshot of the manual of WebSim-MILQ with detailed description of the configuration of the plate heat exchanger model.

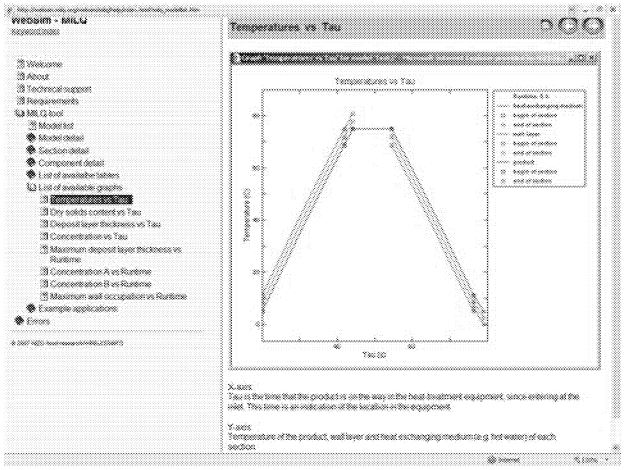

Figure 5. Screenshot of the manual of WebSim-MILQ with detailed description of the graph showing the simulated temperature – time profile of a pasteurizer.

Conclusions

A web-based version of NIZO Premia QSIM (WebSim-MILQ) was successfully developed and applied in 16 SMEs producing various dairy products. This web-based version of NIZO Premia in combination with an appropriate optimisation strategy for heat treatment processes resulted in concrete benefits for the SME's with respect to reducing processing costs and increasing product yield and quality. Future developments will focus on new predictive tools for assessment of efficient water use and reducing energy consumption in dairy production processes. It is also intended to develop predictive tools that support cheese producing companies to increase cheese yield and enhance cheese production efficiency without affecting the taste and appearance of the cheese.

References

1. De Jong, P., Straatsma, J. Otten, Z.E.H., Siezen, R.J., and van der Horst, H.C., 1999. Computer modelling of raw material, process and product, Proceedings 25th IDF Congress, 87-97.
2. De Jong, P., te Giffel, M.C., and Kiezenbrink M.C., 2002b. Prediction of the adherence, growth and release of microorganisms in production chains. International Journal of Food Microbiology 74, 13-25.
3. De Jong, P., te Giffel, M.C., Straatsma, J., and Vissers, M.M.M., 2002a. Reduction of fouling and contamination by predictive kinetic models. International Dairy Journal 12, 285-292.
4. Schutyser M., Straatsma J., Keijzer P., Vissers M., Verschueren M., De Jong P., and Horak P. A new web-based modelling tool (Websim-MILQ) aimed at optimization of heating processes in the dairy industry (2007). Proceedings International congress on Predictive modelling in Foods 16-19 September 2007, Athens, Greece.

SUSTAINABLE FOOD PRODUCTION

INTEGRATED SIMULATION TECHNOLOGY FOR SAFE, SUSTAINABLE FOOD PROCESSES

Karin Östergren
Hans Janestad
Johanna Berlin
Ulf Sonesson
SIK –The Swedish Institute for Food and Biotechnology
SE-40129 Gothenburg, Sweden
E-mail: karin.ostergren@sik.se

KEYWORDS
Simulation, Life Cycle Assessment, Sustainable Manufacturing, Food Production.

ABSTRACT

In the development of sustainable process lines, various aspects must be considered such as quality, microbiological risks and process economy as also environmental impact throughout the development phase of the process. A general *process-driven* simulation tool has been developed to facilitate the rapid and efficient evaluation of alternative processes, taking into account technological, environmental and microbiological aspects. The tool has been used to analyse a proposed process line for product in the form of a snack using brewers' spent grain (BSG) as one major ingredient. From simulations based on data from a pilot scale trail it could be concluded that the handling and choice of ingredients are critical steps from a microbiological and environmental point of view as well as from the point of view of costs. From a process point of view the drying step is the most critical due the large amount of energy required, which influences both costs and the environmental impact. By pressing the BSG before processing and possibly by drying the product at the brewery using e.g. excess steam from the brewing process the environmental impact as well as production costs can be decreased.

INTRODUCTION

Modelling is widely used as a method of making process design more efficient by avoiding expensive mistakes and by facilitating a systematic search for the most advantageous solutions. A vast number of models for food processes have been published, ranging from mechanistic mass- and heat transfer models to integrated process line models which include product quality and economy and models for predicting food safety (e.g. McMeeking et al., 1993). A number of publications focus on industrial modelling with the life cycle assessment (LCA) perspective (e.g. Jödicke et al., 1999; Alexander et al., 2000; Azapagic and Clift, 1999; Kheawhom and Hirao, 2004 and Gäbel and Tillman, 2005). However, there are few, if any, industrial models taking into account, at one and the same time, process economy, microbiological risks and the environmental impact.

Process economy as well as food safety are crucial areas that must be to investigated in the development of new industrial process lines. Environmental sustainability is another aspect that has become increasingly more important and has therefore also become a crucial area. In developing new process lines or exploring possible improvements of existing process lines compromises have to be made between different aspects such as process economy, level of safety, sensory and nutritional quality and now also the expected environmental impact. The earlier in the development phase weak points are discovered the easier and less costly it is to introduce changes. To be able to perform a structured analysis, and taking into account several different aspects, a new simulation tool has been developed in order to gain a simple overview of the impact of various changes.

MODELLING APPROACH

The simulation tool developed combines three areas, namely, economic/technical performance, microbiological safety and environmental impact. The modelling strategy is process-driven, which means that it is the changes in the process conditions that determine the environmental impact and microbiological load. The process line model is built up by combining a set of components describing each unit operation. The components are built up using a pre-defined structure so that they can easily be incorporated or excluded from the model. Global parameters evaluated are typically the number of micro-organisms, the product yield, losses, emissions, water and energy consumption and costs. The global parameters can be chosen freely as the model is being set up and can also easily be added afterwards. Local parameters are used to describe the single components of the model describing the units operation included in the process line model. The model is static in time.

Based on appropriate mathematical models and local process parameters (e.g. the concentration of various ingredients, temperature and residence time), product quality parameters, energy consumption, yield and microbiological status (based on growth, survival and reduction models) are evaluated for each process step. *Economic/Technical performance* is then assessed by evaluating the mass balances and energy calculations and the *microbiological safety* is assessed by simulating the number of micro-organisms in the product along the process line. To evaluate the *environmental impact* the model calculates both direct emissions caused by the

industrial process as well as indirect effects upstream of the industry (e.g. raw material acquisition for ingredients).

For the environmental impact calculations, life cycle assessment (LCA) methodology was used. Life cycle assessment is a tool for evaluating the environmental impact associated with a product, process or production during its life cycle. This is accomplished by identifying and quantitatively or qualitatively describing its requirements of energy and materials, and the emissions and waste released to the environment. Either the total life cycle or part of it is included in the assessment, which means that the product being studied is followed from the initial extraction and processing of the raw materials through manufacturing, distribution, and use, to final disposal, including the transports involved. Besides identifying and quantifying the environmental impact of the product or activity, LCA also identifies those activities in the life cycle of the product which are the main contributers to this impact. An LCA is an ISO standardised tool (ISO, 2006a, 2006b).

The model is implemented in Simulink using an embedded Matlab code to describe the functions associated with each component. The use of the Simulink GUI in combination with the pre-defined structure applied makes it easy to add or take away and re-arrange the components in a process line, as well as to change the local parameters. Below, the model is demonstrated as a tool in developing a new process line for the production of a type of snacks.

MODELLING THE PRODUCTION OF A SNACK

Brewers spent grain (BSG) is a rich source of dietary fibre. The process developed (Ibanoglu et.al 2006, Ainsworth. et al., 2007) aims at developing a nutritious snack at the same time as finding application areas for a by-product from the brewery industry which is commonly not taken advantage of. The major process steps (Figure 1) are the transport of the BSG from the brewery, blast chilling of the incoming BSG, drying and milling the BSG, mixing the BSG with the additional ingredients, extrusion of the snack, packaging and storage of the final product. Storage steps between the major processing steps are included in the simulation model in order to be able to make a feasible judgement of energy costs and microbiological status during the time the raw material/final product is not being processed.

The *quality aspects* of the final product evaluated in the model were expansion, bulk density, fracture stress and hardness. A multivariate PLS model (SIMCA, Umetrics) based on experimental data namely screw speed (100-300 rpm), extrusion moisture (10-20%), BSG concentration (0 - 30%), through-put (10-35 kg/h) and, barrel temperature (80-140 C), was implemented. The accuracy of the model was fair (R2=0.87, Q2=0.645)

Environmental impact data for the ingredients, transport, energy system and waste treatment were collected using an environmental database (EcoInvent, 2003). The environmental impact for the ingredient BSG was assumed to be zero since it is a byproduct from another process.

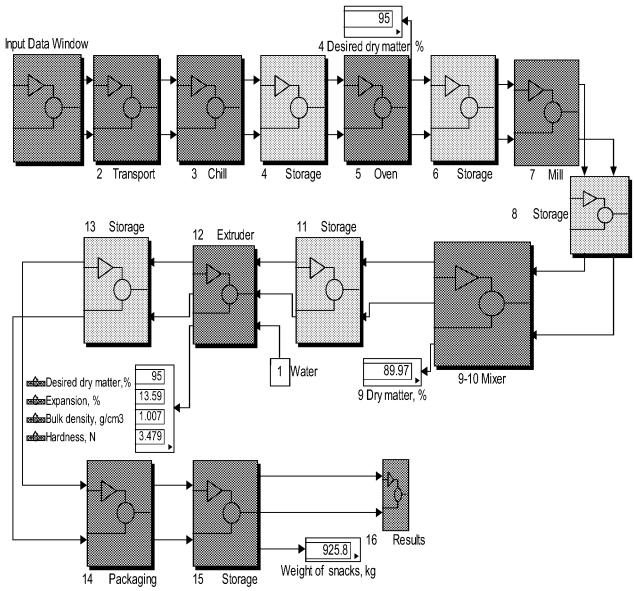

Figure 1: The Simulink GUI (top level) showing the process line being modelled

Bacillus cereus was chosen to represent the microbiological hazard since it can occur in the ingredients. *B. cereus* forms spores which have the ability to survive heat and thus this choice of hazard gives a "worst case" scenario. The kinetic models were taken from Nauta (2001). The reduction of *B.cereus* was based on kinetics valid for spores. It was further assumed that no growth took place at a water activity of < 0.9. Costs of ingredients, packaging and energy were implemented assuming a production site in Great Britain. The data and the models for energy consumption for each process step were taken from data sheets with the exception of the model for energy consumption for the blast chill which was obtained from experimental data. All experimental and process data were kindly provided by Ainsworth and co-workers.

RESULTS

The production of the snack using 1000 kg BSG with a dry matter content of 20% was simulated on the bases of a formulation of 21% BSG , 9% rice flour, 30% chickpea flour and 20% maize flower as the main ingredients. In addition small amounts of spices, salt, yeast, gum Arabicum and oil were added. Of 1000 kg BSG 926 kg of the snack were obtained. A Western European energy system was assumed. It was further assumed that there was no microbiological contamination in any process step. In the reference scenario it was assumed that 10% of the waste went to landfill, 30% to incineration and 40% was used as compost and 20% as animal fodder. The cost of handling losses of the product during production was assumed to be negligible and was thus set to zero.

Selected output data are given in Figures 2-5. From Figure 2 it can be concluded that the drying step of 240 minutes, assuming a surface temperature of 100°C, efficiently reduces

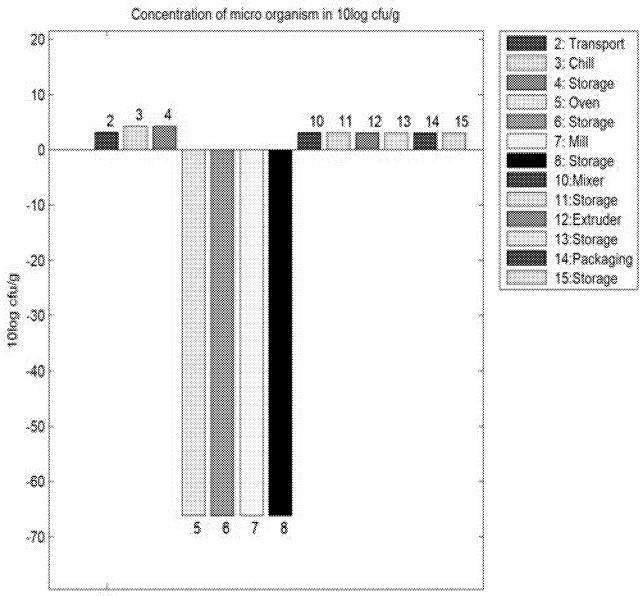

Figure 2: Level of *B. cereus* in each process step. The initial load was: BSG =10^3 cfu/g; tomato powder, carrot powder, onion powder = 10^4 cfu/g; fresh herbs= 10^3 cfu/g; flour = 1 cfu/g

the level of *B. cereus* from the incoming BSG. Due to the low water activity after the drying step and in the final product, the growth of *B. cereus* is efficiently inhibited.

The environmental impact presented in the environmental categories, namely, global warming potential (GWP), acidification, eutrophication and total energy consumption per ton "upgraded" BSG is given in Figure 3. The ingredients added to the BSG to produce a snack are the largest contributors to all impact categories.The ingredients contribute most to the category eutrophication potential (>90%). The process influences the level of total energy (~50%), acidification (~40%), global warming potential (~30%) and eutrophication potential (<10%). The relation found between process-related and ingredient-related environmental impact categories is common for many food processes. From Figure 4 it can be seen that the drying step consumes by far the most energy. Compared to the overall production costs (Figure 5) the energy cost is, however, low, being only 0.9 Euro/kg dry BSG. It is also worth noting that it is a minor ingredient, gum arabicum, that dominates the production costs (excluding equipment and personnel). The costs of the ingredients for upgrading 1 kg of dried BSG to snacks is predicted to be 16 Euros.

DISCUSSION

Ingredients: In order to reduce the environmental impact of the ingredients alternatives to the original ingredients may be considered. E.g. the rice flour (7294 g $C0_2$ eq./kg), which is a major ingredient, contributes five times more to the GWP than maize flour. Tomato powder and onion powder are other (minor) ingredients which have a high environmental impact.

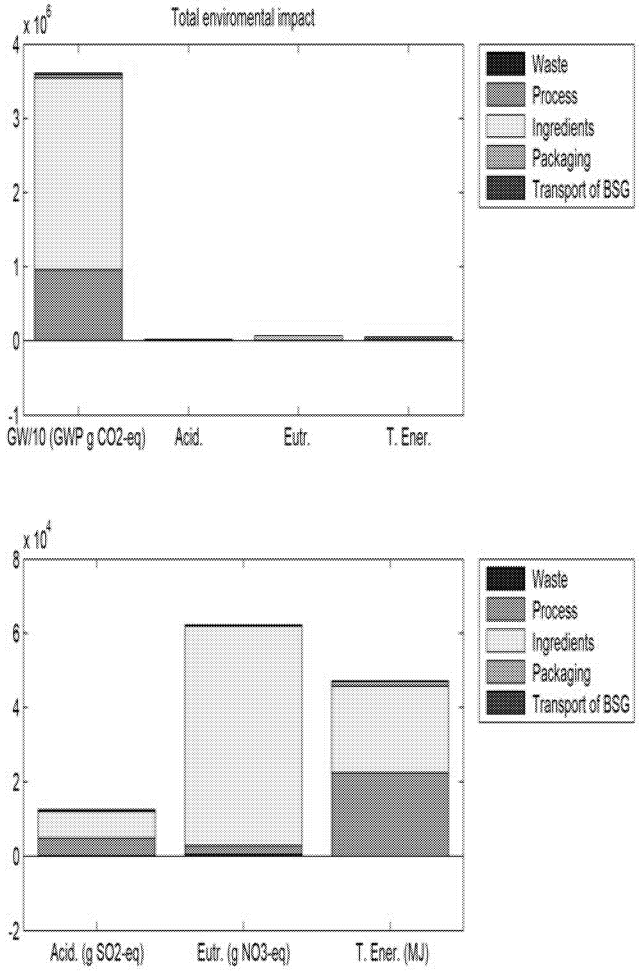

Figure 3: Environmental impact/ 1000 kg processed BSG

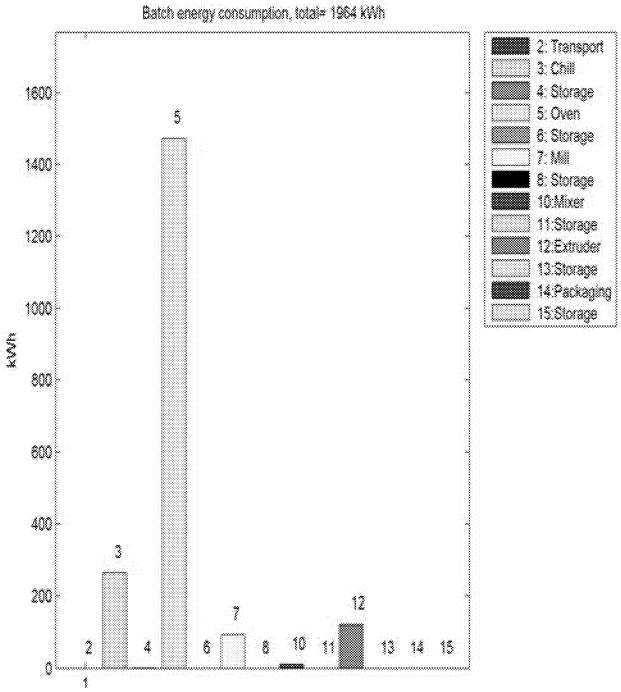

Figure 4: Electricity consumption/ process step when processing 1000 kg BSG

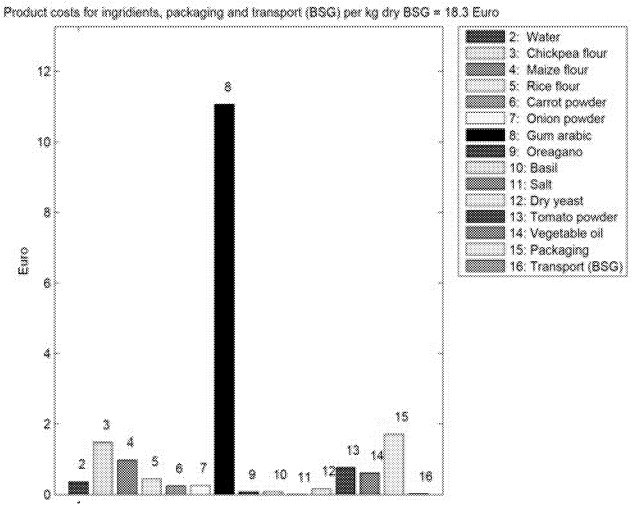

Figure 5: Costs of ingredients and transport per kg BSG

To reduce the overall production costs alternatives to gum arabicum may be considered. Due to the long drying step (step 5), it is the number of micro-organisms in the ingredients added after this drying step that will determine the level of *B. cereus* in the final product. Assuming a maximum contamination of BSG to be 10^4 cfu/g and a minimum contamination in the other ingredients (flour, tomato powder, carrot powder, onion powder, fresh herbs) to be 1 cfu/g, an average level of *B. cereus* in the final product of less than 2 cfu/g is predicted. This result can be compared to a level of 10^3 cfu/g, which was predicted in the simulations shown in Figure 2, where the ingredients added after the drying step were assumed to contain a higher level of contamination.

Processing: The process step requiring most energy is the drying step. By combining drying and mechanical dewatering the energy consumption could be decreased substantially. The energy consumption of a pulp press has for example been reported by M. Schuttenhelm (1999) to be 45kWh/t dry substance. By combining dewatering with an electric field the percent of solids could be increased by up to 49 % for BSG (Orsat et al., 1996). Simulations showed that it was possible to decrease the energy consumption from 2.1 kWh/kg produced snacks to 1 kWh per kg produced snacks assuming an increase from 20% dry mater content to 40% dry matter content in the feed.

The difference in environmental impact for producing 96 kg of snacks with and without adding any BSG was also investigated using the original process design in order to evaluate the benefits of upgrading BSG compared to producing a more conventional type of snack. From these simulations it could be concluded that the BSG adds quite a substantial environmental impact to the process. For the pilot scale process the processing steps before mixing the ingredients, i.e. the production of BSG flour (chilling, drying and milling), contributed more to the environmental impact than the rice flour used instead of BSG when producing a conventional type of snack. Thus the energy consumption of these process steps (chilling, drying and milling) must be decreased substantially in order to gain any environmental benefits in the upgrading of BSG to a snack.

Based on the evaluation of the pilot scale run a potentially best case was defined assuming that the production of the BSG takes place at the site of a brewery and excess heat from the brewery is used in the drying step. This implies that we can omit the transport, the chill step and the environmental impact of the drying step. The environmental impact of the improved process is shown in Figure 6. From

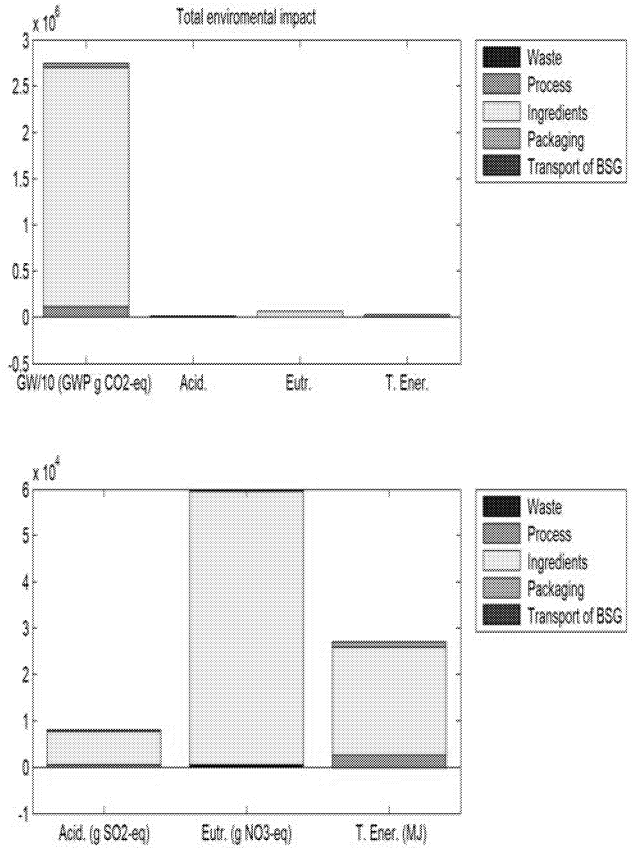

Figure 6: Environmental impact/1000 kg processed BSG assuming that the production of the BSG takes place at the site of the brewery from which excess heat for the drying is used

this it can be concluded that by carefully choosing a production site and by optimising the drying step the environmental impact of the process can be decreased considerably.

CONCLUSIONS

A general, integrated, *process driven* simulation tool has been developed and demonstrated. The simulation framework combines three areas namely economic/technical performance, microbiological safety and environmental impact. Based on the data obtained from a pilot scale trail improvements regarding ingredients, process conditions and microbiological safety could be evaluated.

ACKNOWLEDGEMENTS

This work was supported by the European Commission Project number FOOD-CT-2005-006922. We would also like to acknowledge our dept of thanks to Professor Paul Ainsworth, Andrew Plunkett and Valentina Stojceska at The Manchester Metropolitan University, Senol Ibanoglu at Gaziantep Univeristy and Alexander Milanov, Process Hygiene, SIK for kindly providing data and taking part in all discussions on the implementation and evaluation of the model.

REFERENCES

Ainsworth, P.; S. Ibanoglu; A. Plunkett; E.Ibanoglu; and V. Stojceska. 2007. "Effect of brewers spent grain addition and screw speed on the selected and nutrional properties of an extruded snack." *Journal of Food Engineering,* 81, 702-709.

Alexander, B.; G. Barton; J. Petrie; and J. Romagnoli. 2000. "Process synthesis and optimization tools for environmental design: methodology and structure." *Computers and Chemical Engineering*, 24, 1195-1200.

Azapagic, A. and R. Clift. 1999. "Life Cycle Assessment as a Tool for Improving Process Performance: A Case Study on Boron Products." *International Journal of Life cycle Assessment*, Vol. 4(3), 133-142.

Ecoinvent Centre. 2003. Ecoinvent data v1.01, Final reports ecoinvent 2000 No.1-15, Swiss Centre for Life Cycle Inventories, Dübendorf, CD-ROM.

Gäbel, K. and A-M. Tillman. 2005. Simulating operational alternatives for future cement production, *Journal of Cleaner Production,* 13(13-14), 1246-1257.

Ibanoglu, S.; P. Ainsworth; E.A. Özer; and A.Plunkett. 2006. "Physical and sensory evaluation of a nutritionally balanced gluten-free extruded snack." *Journal of Food Engineering,* 75, 469-472.

ISO 2006a. "Environmental management – Life cycle assessment – Principles and framework." *ISO 14040:2006(E).* Geneva. Switzerland: International Organization for Standardization.

ISO 2006b." Environmental management – Life cycle assessment – Requirements and guidelines." *ISO 14044:2006(E).* Geneva. Switzerland: International Organization for Standardization.

Jödicke, G.O.; A. Zenklusen; Weidenhaupt; and K. Hungerbühler. 1999. "Developing environmentally sound processes in the chemical industry: a case study on pharmaceutical intermediates", *Journal of Cleaner Production*, 7, 159-166.

Kheawhom, S. and M. Hirao. 2004. "Decision support tools for environmentally benign process design under uncertainty." *Computers and Chemical Engineering*, 28, 1715-1723.

Mc Meekin T.A.; J.N. Olley; T. Ross; and D.A. Ratkowsky. 1993. *Predictive Microbiology –theory and application.* A.N. Sharp (ed), Research Studies Press LTD, Taunton, Somerset, England

Nauta, M. J. 2001. *RIVM report* 14916007.

Orsat, V.; G.S. Raghavanet; and E.R. Norris. 1996. "Food processing waste dewatering by electro-osmosis." *Canadian Agricultural Engineering 38(1), 63-67.*

Schuttenhelm, M. 1999. "Pulp press performance measurements in Offstein sugar factory", *Zuckerindustrie 124* (9), 691-696.

AUTHOR BIOGRAPHY

KARIN ÖSTERGREN, PhD in Food Engineering, Lund University ,senior researcher and project leader at SIK. Her research interest is in food engineering and food production engineering. For the past ten years she has been project leader for a variety of projects focusing on exploring the benefits of combining food process engineering and environmental system analysis for sustainable industrial food production. koe@sik.se

HANS JANESTAD, B.Sc. in mathematics, statistics and programming, has been working at SIK with modelling in food engineering for the past 18 years. hj@sik.se

JOHANNA BERLIN, PhD in Environmental Systems Analysis from Chalmers University of Technology. senior researcher and project leader at SIK. Her research interests are environmental system analysis, in particular within the field of sustainable industrial food production, improvement assessment and scenario development. jbe@sik.se

ULF SONESSON is research coordinator for environmental research at SIK and has a PhD in Environmental Systems Analysis. His main research interests are within LCA-based environmental assessment of novel processes and products, as well as adapting the LCA methodology for food products and scenario methodology. For the past ten years he has been working as a project leader both nationally and internationally. usn@sik.se

MODELLING PRODUCT QUALITY IN FOOD SUPPLY CHAINS

Martin Grunow, Renzo Akkerman, Aiying Rong
Department of Management Engineering
Technical University of Denmark
Produktionstorvet 425
2800 Kgs. Lyngby (Copenhagen)
Denmark
E-mail: grunow@ipl.dtu.dk / rak@ipl.dtu.dk / ar@ipl.dtu.dk

KEYWORDS
Food industry, Product quality, MILP, Production and distribution planning

ABSTRACT

The food industry has a variety of distinct characteristics that make effective supply chain management a difficult task. One of the most important characteristics to consider is the perishable nature of food products. It relates to important issues like food safety, health and nutrition, and poses significant challenges in food supply chain management. In this paper, we present a mixed-integer linear programming model (MILP) integrating food quality planning in production and distribution planning.

INTRODUCTION

The food industry has a variety of distinct characteristics that make effective supply chain management (SCM) a difficult task. SCM can be defined as the task of integrating organizational units along the supply chain and coordinating material, information and financial flows in order to fulfil (ultimate) customer demands with the aim of improving competitiveness of a supply chain as a whole (Stadtler and Kilger, 2008).

In food supply chains, one of the most important characteristics to consider is food quality (e.g. Smith and Sparks, 2004). Food quality is heavily affected by the environmental conditions of storage and transportation facilities (see e.g. Labuza, 1982). As Van der Vorst et al. (2007) argue, the importance of food quality in food supply chains requires "quality controlled logistics", which aims at an integrative view on logistics and product quality. For instance, this may include a differentiation of product flows based on the products' quality attributes.

In this paper, we aim to integrate food quality modelling in logistics decision-making. More specifically, we combine decisions on storage and transportation activities together with decisions on temperature setting for the different stages in the supply chain. To capture the dynamics of the quality degradation and the distribution, we develop a multi-period mixed-integer linear programming model for production and distribution planning. Food quality can hereby be actively managed.

RELATED LITERATURE

The basics of production and inventory systems with deteriorating items have been extensively studied, as reported in review articles by Nahmias (1982), Raafat (1991) and Goyal and Giri (2001). These articles distinguish between two types of perishability: fixed lifetime and random lifetime. In the former case, products may be retained in stock for some fixed time after which they must be discarded; in the later case, items are discarded when they spoil and time to spoilage is uncertain. Most of the literature focuses on perishable products with fixed life span. For food products, the moment of spoilage is variable, and highly dependent on environmental conditions such as temperature, which is not covered by inventory-theory-based modelling approaches.

In this paper, the focus is on production and distribution planning. Related work by Eksioglu and Jin (2006) resulted in a planning model that integrated production, inventory and transportation decisions in a two-stage supply chain for perishable products. But their model does not consider transportation between the facilities and further also enforces that each retailer is assigned to exactly one facility. Ahuja et al. (2007) studied a two-stage logistic network similar to that by Eksioglu and Jin (2006) with additional production and inventory capacity constraints. In Ahuja et al. (2007) and Eksioglu and Jin (2006), as well as in Lütke Entrup et al. (2005) and Myers (1997), product quality was implicitly considered by constraining the shelf life of the product.

A more advanced way of including product quality can be seen in Zhang et al. (2003), who considered a three level distribution system with fixed plant locations, potential central and distribution warehouses, as well as retailers. In their study, product quality is represented as a function of time and temperature for production, transportation, and storage. But their approach is still a traditional network approach and product quality degradation is not captured in the representation of the network explicitly. That is, the model itself treats quality degradation as a given. In Rong et al. (2008), product quality degradation is explicitly included. They integrate decisions on production and transportation with the choices of warehouse transportation temperatures.

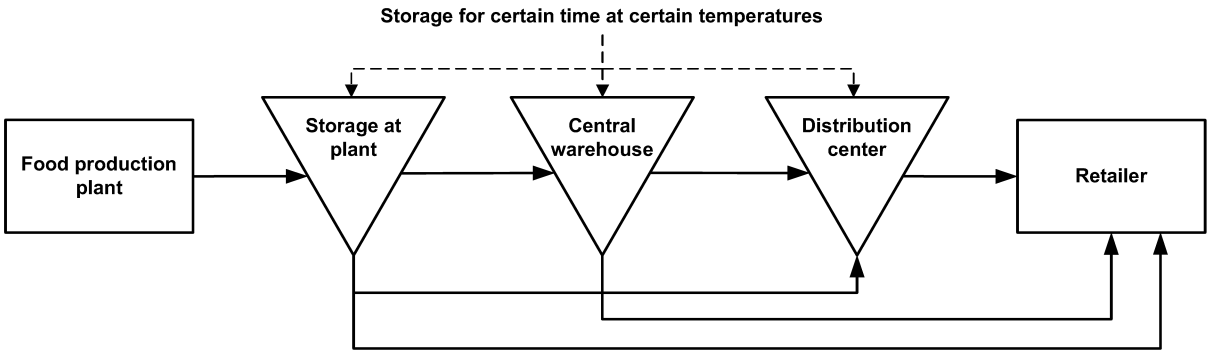

Figure 1: Structure of the Food Supply Chain

MODELLING FOOD QUALITY DEGRADATION

In general, quality degradation of food products during storage or transportation is dependent on storage time and temperature, and various constants (e.g., activation energy, gas constant). Most often, quality degradation is linear or exponential in relation to time (for a given temperature). For a more detailed discussion, we refer to Labuza (1982) or Man and Jones (1994). Quality prediction of food products is a complex task, due to the range and dynamics of product characteristics and storage conditions. Numerous models have been developed for specific food products (e.g., McDonald and Sun, 1999; Lukasse and Polderdijk, 2003), and some are even included in widely used decision support software (e.g., Dalgaard et al., 2002).

Obviously, temperature is an important factor in controlling product quality in supply chains. The rate of quality degradation k is therefore often based on the Arrhenius equation, a formula for the temperature dependence of a chemical reaction. The general form of this equation is:

$$k = k_0 \exp\left[-E_a / RT\right], \tag{1}$$

where k_0 is a constant, E_a the activation energy (an empirical parameter characterizing the exponential temperature dependence), R the gas constant, and T the temperature.

For the prediction of quality levels, we can use this equation to estimate the quality level of a product at a certain location in the production and distribution network based on an initial quality, and subsequent storage periods, leading to a way to calculate the expected quality of food products after storage at given time periods and temperatures. For a given temperature, this relationship is mostly linear or exponential, but the exponential relationship can then be transformed to a linear relationship. This means the quality change during a specified time period can be determined for each possible storage or transportation temperature, and the outcome can be used as parameters in the production and distribution planning model developed in this paper. This leads to the following quality change (or logarithmic quality change) ΔQ for a time period with length τ and temperature T:

$$\Delta Q(\tau, T) = -k_0 \tau \cdot \exp\left[-E_a / RT\right]. \tag{2}$$

We specifically choose to use this general way of modelling quality degradation to keep the production and distribution planning approach presented in this paper applicable to a wide variety of food industries. For each application, a specific quality degradation function is used.

PROBLEM FORMULATION

In this paper, we consider a single-product food supply chain, consisting of production sites, central warehouses, distribution centres, and retailers. The supply chain is illustrated in Figure 1. The figure also shows that storage of products occurs in the first three stages. The chain is driven by the product demand of retailers. This demand is not only expressed in product volumes, but also in product quality requirements - which are normally related to a certain remaining shelf life and can differ between the retailers.

The model explicitly considers product quality throughout the supply chain. Product flows are distinguished by the product quality, and quality degradation occurs during storage and transport. For this, we discretize product quality in such a way that that quality changes during storage and transportation are integers. We use the linear (or linearized) quality degradation described earlier, so quality decay is linearly related to the storage time. This is essential in reducing the complexity of the resulting decision support model. Figure 2 illustrates quality degradation in the distribution network for given temperatures for storage and transportation facilities. In the example, a product is first stored at the producer (P_1), subsequently transported to a distribution centre (D_3), where it is also stored for a certain time, and finally, the product is transported to a retailer (R_2). The quality level of the product (starting at $q_{\max}$) is subject to decrease as time goes on.The decrease depends on the temperature in storage and during transportation which is an outcome of the solution approach.

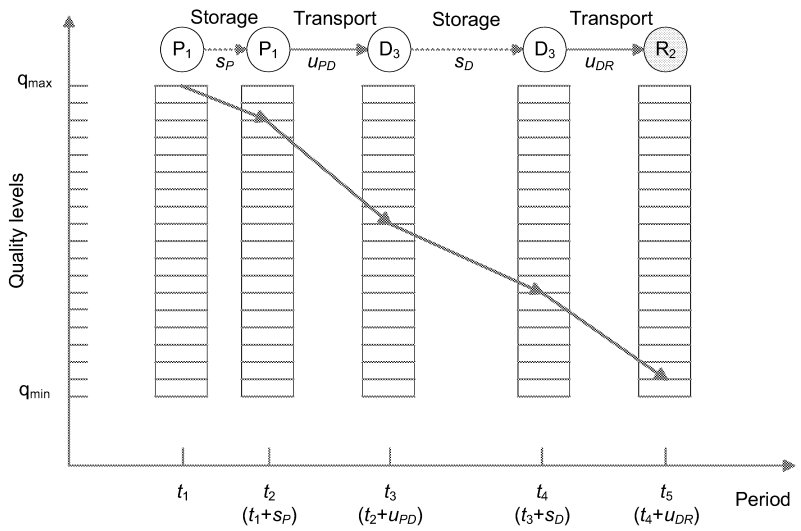

Figure 2: Illustration of Quality Degradation using Discrete Quality Levels

Next to the traditional decisions on production quantities and product shipments, the model also includes decision-making on the temperatures for the storage facilities. In this way, product quality is not only tracked through the chain, but can also be influenced. Temperatures in the transportation facilities are assumed to be fixed, but do affect product quality.

Several assumptions are made in relation to the modelling:

- The discretization of quality levels is performed in such a way that each storage or transportation activity will at least lead to one level of quality change.
- Only products that satisfy the quality requirements are considered in product flow. Other product is considered as waste at the end of each period.
- The quality levels for each of the production batches can be different, reflecting variability in raw material quality.
- Shipments are made at the end of each period.

The following notation is introduced for modelling:

Indices:

i	node index (for production facilities, storage facilities, and retailers),
i,j	index pair, (i,j), referring to an arc from node i to node j,
q	quality index, $q \in Q$,
k	temperature index, $k \in \{1,\ldots,S\}$,
t	time index, referring to a planning period. (A time period $\omega_{\max}$ is added to the planning horizon to facilitate distribution lead times.)

Sets:

P	set of plants,
W	set of potential central warehouses,
D	set of potential distribution centres,
R	set of retailers,
U	set of production and storage facilities, $U = P \cup W \cup D$,
N	set of all nodes: $N = P \cup W \cup D \cup R$,
A	set of all arcs ($A \subset N \times N$),
Q	set of all quality levels q, $Q = \{1,\ldots,B\}$,
$n(i)$	set of successor nodes for node i,
$v(i)$	set of predecessor nodes for node i.

Parameters:

M	a large positive value,
$\omega_{\max}$	maximum planned transport lead time from production sites to retailers,
$a_{i,t}$	production capacity for plant $i \in P$ in period t,
$f_{i,j}$	cost for transporting one product unit on arc (i,j),
$g_{i,k}^{(1)}$	fixed cost (includes cooling) for facility $i \in U$ per period at temperature choice k,
$g_{i,k}^{(2)}$	variable storage cost for one product unit per period in facility $i \in U$ at temperature choice k,
$p_{i,t}$	cost for producing one product unit in facility $i \in P$ in period t,
w_i	waste disposal cost for one product unit, which is incurred when product quality falls below the required quality level in facility i,
$d_{j,t}$	demand by retailer $j \in R$ in period t,
$q_{\max}$	maximal quality level for products,
$q_{i,\min}$	minimum quality level for products in node i,
s_i	batch size in plant $i \in P$,
$\Delta q_i^{(k)}$	quality degradation in one period for products stored in facility $i \in U$ at temperature choice k,
$\Delta q_{i,j}$	quality degradation for products transported on arc (i,j),
$u_{i,j}$	number of periods transportation lasts on arc (i,j).

Decision variables:

$I_{i,q,k,t}$	inventory with quality level q in facility i with temperature choice k at the beginning of period t,
$x_{i,j,q,t}$	flow quantities on arcs (i,j) in period t with quality level q at the (starting) node i,

$z_{i,k,t}$ binary variable indicates whether the facility i has temperature choice k in period t,
$y_{i,t}$ number of batches required to be produced in plant i in period t,
$\Omega_{i,t}$ amount of waste at facility i in period t.

The quality-based multi-period production and distribution planning problem can now be formulated as follows.

$$\min \sum_{t=1-\omega_{\max}}^{H} \sum_{i \in P} p_{i,t} s_i y_{i,t} + \sum_{t=1-\omega_{\max}}^{H} \sum_{i \in U} w_i \Omega_{i,t} + \sum_{t=1-\omega_{\max}}^{H} \sum_{(i,j) \in A} \sum_{q \geq q_{j,\min} + \Delta q_{i,j}} f_{i,j} x_{i,j,q,t} + \sum_{t=1-\omega_{\max}}^{H} \sum_{k=1}^{S} \left(\sum_{i \in U} g_{i,k}^{(1)} z_{i,k,t} + \sum_{i \in U} \sum_{q \geq q_{i,\min} + \Delta q_i^{(k)}} g_{i,k}^{(2)} I_{i,q,k,t} \right) \quad (3)$$

subject to

$$\sum_{k=1}^{S} I_{i,q,k,t+1} = \sum_{k=1}^{S} I_{i,q+\Delta q_i^{(k)},k,t} + s_i y_{i,q,t} - \sum_{\substack{j \in n(i) \\ q \geq q_{j,\min} + \Delta q_{i,j}}} x_{i,j,q,t}, \quad \forall i \in P, \forall q \in \{Q | q_{i,\min} \leq q \leq q_{\max}\}, \quad \forall t \in \{1-\omega_{\max}, \ldots, H\}, \quad (4)$$

$$\sum_{k=1}^{S} I_{i,q,k,t+1} = \sum_{k=1}^{S} I_{i,q+\Delta q_i^{(k)},k,t} + \sum_{j \in v(i)} x_{j,i,q+\Delta q_{j,i},t-u_{ji}} - \sum_{\substack{j \in n(i) \\ q \geq q_{j,\min} + \Delta q_{i,j}}} x_{i,j,q,t}, \quad \forall i \in W \cup D, \forall q \in \{Q | q_{i,\min} \leq q \leq q_{\max}\}, \quad \forall t \in \{1-\omega_{\max}, \ldots, H\}, \quad (5)$$

$$\Omega_{i,t} = \sum_{k=1}^{S} \sum_{q=q_{i,\min}}^{q_{i,\min} + \Delta q_i^{(k)} - 1} I_{i,q,k,t-1}, \quad \forall i \in U, \forall t \in \{1-\omega_{\max}, \ldots, H\}, \quad (6)$$

$$\sum_{j \in v(i)} \sum_{q \geq q_{i,\min}} x_{j,i,q+\Delta q_{j,i},t-u_{ji}} = d_{i,t}, \forall i \in R, \forall t \in \{1, \ldots, H\}, \quad (7)$$

$$I_{i,q,k,t} \leq M \cdot z_{i,k,t}, \forall i \in U, \forall q \in \{Q | q \geq q_{i,\min}\}, \quad \forall k \in \{1, \ldots, S\}, \forall t \in \{1-\omega_{\max}, \ldots, H\}, \quad (8)$$

$$\sum_{k=1}^{S} z_{i,k,t} = 1, \forall i \in U, \forall t \in \{1-\omega_{\max}, \ldots, H\}, \quad (9)$$

$$\sum_{q \geq q_{i,\min}} s_i y_{i,q,t} \leq a_{i,t}, \forall i \in P, \forall t \in \{1-\omega_{\max}, \ldots, H\}, \quad (10)$$

$$I_{i,q,k,t} \geq 0, \quad \forall i \in U, \forall q \in \{Q | q \geq q_{i,\min}\}, \quad \forall k \in \{1, \ldots, S\}, \forall t \in \{1-\omega_{\max}, \ldots, H\}, \quad (11)$$

$$x_{i,j,q,t} \geq 0, \forall (i,j) \in A, \forall q \in \{Q | q \geq q_{i,\min}\}, \quad \forall t \in \{1-\omega_{\max}, \ldots, H\}, \quad (12)$$

$$z_{i,k,t} \in \{0,1\}, \forall i \in U, \forall k \in \{1, \ldots, S\}, \quad \forall t \in \{1-\omega_{\max}, \ldots, H\}, \quad (13)$$

$y_{i,q,t} \geq 0$ and integer, $\forall i \in P, \forall q \in \{Q | q \geq q_{i,\min}\}, \forall t \in \{1-\omega_{\max}, \ldots, H\}$. (14)

In the above formulation, the objective function (3) aims to minimize the total costs, consisting of production costs, waste disposal costs, transportation costs, and storage costs. Constraints (4) enforce the inventory balances for production plants, and constraints (5) reflect the inventory balances for warehouses and distribution centres. Constraints (6) cause products with quality levels between $q_{i,\min}$ and $q_{i,\min} + \Delta q_i^{(k)}$ to be transferred to waste in variables $\Omega_{i,t}$. Constraints (6) also make sure that there is no inventory for products with quality level less than $q_{i,\min}$. These products cannot be used anymore to satisfy the next periods' demand. Constraints (7) reflect that the retailers' demand and quality requirement must be satisfied. Constraints (8) determine the inventory under different temperature choices. Each facility can only be operated at a single temperature level. Hence, constraints (9) imply that one temperature must be selected for each storage facility. Constraints (10) enforce the production capacity constraints. The remaining constraints (11)-(14) are non-negativity constraints and integer restrictions on the decision variables.

CONCLUSIONS

This paper presented a mixed-integer linear programming model for the planning of food production and distribution. It is based on a generic food supply chain configuration and a general way of describing quality degradation of food products, so as to facilitate application in a wide variety of food industries. The main contribution lies in the inclusion of product quality in the model, and in the differentiation of product flows based on product quality. The model presented is therefore a useful tool in the operation of production and distribution systems in the food industry.

Initial test runs with the model (using ILOG's OPL software in combination with CPLEX) have proven successful, and solution times were within limits acceptable for use of the model in industrial practice. Currently, research efforts are aiming at an implementation of the model in a typical fresh food industry. Next to outcomes such as the evaluation of potential supply chain configurations, this application will allow us to study the performance of the model on the operational level.

ACKNOWLEDGEMENTS

The authors would like to thank the FoodDTU research centre (www.fooddtu.dk) at the Technical University of Denmark for partial funding of this research.

REFERENCES

Ahuja, R.K.; W. Huang; H.E. Romeijn; and D.T. Morales. 2007. "A heuristic approach to the multi-period single-sourcing problem with production and inventory capacities and perishability constraints". *INFORMS Journal on Computing* 19, 14-26.

Dalgaard, P.; P. Buch; and S. Silberg. 2002. "Seafood Spoilage Predictor—development and distribution of a product specific application software". *International Journal of Food Microbiology* 73, 343-349.

Eksioglu, S.D. and M. Jin 2006, "Cross-facility production and transportation planning problem with perishable inventory". In: *ICCSA 2006, Lecture Notes in Computer Science 3982*, M.L. Gavrilova; O. Gervasi; V. Kumar; C.J.K. Tan; D. Taniar; A. Laganà; Y. Mun; and H. Choo (Eds.). 708-717.

Goyal, S.K. and B.C. Giri. 2001. "Recent trends for modeling deteriorating inventory". *European Journal of Operational Research* 134, 1-16.

Labuza, T.P. 1982. *Shelf-life dating of foods*. Food & Nutrition Press, Westport, CT, USA.

Lukasse, L.J.S., and J.J. Polderdijk. 2003. "Predictive modelling of post-harvest quality evolution in perishables, applied to mushrooms". *Journal of Food Engineering* 59, 191-198.

Lütke Entrup, M.; H.-O. Günther; P. van Beek; M. Grunow; and T. Seiler. 2005. "Mixed-integer linear programming approaches to shelf-life-integrated planning and scheduling in yoghurt production". *International Journal of Production Research* 43, 5071-5100.

Man, C.M.D. and A.A. Jones. 1994. *Shelf life evaluation of foods*. Blackie Academic & Professional, Glasgow, UK.

McDonald, K. and D.-W. Sun. 1999, "Predictive food microbiology for the meat industry: A review". *International Journal of Food Microbiology* 52, 1-27.

Myers, D.C. 1997. "Meeting seasonal demand for products with limited shelf lives". *Naval Research Logistics* 44, 473-483.

Nahmias, S. 1982. "Perishable inventory theory: A review". *Operations Research* 30, 680-708.

Raafat, F. 1991. "Survey of literature on continuously deteriorating inventory models". *Journal of the Operational Research Society* 42, 27-37.

Rong, A.; R. Akkerman; and M. Grunow. 2008. "Mixed-integer linear programming approach for food production and distribution planning". In *Pre-prints of the Fifteenth International Working Seminar on Production Economics* (Innsbruck, Austria , March 3-7, 2008), Vol. 2, 559-570.

Smith, D. and L. Sparks. 2004. "Temperature controlled supply chains". In: *Food supply chain management*, Bourlakis, M.A. and P.W.H. Weightman (Eds.). Blackwell Publishing, Oxford, UK, pp. 179-198.

Stadtler, H. and C. Kilger (Eds). 2008. *Supply chain management and advanced planning: Concepts, models, software, and case studies*. Fourth edition, Springer-Verlag, Berlin, Germany.

Van der Vorst, J.G.A.J.; O. van Kooten; W. Marcelis; P. Luning; and A.J.M. Beulens. 2007. "Quality controlled logistics in food supply chain networks: integrated decision-making on quality and logistics to meet advanced customer demands". In: *Proceedings of the 14th International EurOMA Conference* (Ankara, Turkey, June 17-20, 2007).

Zhang, G.; W. Habenicht; and W. Spieβ. 2003. "Improving the structure of deep frozen and chilled food chain with tabu search procedure". *Journal of Food Engineering* 60, 67-79.

AUTHOR BIOGRAPHIES

MARTIN GRUNOW is professor of Operations Management and leader of the theme "Catering and convenience, freshness and supply chains" in the FoodDTU Center at the Technical University of Denmark. Earlier, he worked at the Technical University Berlin and at Degussa AG's R&D department. His research interests are in production and logistics management with a focus on supply chain management in the process industries, including food. He has coauthored more than 80 publications amongst others in International Journal of Production Economics, International Journal of Production Research, European Journal of Operational Research, CIRP Annals, and OR Spectrum. For the latter journal, he also acts as an editor (since 2001).

RENZO AKKERMAN is a H.C. Ørsted postdoctoral research fellow at the Technical University of Denmark in the field of Operations Management. He obtained his Ph.D. in Operations Management from the University of Groningen in The Netherlands, where he previously received an M.Sc. in Econometrics & Operations Research. His research interests are in operations management and supply chain management, mainly related to the food industry, but also in the health care sector. His research has been published in, amongst others, International Journal of Production Economics, International Journal of Production Research, British Food Journal, and Health Care Management Science.

AIYING RONG received her master degree in Industrial Engineering and Engineering Management at Hong Kong University of Science and Technology in 2003 and her Ph.D. degree in Computer Science (Algorithmics) at the University of Turku, Finland in 2006. Currently, she is working as a postdoctoral researcher in the Department of Management Engineering at the Technical University of Denmark and is involved in research on supply chain management in the food industry. Her research interests include operations, planning and scheduling of production activities in different industrial sectors such as the energy industry, the food industry, and the iron & steel industry.

AUTHOR LISTING

AUTHOR LISTING

AUTHOR LISTING